Rigid, Dianionic Carbene Scaffolds for Phosphenium Catalysis

Chloe L. Shaves

School of Physical Sciences

University of Kent

Canterbury

Thesis submitted for the degree of

Master of Science

September 2019

Declaration

I hereby certify that the research presented in this thesis was carried out by myself at the University of Kent, unless otherwise stated in the text. I declare that I am the sole author of this thesis and that this work has not been previously published or submitted, in whole or in part, for any other degree award in any other university. All supporting literatures, quotes and resources have been referenced and acknowledged to the authors and to the best of my knowledge this thesis does not infringe anybody's copyright. I also declare that the copyright of this thesis resides with the author.

Chloe L. Shaves

September 2019

Acknowledgements

Abbreviations

AO	Atomic Orbital
DCM	Dichloromethane
HMDS	Hexamethyldisilazane
HOMO	Highest Occupied Molecular Orbital
LUMO	Lowest Occupied Molecular Orbital
MO	Molecular Orbital
NHC	*N*-Heterocyclic Carbene
NMR	Nuclear Magnetic Resonance
SCXRD	Single Crystal X-Ray Diffraction
THF	Tetrahydrofuran
TMS	Trimethylsilyl
TBDMS	*tert*-butyldimethylsilyl
VT	Variable Temperature

Definition of Units

Å	Angstrom
g	grams
h	Hour(s)
Hz	Hertz
K	Kelvin
mmol	millimole
ppm	parts per million
t	Time
δ	chemical shift (ppm)
°C	Celsius

Definition of Chemical Terms

Ar	aryl
BAr^{Cl}	*tetrakis*(3,5-dichlorophenyl)borate
BAr^{F}	*tetrakis*[3,5-*bis*(trifluoromethyl)phenyl]borate
Cp	cyclopentadienyl
Dipp	2,6-diisopropylphenyl
Et	ethyl
IAd	1,3-diadamantylimidazol-2-ylidene
ICy	1,3-dicyclohexylimidazol-2-ylidene
^{i}Pr	isopropyl
I^{i}Pr^{Me}	1,3-diisopropyl-4,5-dimethylimidazol-2-ylidene
IMes	1,3-bis(2,4,6-trimethylphenyl)imidazol-2-ylidene
IMes^{Me}	1,3-bis(2,4,6-trimethylphenyl)-4,5-dimethylimidazol-2-ylidene
IPr	1,3-bis(2,6-diisopropylphenyl)imidazole-2-ylidene
Me	methyl
Mes	2,4,6-trimethylphenyl
o	*ortho*
OTf	trifluoromethanesulfonate, triflate
p	*para*
Ph	phenyl
R	variable group
SIMes	1,3-bis(2,4,6-trimethylphenyl)-4,5-dihydroimidazol-2-ylidene
SIPr	1,3-bis(2,6-diisopropylphenyl)-4,5-dihydroimidazol-2-ylidene
^{t}Bu	*tert*-butyl
X	halide, pseudo-halide, or anion

Abstract

A viable synthetic method for the preparation of a novel imidazolium NHC precursor, 1,3-bis(2-methoxyphenyl)-4,5-dimethylimidazolium ([IAnis^{Me}H]$^+$), was developed, and several salts with different anions prepared. Said precursor was converted to another novel NHC precursor, 1,3-bis(2-hydroxyphenyl)-4,5-dimethylimidazolium ([IPhenol^{Me}H]$^+$), by demethylation of the *o*-anisole substituents and two different salts were prepared. Having synthesised the imidazolium precursors to two novel NHCs, deprotonation of both species proved to be challenging. The best methods for the *in situ* synthesis of the corresponding free NHCs were either the addition of NaH/^{t}BuOK or LiHMDS depending on the precursor employed.

The coordination of IAnis^{Me} was explored with the transition metals such as copper, nickel, and silver and with the metalloid, selenium. Thus, several mono-NHC complexes were synthesised along with one homoleptic, cationic copper complex, to show the versatility of the ligand and gain an understanding of the ligand's electronic properties. All the metal complexes were characterised by multinuclear NMR, single crystal X-ray diffraction, and combustion analysis where possible.

Furthermore, coordination of both IAnis^{Me} and IPhenolate^{Me} to phosphorus was attempted, however no conclusive proof of target complex formation was acquired. The formation of the desired phosphenium cation targets remains speculative as a result.

Table of Contents

Chapter One

Introduction

"If you don't know where you are going any road can take you there"

Lewis Carroll, Alice in Wonderland

1.1 Introduction to catalysis

It has been known since antiquity that the addition of substoichiometric quantities of a specific material could vastly affect the composition of other materials.[1] However, the term "catalysis" was first coined in 1835 by Berzelius and it was not until 1894 that Ostwald introduced a suitable definition: "Catalysis is the acceleration of a slow chemical process by the presence of a foreign material".[1,2]

A catalyst is therefore a substance that, upon adding small quantities to a reaction, accelerates the rate of the chemical reaction (*via* reducing its activation energy) without altering the Gibbs free energy of the reaction or modifying the position of the equilibrium, and is not itself consumed during the reaction but instead regenerated.[3-5] This process is called catalysis, and a catalytic reaction is a cyclic process in which the catalyst and reactant(s) interact with each other to form a complex which allows a different reaction pathway with a lower activation energy barrier for their transformation into the product(s).[2,3]

In general, catalysts can be split into many different types but within these, the main two are heterogeneous or homogeneous catalysts. A heterogeneous catalytic reaction occurs when the catalyst (typically a porous solid or surface) and the reagent(s) (typically dissolved in a solvent) exist in two different physical phases.[6] Heterogeneous catalysts are typically inorganic solids such as oxides, sulphides, metals, and metal salts, and are of particular importance in chemical and energy industries.[5,7] A homogeneous catalytic reaction occurs when the catalyst and reagent(s) exist in the same phase (both dissolved in a solvent).[4,6] Homogeneous catalysts are commonly metal salts, organometallic complexes, and organic acids. An example of an application of homogeneous catalysis is asymmetric catalysis which employs a chiral catalyst to catalyse the generation of a chiral compound, favouring the formation of one specific stereoisomer. In 2001, the chemistry Nobel prize was awarded to William S. Knowles, Ryoji Noyori, and K. Barry Sharpless for their research in chiral transition metal catalysis for stereoselective hydrogenation and oxidations.[8] Other types include photocatalysis, biocatalysis, nanocatalysis, and electrocatalysis.

Catalysis is hugely important and widely utilised in the chemical and pharmaceutical industries, and catalysts are crucial to the production of materials and chemicals upon which our modern civilisation depends *e.g.* polymers and pharmaceuticals.[6,9] Although catalysts offer increased efficiencies, they also come with environmental concerns as the majority of catalysts are organometallic catalysts employing precious metals.[9,10] The most commonly employed rare and expensive precious metals are rhodium, platinum and palladium.[11]

The problems associated with these metals are the carbon footprint of extracting them, their toxicity, and their cost.[9] Research has therefore focused on discovering alternative catalysts based on earth abundant elements such as first row transition metals.[6,9] However, these catalysts still contain metals and thus in the late 1990s and early 2000s a new concept came about: organocatalysis, or metal-free catalysis.[9,12] This involves essentially four types of organocatalysts (Lewis acids, Lewis bases, Brønsted acids and Brønsted bases)[12] of which Lewis acid catalysts form the focus of this work.

1.1.1 Lewis acid catalysis

Lewis acid catalysis is a very versatile and commonly employed strategy for the catalytic activation of organic molecules, and is utilised in many synthetically important transformations.[13] A Lewis acid is a species with a vacant, low-lying orbital which is exploited in reactions.[10,14] Consequently Lewis acid catalysts initiate their catalytic cycles by accepting electrons from a substrate into their vacant orbital, which is often localised on a positively charged centre.[12,15]

Traditionally Lewis acid catalysts are associated with metal halides such as aluminium chloride, titanium chloride, and zinc chloride, as well as other metal- (Al, Cu, Li, Mg, Ti…) or metalloid-based compounds.[10,13] However they are not the only Lewis acids known.[10] A range of other compounds such as imidazolinium salts, phosphenium, carbenium, silylium, and selenonium cations, and hypervalent systems based on phosphorus and the other group 15 elements all display Lewis acid catalytic acitivity.[10,15-18] These compounds dominate the research areas of Lewis acid organocatalysts and metal-free Lewis acids.

One such example is silicon Lewis acids (SLAs). In these, silicon can be considered as Lewis acidic due to its tendency to expand its valence shell to give rise to five- and six-coordinate intermediates.[19] SLAs can be employed as mediators in carbon-carbon bond formations *e.g.* reaction of acetals with nucleophiles (enol ethers and allylic reagents), carbonyl compounds with nucleophiles, and three component coupling of a carbonyl compound, alkoxysilane and a nucleophile.[19] One advantage of SLAs over metal halide Lewis acids is that they are compatible with many carbon nucleophiles, such as allyl organometallic reagents, cuprates and silyl enol ethers. They are also not prone to aggregation and their structure can be finely controlled by modifying the steric volume of their substituents.

Most examples of SLAs are based on achiral species, but in 1998 Jørgensen and Helmchen reported the synthesis of the first chiral cationic SLA salt (*figure 1.1*).[10,20]

(S)-**I**
a. X = [B(C$_6$F$_5$)$_4$]
b. X = BAr^F
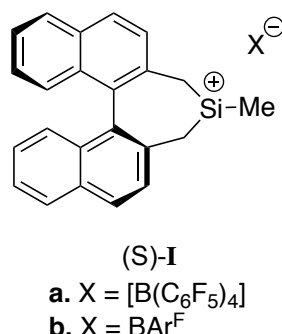
Figure 1.1. Structure of the first chiral cationic salt.

The counter anions [B(C$_6$F$_5$)$_4$]$^-$ and [BAr^F]$^-$ were used, as they are both considered almost chemically inert and non-coordinating and thus ensured that the silyl salt had a high reactivity.[10,20] These cations react rapidly with DCM, abstracting Cl$^-$, but form solvates in MeCN, confirming their Lewis acidity and emphasising the importance of solvent choice in this chemistry.[19] Thus, the solvent in a catalytic reaction plays an important role, for instance a polar solvent in combination with a cationic catalyst has led to increased activity of the catalytic system and therefore an improvement in isolated yield.[20,21] On the other hand, there is the possibility that a polar solvent can coordinate too strongly to the cationic centre and instead inhibit the catalyst from catalysing reactions. Therefore, tuning the structure of the

catalyst such as counter anion and solvent can ultimately affect the catalytic activity, enabling improvements.

The chiral silyl cation salt (S)-**Ia** was tested as a Lewis acid catalyst in the Diels-Alder reaction between acryloyl oxazolidione and 1,3-cyclohexadiene (*scheme 1.1*). The product was obtained in 95 % yield, with greater than 95 % *endo* selectivity. Unfortunately, the enantioselectivity was moderate and approximately 10 % ee was achieved.[10,20]

95%
10% ee
> 95% *endo*
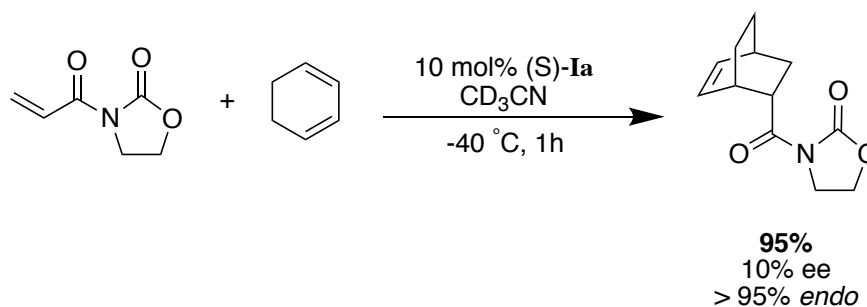
Scheme 1.1. Diels-Alder reaction between acryloyl oxazolidione and 1,3-cyclohexadiene catalysed by (S)-**Ia**.

Catalyst (S)-**Ia** was also able to catalyse the hetero-Diels-Alder reaction between benzylidene-2-methoxyaniline and Danishefsky's diene (*scheme 1.2*). The product was obtained in 74 % yield, as a racemic mixture.

74%
rac
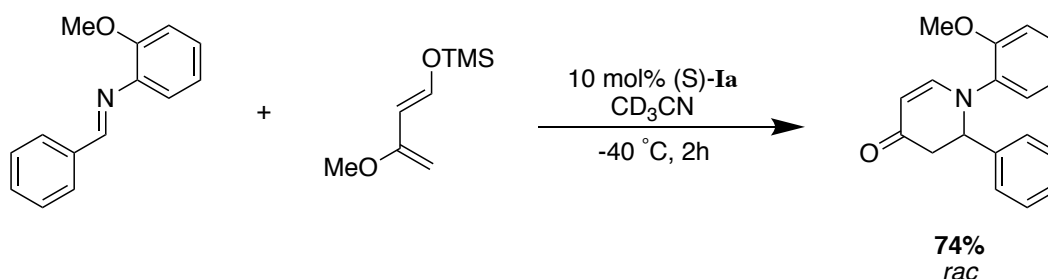
Scheme 1.2. Hetero-Diels-Alder reaction between benzylidene-2-methoxyaniline and Danishefsky's diene catalysed by (S)-**Ia**.

Carbocation-based catalysts, analogous to the silyl cations discussed above, are also known but less studied in comparison.[10] The first isolable carbocation was discovered in 1891 by Merling, but was not structurally confirmed to be the tropylium cation **II** (*figure 1.2*) until 1954 by Doering and Knox.[22,23] Following that, it was not until 1984 that the first carbenium species, trityl salts (TrX) **III** (*figure*

1.2), were utilised as Lewis acid catalysts in the Mukaiyama aldol, Michael, and Sakurai allylation reactions.[10,13,24]

II   **III**

a. X = ClO$_4$
b. X = TfO
c. X = SbCl$_4$
d. X = BF$_4$
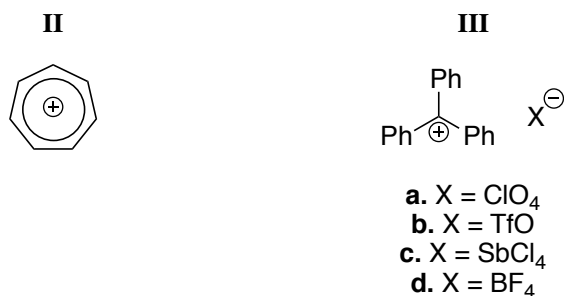
Figure 1.2. Tropylium cation **II** and trityl salt **III**.

Mukaiyama and co-workers reported that 5 mol% of trityl perchlorate, **IIIa**, catalyses the Mukaiyama aldol reaction of trimethylsilyl enol ether and benzaldehyde (*scheme 1.3*) very efficiently.[13,24] This gave high yields of the corresponding β-hydroxy ketones with low diastereoselectivity. However, increasing the steric bulk of the substituent attached to silicon *e.g.* swapping trimethyl silyl enol ether for *tert*-butyldimethylsilyl enol ether, preferentially favoured the thereo aldol and gave high diastereoselectivity in high yields.[24]

X = TMS (**74%**, erythro:thereo 51:49)

X = TBDMS (**89 %**, erythro:thereo 16:84)
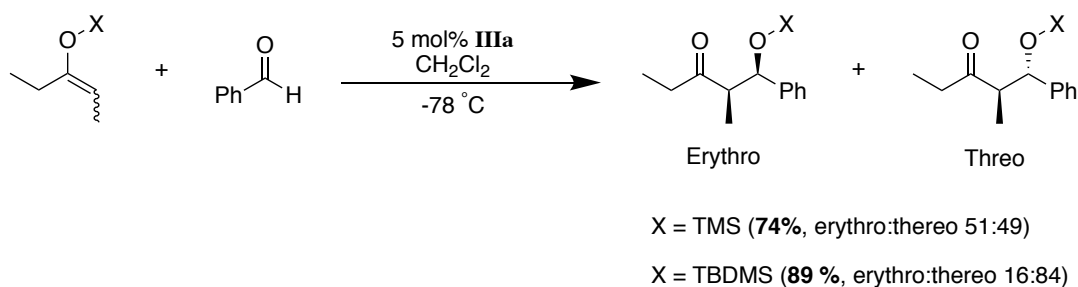
Scheme 1.3. Mukaiyama aldol reactions catalysed by trityl perchlorate **IIIa**.

1.2 Phosphenium cations

P(III) compounds in particular are usually considered as Lewis bases as a result of the accessible lone pair of electrons.[25,26] Nevertheless, phosphenium cations ($[R_2P:]^+$) contain a divalent two-coordinate phosphorus centre in a +3 oxidation state, with a high degree of positive charge accumulation at the phosphorus centre.[27] Notably, singlet phosphenium cations are isolobal and isoelectronic with singlet carbenes, silylenes, and nitrenium cations (*figure 1.3*).[28] Like their congeners, phosphenium cations contain a lone pair of electrons and a vacant p orbital at the reactive phosphorus centre (depicted in *figure 1.3*) and can therefore adopt different multiplicities *e.g.* singlet or triplet ground states.[25] Due to their

electronic structure, singlet species are expected to display amphoteric properties; able to function either as a Lewis acid due to their electrophilic character, or a Lewis base able to form dative bonds though their lone pairs *e.g.* able to act as ligands toward metal carbonyls, azides, *etc* and so exhibit rich coordination chemistry.[25,26,29,30]
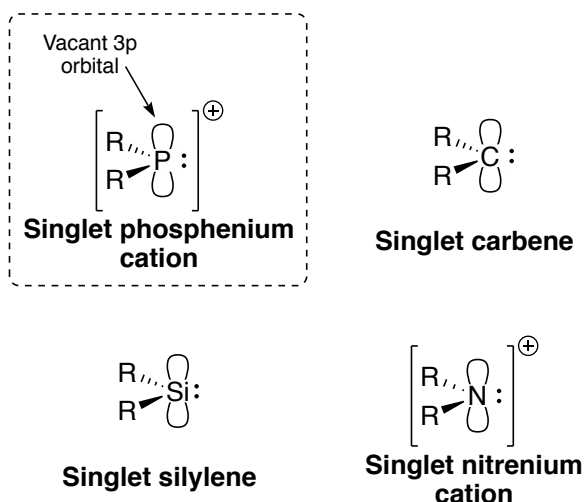
Figure 1.3. A phosphenium cation and congeners.

Hence the chemistry and properties of these phosphenium cations and their congeners are likely to be similar, making them versatile and useful reagents for fundamental perspectives and catalysis.[25,31] Because phosphenium cations are highly reactive species due to a paucity of electron density at the phosphorus centre, a combination of electronic and kinetic stabilisations are employed to synthesise and isolate stable phosphenium cations.[25] The first stable phosphenium cations (**IV** and **V**, *figure 1.4*) were discovered in 1964 by Dimroth and Hoffmann.[32]

$R^1 = CH_3, C_2H_5; R^2 = H, OCH_3$ $R^1 = C_2H_5; R^2 = H, CH_3$
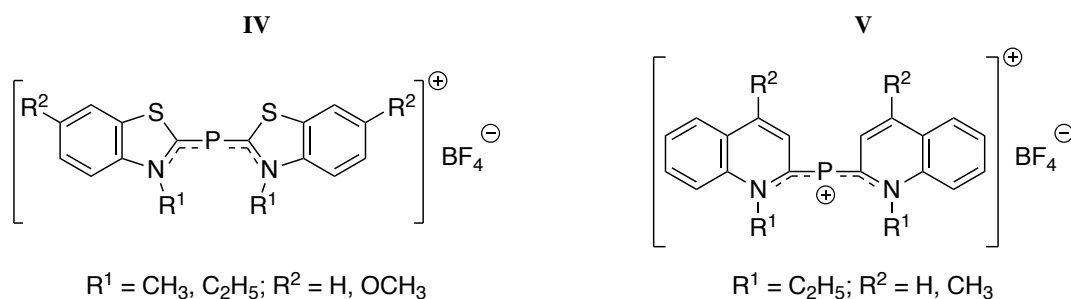
Figure 1.4. The first stable phosphenium cations.

However, it was not until 1972 that the first stabilised cyclic phosphenium cations were reported independently, both examples were synthesised *via* halide abstraction (*e.g.* BF_3, PF_5, PCl_5, $AlCl_3$) from the precursor diaminohalophosphines.

Fleming *et al.*[33] first reported **VI** and Maryanoff and Hutchins[34] described **VII** shortly thereafter (*figure 1.5*). A few years after that, Perry and co-workers[35] broadened the scope of phosphenium cations significantly, with the preparation of the first acyclic, donor-stabilised phosphenium cations **VIII** and **IX** (*figure 1.5*). From then onwards, interest in phosphenium cation chemistry has grown steadily.
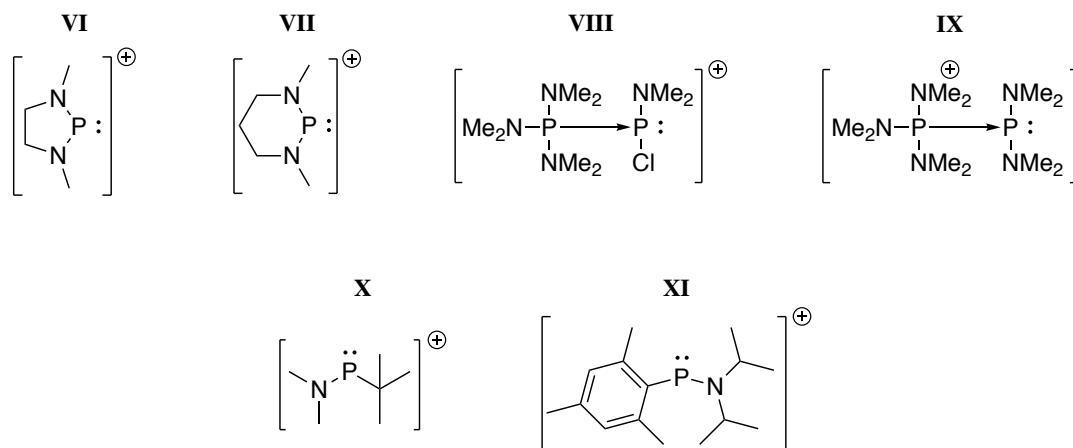
Figure 1.5. Examples of cyclic, acyclic and mono-amido-substituted phosphenium cations.

Their stability and isolability depends on having either π-electron donating substituents adjacent to the cationic phosphorus centre and/or substituents which are able to delocalise/disperse the positive charge build up around the cationic phosphorus centre.[30] The majority of phosphenium cations are stabilised by the former and thus are usually bonded to at least one amido group for thermodynamic stabilisation *via* p_π-p_π delocalisation, *e.g.* **VI**, **VII**, **X** (the first isolated example containing a P-C bond and exhibiting the highest published ^{31}P chemical shift at δ 513.2 ppm for a phosphenium cation), and **XI** (*figure 1.5*).[36,37]

The phosphenium cation $[(H_2N)_2P]^+$ is stabilised by the dative π-bonding between the nitrogen lone pairs and phosphorus vacant 3p orbital, thus relieving the positive charge on the phosphorus centre, depicted in *figure 1.6*.

π-electron donating
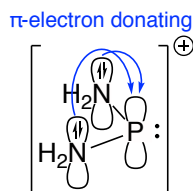
Figure 1.6. Stabilisation *via* dative π-bonding between nitrogen lone pairs and phosphorus vacant 3p orbital on $[(H_2N)_2P]^+$.

Ab initio MO calculations of $[(H_2N)_2P]^+$, carried out by Cowley *et al.* in 1980, highlight the necessity for π-bonding between phosphorus and adjacent ligand(s) for stabilisation of the phosphenium cation as portrayed in *figure 1.7*.[38] The HOMO possesses $2a_2$ symmetry and is non-bonding and is the combination of N(2p) AOs; the second occupied MO possesses $3a_1$ symmetry and essentially corresponds to phosphorus lone pair of electrons.[38] The LUMO is an N-P π-antibonding MO and possesses $5b_1$ symmetry. Thus, the first occupied MO shown, possessing $4b_1$ symmetry, is bonding and considered to be the N→P π-bonding,[38] and hence plays a vital role in the stabilisation of the cation.
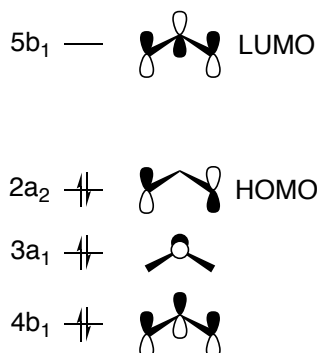
Figure 1.7. Molecular orbital diagram showcasing the important MO of $[(H_2N)_2P]^+$.

The cationic phosphorus centre can also be stabilised by being incorporated into a conjugated π-system, with examples such as **XII**, **XIII** and **XIV** in which the cationic centre is stabilised by a more extensive 6π-delocalisation.[39-41] Multihapto bonding to the cationic phosphorus centre *e.g.* **XV**, can contribute to delocalisation of the positive charge and therefore, partially stabilise the cation.[42] Not only that, the synthesis of $[(Ferrocenyl)_2P]^+$, the first phosphenium cation which featured two P-C bonds, demonstrates that ferrocenyl moieties can stabilise the cationic phosphorus centre *via* delocalisation of the positive charge (*figure 1.8b*).[36,43]

9

a)

XII XIII XIV XV

b)
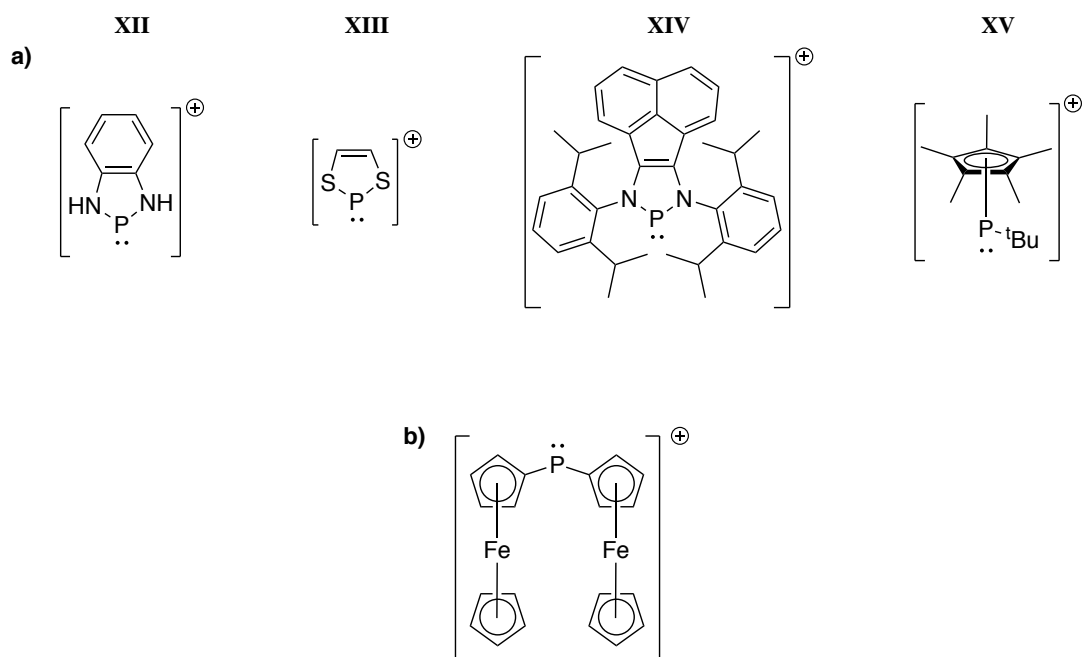
Figure 1.8. a) Phosphenium cations stabilised *via* extensive π-systems; b) Structure of [(Ferrocenyl)$_2$P]$^+$.

Structures **XIII** and **XV** demonstrate that it is not only amido substituents that can stabilise phosphenium cations, and therefore a whole array of phosphenium cations have been prepared.

Kinetic stabilisation of phosphenium centres can be achieved *via* either steric bulk about the phosphorus centre, or their interaction with the counter ion which moderates their Lewis-acidic properties through aggregation in solution.[44,45] Burford *et al.*, in 1993, described the importance of anionic protection, when they showed that [(^{i}Pr$_2$N)$_2$P]GaCl$_4$ is stable in DCM whereas [(^{i}Pr$_2$N)$_2$P]BPh$_4$ reacts with DCM giving rise to a number of phosphorus containing species.[45] One observed species, generated through the oxidative addition of a DCM molecule to the phosphenium centre in the BPh$_4$ salt, was [(^{i}Pr$_2$N)$_2$PCl(CH$_2$Cl)], depicted in *scheme 1.4.*
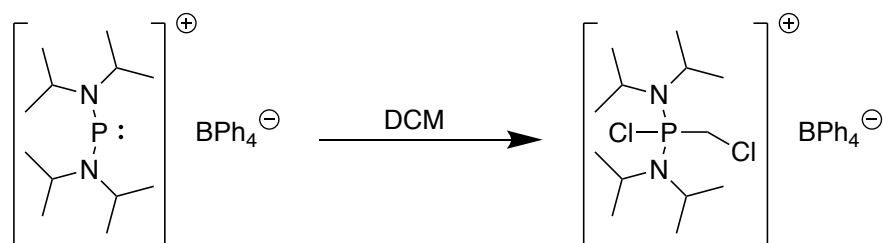
Scheme 1.4. Formation of [(^{i}Pr$_2$N)$_2$PCl(CH$_2$Cl)] *via* oxidative addition.

This difference in reactivity can be attributed to either the considerably greater basicity of the electron rich [GaCl$_4$]$^-$ anion, relative to the [BPh$_4$]$^-$ anion or the aggregation of the former to the latter in solution.[45] Such effects render the phosphenium cation with the [GaCl$_4$]$^-$ anion less susceptible to attack from the polar solvent.

1.2.1 Synthesis and characterisation of phosphenium cations

1.2.1.1 Synthesis *via* halide abstraction

The most commonly used method for the synthesis of phosphenium cations is *via* halide abstraction from the corresponding halophosphine precursor. Some of the Lewis acids which are typically employed are: AlCl$_3$, Me$_3$SiOTf, GaCl$_3$, FeCl$_3$, PCl$_3$, PF$_5$, and BF$_3$.[30] There is not only one halide abstraction agent which is the best for all cases. It depends specifically on the halophosphine precursor used, as not all phosphenium cations can be formed/isolated using all the reagents above. In general, the preparation of phosphenium cations (salts) is by mixing the halophosphine precursor with stoichiometric quantities of a Lewis acid in a suitable solvent (typically DCM - as its moderately high dielectric constant allows the solubilisation of most phosphenium salts, but THF and toluene sometimes also work), shown in *scheme 1.5.*[25]

R = ^{i}Pr or Ph
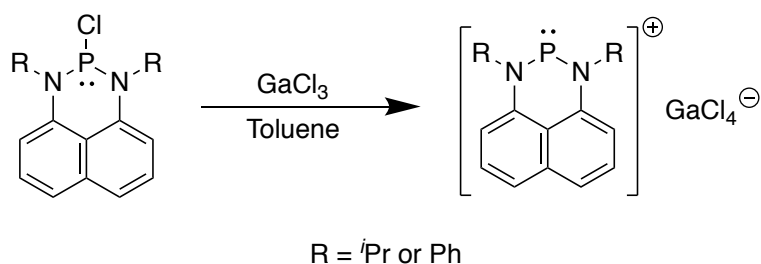
Scheme 1.5. Formation of phosphenium cations *via* chloride abstraction using GaCl$_3$.

Other halide abstraction agents which have been employed are: NaBAr^F, NaBAr^{Cl}, NaBPh$_4$, AgOTf, and TlBAr^F, which upon abstraction of the halide form insoluble metal-halide salts, driving these reactions, depicted in *scheme 1.6*.[46-48]
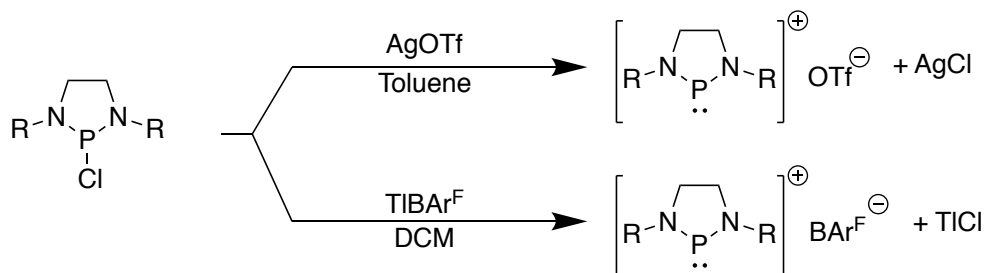
R = *p*-MeOPh, Dipp, Mes

Scheme 1.6. Formation of phosphenium cations *via* chloride abstraction using AgOTf or TlBAr^F.

1.2.1.2 Synthesis *via* autoionisation

In some cases, the phosphenium cation is formed spontaneously from the corresponding halophosphine precursor *via* extrusion of the halide without the addition of a halide abstraction reagent.[30] This is known as autoionisation. For example, the reaction of two moles of an aminoketone with Et$_3$N and PCl$_3$ afforded the donor-stabilised phosphenium cation **XVI** (*scheme 1.7*), rather than the corresponding halophosphine.[49]
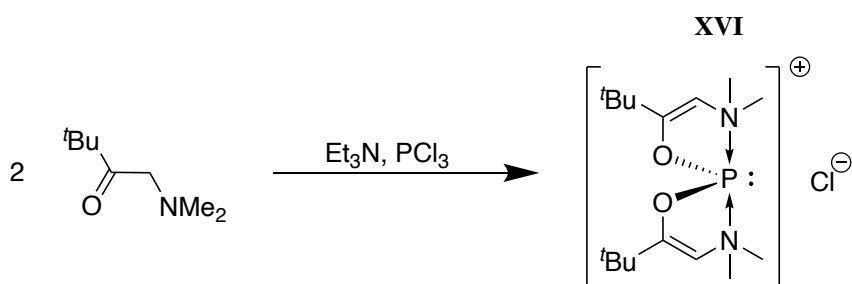
Scheme 1.7. Treatment of two moles of an aminoketone with Et$_3$N and PCl$_3$ yields the phosphenium cation **XVI**, rather than the corresponding halophosphine, *via* autoionisation.

Autoionisation in solution *via* dissociation of the P-X bond can be confirmed by anion metathesis, as represented in *scheme 1*.8. When the counter ion Cl$^-$ of the spirocyclic cation **XVI** is exchanged for BPh$_4^-$ to form **XVII**, both ^{31}P chemical shifts are identical at δ 103 ppm, confirming that **XVI** was autoionised.[44,49]

XVI   XVII

δ_p 103 ppm δ_p 103 ppm
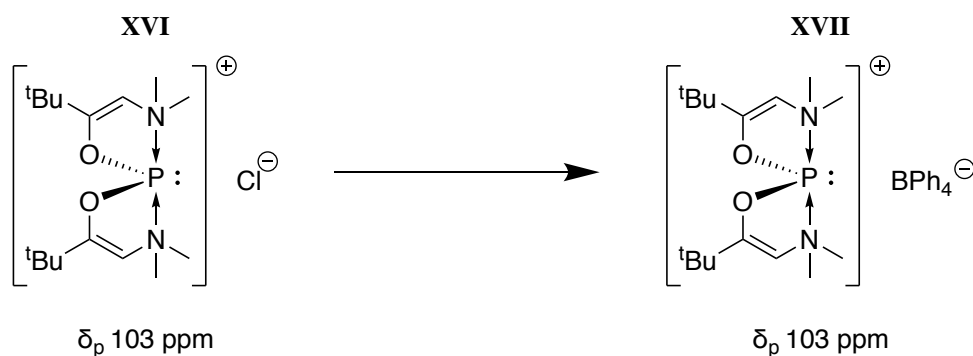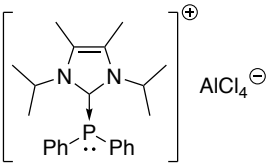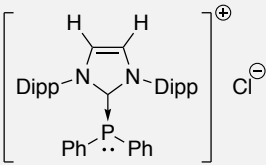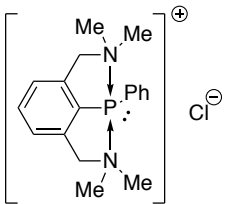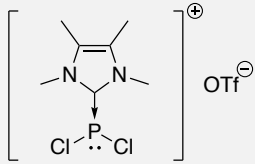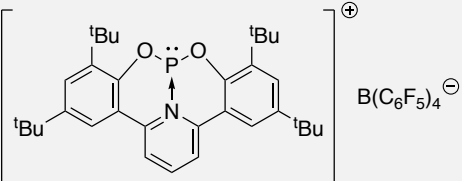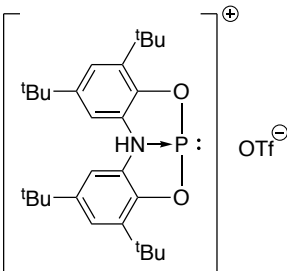
Scheme 1.8. Anion metathesis of Cl- to BPh_4^-.

1.2.1.3 Characterisation by ^{31}P NMR spectroscopy

^{31}P NMR spectroscopy is the most important spectroscopic technique for the identification/characterisation of phosphenium cations and for the study of their further reactions.[30] Generally, phosphenium cations ^{31}P chemical shifts are downfield, due to the paucity of electron density at the phosphorus centre and consequently fall in the region of δ +111.0 to δ +513.2 ppm.[30] However, this is not the case for all phosphenium cations as shown in *table 1.1*.

Typically, phosphenium cations are shifted a further δ >100 ppm downfield relative to their corresponding halophosphine precursor.[30] One exception is $[(Me_5C_5)(Me_2N)P]^+$, which has a ^{31}P NMR chemical shift of δ 111.0 ppm which is 33.8 ppm upfield from its corresponding halophosphine precursor (*table 1.1, entry 6*).[50] Such upfield shift is attributed to the multihapto bonding of the Me_5C_5 ligand and phosphorus centre.[50] Another trend which can be observed is the downfield shifts of complexes which have reduced conjugating ability such as, $[(Me_2N)(^tBu)P]^+$, **X**, which possess a ^{31}P chemical shift of δ 513.2 ppm, due to the lack of π-electron donating substituents (*table 1.1, entry 10*).

13

Entry	Phosphenium Cation	^{31}P NMR Chemical Shift (δ) in ppm	Reference
1	$[(Bu_3P)_2P]^+AlCl_4^-$	-229	51
2		-26.95	52
3		-12.9	53
4		+93.2	54
5		+107	55
6	$[(Me_5C_5)(Me_2N)P]^+AlCl_4^-$	+111.0	50
7		+126	56
8		+155.5	57
9	$[(Mes)(^iPr_2N)P]^+AlCl_4^-$	+500	37
10	$[(Me_2N)(^tBu)P]^+AlCl_4^-$	+513.2	36

Table 1.1. ^{31}P chemical shifts for an array of phosphenium cations.

Whether the compound exists as a neutral complex (to which the anion is bound), or is in equilibrium with its corresponding phosphenium cation, is dependent upon the solvent in which it is dissolved.[56] Dobrovetsky suggested that **XVIII** (neutral species) exists in equilibrium with **XIX** (cationic species) influenced by solvent polarity. Thus, in less polar solvents (*e.g.* C_6H_5Br) the equilibrium lies to the left and favours the neutral complex **XVIII**, whereas, in polar solvents (*e.g.* MeCN) the equilibrium lies to the right and favours the cationic species **XIX** (*scheme 1.9*).[56] This was determined due to the ^{31}P NMR chemical shifts of **XVIII** shifting downfield upon increasing polarity of the solvent. In C_6H_5Br, **XIX** possesses a ^{31}P chemical shift of δ 92 ppm, whereas in CH_2Cl_2 it is δ 117 ppm, and in MeCN, δ 126 ppm.[56]

XVIII		XIX
Low polarity solvent		High polarity solvent

C_6H_5Br	<	CH_2Cl_2	<	MeCN
δ_p 92 ppm		δ_p 117 ppm		δ_p 126 ppm
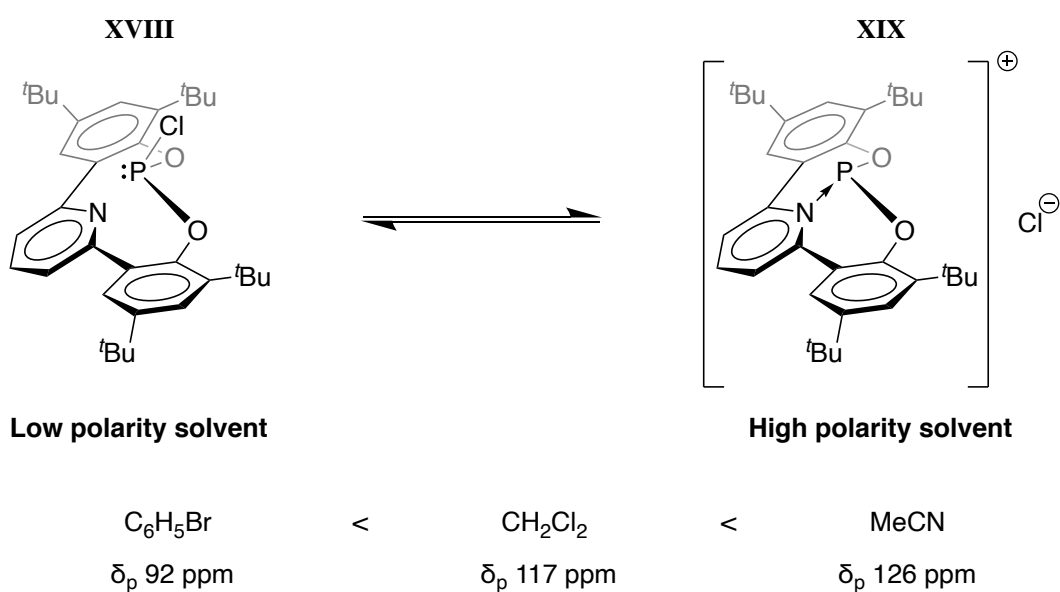
Scheme 1.9. Solvent polarity influencing neutral or cationic equilibrium.

1.2.2 Phosphenium cations stabilised *via* adduct formation

Many isolable phosphenium cations are stabilised by covalent π bonding to relieve the positive charge at the phosphorus centre. However, phosphenium cation stabilisation can also be achieved by coordination of a neutral donor to the phosphorus centre, as illustrated by cations **XX** and **XXI**.[52,54]

XX   **XXI**

Figure 1.9. Cations stabilised by adduct formation.

The ^{1}H NMR spectrum of cation **XX** displays two -CH$_3$ environments as a result of the magnetically inequivalent methyl groups (*figure 1.10*), consistent with the N-P-N bonding mode being present in solution.[54]
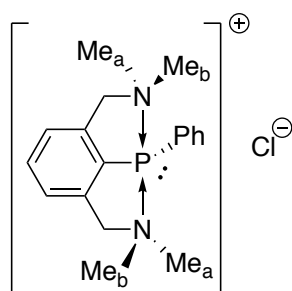
Figure 1.10. Magnetically inequivalent methyls on the N(Me)$_2$ moieties of **XX**.

Cationic P^I species can also be stabilised *via* N→P adduct formation and be generated by anion displacement *e.g.* phosphines bearing good leaving groups can undergo displacement of the original ligand by introduction of a neutral ligand (a stronger donor). The resulting ionic system therefore has an additional electrostatic component, hence the P^I salt is the thermodynamic preference and drives the reaction.[58] An example, is an iminophosphine undergoes the displacement of triflate with either quinuclidine or pyridine forming the corresponding cationic complexes **XXII** or **XXIII** (*scheme 1.10*) stabilised *via* N→P adduct formation.[59]

XXII

XXIII
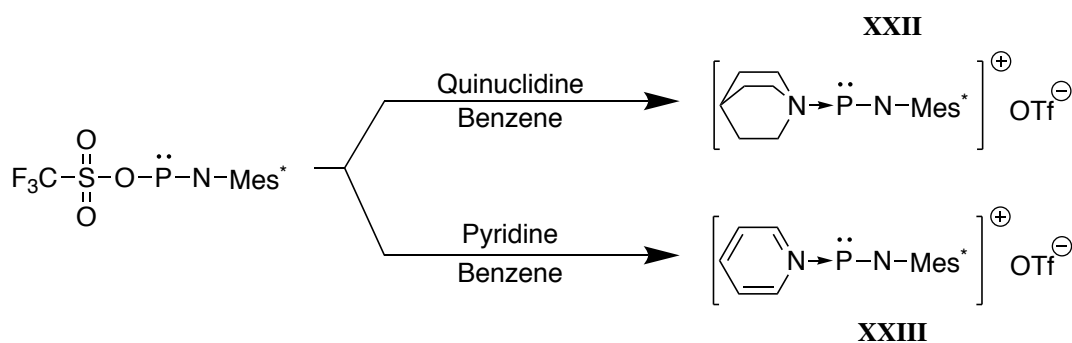
Scheme 1.10. Displacement of triflate forming the corresponding cationic complexes.

1.2.2.1 Geometrically constrained phosphenium cations

Van Korton and co-workers demonstrated that the tridentate pincer ligand **XXIV** (*figure 1.11*) can be utilised for the stabilisation/isolation of cationic species *e.g.* stannonium cations.[60,61]
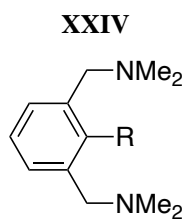
XXIV

Figure 1.11. Chelating tridentate pincer ligand.

After this, in 1997 Corriu used the same pincer ligand **XXIV** to synthesise the phosphenium cation **XX**, which was the first geometrically constrained phosphenium cation,[54] stabilised by two dialkylamino group N→P intermolecular interactions and one covalent bond. The cation **XX** was synthesised *via* the reaction of the appropriate organolithium species with PhPCl$_2$ with subsequent autoionisation, illustrated in *scheme 1.11*.

XX
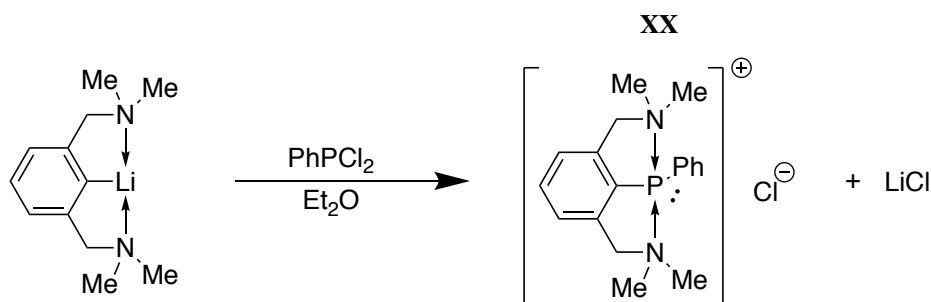
Scheme 1.11. Synthesis of the 'first' geometrically constrained phosphenium cation.

Since then, there have only been a handful of geometrically constrained phosphenium cations reported but there have been a few examples of neutral P[III] geometrically constrained species described, which are all capable of activating small molecules. The compound that really sparked curiosity into this particular field was Arduengo's synthesis of the neutral P[III] species **XXV**, a tridentate pincer ligand coordinated to a P[III] atom *via* a O,N,O-binding motif.[62] Arduengo examined the reactivity of **XXV** with halogens, alcohols, α-dicarbonyls, acetylenes, Bronsted acids, alkynes and transition metal complexes.[62,63] 25 years after it was reported, Radosevich showed that **XXV** was capable of reversible redox cycling between P[III]/P[V] oxidation states,[64] and as such could be harnessed for catalytic transfer hydrogenation reactions, *e.g.* the hydrogenation of diazobenzene, depicted in *scheme 1.12*.[64] Such ability is rare for non-metal based platforms, as traditionally it was considered exclusive to transition metals (d-block metals).
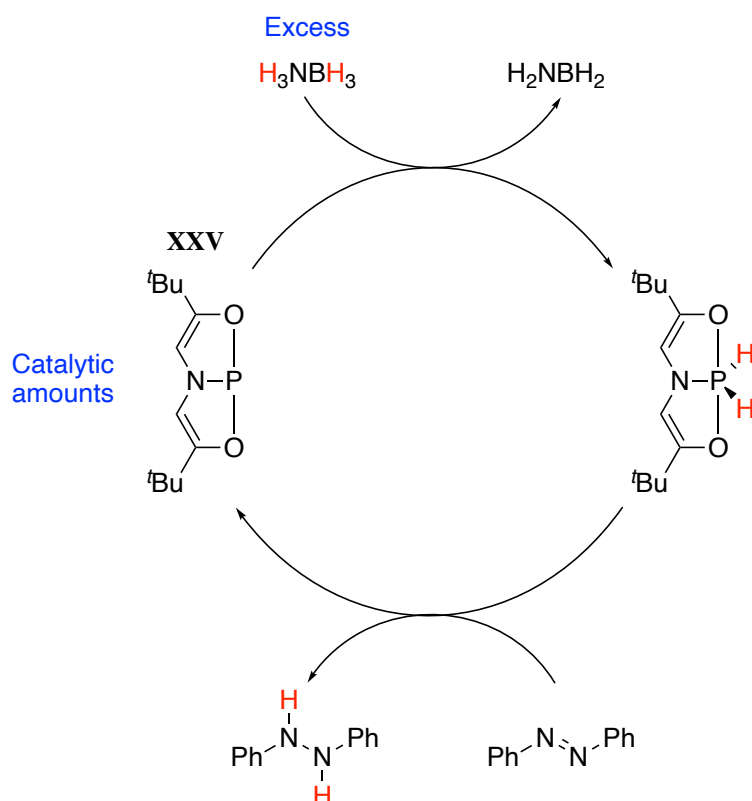
Scheme 1.12. Catalytic cycle of the catalytic transfer hydrogenation of diazobenzene *via* phosphorus platform **XXV**.

Following that, the same group also demonstrated that **XXV** can undergo intermolecular N-H oxidative addition of ammonia, alkyl- and aryl-amines at the P[III]

centre leading to a P^V species.[65] Radosevich and Kinjo subsequently synthesised the geometrically constrained neutral P^{III} species **XXVI** and **XXVII** respectively. Here, **XXVI** is capable of reversible intermolecular E-H (E = OR, NHR) oxidative addition which affords the corresponding P^V species and therefore shows potential in catalysis.[66] Notably, such phosphorus platforms (**XXVI**, **XXVII** and **XXVIII**) can perform small-molecule bond activation due to their pronounced geometric distortions, a result of their pincer ligand binding motifs, which causes substantial electrophilic (δ+) character at their phosphorus centres.[66]

XXVI	**XXVII**	**XXVIII**
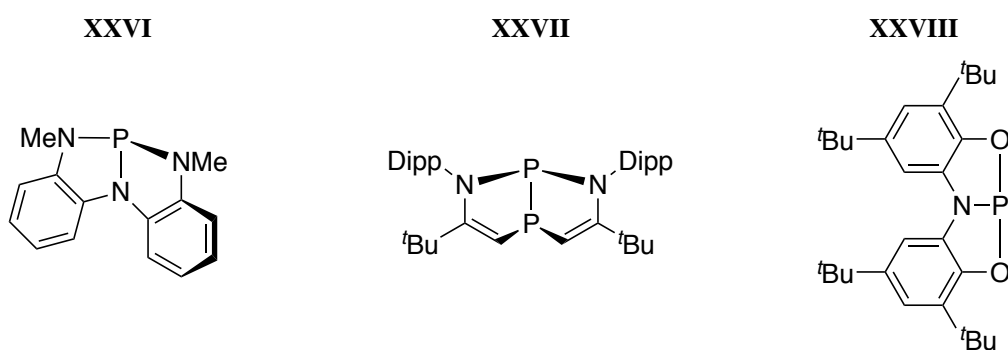
Figure 1.12. Geometrically constrained neutral P^{III} species.

Compound **XXVII** can activate ammonia by σ-bond metathesis between an N-H bond on ammonia and one of the P-N endocyclic bonds on **XXVII**.[67] In this process, the phosphorus oxidation state does not change and thus it is not oxidative addition. Such activation was induced by the bent geometry of **XXVII** established due to the two phosphorus atoms binding at the bridgehead.[67] The other tridentate neutral P^{III} species worth noting is **XXVIII**, reported by Aldridge and Goicoechea, which too is able to activate ammonia and water *via* E-H oxidative addition leading to the formation of the corresponding P^V species, similar to compound **XXVI**.[68] Thus all 3 studies emphasize that P^{III}-based pincer complexes with distorted geometries can activate a range of E-H bonds (E = O or N) and therefore presents new ways of non-metal catalysis employing group XV elements.

A few years later the same group (Aldridge and Goicoechea) reported two geometrically constrained phosphenium cations derived from **XXVIII**.[57] Cations **XXIX** and **XXX** were prepared when studying the reactivity of **XXVIII** with electrophiles, specifically whether electrophilic substrates would associate with the

P^{III} centre or with the more electronegative O,N,O atoms on the ligand backbone, as shown in *scheme 1.13*.[57]
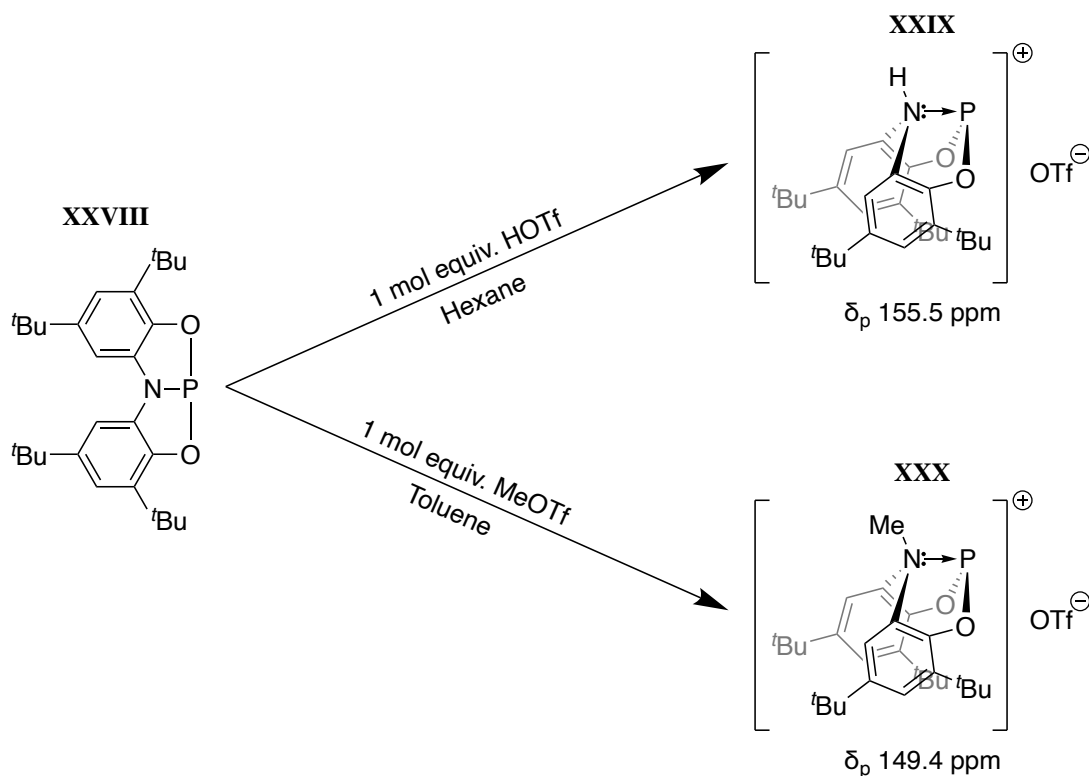
Scheme 1.13. Syntheses of the geometrically constrained P^{III} cations **XXIX** and **XXX**.

They were surprised to report that protonation/methylation did not occur directly with the P^{III} centre, but instead the electrophilic groups associated with the nitrogen centre of the chelating tridentate ligand.[57] Upon functionalisation of the nitrogen atom, in both cationic species **XXIX** and **XXX**, the P^{III} centres and OTf anions were in close proximity of each other in the crystal structures, suggesting significant positive charge accumulation on the P^{III} centre.[57] Also both **XXIX** and **XXX**, adopt a distorted tetrahedral geometry around the nitrogen atom and exhibit notable elongation of their P-N bonds compared to **XXVIII** (P-N bond distances for **XXVIII**, **XXIX** and **XXX**, respectively: 1.757(1), 1.926(2), and 1.955(2) Å).[57] This indicates that the P-N interaction is comparatively weak. The two P-O bond distances for **XXVIII** undergo a slight contraction upon protonation/methylation of the nitrogen atom, from 1.659(1) and 1.652(1) Å to 1.615(2) and 1.619(2) Å in **XXIX** upon protonation of the nitrogen atom, and contract to 1.626(2) and 1.626(2) Å upon methylation of the nitrogen atom in **XXX**. Interestingly, upon

addition of an acid such as HCl (in which the counter-anion Cl⁻ is more nucleophilic than OTf⁻) to **XXVIII**, yielded the corresponding P^V species as a result of oxidative addition.[57] This opens the possibility that other phosphenium cations with a pincer ligand system containing a binding nitrogen atom may be synthesised *via* functionalisation of the binding nitrogen atom and stabilised by the formation of an N→P interaction or base-stabilised through close contact with anion. However, this may be expected only in the presence of weak nucleophiles like OTf⁻ anions otherwise oxidative addition will most likely occur instead.

The other geometrically constrained phosphenium cation recently described, which is of importance to this project, is the cationic species **XIX** reported by Dobrovetsky.[56] As geometrically constrained neutral P^{III} compounds, show enhanced reactivity when incorporated into a tridentate ligand system *vide supra*, such approaches could lead to the enhancement of the amphoteric nature of P^{III} cationic centres.[56,66] Hence a cationic species constrained by a tridentate ligand was prepared by Dobrovetsky *via* halide abstraction from the natural P^{III} halophosphine precursor **XVIII** using potassium tetrakis(pentafluorophenyl)borate (*scheme 1.14*).[56,62]

Scheme 1.14. Two step, two pot synthesise of the geometrically constrained phosphenium cation **XIX**.
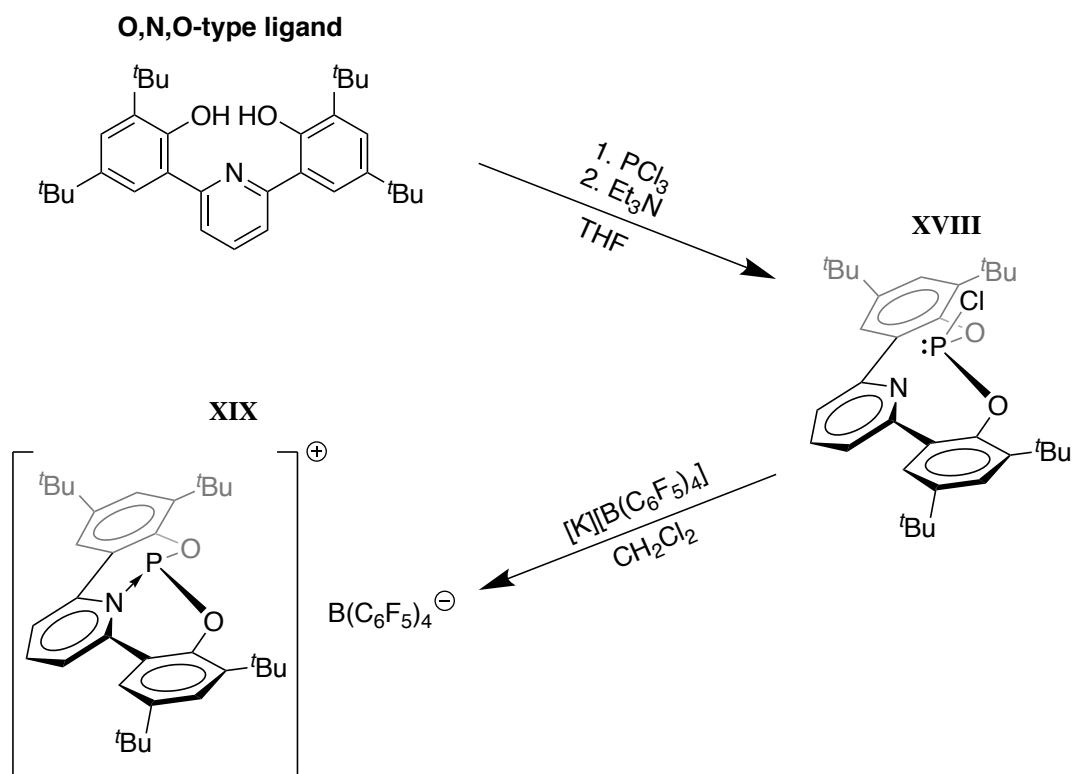
The geometry around the phosphorus cationic centre of **XIX** is significantly distorted. The P-O bonds of **XIX** (1.61 Å) are similar to the P-O bonds of the closely related cations **XXIX** and **XXX** (1.615-1.626 Å).[56,57] However, the P-N bond of **XIX** is 1.81 Å, short relative to **XXIX** and **XXX** (1.926(2) and 1.955(2), respectively).[56,57] this suggests that the N→P interaction in **XIX** is stronger than those in **XXIX** and **XXX**, and of a very similar length to **XXVIII** which has a formal P-N bond.[56]

They reported that **XIX** could undergo oxidative addition with H_2O (stoichiometric amounts), MeOH, ^{i}PrOH, ^{t}BuOH, and NH_3, depicted in *scheme 1.15*.[56] Such addition to **XIX** synthesises the phosphonium cations **XXXI, XXXII, XXXIII, XXXIV,** and **XXXV** respectively, and the formation of a P-H moiety was confirmed, by the appearance of doublets with complementary coupling in their ^{31}P and ^1H NMR spectra.
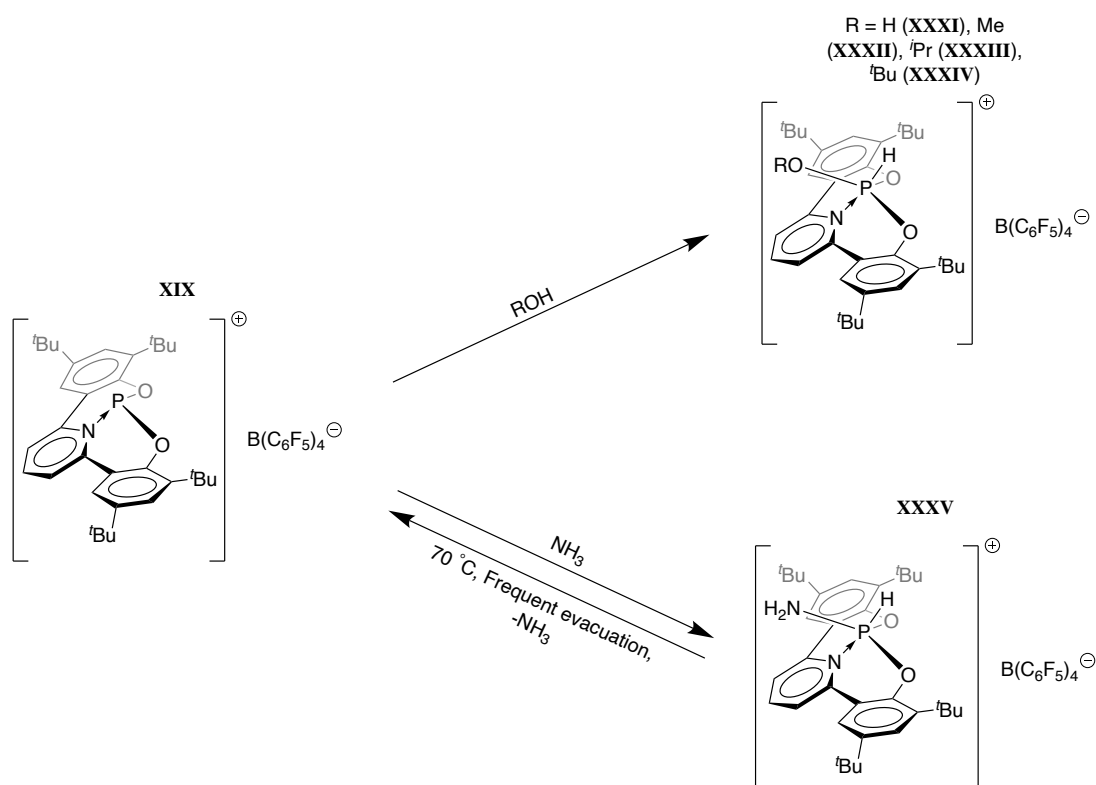
Scheme 1.15. Oxidative addition of **XIX** with H_2O, MeOH, ^iPrOH, ^tBuOH and NH_3.

In the case of the H_2O activated species **XXXI**, such reactivity has not been reported/observed beforehand with monocationic phosphenium cations.[56] Also, noteworthy is that the reaction of **XIX** with NH_3 is reversible. Thus, **XIX** undergoes reversible redox cycling first *via* the oxidative addition of NH_3 forming the corresponding phosphonium cation **XXXV**, then surprisingly the reductive elimination of NH_3 upon heating **XXXV** to 70 $^{\circ}$C and frequent evacuation, regenerating the phosphenium cation, **XIX**. This reversible redox cycling was not reported/observed for the NH_3 oxidative addition products, of **XXV**, **XXVI** and **XXVIII** (neutral geometrical constrained P^{III} compounds) and furthermore such addition has never been observed/reported with other phosphenium cations.[56]

This work highlights how such geometrically constrained phosphenium cations can be of specific use in the controlled activation of polar small molecules, such as water and ammonia in terms of H-OH and H-NH_2 bond activation, which therefore provides functionality to unactivated bonds which are thus challenging and highly sort after targets, for the generation of renewable energy (e.g. water splitting, H_2O into H_2 and ½ O_2, for the production of solar fuel) and the chemical synthesis of

value-added products (*e.g.* the catalytic addition/coupling of ammonia to olefins/arenes to yield primary amines/anilines are very sort after goals in catalysis).[68-70] Inspired by these results, the target of this thesis is to synthesise the geometrically constrained phosphenium cation, **XXXVI**. This cation uses an NHC→P interaction for the stabilisation of the cationic phosphorus and reduces the steric bulk on the adjacent phenyl rings relative to **XIX**. The overall aim of this project was to determine how these changes affect the Lewis acidity of the phosphenium cation, and explore the use of this cation for small molecule activation and catalysis.
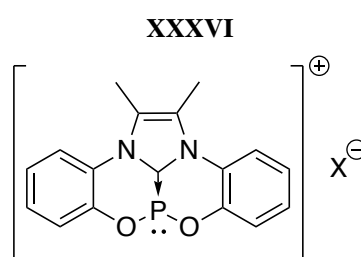
XXXVI

Figure 1.13. Novel geometrical constrained phosphenium cation **XXXVI**.

1.2.2.2 Carbene ligands for adduct formation

1.2.2.2.1 *N*-Heterocyclic carbenes

N-Heterocyclic carbenes (*figure 1.14*) are neutral heterocyclic species which contain a divalent, cyclic carbene carbon which is stabilised *via* (at least one) nitrogen heteroatom(s) and their substituents, both at N and on the backbone.[71,72]
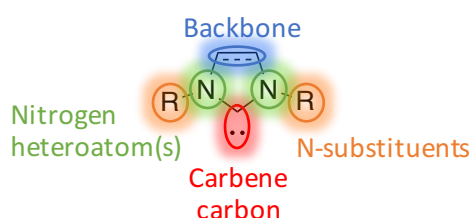
Figure 1.14. NHCs structural features.

In most NHCs, the carbene carbon atom is in a singlet ground state. NHCs most commonly have two nitrogen heteroatoms adjacent to the carbene carbon atom (C_2) which provide electronic stabilisation. Not surprising, nitrogen atoms are σ-electron withdrawing (inductive effect) and π-electron donating (mesomeric effect) and it is well established that these effects favour the singlet ground state (*figure 1.15*).[73]
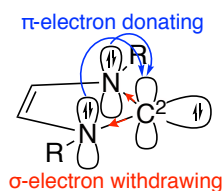
Figure 1.15. Singlet ground state electronic structure of a typically NHC, depicting how nitrogen heteroatoms stabilise/favour this state *via* inductive and mesomeric effects, respectively.

The N-substituents are generally bulky substituents which provide kinetic stabilisation as they sterically disfavour dimerisation of two NHCs together.[71] Furthermore, steric effects of these bulky substituents can also influence the ground-state multiplicity of the adjacent carbene carbon.[73]

The backbone of the heterocyclic ring can also provide kinetic stabilisation and further favours the singlet ground state as the backbone imposes an angular constraint and inhibits the twisting of the N-C-N bonds which arranges the carbene carbon in a bent geometry.[71,73] Substituents can be attached to the backbone, which can also influence the carbenic carbon's electronic properties.[71] Moreover, the heterocyclic ring can also be aromatic, *e.g.* an unsaturated species (imidazolylidene), or not *e.g.* a saturated species (imidazolinylidene), depicted in *figure 1.16*. If the backbone is aromatic, this adds additional electronic stabilisation to the species as this effect enhances p_π-p_π delocalisation around the ring.[71,74] The cyclic delocalisation significantly increases the mesomeric effect favouring the singlet ground state.[71,74]
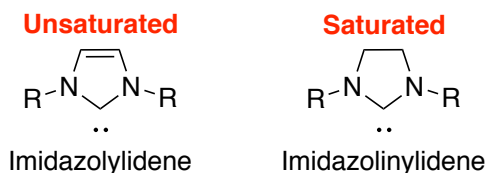
Figure 1.16. NHCs structural feature: unsaturated or saturated.

However, within NHCs general properties as described above fall a whole host of different classes *e.g.* different heteroatoms, different numbers of heteroatoms, and differing ring size of the heterocycles, though five-membered heterocycles are the most common.[71,73]

1.2.2.2.2 NHC-stabilised phosphenium cations

Numerous phosphenium cations have been synthesised over the years, however, the majority of them require stabilisation *e.g.* adduct formation with Lewis bases.[75] One way in which P[III] Lewis acid acceptor centres have been stabilised is *via* their coordination with NHCs. These ligands have strong Lewis basic character (due to lone pair bearing) and therefore are an ideal stabilising ligand for P[III] cations.[58] The coordination chemistry/stabilisation of these types of donor-acceptor adducts is attributed to a dative bonding interaction (C→P interaction) between a neutral two-electron carbon donor with a P[III] centred-cation acceptor (regardless of its lone pair), and the resultant cations are best described as NHC→phosphenium adducts (*figure 1.17a*).[58,76,77] However, such complexes can also be regarded as NHC-substituted P complexes that bear a positive charge on the NHC imidazole ring (*figure 1.17b*).[76-78]
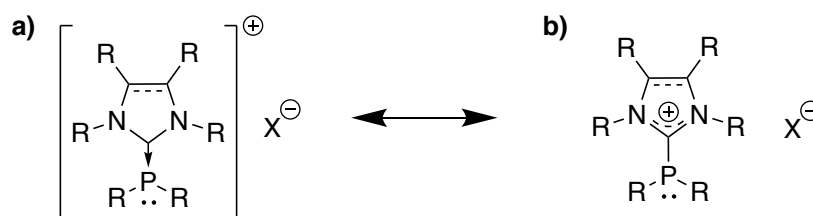
Figure 1.17. a) Dative representation of NHC→phospheniums adducts; b) Lewis representation of imidazoliophosphine.

Macdonald and co-workers have shown that the C→P bond in the phosphenium cation **XXXVII** can be described as a donor-acceptor bond (**XXXVIIa**), where the NHC moiety acts exclusively as a Lewis donor and thus, the phosphenium moiety behaves solely as a Lewis acceptor, instead of forming a C-P multiple bond (**XXXVIIb**).[26] This is explained by the Carter-Goddard-Malrieu-Trinquier (CGMT) model and is attributed to the NHC and phosphenium cation fragments profound electronic preference of the singlet state rather than the triplet state (*figure 1.18b*) due to their significantly large singlet-triplet energy difference ($\Delta E_{s \to t}$).[26,79] As such, this enforces pyramidal configuration at the P centre, hence the absence of a double bond.[26,80]
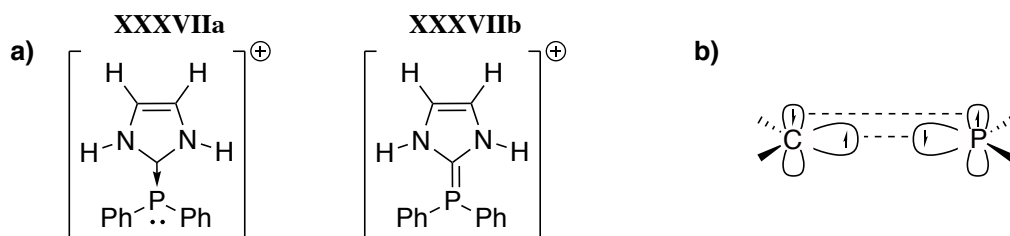
Figure 1.18. a) Canonical structures of **XXXVII**; b) Coupling of two triplet fragments forming a multiple bond.

The work by Kuhn *et al.* in 1999 led to the synthesis of the first phosphenium cation stabilised *via* coordination with an NHC.[52] Treatment of imidazole-2-ylidene **XXXVIII** with chlorodiphenylphosphine gave the desired product **XXXIX** (^{31}P chemical shift of δ -27.05 ppm) and was further reacted with aluminium trichloride to give the corresponding tetrachloroaluminate salt **XL** (^{31}P chemical shift of δ -26.95 ppm), depicted in *scheme 1.16*.[52,73] The exchange of the counterions (anion metathesis) from the nucleophilic chloride to the largely inert tetrachloroaluminate, caused only a marginal difference in their ^{31}P chemical shifts,[52] which confirmed that the chloride had already dissociated from the phosphorus moiety forming the cation rather than a carbene-halophosphine adduct. They also report that **XL** has a low solubility in non-polar solvents and is only stable in aprotic solvents for approximately 30 minutes.[52]
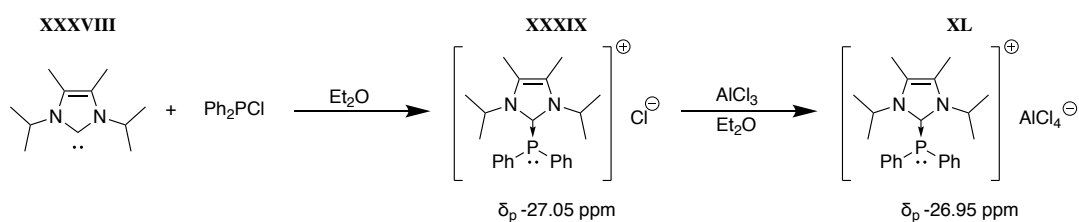
Scheme 1.16. Preparation of the first carbene-stabilised phosphenium cation.

Subsequently, quite a few carbene-stabilised phosphenium cations have been successfully synthesised and characterised, and there are various ways in which such cations can be prepared. One method is the reactions of imidaol-2-ylidene (bulky NHCs with N-subsitiuents such as Dipp, ^{t}Bu or adamantyl and so forth) with halophosphines (*scheme 1.17a*)[81,82] or phosphine-stabilised phosphenium salts (*scheme 1.17b*)[83] to yield either the hypervalent NHC→halophosphine adduct **XLI** or the phosphenium salt immediately **XLII** or upon treatment with a metathesis reagents (AlCl$_3$, GaCl$_3$, NaBAr^{Cl}, NaBAr^F, NaOTf).
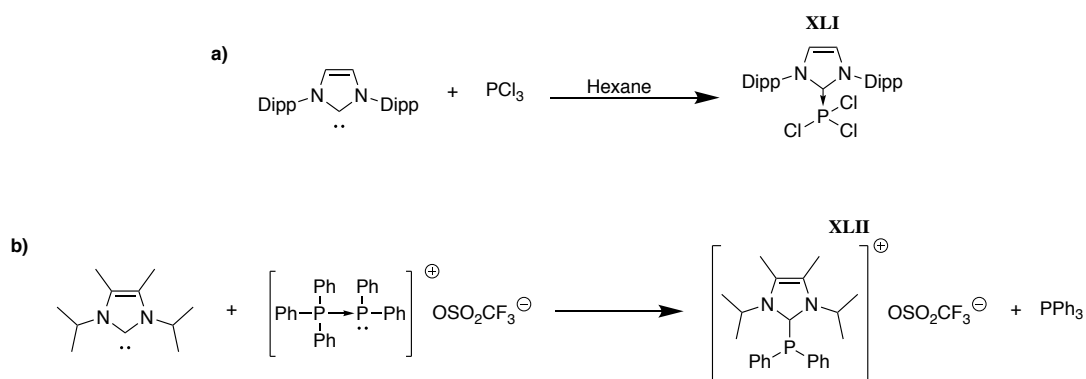
Scheme 1.17. a) Treatment of an NHC with PCl_3 which yields an NHC→PCl_3 adduct; b) Reaction of an NHC with a penta-phenylphosphinophosphonium salt which forms a phosphenium cation.

Macdonald reported that upon reacting PCl_3 with NHCs bearing less bulky N-substituents, such as Et, ^{i}Pr and Mes, a redox reaction occurs yielding the P^I cations **XLIII** and **XLIV** as a result of the formal sequestration of Cl_2, illustrated in *scheme 1.18*, rather than the formation of the desired corresponding P^{III} species.[82,84]

R_1 = Et, ^{i}Pr, Mes; R_2 = Me (Et & ^{i}Pr), H (Mes)
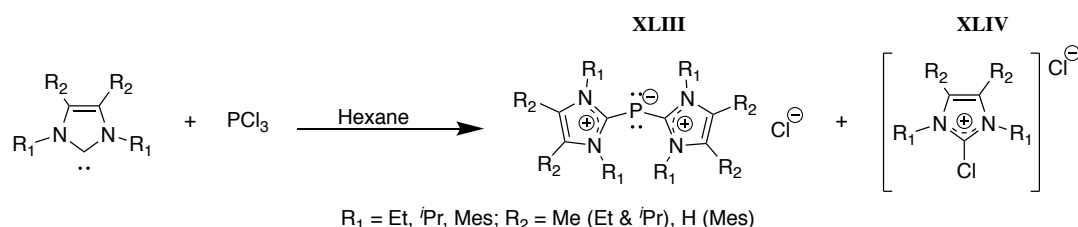
Scheme 1.18. Treatment of less bulky NHCs with PCl_3 triggers a redox reaction to yield the corresponding P^I cations and 2-chloro-imidazolium chlorides, instead of the desired P^{III} species.

To prevent the reduction of P^{III} species from occurring with less bulky NHCs, the "free" NHCs can be transformed into protected NHCs *via* adduct formation and can be described as "onio-substituent transfer agents".[82,85] Protection can be obtained by carboxylation or silylation, generating imidazolium-2-carboxylates (NHC-CO_2 adducts)[86] or 2-(trimethylsilyl)imidazolium salts (NHC-silylium adducts)[87]. These agents can be treated with halophosphines (*e.g.* PCl_3) and yield the corresponding hypervalent NHC→halophosphine adduct or the phosphenium salt immediately depending on its stability.[77,81b] In the case of the TMS-imidazolium salt **XLV** with excess PCl_3 yielded the carbene-stabilised phosphenium cation **XLVI**, reaction outlined in *scheme 1.19*.[82]
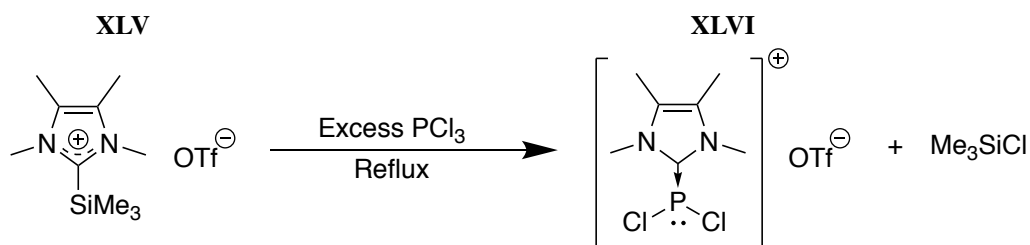
Scheme 1.19. Reaction of a protected NHC with PCl$_3$ to yield a P^{III} cation.

1.3 Conclusion

Geometrically constrained phosphenium cations show great potential in main group Lewis acid catalysis, with virtually all such species reported in the literature capable of activating E-H bonds (e.g. H-OH, RO-H and H-NH$_2$). Thus, this work targeted the synthesis of donor-stabilised phosphenium cations, specifically targeting a rigid carbene-stabilised phosphenium cation with the intention to explore its Lewis acidity and potential as a main group Lewis acid catalyst. This first required the development of a synthetic method for necessary novel dianionic carbene ligands.

1.4 References

1. G. Ertl, *Angew. Chem. Int. Ed.*, 2009, **48**, 6600-6606.

2. E. Roduner, *Chem. Soc. Rev.*, 2014, **43**, 8226-8239.

3. H. Spinney, I. Korobkov, G. DiLabio, G. Yap and D. Richeson, *Organometallics*, 2007, **26**, 4972-4982.

4. O. Deutschmann, H. Knozinger, K. Kochloefl and T. Turek, *Ullmann's Encycl. Ind. Chem.*, 2011.

5. P. Wells, *Encyclopedia of Materials: Science and Technology*, 2001, 1020-1025.

6. A. Hagemeyer and A. Volpe, *Reference Module in Materials Science and Materials Engineering*, 2016.

7. L. Chmielarz, M. Rutkowska and A. Kowalczyk, *Adv. Inorg. Chem.*, 2018, **72**, 323-383.

8. D. Murzin and T. Salmi, *Catalytic Kinetics*, 2005, 27-72.

9. J. Bayne and D. Stephan, *Chem. Soc. Rev.*, 2016, **45**, 765-774.

10. O. Sereda, S. Tabassum and R. Wilhelm, *Top. Curr. Chem.*, 2009, 349-393.

11. R. Bullock, *Catal. Precious Met.*, Wiley, Somerset, 2011.

12. B. List, *Chem. Rev.*, 2007, **107**, 5413-5415.

13. V. Naidu, S. Ni and J. Franzén, *ChemCatChem*, 2015, **7**, 1896-1905.

14. W. Jensen, *Chem. Rev.*, 1978, **78**, 1-22.

15. O. Sereda, N. Clemens, T. Heckel and R. Wilhelm, *Beilstein Jour, Org. Chem.*, 2012, **8**, 1798-1803.

16. V. Jurčík and R. Wilhelm, *Org. Biomol. Chem.*, 2005, **3**, 239-244.

17. C. Chen, S. Chao, K. Yen, C. Chen, I. Chou and S. Hon, *J. Am. Chem. Soc.*, 1997, **119**, 11341-11342.

18. X. He, X. Wang, Y. Tse, Z. Ke and Y. Yeung, *Angew. Chem. Int. Ed.*, 2018, **57**, 12869-12873.

19. A. Dilman and S. Ioffe, *Chem. Rev.*, 2003, **103**, 733-772.

20. M. Johannsen, K. Jørgensen and G. Helmchen, *J. Am. Chem. Soc.*, 1998, **120**, 7637-7638.

21. M. Johannsen and K. Jørgensen, *J. Chem. Soc., Perkin Trans. 2*, 1997, 1183-1186.

22. G. Merling, *Ber. Dtsch. Chem. Ges.*, 1891, **24**, 3108-3126.

23. W. Von E.Doering and L. Knox, *J. Am. Chem. Soc.*, 1954, **76**, 3203-3206.

24. T. Mukaiyama, S. Kobayashi and M. Murakami, *Chem. Let.*, 1985, **14**, 447-450.

25. H. Spinney, I. Korobkov, G. DiLabio, G. Yap and D. Richeson, *Organometallics*, 2007, **26**, 4972-4982.

26. B. Ellis, P. Ragogna and C. Macdonald, *Inorg. Chem.*, 2004, **43**, 7857-7867.

27. A. Cowley and R. Kemp, *Chem. Rev.*, 1985, **85**, 367-382.

28. J. Harrison, R. Liedtke and J. Liebman, *J. Am. Chem. Soc.*, 1979, **101**, 7162-7168.

29. A. Cowley, M. Cushner and J. Szobota, *J. Am. Chem. Soc.*, 1978, **100**, 7784-7786.

30. A. Cowley and R. Kemp, *Chem. Rev.*, 1985, **85**, 367-382.

31. N. Hardman, M. Abrams, M. Pribisko, T. Gilbert, R. Martin, G. Kubas and R. Baker, *Angew. Chem. Int. Ed.*, 2004, **43**, 1955-1958.

32. K. Dimroth and P. Hoffmann, *Angew. Chem. Int. Ed. Engl.*, 1964, **3**, 384-384.

33. S. Fleming, M. Lupton and K. Jekot, *Inorg. Chem.*, 1972, **11**, 2534-2540.

34. B. Maryanoff and R. Hutchins, *J. Org. Chem.*, 1972, **37**, 3475-3480.

35. a) R. Kopp, A. Bond and R. Parry, *Inorg. Chem.*, 1976, **15**, 3042-3046. b) C. Schultz and R. Parry, *Inorg. Chem.*, 1976, **15**, 3046-3050.

36. A. Cowley, M. Lattman and J. Wilburn, *Inorg. Chem.*, 1981, **20**, 2916-2919.

37. R. Reed, Z. Xie and C. Reed, *Organometallics*, 1995, **14**, 5002-5004.

38. A. Cowley, M. Cushner, M. Lattman, M. McKee, J. Szobota and J. Wilburn, *Pure Appl. Chem.*, 1980, **52**, 789-797.

39. D. Schmid, S. Loscher, D. Gudat, D. Bubrin, I. Hartenbach, T. Schleid, Z. Benkő and L. Nyulászi, *Chem. Commun.*, 2009, 830-832.

40. M. MacLennan and K. Darvesh, *Can. J. Chem.*, 1995, **73**, 544-549.

41. G. Reeske, C. Hoberg, N. Hill and A. Cowley, *J. Am. Chem. Soc.*, 2006, **128**, 2800-2801.

42. A. Cowley and S. Mehrotra, *J. Am. Chem. Soc.*, 1983, **105**, 2074-2075.

43. S. Baxter, R. Collins, A. Cowley and S. Sena, *Inorg. Chem.*, 1983, **22**, 3475-3479.

44. D. Gudat, *Coord. Chem. Rev.*, 1997, **163**, 71-106.

45. N. Burford, P. Losier, P. Bakshi and T. Cameron, *J. Chem. Soc., Dalton Trans.*, 1993, 201-202.

46. C. Caputo, J. Price, M. Jennings, R. McDonald and N. Jones, *Dalton Trans.*, 2008, 3461.

47. E. Clark, A. Borys and K. Pearce, *Dalton Trans.*, 2016, **45**, 16125-16129.

48. N. Burford, P. Losier, C. Macdonald, V. Kyrimis, P. Bakshi and T. Cameron, *Inorg. Chem.*, 1994, **33**, 1434-1439.

49. Y. Balitzky, S. Pipko, A. Sinitsa, A. Chernega, Y. Gololobov and A. Nesmeyanov, *Phosphorus, Sulfur, and Silicon and the Related Elements*, 1993, **75**, 167-170.

50. S. Baxter, A. Cowley and S. Mehrotra, *J. Am. Chem. Soc.*, 1981, **103**, 5572-5573.

51. A. Schmidpeter, S. Lochschmidt and W. Sheldrick, *Angew. Chem. Int. Ed. Engl.*, 1985, **24**, 226-227.

52. N. Kuhn, J. Fahl, D. Bläser and R. Boese, *Z. Anorg. Allg. Chem.*, 1999, **625**, 729-734.

53. D. Mendoza-Espinosa, B. Donnadieu and G. Bertrand, *J. Am. Chem. Soc.*, 2010, **132**, 7264-7265.

54. F. Carré, C. Chuit, R. Corriu, A. Mehdi and C. Reyé, *J. Organomet. Chem.*, 1997, **529**, 59-68.

55. F. Henne, A. Dickschat, F. Hennersdorf, K. Feldmann and J. Weigand, *Inorg. Chem.*, 2015, **54**, 6849-6861.

56. S. Volodarsky and R. Dobrovetsky, *Chem. Comm.*, 2018, **54**, 6931-6934.

57. T. Robinson, S. Lo, D. De Rosa, S. Aldridge and J. Goicoechea, *Chem. - Eur. J.*, 2016, **22**, 15712-15724.

58. N. Burford and P. Ragogna, *J. Chem. Soc., Dalton Trans.*, 2002, 4307-4315.

59. N. Burford, P. Losier, A. Phillips, P. Ragogna and T. Cameron, *Inorg. Chem.*, 2003, **42**, 1087-1091.

60. G. van Koten, J. Jastrzebski, J. Noltes, A. Spek and J. Schoone, *J. Organomet. Chem.*, 1978, **148**, 233-245.

61. J. Jastrzebski and G. Van Koten, *Adv. Organomet. Chem.*, 1993, 241-294.

62. A. Arduengo, C. Stewart, F. Davidson, D. Dixon, J. Becker, S. Culley and M. Mizen, *J. Am. Chem. Soc.*, 1987, **109**, 627-647.

63. a) A. Arduengo, D. Dixon and C. Stewart, *Phosphorus and Sulfur and the Related Elements*, 1987, **30**, 341-344. b) A. Arduengo, H. Rasika Dias and J. Calabrese, *Phosphorus, Sulfur, and Silicon and the Related Elements*, 1994, **87**, 1-10.

64. N. Dunn, M. Ha and A. Radosevich, *J. Am. Chem. Soc.*, 2012, **134**, 11330-11333.

65. S. McCarthy, Y. Lin, D. Devarajan, J. Chang, H. Yennawar, R. Rioux, D. Ess and A. Radosevich, *J. Am. Chem. Soc.*, 2014, **136**, 4640-4650.

66. W. Zhao, S. McCarthy, T. Lai, H. Yennawar and A. Radosevich, *J. Am. Chem. Soc.*, 2014, **136**, 17634-17644.

67. J. Cui, Y. Li, R. Ganguly, A. Inthirarajah, H. Hirao and R. Kinjo, *J. Am. Chem. Soc.*, 2014, **136**, 16764-16767.

68. T. Robinson, D. De Rosa, S. Aldridge and J. Goicoechea, *Angew. Chem. Int. Ed.*, 2015, **54**, 13758-13763.

69. J. van der Vlugt, *Chem. Soc. Rev.*, 2010, **39**, 2302–2322.

70. W. Piers, *Organometallics*, 2011, **30**, 13-16.

71. M. Hopkinson, C. Richter, M. Schedler and F. Glorius, *Nature*, 2014, **510**, 485-496.

72. M. Jahnke and F. Hahn, *N-Heterocyclic Carbenes: From Laboratory Curiosities to Efficient Synthetic Tools, 2nd Edition*, 2017, 1-45.

73. D. Bourissou, O. Guerret, F. Gabbaï and G. Bertrand, *Chem. Rev.*, 2000, **100**, 39-92.

74. C. Boehme and G. Frenking, *J. Am. Chem. Soc.*, 1996, **118**, 2039-2046.

75. J. Weigand, K. Feldmann and F. Henne, *J. Am. Chem. Soc.*, 2010, **132**, 16321-16323.

76. I. Abdellah, C. Lepetit, Y. Canac, C. Duhayon and R. Chauvin, *Chem. - Eur. J.*, 2010, **16**, 13095-13108.

77. a) S. Gaillard and J. Renaud, *Dalton Trans.*, 2013, **42**, 7255. b) C. Maaliki, C. Lepetit, Y. Canac, C. Bijani, C. Duhayon and R. Chauvin, *Chem. - Eur. J.*, 2012, **18**, 7705-7714. c) K. Schwedtmann, M. Holthausen, K. Feldmann and J. Weigand, *Angew. Chem. Int. Ed.*, 2013, **52**, 14204-14208.

78. K. Schwedtmann, M. Holthausen, K. Feldmann and J. Weigand, *Angew. Chem. Int. Ed.*, 2013, **52**, 14204-14208.

79. H. Cheng, C. Lin and S. Chu, *J. Phys. Chem. A*, 2007, **111**, 6890-6893.

80. C. Lepetit, V. Maraval, Y. Canac and R. Chauvin, *Coordi. Chem. Rev.*, 2016, **308**, 59-75.

81. a) Y. Wang, Y. Xie, M. Abraham, R. Gilliard, P. Wei, H. Schaefer, P. Schleyer and G. Robinson, *Organometallics*, 2010, **29**, 4778-4780. b) Y. Canac, C. Maaliki, I. Abdellah and R. Chauvin, *New J. Chem.*, 2012, **36**, 17-27.

82. J. Weigand, K. Feldmann and F. Henne, *J. Am. Chem. Soc.*, 2010, **132**, 16321-16323.

83. N. Burford, T. Cameron, P. Ragogna, E. Ocando-Mavarez, M. Gee, R. McDonald and R. Wasylishen, *J. Am. Chem. Soc.*, 2001, **123**, 7947-7948.

84. B. Ellis, C. Dyker, A. Decken and C. Macdonald, *Chem. Comm.*, 2005, 1965–1967.

85. G. Bouhadir, R. Reed, R. Réau and G. Bertrand, *Heteroat. Chem.*, 1995, **6**, 371-375.

86. a) M. Fèvre, P. Coupillaud, K. Miqueu, J. Sotiropoulos, J. Vignolle and D. Taton, *J. Org. Chem.*, 2012, **77**, 10135-10144. b) T. Olszewski and D. Jaskólska, *Heteroat. Chem.*, 2012, **23**, 605-609.

87. M. Silva Valverde, E. Theuergarten, T. Bannenberg, M. Freytag, P. Jones and M. Tamm, *Dalton Trans.*, 2015, **44**, 9400-9408.

Chapter Two

Optimising Ligand (NHC) Syntheses

"The triumph can't be had without the struggle"

Wilma Rudolph

2.1 Introduction to NHCs

The existence of carbenic carbon centres was first hypothesised back in 1835 by Duman and Pelgot, who considered the existence of the simplest carbene carbon known: methylene, CH_2.[1,2] The first (heteroatom-stabilised) carbene carbon to be synthesised was Chugaev's salt, *via* the reaction of tetrachloroplatinate(II) with methylisocyanide and hydrazine in 1915, with the formula $[Pt(C_4H_9N_4)(MeNC)_2]Cl$ and structure represented in *figure 2.1*.[3] However, it was not confirmed to be a heteroatom-stabilised carbene carbon until 1973, when the definitive structure was determined *via* ^{1}H NMR and single-crystal X-ray diffraction.[4,5]
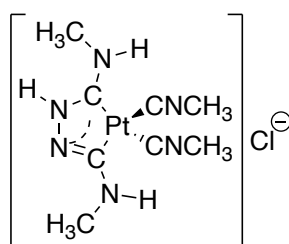
Figure 2.1. Definite structure of $[Pt(C_4H_9N_4)(MeNC)_2]Cl$.

In 1968, Wanzlick and Öfele independently reported the synthesis and characterisation of the first NHC-metal complexes, and discovered that NHCs are excellent ligands for transition metals, which today is one of their many applications.[1,5] However, it was not until 1991 that the first free and isolable NHC was successfully synthesised by Arduengo and co-workers *via* the deprotonation of the corresponding imidazolium salt (NHC precursor) affording 1,3-bis-1-adamantyl-imidazol-2-ylidene (IAd, *figure 2.2*) which was stable under an inert atmosphere.[1,6,7]
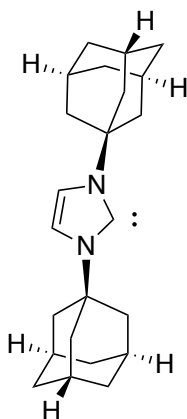
Figure 2.2. Structure of IAd.

After these discoveries, the field expanded exponentially and is ever growing, leading to the synthesis of an enormous array of novel NHCs to understand more about their chemistry and their potential applications.

2.2 Results and discussion

2.2.1 Synthesis of formamidine precursors

Two formamidine precursors were synthesised, the first was *N,N'*-bis(2-methoxyphenyl)formamidine, **1a**, which is a known compound and was prepared *via* a solvent-free one-step reaction of 2-methoxyaniline, triethyl orthoformate, and catalytic acetic acid (*scheme 2.1a*).[8] The second was the lithiated version of **1a** *N,N'*-bis(2-methoxyphenyl)lithiumformamidine, **1b,** and was prepared *via* metalation of **1a** with ^{n}BuLi to give a pale-yellow solid in good yield (*scheme 2.1b*).
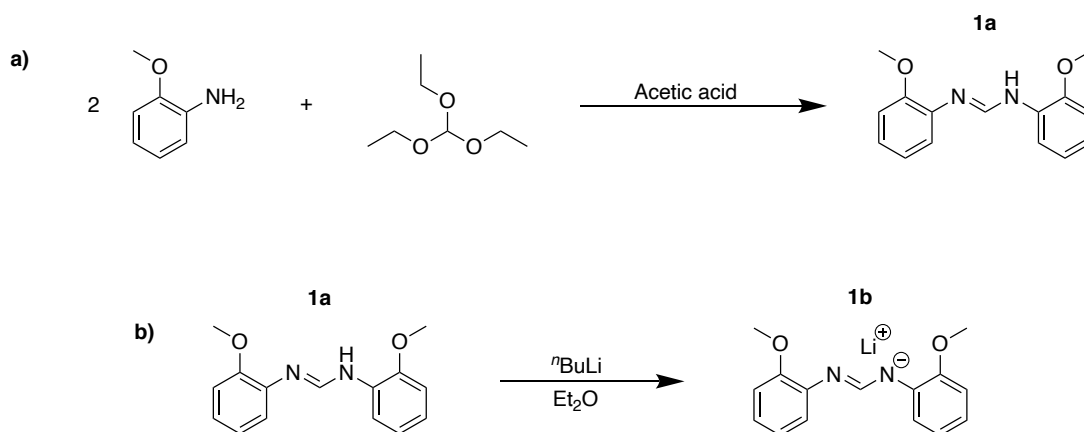
Scheme 2.1. Synthesis of: a) **1a** *via* a solvent-free one-step reaction; b) **1b** *via* metalation of **1a**.

2.2.2 Syntheses of 1,3-bis(2-methoxyphenyl)-4,5-dimethylimidazolium salts (NHC precursor)

2.2.2.1 Synthesis of 1,3-bis(2-methoxyphenyl)-4,5-dimethylimidazolium chloride, 2a

2.2.2.1.1 Initial large scale efforts

The imidazolium precursor targeted, 1,3-bis(2-methoxyphenyl)-4,5-dimethylimidazolium chloride, **2a**, was first synthesised in an impure state in an undergraduate project. It was prepared *via* amine alkylation followed by dehydration by a modified preparation by Glorius.[8] The treatment of **1a** with 3-chlorobutan-2-one and *N,N*-diisopropylethylamine in acetonitrile under an inert

atmosphere and heating at 110 °C, gave the hemi-aminal intermediate (*scheme 2.2*). Following removal of the solvent, the residue was suspended in toluene and TMSCl and a minuscule quantity of HCl(aq), were added, and the reaction mixture was heated at 90 °C to trigger the dehydration of the hemi-aminal intermediate and form **2a** (*scheme 2.2*). After work-up, the reaction yielded a brown sticky solid which was identified as impure **2a** by ^{1}H NMR.
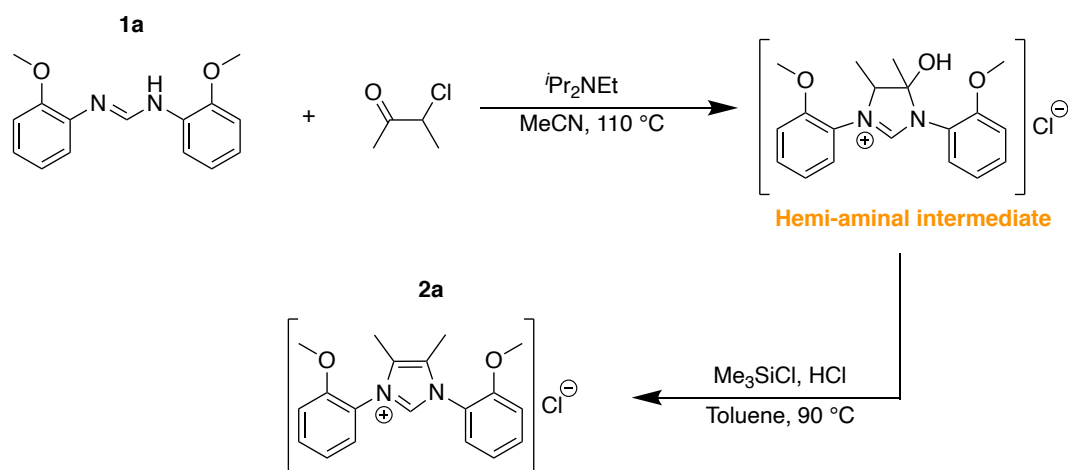
Scheme 2.2. Synthesis of **2a** from **1a**, *via* a two-pot two-step synthesis.

Following this, it was questioned why the reaction needed the addition of HCl, and speculated that just the addition of TMSCl should suffice. It was expected that silylation of the alcohol group would activate the oxygen as a leaving group (E2 mechanism, *scheme 2.3*) affording **2a**.
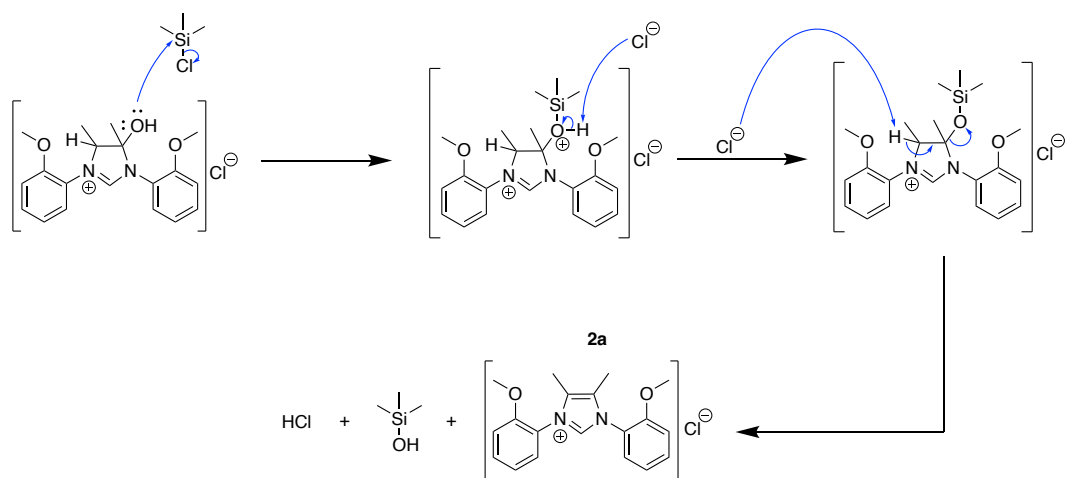
Scheme 2.3. Proposed mechanism for the dehydration of the hemi-aminal intermediate *via* TMSCl, affording the NHC precursor, **2a**.

Subsequently, the same preparation was repeated without the addition of HCl(aq) but unfortunately also yielded impure **2a** and after many purification attempts was still impure.

Exploring the synthesis was slow as formation of the hemi-aminal intermediate under literature conditions required long reaction times. Therefore, the synthesis of **2a** *via* the reaction of **1b**, formed by deprotonation of **1a** with ^{n}BuLi, with 3-chlorobutan-2-one in THF was attempted (*scheme 2.4*). It was expected that using **1b** as a stronger nucleophile would speed up the reaction. After one hour, *in situ* ^{1}H NMR data confirmed that virtually all the 3-chlorobutan-2-one had been consumed and it was therefore likely that the intermediate had been formed. The solution was further heated to see if spontaneous dehydration of the backbone would occur, but this was not observed after 12 hours reflux (dehydration condition A, *scheme 2.4*). TMSCl was therefore added and the resulting solution was heated in the hope of silylating the backbone and promoting dehydration (dehydration condition B, *scheme 2.4*). However, work-up afforded a dark brown solid which was identified as *N*-(2-methoxyphenyl)formamide by ^{1}H NMR, indicating decomposition of **1b**.
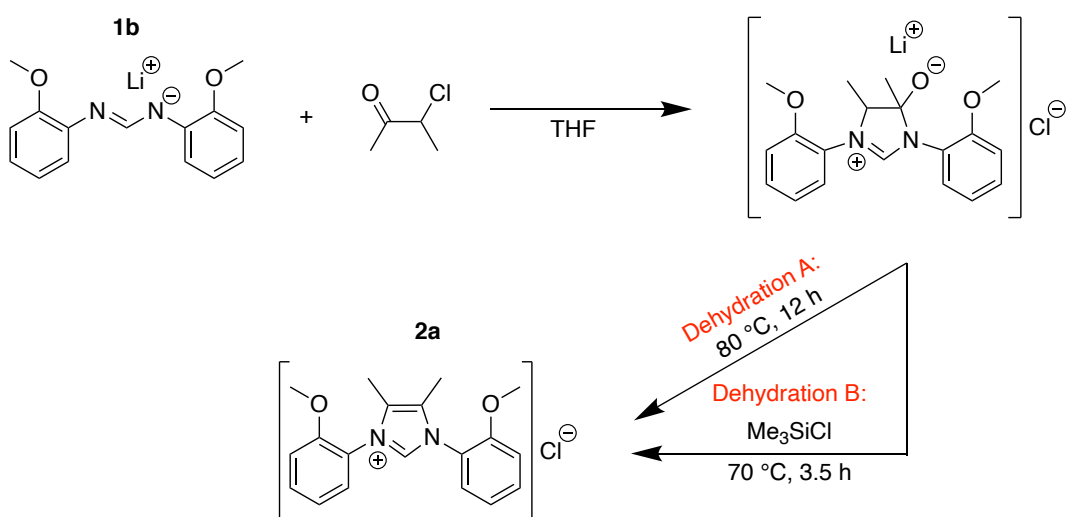
Scheme 2.4. Proposed reaction scheme for the synthesis of **2a** from **1b**.

As all initial bulk syntheses were shown to be unsuccessful, multiple NMR-scale reactions were carried out to gain an understanding of what was happening. Although the reactions above were heated at higher temperatures, all subsequent reactions were heated at 80 °C for both steps, unless otherwise specified, as no

difference was observed from heating at increased temperature as reported by Glorius.[8]

2.2.2.1.2 Preliminarily NMR-scale reactions

Multiple NMR-scale reactions were carried out and monitored *via in situ* ^{1}H NMR. The general procedure was the treatment of **1a** with 3-chlorobutan-2-one, *N,N*-diisopropylethylamine, and additive (*vide infra*) in MeCN and subsequent heating until full consumption of **1a** (step one). The conversion was monitored by ^{1}H NMR, whereby the methoxy singlet at approximately 3.8 ppm, disappeared while two methoxy singlets due to the unsymmetrical hemi-aminal intermediate grew, indicating the formation of the hemi-aminal intermediate, depicted in *figure 2.3*.
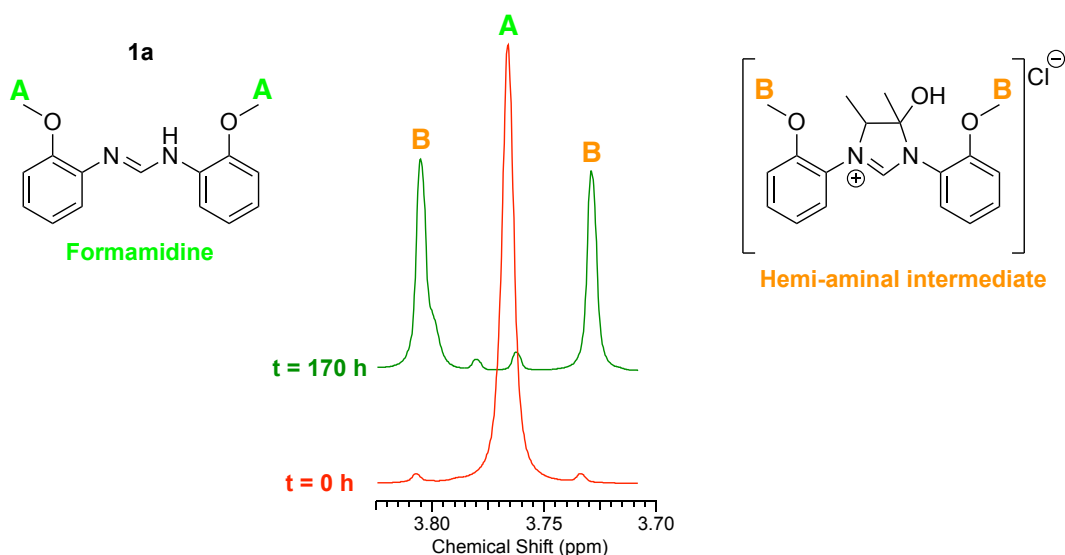
Figure 2.3. Full conversion of **1a** into the hemi-aminal intermediate, represented by ^{1}H NMR spectra.

After this, subsequent steps were varied. Initially, the previously tried method was repeated: **1a** with 3-chlorobutan-2-one and *N,N*-diisopropylethylamine in acetonitrile, after which the solvent was removed under reduced pressure followed by the addition of TMSCl, and toluene, and subsequent heating. An *in situ* ^{1}H NMR spectrum implied the possible formation of **2a**, but this was not conclusive as toluene and MeCN peaks obscured several diagnostic signals. The solution was therefore worked-up and was shown to be impure **2a** by ^{1}H NMR (*figure 2.4*) with incomplete conversion.
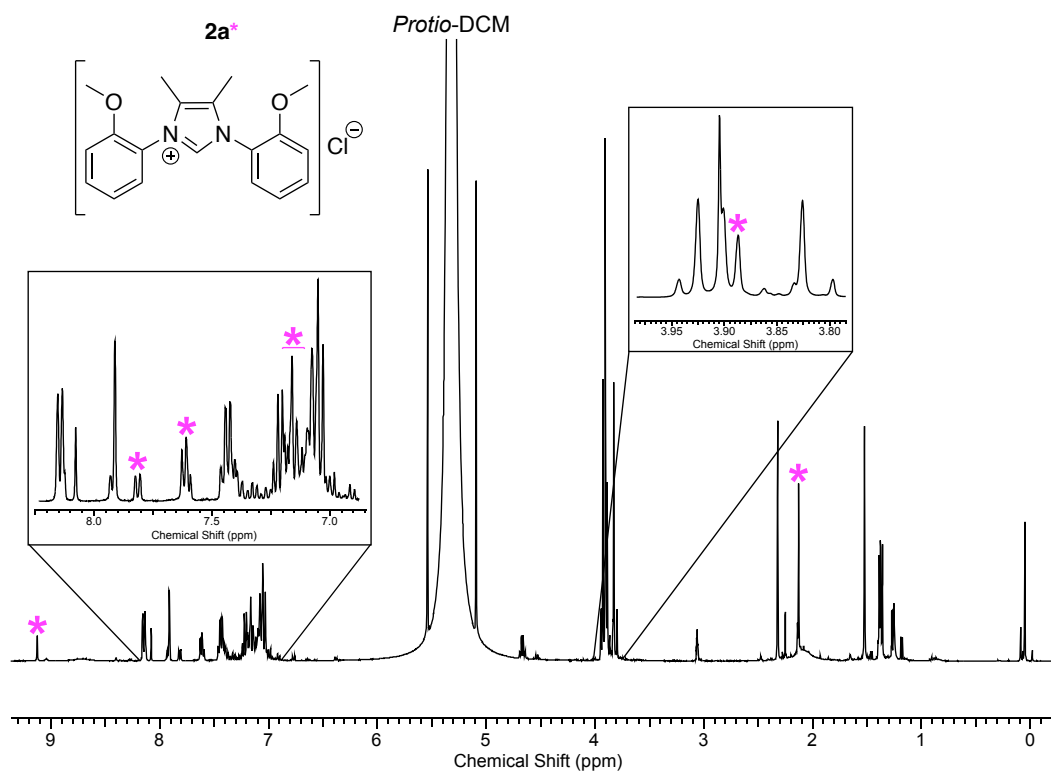
Figure 2.4. ^{1}H NMR spectrum suggesting impure **2a**.

In view of this result, it was hypothesised that a one-pot one-step synthesis might proceed more efficiently. Such synthesis was proposed, since during the reaction the aryl region of the ^{1}H NMR data could still be monitored in MeCN, unlike in toluene, and as the addition of the dehydrating agent TMSCl in the beginning may limit/halt side reactions, affording cleaner **2a**. Thus, the general procedure (**1a** with 3-chlorobutan-2-one and *N,N*-diisopropylethylamine in acetonitrile) was performed with the addition of TMSCl. After 111 hours, *in situ* ^{1}H NMR data suggested full consumption of **1a** and indicated the generation of a mixture of products including the hemi-aminal intermediate, silylated intermediate, and **2a**, depicted in *figure 2.5*.
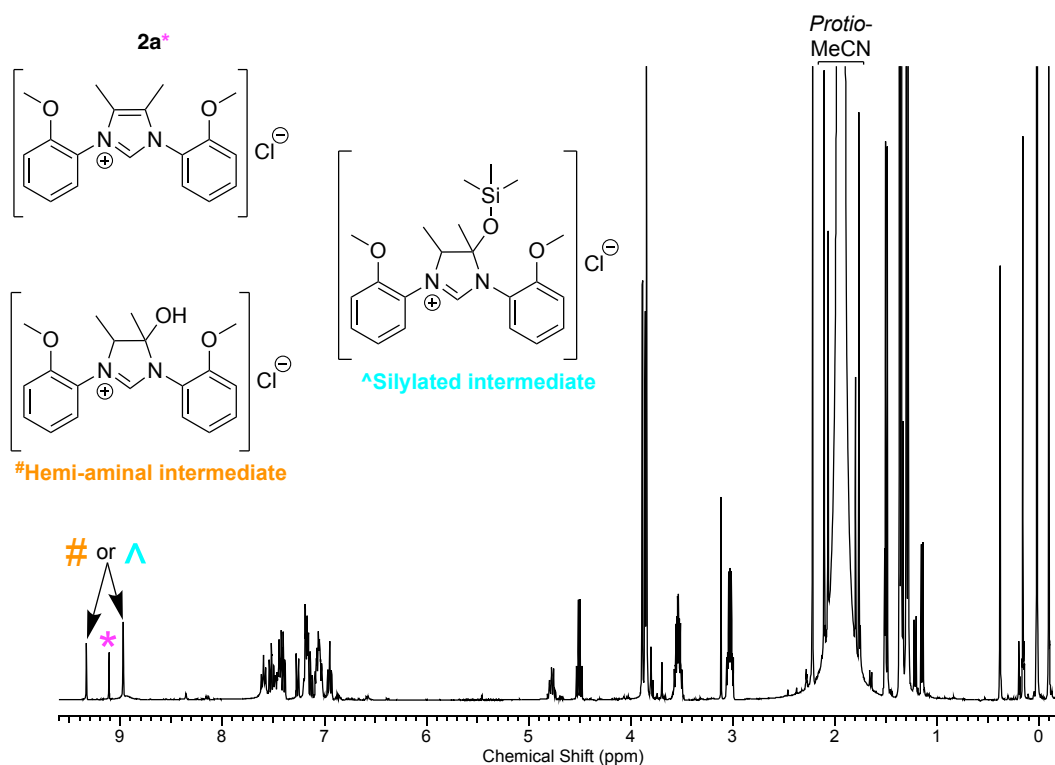
Figure 2.5. *In situ* ^{1}H NMR spectrum suggesting a mixture of intermediates along with **2a**.

The solution was further heated to try and drive the reaction through to completion (full dehydration), but the *in situ* ^{1}H NMR spectra were ambiguous. The reaction was worked-up and the product was confirmed as impure **2a** by ^{1}H NMR with a 7 to 3 ratio of **2a** to unconverted intermediate by integration of signals for methyl groups on the backbone.

Due to the slowness of the first step (mechanism illustrated in *scheme 2.5*), KI was added to subsequent reactions as an additive to decrease the reaction time by inducing a Finkelstein reaction.[9] Since iodide is a better leaving group than chloride, this was expected to speed up the reaction time, albeit producing a mixture of the imidazolium iodide and chloride.
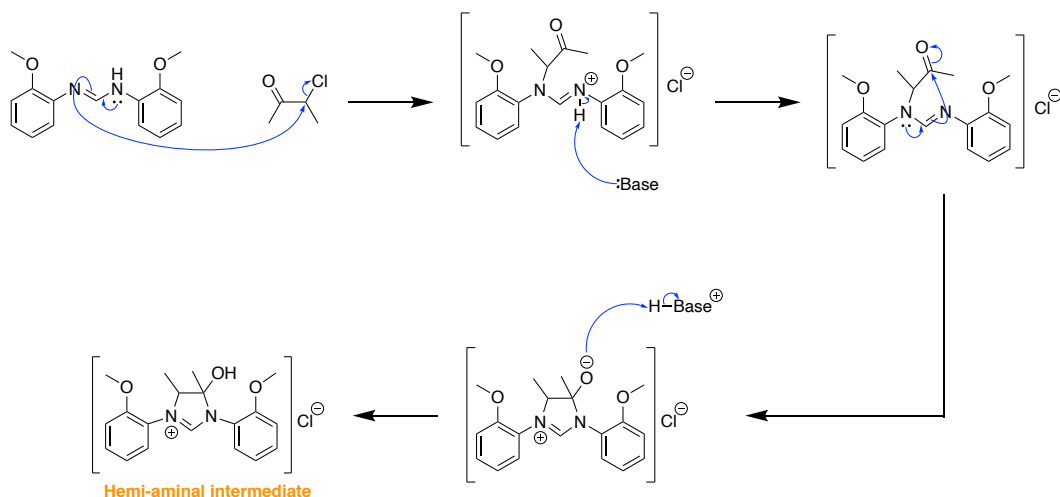
Scheme 2.5. Proposed mechanism for the formation of the intermediate by treatment of **1a** with 3-chlorobutan-2-one.

Given the unsuccessful one-pot synthesis, further test reactions were carried out in which the hemi-aminal intermediate was formed *in situ* and then a dehydrating agent was added. This would be expected to lead to fewer side reactions due to only having one species present (the hemi-aminal intermediate) rather than many (e.g. **1a**, the hemi-aminal intermediate, silylated intermediate, and **2a**). Unfortunately, this was unsuccessful and the ^{1}H NMR data suggested that the oxygen on the backbone had been silylated (O-SiMe$_3$) with changes in the chemical shifts of the signals corresponding to the inequivalent methyls on the backbone upon addition of TMSCl (*figure 2.6*). Only a small quantity of **2a** was generated, as suggested by the singlet at approximately 8.6 ppm (*figure 2.6*). Thus, it was concluded that TMSCl was not a suitable reagent for the dehydration of the hemi-aminal intermediate.
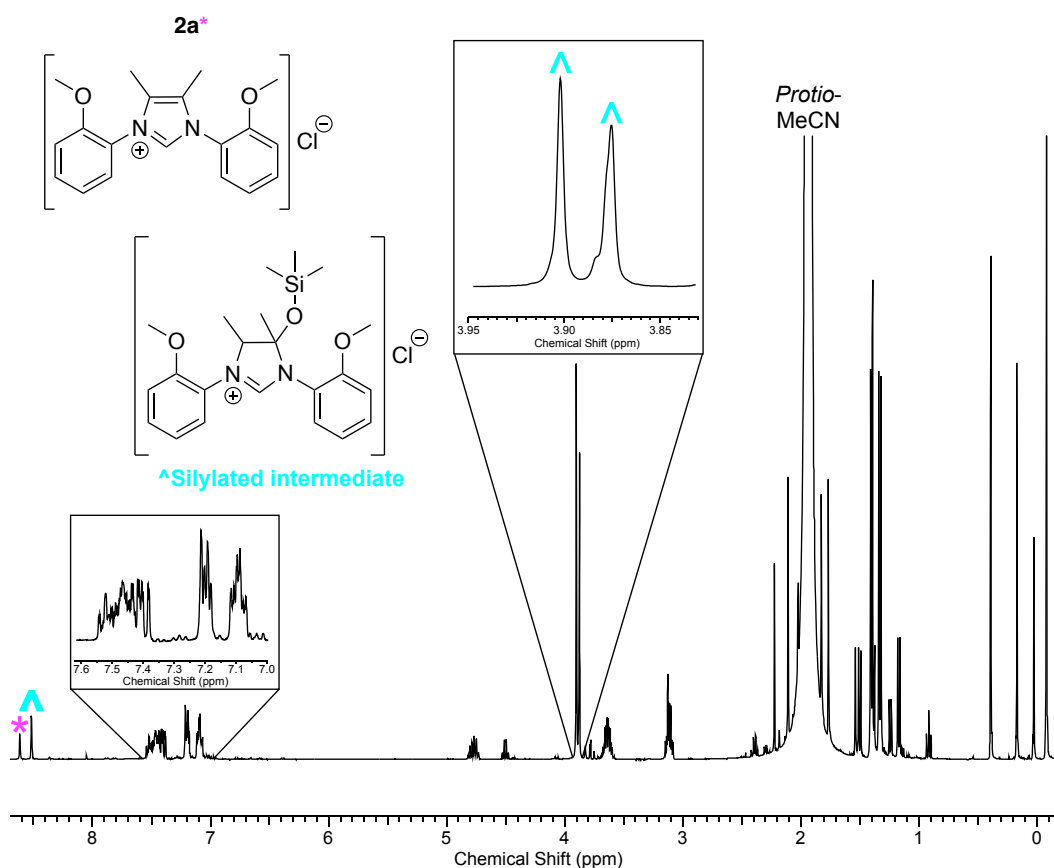
Figure 2.6. ^{1}H NMR spectrum displaying silylation of the intermediate and the generation of a small quantity of **2a**.

Given that utilising TMSCl did not proceed as expected, two similar preparations to the literature method[8] were attempted. Step one proceeded as before (reaction of **1a** with 3-chlorobutan-2-one and *N,N*-diisopropylethylamine in acetonitrile), after that two different dehydration conditions were attempted in parallel. The first was the removal of the solvent, followed by the suspension of the residue in toluene and Ac_2O (two-pot two-step synthesis) and the second was the addition of Ac_2O and HCl(aq) to the resulting solution (one-pot two-step synthesis). Nevertheless, the attempted dehydration *via* a one-pot two-step synthesis, was shown to be ineffective by ^{1}H NMR. Therefore, no work-ups were carried out on either of the attempts.

At this point, it was wondered why the Glorius route uses the addition of both HCl(aq) and Ac_2O. Therefore, it was speculated that the addition of HCl(aq) alone should be enough to dehydrate the intermediate. Specifically, protonating the OH

43

group on the backbone would form water as a leaving group, and permit overall elimination and dehydration, illustrated in *scheme 2.6*.
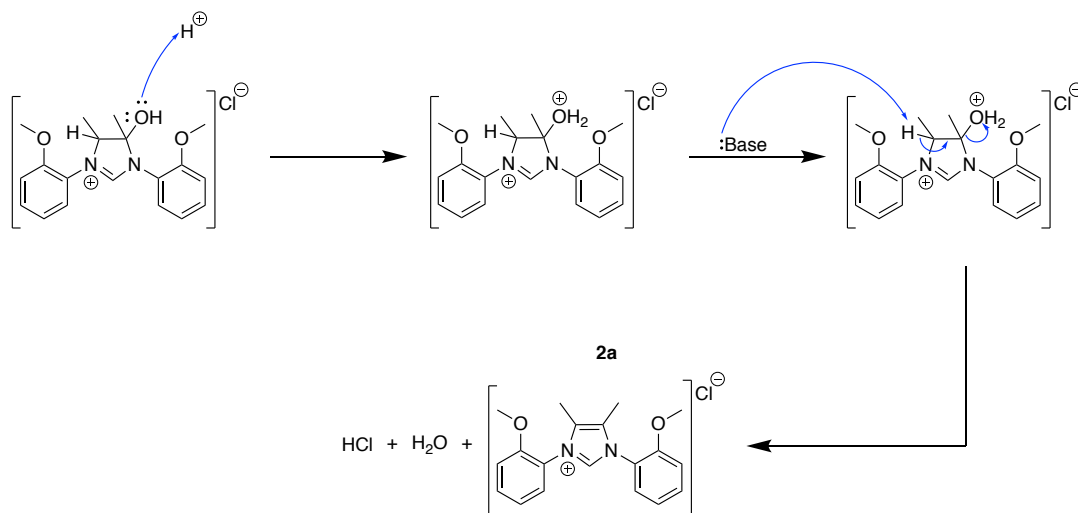
Scheme 2.6. Proposed mechanism for the dehydration of the hemi-aminal intermediate *via* HCl(aq), affording the NHC precursor, **2a**.

The hypothesis was tested in a one-pot, two-step synthesis involving the addition of HCl(aq) after complete consumption of **1a.** This led to the clean formation of **2a**, indicating that HCl(aq) is more than sufficient to carry out this transformation. This was amenable to scale-up, giving a good yield of pure **2a** (49 %) after work-up, albeit requiring extremely long reaction times to form the intermediate (110 hours). Poor quality crystals of **2a** suitable for single-crystal X-ray diffraction were grown by the slow evaporation of DCM. Compound **2a** crystallises in the space group P-1 with a molecule of **2a** and two molecules of water in the asymmetric unit, with the anisole rings of the NHC adopting an anti-configuration, depicted in *figure 2.7*. Although the quality of the data is sufficient to unambiguously assign atom connectivity and spatial orientation, it is insufficient for discussion of specific bond distances and angles.
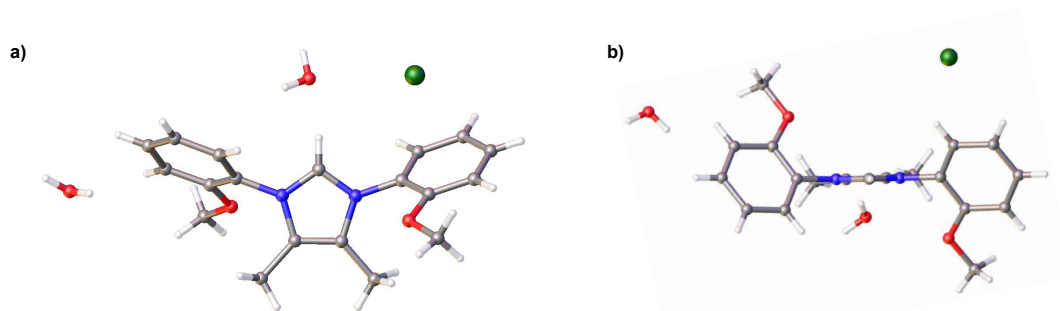
Figure 2.7. Crystal structure of **2a**: a) Top-down view; b) View down imidazolium C-H axis.

As the imidazolium chloride, **2a**, proved very hard to dry and trace quantities of water interfered with subsequent reactions, other anions were investigated in the hope that they could be dried.

2.2.2.2 Synthesis of 1,3-bis(2-methoxyphenyl)-4,5-dimethylimidazolium iodide, 2b

1,3-bis(2-methoxyphenyl)-4,5-dimethylimidazolium iodide, **2b**, was targeted in the hope that addition of KI as a nucleophilic catalyst would reduce reaction times. Additive potassium iodide reduced the first step reaction time from 110 hours (without the additive) to 2 hours. Subsequent dehydration and work-up gave clean isolation of **2b** in 49 % yield.

2.2.2.3 Synthesis of 1,3-bis(2-methoxyphenyl)-4,5-dimethylimidazolium tetrafluoroborate, 2c

1,3-Bis(2-methoxyphenyl)-4,5-dimethylimidazolium tetrafluoroborate, **2c**, was prepared cleanly *via* anion metathesis of **2a** with $NaBF_4$ in water.

Additionally, anion metathesis of **2b** into **2c** was attempted by a modified preparation of halogen exchange by Cisnetti.[10] Firstly, a solution of $NaBF_4$ in water was added dropwise to a solution of **2b** in acetone. No precipitate formed initially but upon adding additional water, a dark precipitate appeared. However, this was identified as **2b** by ^1H NMR, and the absence of signals in the ^{11}B and ^{19}F NMR spectra. Reversing the order of addition gave the same result of recovered starting material and so no further attempts were made.

2.2.3 Synthesis of 1,3-bis(2-methoxyphenyl)-4,5-dimethylimidazol-2-ylidene (free NHC), 3

After successful syntheses of imidazolium salts **2a**, **2b**, and **2c**, it was sought to deprotonate the imidazolium, forming the corresponding free NHC for subsequent coordination to phosphorus. A variety of different bases have been employed to synthesise free NHCs from their corresponding imidazolium precursors, including, NaH/^{t}BuOK or ^{t}BuOH in catalytic amounts, ^{t}BuOK, LiHMDS, KHMDS and others.[10,11]

Initial attempts to deprotonate **2a** with a range of bases failed, with the recovery of the imidazolium chloride, **2a**. It was found that despite the absence of visible H_2O in the ^{1}H NMR spectrum (*figure 2.8*), the isolated **2a** nevertheless contained several equivalents of water, perhaps unsurprising given the water of crystallisation in the crystal structure.
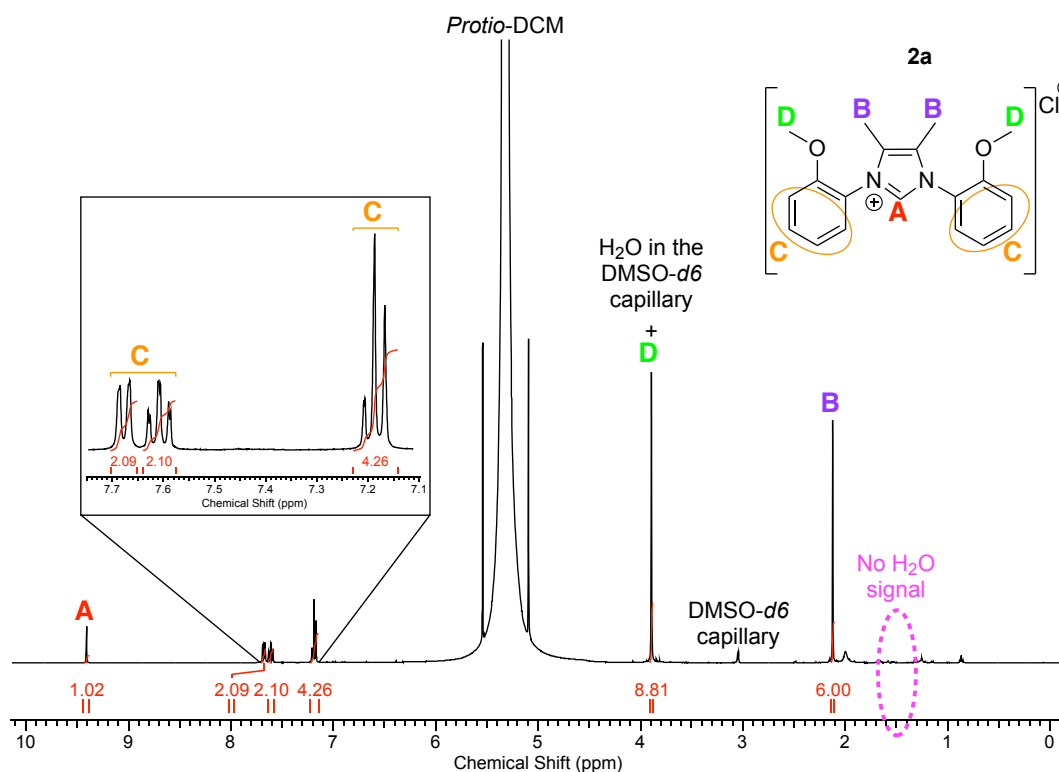
Figure 2.8. ^{1}H NMR spectrum of **2a**, illustrating no water signal.

As no H_2O signal was visible in the ^{1}H NMR spectra of **2a** it must be in either fast exchange and/or hydrogen bonding with the imidazolium C-H. However, since no water signal appeared, the amount of water present could not be quantified and therefore the appropriate amount of base to counteract such reaction could not be

determined. To complicate the problem, extra base could not be added as leftover base would cause problems further down the line when reacting with a phosphorus species. As it had been deduced **2a** was not dry, attempts were made to dry **2a** with TMSCl, but it was not possible to confirm if this had been successful due to the absence of a water signal in the ^{1}H NMR. Thus, the **2a** dried with TMSCl, one equivalent LiHMDS, and THF were combined. Nonetheless, after work-up yielded a yellow tar which was identified as a mixture of **2a** and **3**, by ^{1}H NMR in *protio*-DCM.

Due to all previous attempts being unsuccessful, preliminary NMR-scale reactions were performed. **2a** (dried with TMSCl) and two equivalents of base (such as LiHMDS or ^{t}BuOK) in THF or Et$_2$O were mixed and *in situ* ^{1}H NMR spectra of the preliminary reaction solutions all implied the existence of **3**, by the disappearance of the diagnostic imidazolium C-H resonance. However, small amounts of brown solid were still present in all of the NMR tubes, which was presumed to be unconverted **2a**. To confirm the poor solubility of **2a** in THF and Et$_2$O, further tests were carried out. **2a** was suspended in THF and Et$_2$O and *in situ* ^{1}H NMR data confirmed only trace amounts of **2a** were present in THF, and no traces of **2a** were observed in Et$_2$O. Successively, two equivalents of base (LiHMDS or ^{t}BuOK respectively) were added to each solvent. In each case, the resulting mixtures were a yellow/cream supernatant with brown solid present (still presumed to be **2a**, given the very low solubility in the solvents employed) and *in situ* ^{1}H NMR spectra of both indicated the formation of **3**.

Deprotonation of **2c** which had not previously been dried by special measures was also attempted. **2c** was suspended in THF and *in situ* ^{1}H NMR data indicated that only trace amounts of **2c** were present in solution. Following the addition of one equivalent of LiHMDS, the resulting mixture still had a small amount of brown solid (presumed to be **2c**) present, implying that **2c** was wet. Nevertheless, *in situ* ^{1}H NMR data suggested only **3** was present in solution. By virtue of this observation, **2c** was dried *in vacuo* at 80 °C and deprotonation was attempted with equimolar amounts of LiHMDS in THF. In this case, no solid was observed indicating that **2c**

was completely dry, and *in situ* ¹H NMR data indicated only **3** was present, illustrated in *figure 2.*9, by the absence of the imidazolium signal.
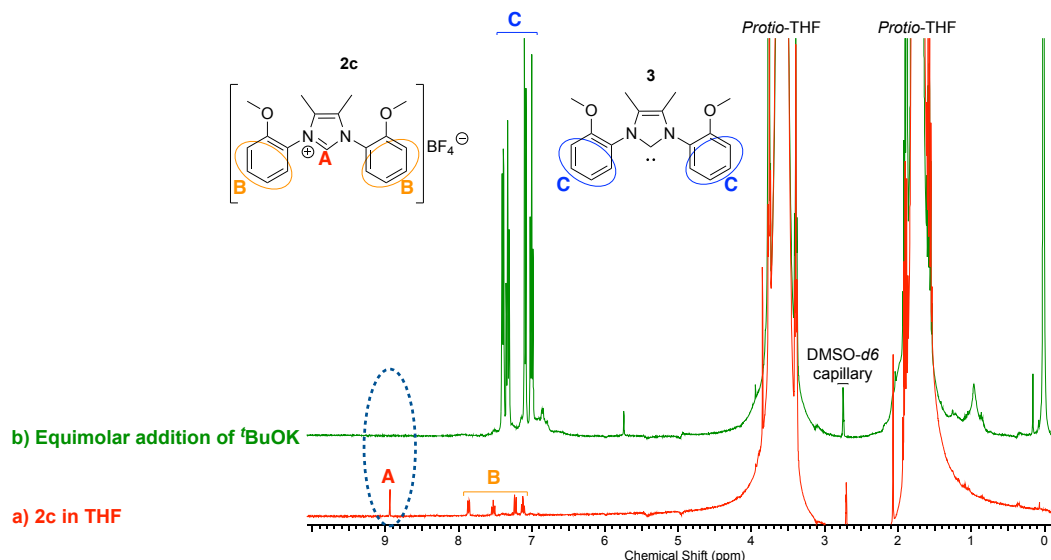
Figure 2.9. ¹H NMR spectra: a) **2c** suspended in THF b) After the equimolar addition of LiHMDS.

As drying in vacuo at 80 °C worked for **2c**, the same procedure was attempted for drying **2a**, as an alternative to drying with TMSCl which proved to be unsuccessful. Initially, **2a** was dried in a vacuum oven at 80 °C for 69 hours in the hope to remove all trace of water. This sample was then stored in air because it was not presumed to be hygroscopic and it was assumed that it just had water trapped inside. Unfortunately, after reacting this with equimolar amounts of LiHMDS, a brown solid (**2a**) was still present confirming that **2a** was not completely dry. Thus, another portion of one equivalent LiHMDS was added, consuming the remaining solid; *in situ* ¹H NMR data confirmed only **3** was present, revealing that the **2a** was at least dryer than formerly. Deprotonation of **2b** (dried *in vacuo*) with one equivalent of LiHMDS in toluene was attempted, but the results were ambiguous.

Thus, it was determined that **3** could be synthesised from either **2a** or **2c**, however **2c** only required equimolar addition of base whereas **2a** needs unquantifiable and unpredictable amounts of base. By virtue of this, it was decided that the most effective method to yield **3** was excess NaH with catalytic *t*BuOH present for the *in situ* production of *tert*-butoxide. This would ensure more than sufficient quantities

of base NaH were present, however, only trace quantities of base ^{t}BuONa were present in solution, subsequently causing no substantial problems further down the line. Hence large-scale preparations of **3** employing this approach from both **2a** and **2c** were attempted. The attempt with **2c**, after work-up, afforded a brown solid which was identified as mostly **3** along with a small amount of **2c** by ^{1}H NMR and it was assumed that water must have contaminated the solution somehow. To minimise this in future syntheses, eight equivalents of NaH were subsequently used. Thus, deprotonation of **2a** with eight equivalents of NaH and catalytic amounts of ^{t}BuOH proceeded successfully and afforded a brown solid which was identified as **3** by ^{1}H NMR in *protio*-THF. Running an ^{1}H NMR of the solid in *protio*-DCM led to broad peaks appearing suggesting that the free carbene reacts with DCM, and hence the first attempts at deprotonation may have worked somewhat.

2.2.4 Syntheses of protected NHCs

Due to the relative instability of free NHC, **3**, on exposure to air and moisture the synthesis of masked NHCs were attempted, as a way of circumventing this limitation.[12]

2.2.4.1 Synthesis of 1,3-bis(2-methoxyphenyl)-4,5-dimethylimidazolium-2-carboxylate, 4a

Among the many masked NHC types known, the CO_2 adducts were identified as particularly interesting targets. Many have been reported as relatively stable to air and moisture and, upon generating the free NHC, the only by-product is CO_2 (a gas) making subsequent purification trivial and production of the NHC entropy driven (thermodynamically favourable). Accordingly, preparations of 1,3-bis(2-methoxyphenyl)-4,5-dimethylimidazolium-2-carboxylate, **4a**, were attempted. All subsequent approaches started off with the synthesis of **3** *in situ* by deprotonation of **2c** with varied amounts of LiHMDS (ranging from 1.1 to 2 equivalents), followed by various carboxylation steps (*scheme 2.7*). However, all efforts proved to be unsuccessful and the isolated solids were all identified as mixtures of **2c** and **4a** by ^{1}H NMR. Initially, sublimate from dry ice was employed as a CO_2 source which, as it was unsuccessful, indicated that the dry ice was wet. Subsequently, carboxylation by introducing CO_2 from a gas cylinder was attempted, but this was also ineffective

and imidazolium was recovered. As the initial attempt at direct carboxylation with CO_2 from a gas cylinder was met with hydrolysis, the reaction was repeated with a drying step and a further 0.4 equivalence of base. CO_2 from a gas cylinder was first passed though molecular sieves before being introduced to the *in situ* generated free NHC, **3**, however this too was unsuccessful at producing clean **4a**. As all attempts demonstrated that above methods were not viable at yielding only **4a**, no further methods were tried.
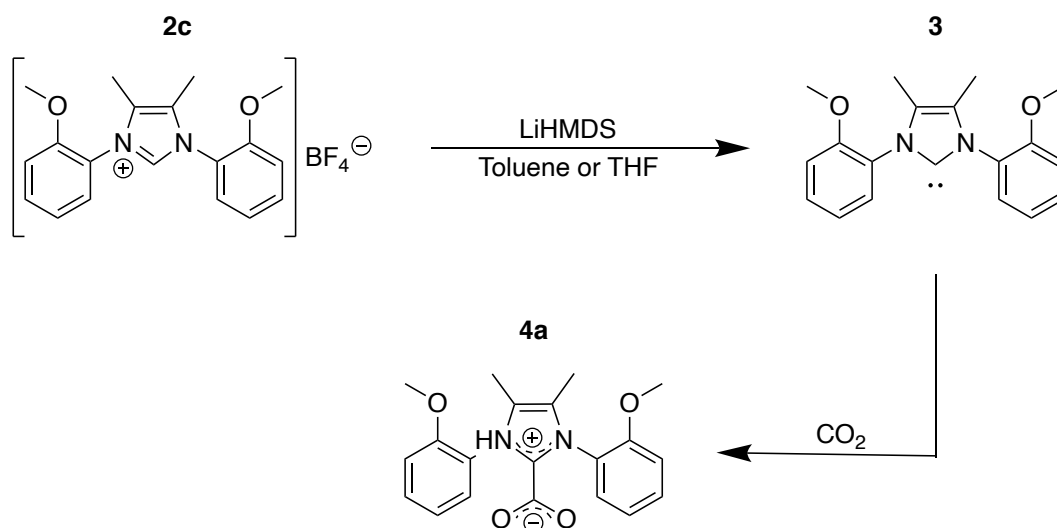
Scheme 2.7. Proposed reaction scheme for the carboxylation of **3**.

2.2.4.2 Synthesis of 1,3-bis(2-methoxyphenyl)-4,5-dimethyl-2-(trimethylsilyl)imidazolium chloride, 4b

All efforts to afford 1,3-bis(2-methoxyphenyl)-4,5-dimethyl-2-(trimethylsilyl)imidazolium chloride, **4b**, by the addition of TMSCl to **3**, either isolated or generated *in situ*, were shown to be unsuccessful (*scheme 2.8*). The *in situ* ^{1}H NMR spectra were either ambiguous or, upon the removal of THF *in vacuo* and addition of *protio*-DCM (as the protected carbene was assumed stable in DCM), confirmed **2a** as the majority product.
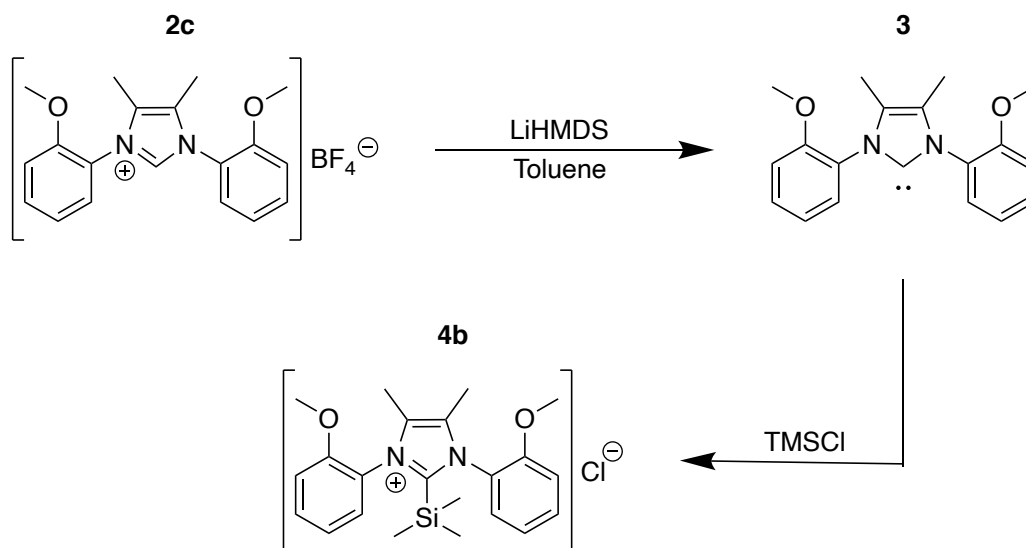
Scheme 2.8. Proposed reaction scheme for the silylation of **3**.

2.2.5 Synthesis of 1,3-bis(2-hydroxyphenyl)-4,5-dimethylimidazolium salt

2.2.5.1 Synthesis of 1,3-bis(2-hydroxyphenyl)-4,5-dimethylimidazolium tetrafluoroborate, 5a

Initial attempts at isolating 1,3-bis(2-hydroxyphenyl)-4,5-dimethylimidazolium tetrafluoroborate **5a** by the addition of 2.1 equivalents BBr_3 to **2c** in DCM were unsuccessful, affording grey tars which were identified as a mixture of mono- and di-demethylated product by ^{1}H NMR. Thus, 4.2 equivalents of BBr_3 and **2c** were mixed in DCM and, after work-up, afforded a grey/brown tar which was identified as **5a** by ^{1}H NMR.

2.2.5.2 Synthesis of 1,3-bis(2-hydroxyphenyl)-4,5-dimethylimidazolium bromide, 5b

With no hypothesis or evidence to suggest that making the BF_4 salt would be beneficial for subsequent reactivity, and given that the product after the first step in the preparation of **5a** should be predominantly 1,3-bis(2-hydroxyphenyl)-4,5-dimethylimidazolium bromide, **5b**, synthesis of the bromide salt itself was attempted. Reaction of **2a** with BBr_3 (4.2 equivalents) in DCM, followed by an altered work-up with NaBr(aq) to drive bromide formation and extraction into DCM, afforded a brown tar identified as **5b** by ^{1}H NMR in good yield (*scheme 2.9*). Upon scaling-up the reaction and carrying out the work-up, it was found that **5b** was not very soluble in DCM or water, leading to a low overall yield. Repeating the

same method but altering the work-up to accommodate the fact that the majority of the **5b** precipitates out upon adding NaBr(aq), afforded a more satisfactory yield.
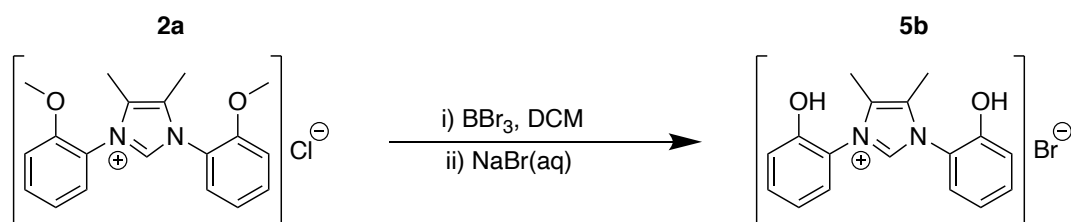
Scheme 2.9. Demethylation of **2a**, *via* the addition of BBr₃.

Crystals suitable for SCXRD analysis were obtained *via* the slow diffusion of hexane into a concentrated solution of DCM. Compound **5b** crystallised in the space group Pbca with one molecule of **5b** in the asymmetric unit, with the phenol rings of the NHC adopting a syn-configuration, depicted in *figure 2.10*. This contrasts with the anisole rings of **2a** which adopt an anti-configuration in the solid state (*figure 2.7*).
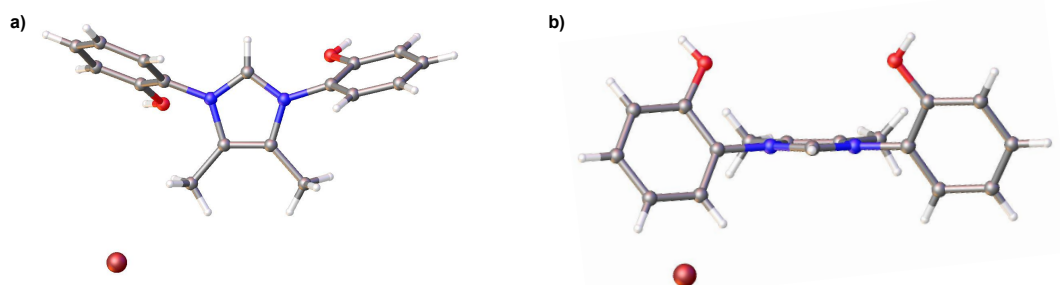
Figure 2.10. Crystal structure of **5b**: a) Top-down view; b) View down imidazolium C-H axis.

2.2.6 Attempted syntheses of potassium/sodium/lithium 2,2'-(4,5-dimethylimidazole-1,3-diyl)diphenolate (depending on the base employed), 6

Synthesis of the potassium/sodium/lithium 2,2'-(4,5-dimethylimidazole-1,3-diyl)diphenolate, **6**, was attempted *via* triple deprotonation of the three acidic protons on **5b** (the imidazolium and OH groups on the phenol rings, illustrated in *scheme 2.10*), in the hope of creating a pincer ligand for subsequent coordination to phosphorus. Initial attempts at isolating **6** from **5b** *via* NaH/ᵗBuOK were inconclusive.
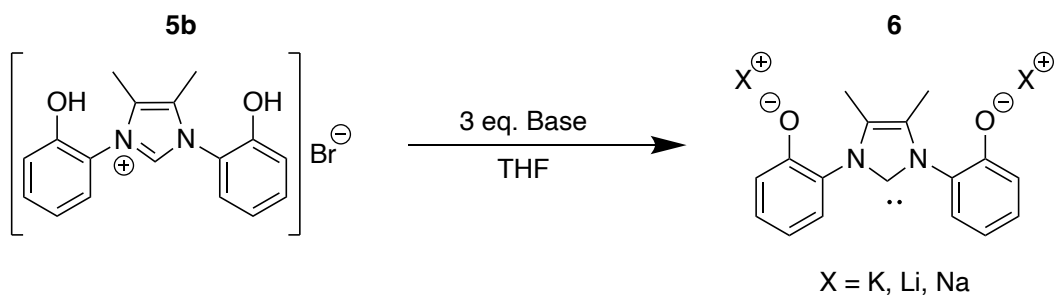
Scheme 2.10. Synthesis of **6** *via* deprotonation of the three acidic protons on **5b**.

Thus, unsure as to what was occurring, a preliminary NMR-scale study was performed. **5b** was suspended in THF and *in situ* ^{1}H NMR data confirmed only trace amounts of **5b** were present in solution, indicating that **5b** is sparingly soluble in THF (*figure 2.11a*). Successively, three equivalents of ^{t}BuOK were added and *in situ* ^{1}H NMR data was thought to suggest the presence of **6** (with potassium counterions) and a small amount of **5b**, but was not conclusive due to the signals being very broad (*figure 2.11b*). Thus, another three equivalents of ^{t}BuOK were added and *in situ* ^{1}H NMR data was believed to indicate the formation of only **6** (*figure 2.11c*) by the appearance of sharper, more resolved peaks.
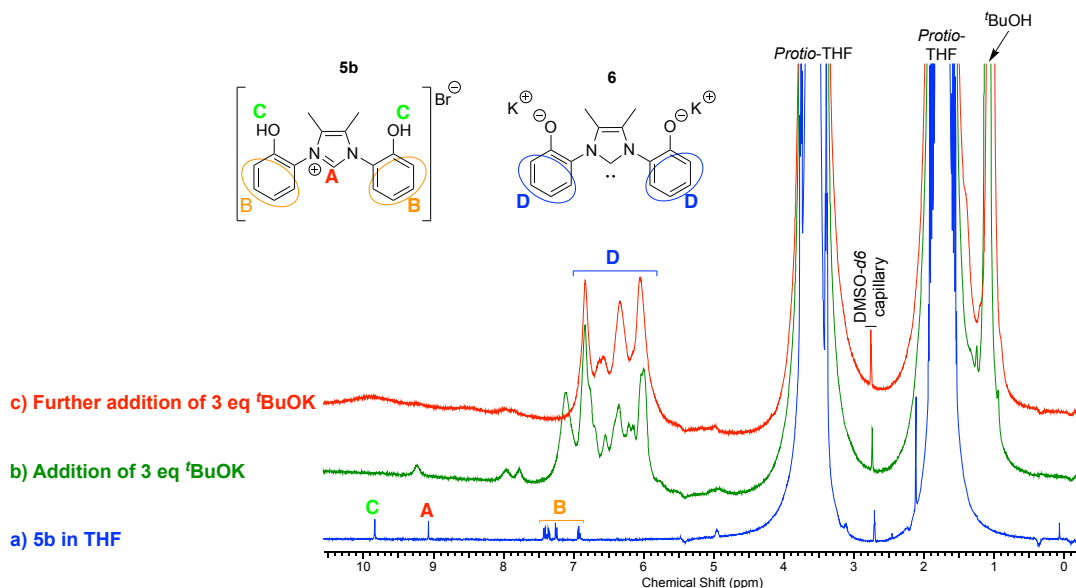
Figure 2.11. ^{1}H NMR spectra: a) **5b** suspended in THF (trace quantities of **5b** present in solution); b) Addition of three equivalents ^{t}BuOK; c) Further addition of three equivalents ^{t}BuOK.

Since adding six equivalents ^{t}BuOK showed promise on a small-scale, preparation was attempted on a larger scale. However, the large-scale reaction yielded a white

solid which did not dissolve in THF, implying that the solid was not **6** and most likely still **5b**. In the hopes that changing the base/metal ions would be successful, a preliminary NMR-scale reaction utilising **5b** and three equivalents of LiHMDS in THF showed promise, with *in situ* ^{1}H NMR data indicating only the presence of **6** (with lithium counterions). Addition of a further three equivalents of LiHMDS led to dissolution of more of the brown solid (**5b**) and increased signal intensity for the putative **6**, as shown by the increased intensity of the aryl peaks in the *in situ* ^{1}H NMR spectra (i.e. more of **5b** was converted into **6**), illustrated in *figure 2.12*.
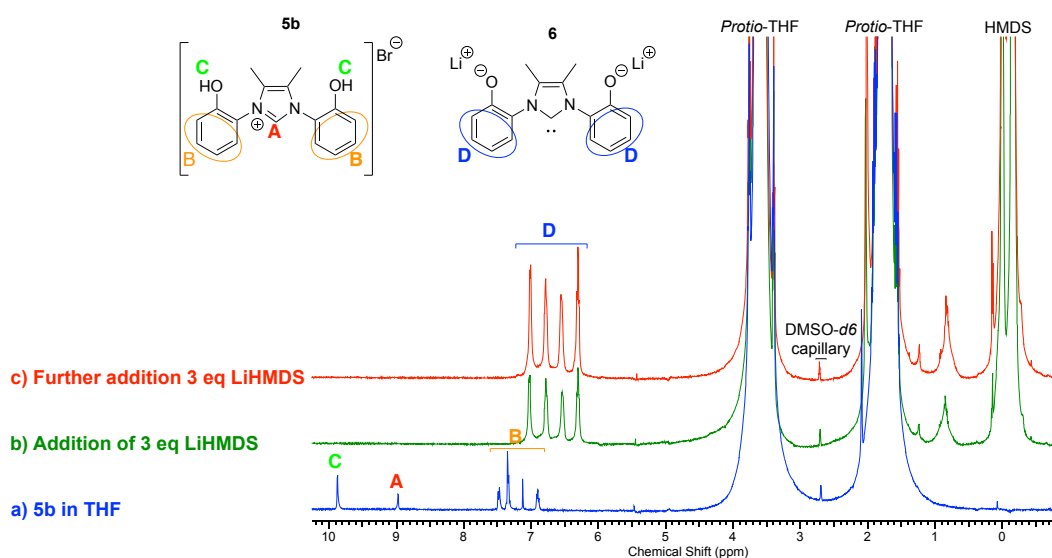
Figure 2.12. ^{1}H NMR spectra: a) **5b** suspended in THF (trace quantities of **5b** present in solution); b) Addition of three equivalents LiHMDS; c) Further addition of three equivalents LiHMDS.

Due to the encouraging results of the small-scale synthesis, a modified large-scale synthesis was attempted. This time 3.1 equivalents of LiHMDS and **5b** in THF were combined and the resulting mixture was worked-up to give a brown solid. The ^{1}H NMR data of the afforded brown solid was ambiguous as the aryl peaks were broad and, as *protio*-THF was used as the NMR solvent, the alkyl signals were obscured and thus the solid may or may not have been **6** (with lithium counterions). It was therefore concluded to be likely that **6** (with lithium counterions) could be generated *in situ*, however, isolation was unsuccessful and henceforth it should be reacted on immediately.

2.3 Conclusion

After many unsuccessful attempts, a practical preparation for the synthesis of **2a** in good yield was developed. The corresponding iodide and tetrafluoroborate salts were also prepared; the iodide salt was accessible *via* the fast-synthetic route (as the additive KI dramatically reduced the first step reaction time, and therefore the overall synthesis time), whilst the tetrafluoroborate salt was easiest to prepare in dry form. The best method for synthesis of the free IAnis^{Me} NHC, **3**, was *via* NaH/^{t}BuOH from the corresponding imidazolium salts, **2a** or **2c**. Demethylation of **2a** or **2c** using BBr$_3$ resulted in another novel NHC precursor, **5**. All attempts at isolating the deprotonated version, **6**, were unsuccessful, but nevertheless it was formed *in situ,* moderately effectively with the base LiHMDS.

2.4 Experimental

2.4.1 Syntheses of formamidines

2.4.1.1 *N,N'*-Bis(2-methoxyphenyl)formamidine, 1a

In air, 2-methoxyaniline (13.6 cm^3, 120 mmol), triethyl orthoformate (10 cm^3, 60 mmol), and acetic acid (4 drops) were combined, and refluxed at 140 °C for 4 h. The resulting mixture was left to cool without stirring, after which the cold saturated mixture was stirred (which sometimes induced nucleation straight away) and hexane (50 cm^3) was added to aid precipitation. The resulting mixture was filtered, and the precipitate was washed with hexane (15 cm^3) to afford a white powder (11.947 g, 46.6 mmol, 78 %). **^{1}H NMR** (400 MHz, DCM, 25.0 °C): δ 8.17 (s, 1H), 7.20 (br, 2H), 7.01 (m, 2H), 6.91 (m, 4H), 3.81 (s, 6H). **^{13}C{^{1}H} NMR** (100.52 MHz, DCM, 25.0 °C): δ 150.32 (N*C*HN), 147.77 (*C* phenyl), 135.11 (*C* phenyl), 123.32 (*C*H phenyl), 121.11 (*C*H phenyl), 118.27 (*C*H phenyl), 111.17 (*C*H phenyl), 55.76 (O*C*H$_3$). NMR data in accordance with the literature.[8]

2.4.1.2 *N,N'*-Bis(2-methoxyphenyl)lithiumformamidine, 1b

1a (1.006 g, 3.9 mmol) was suspended in diethyl ether (10 cm^3) and stirred in an ice bath followed by the dropwise addition of ^{n}BuLi in hexane (2.7 cm^3, 1.6 M, 4.29 mmol), upon which a pale precipitate started to crash out with an orange supernatant. The reaction mixture was left to stir at ambient temperature overnight. The yellow supernatant was transferred *via* a filter cannula, and the

residue was washed with hexane (5 cm^3) and dried *in vacuo*, to give a pale-yellow solid which was identified as predominantly **1b** with a small amount of **1a** present by ^{1}H NMR in a 9 to 1 ratio, respectively by integration of the imidazolium CH signals, and subsequently used without further purification.

2.4.2 Syntheses of 1,3-bis(2-methoxyphenyl)-4,5-dimethylimidazolium salts, 2

2.4.2.1 Synthesis of 1,3-bis(2-methoxyphenyl)-4,5-dimethylimidazolium chloride (IAnis^{Me}.HCl), 2a

All attempts were modified preparations from Glorius' synthesis of 4-methyl-1,3-bis-(2,4,6-trimethylphenyl)-3H-imidazol-1-ium chloride.[8]

2.4.2.1.1 Attempted formation of the intermediate from 1a, 3-chlorobutan-2-one, and *N,N*-diisopropylethylamine in MeCN and subsequent dehydration with Me$_3$SiCl and HCl(aq) in toluene

1a (0.770 g, 3 mmol) was suspended in MeCN (6 cm^3) in an J Young's sample flask. Successively 3-chlorobutan-2-one (0.6 cm^3, 6 mmol) and *N,N*-diisopropylethylamine were added, the tube was sealed, and the reaction was subsequently stirred at 110 °C for 40 h. The following steps were then carried out without inert atmosphere techniques. The solvent was removed under reduced pressure, followed by the addition of Me$_3$SiCl (1.1 cm^3, 9 mmol), 37 % aq. HCl (4 drops), and toluene (7.6 cm^3) and was subsequently refluxed at 90 °C for 2.5 h, resulting in a biphasic mixture. Water (50 cm^3) was added and the organic products were extracted into DCM (4 x 50 cm^3). The combined organic extracts were dried with MgSO$_4$, filtered, and the solvent was removed under reduced pressure, to afford a biphasic mixture of a dark brown oil with a light brown oil on top. Hexane (10 cm^3) was added, inducing precipitation and afforded a dark brown solid with a brown supernatant. The supernatant was decanted, leaving behind a dark brown sticky solid, shown to be impure **2a** by ^{1}H NMR.

The sticky solid was dissolved in minimal amounts of DCM (5 cm^3) and added dropwise to stirring hexane (15 cm^3); precipitation occurred instantly. The supernatant was decanted and the precipitate was washed with hexane (5 cm^3) to

afford a dark brown sticky solid. TLC was carried out on the dark brown sticky solid which confirmed the product, **2a**, along with numerous other impurities.

2.4.2.1.2 Attempted formation of the intermediate from 1a, 3-chlorobutan-2-one, and *N,N*-diisopropylethylamine in MeCN and subsequent dehydration with Me₃SiCl in toluene

1a (7.454 g, 29 mmol) was suspended in MeCN (56 cm³) in a J Young's sample flask. Successively 3-chlorobutan-2-one (5.9 cm³, 58 mmol) and *N,N*-diisopropylethylamine (6 cm³, 34.8 mmol) were added, the tube was sealed, and stirred at 110 °C for 64.5 h. The following steps were then carried out without inert atmosphere techniques. The solvent was removed under reduced pressure, affording a dark brown oil to which Me₃SiCl (11 cm³, 87 mmol) and toluene (74 cm³) were added and the resulting mixture was stirred for 3 h at 90 °C. Water (50 cm³) was added to the resulting biphasic mixture and the organic products were extracted into DCM (4 x 30 cm³). The combined organic extracts were dried with MgSO₄, filtered, and the solvent was removed under reduced pressure, affording a dark brown tar which was identified as impure **2a** and **1a** by ¹H NMR.

Attempted purification of **2a:**

Washing the tar with hexane, followed by dissolution in DCM and aqueous and brine washes, still afforded a tarry residue after removal of solvent. High purity, dark crystalline crude could be obtained by dissolving the tar in DCM, filtering through silica, and removal of solvent, but despite repeated attempts and experimentation with solvent systems and washings, pure **2a** was not available by this method.

2.4.2.1.3 Attempted formation of the intermediate from 1b and 3-chlorobutan-2-one in MeCN and subsequent dehydration with Me₃SiCl

1b (0.026 g, 0.1 mmol) was suspended in THF (~1 cm³) in a J Young's NMR tube equipped with a DMSO-*d₆* capillary. 3-chlorobutan-2-one (0.01 cm³, 0.01 mmol) was added and the resulting mixture was heated at 80 °C for 12 h. After cooling Me₃SiCl (0.3 cm³, 2.76 mmol) was added and the reaction was subsequently heated at 70 °C for 3.5 h. The resulting mixture was a dark brown supernatant with a

brown precipitate and ^{1}H NMR data was ambiguous. Therefore, in air, water (5 cm^3) was added to the mixture and the organic products were extracted into DCM (3 x 5 cm^3). The combined organic extracts were dried with MgSO$_4$, filtered, and the solvent was removed under reduced pressure, affording a dark brown solid, identified as N-(2-methoxyphenyl)formamide by ^{1}H NMR.

2.4.2.1.4 NMR-scale reactions

General Procedure: In a J Young's NMR tube equipped with a DMSO-d_6 capillary, **1a** (0.026 g, 0.1 mmol) and additive (*vide infra*), were suspended in acetonitrile (1 cm^3). Successively 3-chlorobutan-2-one (0.02 cm^3, 0.2 mmol) and *N,N*-diisopropylethylamine (0.02 cm^3, 0.12 mmol) were added and the resulting mixture was heated at 80 °C whilst the reaction progress was monitored by *in situ* ^{1}H NMR. After full conversion of the formamidine into the hemi-aminal intermediate, the subsequent steps were varied and the reaction was monitored by *in situ* NMR until complete dehydration was observed and subsequent work-up steps were carried out without inert atmosphere techniques.

2.4.2.1.4.1 Attempted dehydration with Me$_3$SiCl in toluene

Performed according to the general procedure above. The resulting mixture was heated at 80 °C for 170 h affording a yellow solution. The solvent was removed under reduced pressure, followed by the addition of toluene (1 cm^3) and Me$_3$SiCl (0.4 cm^3, 3.15 mmol) and the mixture was subsequently refluxed at 110 °C under elevated pressure for 3.5 h. The resulting mixture was a yellow solution with a grey sand-like precipitate. Water (10 cm^3) was added and the organic products were extracted into DCM (3 x 5 cm^3). The combined organic extracts were dried with MgSO$_4$, filtered, and the solvent was removed under reduced pressure affording a yellow/brown oil, which was identified as impure **2a** in a 2 to 3 ratio, of **2a** to unconverted intermediate by ^{1}H NMR by integration of signals for methyl groups on the backbone.

2.4.2.1.4.2 Attempted dehydration with the addition of Me$_3$SiCl in the first step (a one-pot one-step synthesis)

Performed according to the general procedure above, with Me$_3$SiCl (0.026 cm^3, 0.2 mmol) as an additive and the reaction mixture heated at 80 °C for 111 h. The

resulting light brown solution was shown to be a mixture of the hemi-aminal intermediate, silylated intermediate, and **2a** by ^{1}H NMR. The solution was further heated at 110 °C under elevated pressure for 9 h, to give a dark brown/black reaction mixture. This was presumed to indicate predominant formation of **2a**, due to one main signal at 9.11 ppm in the ^{1}H NMR, however not unambiguous as multiple peaks were present. Thus, water (5 cm^3) was added and the organic products were extracted into DCM (3 x 5 cm^3). The combined organic extracts were dried with MgSO$_4$, filtered, and the solvent was removed under reduced pressure affording a brown tar, which was identified as impure **2a** in a 7 to 3 ratio, of **2a** to unconverted intermediate by ^{1}H NMR by integration of signals for methyl groups on the backbone.

2.4.2.1.4.3 Attempted dehydration with Me₃SiCl, KI additive (a one-pot two-step synthesis)

Performed according to the general procedure above, with KI (0.056 g, 0.34 mmol) as additive and the reaction mixture heated at 80 °C for 2 h resulting in a pale-yellow solution and white precipitate, presumed to be KCl. After cooling Me₃SiCl (0.026 cm^3, 0.20 mmol) was added and the supernatant changed from pale-yellow to orange. After heating the reaction mixture at 80 °C for 1 h the supernatant turned orange/brown and ^{1}H NMR data suggested that the reaction was unsuccessful, **2a** had not been synthesised.

2.4.2.1.4.4 Attempted dehydration with Ac₂O in toluene, KI additive

Performed according to the general procedure above, with KI (0.051 g, 0.31 mmol) as additive and the reaction mixture heated at 80 °C for 16 h. Removal of the solvent under reduced pressure afforded a brown tar to which toluene (1 cm^3) and Ac₂O (0.029 cm^3, 0.30 mmol) were added. The resulting mixture was heated at 80 °C for 24.5 h, but it was unclear whether the reaction had been successful or not due to ^{1}H NMR data being ambiguous, because of *protio*-toluene obscuring the aryl region.

2.4.2.1.4.5 Attempted dehydration with Ac$_2$O and HCl, KI additive (a one-pot two-step synthesis)

Performed according to the general procedure above, with KI (0.052 g, 0.31 mmol) as additive and the reaction mixture heated at 80 °C for 16 h. After cooling Ac$_2$O (0.029 cm^3, 0.30 mmol) was added and the reaction mixture was heated at 80 °C for 2 h; *in situ* ^{1}H NMR data did not indicate the formation of imidazolium. Therefore, 37 % aq. HCl (3 drops) was added and the resulting mixture was heated at 80 °C for 1 h; *in situ* ^{1}H NMR data was ambiguous.

2.4.2.1.4.6 Attempted dehydration with HCl, KI additive (a one-pot two-step synthesis)

Performed according to the general procedure above, with KI (0.055 g, 0.33 mmol) as additive and the reaction mixture heated at 80 °C for 18 h to give a yellow supernatant with white precipitate, presumed to be KCl. After cooling 37 % aq. HCl (2 drops) was added without care to maintain the inert atmosphere and the mixture was subsequently heated at 80 °C for 2 h. The supernatant changed from yellow to orange and ^{1}H NMR data indicated clean formation of the desired imidazolium iodide.

2.4.2.1.5 Formation of the intermediate from 1a, 3-chlorobutan-2-one, and *N,N*-diisopropylethylamine in MeCN and subsequent dehydration with HCl

1a (5.909 g, 23.05 mmol) was suspended in MeCN (50 cm^3) in a J Young's sample flask and 3-chlorobutan-2-one (4.66 cm^3, 46.14 mmol) and *N,N*-diisopropylethylamine (4.82 cm^3, 27.67 mmol) were added and the tube was sealed. The resulting solution was heated at 80 °C for 110 h, after which ^{1}H NMR data of the sample suggested almost full consumption of **1a**. The following steps were then carried out without inert atmosphere techniques. Subsequently, 37 % aq. HCl (8.4 cm^3, 276.47 mmol) was added and the mixture was heated at 80 °C for 2 h. Brine (30 cm^3) was added and the organic products were extracted into DCM (4 x 20 cm^3). The combined organic extracts were dried with MgSO$_4$, filtered, and the solvent was removed under reduced pressure, affording a brown/black oil. The oil was dissolved in DCM (20 cm^3) and added dropwise to stirring EtOAc (75 cm^3), inducing precipitation. The resulting mixture was filtered and the precipitate was

washed with EtOAc (10 cm³) to afford a brown/cream solid which was identified as impure **2a** by ^{1}H NMR, along with 3-chlorobutan-2-one, Hünigs base and HCl. The crude solid was therefore dissolved in DCM (30 cm³) and washed with a saturated aq. $NaHCO_3$ solution (2 x 10 cm³) and the organic products were extracted into DCM (3 x 15 cm³) from the combined aqueous washings. The combined organic extracts were dried with $MgSO_4$, filtered, and the solvent was removed under reduced pressure, affording a light brown solid. The light brown solid was dried in a Schlenk at 80 °C *in vacuo* overnight to give **2a** as a light brown solid (3.5339 g, 10.25 mmol, 44 %). **^{1}H NMR** (400 MHz, DCM, 16.4 °C): δ 9.56 (s, 1H), 7.67 (m, 2H), 7.58 (m, 2H), 7.15 (m, 4H), 3.87 (s, 6H), 2.10 (s, 6H). **^{13}C{^{1}H} NMR** (100.52 MHz, DCM, 17.1 °C): δ 153.91 (N*C*(H)N), 136.57 (*C* phenyl or N*C*(CH₃)), 132.69 (*C*H phenyl), 128.67 (*C*H phenyl), 128.18 (*C* phenyl or N*C*(CH₃)), 121.62 (*C* phenyl or N*C*(CH₃)), 121.32 (*C*H phenyl), 112.52 (*C*H phenyl), 56.16 (O*C*H₃), 8.72 (*C*H₃). Despite multiple attempts only poor X-ray quality crystals of **2a** were grown, by the slow diffusion of hexane into a concentrated solution of DCM. Elemental analysis: Calculated for $C_{19}H_{21}ClN_2O_2$: C, 66.18; H, 6.14; N, 8.12. Found: C, 66.06; H, 6.27; N, 8.00.

2.4.2.1.6 Attempted drying 2a with Me₃SiCl

2a (5.69 g, 16.50 mmol), Me₃SiCl (4.40 cm³, 34.67 mmol), and DCM (20 cm³) were combined and refluxed for 18 h. The solvent was removed *in vacuo* and the solid residue was washed with hexane (10 cm³) and dried *in vacuo* to afford **2a** as a light brown solid; identified by ^{1}H NMR.

2.4.2.1.7 Attempted drying 2a in a vacuum oven

2a (5.239 g) was placed in a vacuum oven and was heated at 80 °C for 69 h, to give a cream solid (4.159 g, ~12.06 mmol) which was identified as **2a** by ^{1}H NMR.

2.4.2.2 Synthesis of 1,3-bis(2-methoxyphenyl)-4,5-dimethylimidazolium iodide (IAnis^Me.HI), 2b

1a (5.234 g, 20.42 mmol) and KI (10.168 g, 61.25 mmol) were suspended in MeCN (40 cm³) and 3-chlorobutan-2-one (4.13 cm³, 40.89 mmol) and *N,N*-diisopropylethylamine (4.27 cm³, 24.51 mmol) were added. The resulting solution was heated at 80 °C for 2 h, after which full consumption of **1a** was shown by ^{1}H NMR on an extract. The following steps were then carried out without inert

atmosphere techniques. To this 37 % aq. HCl (7.6 cm^3, 250.14 mmol) was then added and the mixture was subsequently heated at 80 °C for 2 h. Brine (80 cm^3) was added and the organic products were extracted into DCM (7 x 30 cm^3). The combined organic extracts were dried with MgSO$_4$, filtered, and the solvent was removed under reduced pressure, affording a brown oil. The oil was dissolved in DCM (20 cm^3) and added dropwise to stirring hexane (80 cm^3) which induced deposition of a dark tar. The supernatant was decanted and the tar was dissolved in DCM (25 cm^3) and added dropwise to stirring EtOAc (75 cm^3) which induced precipitation. The resulting mixture was filtered and the precipitate was washed with EtOAc (10 cm^3) to give a brown crystalline solid, identified as **2b** along with starting materials (3-chlorobutan-2-one and Hünigs base) and EtOAc. Water (100 cm^3) was added and the solid did not dissolve even upon heating. The mixture was filtered and the solid was washed with water (50 cm^3) to afford a brown solid shown to be clean **2b** by ^{1}H NMR. The brown solid was dried in a Schlenk at 80 °C *in vacuo* overnight, to give a brown solid (4.3369 g, 9.94 mmol, 49 %). **^{1}H NMR** (400 MHz, DCM, 25.0 °C): δ 8.57 (s, 1H), 7.62 (m, 4H), 7.19 (m, 4H), 3.90 (s, 6H), 2.16 (s, 6H). **^{13}C{^{1}H} NMR** (100.52 MHz, DCM, 25.0 °C): δ 153.98 (NC(H)N), 134.97 (C phenyl or NC(CH$_3$)), 133.07 (CH phenyl), 128.87 (C phenyl or NC(CH$_3$)), 128.43 (CH phenyl), 121.44 (CH phenyl), 121.30 (C phenyl or NC(CH$_3$)), 112.85 (CH phenyl), 56.44 (OCH$_3$), 9.06 (CH$_3$).

2.4.2.3 Synthesis of 1,3-bis(2-methoxyphenyl)-4,5-dimethylimidazolium tetrafluoroborate (IAnis^{Me}.HBF$_4$), 2c

2.4.2.3.1 Anion metathesis of 2a to 2c

In air, **2a** (3.104 g, 9.00 mmol) was dissolved in H$_2$O (15 cm^3) and stirred, followed by the dropwise addition of NaBF$_4$ (1.046 g, 9.53 mmol) in H$_2$O (10 cm^3), upon which a precipitate formed. The mixture was filtered and precipitate was washed with H$_2$O (10 cm^3) and dried in a Schlenk at 80 °C *in vacuo* overnight to afford a cream solid (2.975 g, 7.51 mmol, 83.4 %). **^{1}H NMR** (400 MHz, DCM, 17.1 °C): δ 8.38 (s, 1H), 7.62 (m, 2H), 7.48 (dd, $^3J_{H-H}$ = 1.46 Hz, $^4J_{H-H}$ = 7.79 Hz, 2H), 7.18 (m, 4H), 3.88 (s, 6H), 2.13 (s, 6H). **^{11}B NMR** (128.27 MHz, DCM, 16.4 °C): δ -1.84 (s). **^{19}F** (376.17 MHz, DCM, 16.3 °C): δ -153.36 (s), -153.41 (s) [due to the primary isotope effect, ^{19}F

bound to ^{10}B and ^{11}B]. **^{13}C{^{1}H} NMR** (100.52 MHz, DCM, 17.7 °C): δ 153.99 (NC(H)N), 134.97 (C phenyl or NC(CH$_3$)), 133.00 (CH phenyl), 128.77 (C phenyl or NC(CH$_3$)), 128.22 (CH phenyl), 121.39 (CH phenyl), 112.71 (CH phenyl), 56.20 (OCH$_3$), 8.72 (CH$_3$). Elemental analysis: Calculated for C$_{19}$H$_{21}$BF$_4$N$_2$O$_2$: C, 57.60; H, 5.34; N, 7.07. Found: C, 57.76; H, 5.45; N, 6.95.

2.4.2.3.2 Attempted anion metathesis of 2b to 2c *via* 2b in acetone and a solution of NaBF$_4$ in water added dropwise

In air, **2b** (0.202 g, 0.46 mmol) was dissolved in acetone (3 cm^3) and stirred, followed by the dropwise addition of NaBF$_4$ (0.056 g, 0.51 mmol) in water (1 cm^3). No precipitation occurred and thus water (5 cm^3) was added and a dark precipitate formed. The resulting mixture was filtered and the precipitate was washed with water (10 cm^3) to give a brown solid which was identified as **2b** by ^{1}H NMR as in the ^{11}B and ^{19}F NMR spectra no signals were present, which confirmed no BF$_4$ anion was present.

2.4.2.3.3 Attempted anion metathesis of 2b to 2c *via* the slow addition of 2b to a solution of NaBF$_4$ in acetone

In air, **2b** (0.100 g, 0.23 mmol) was added slowly to a stirring solution of NaBF$_4$ (0.031 g, 0.28 mmol) in acetone (2 cm^3); no precipitation occurred. Water (10 cm^3) was added and a dark precipitate formed. The resulting mixture was filtered to afford a brown solid which was identified as **2b** by ^{1}H NMR, with no signals were present in either the ^{11}B and ^{19}F NMR spectra, confirming that no BF$_4$ anion was present.

2.4.3 Synthesis of 1,3-bis(2-methoxyphenyl)-4,5-dimethylimidazol-2-ylidene, 3

2.4.3.1 Attempted deprotonation of 2a with 2 eq. NaH and ^{t}BuOH (catalytic amounts) in THF

NaH (0.1166 g, 60wt % in mineral oil, 4.86 mmol) was first washed with THF (2 x 5 cm^3) and then suspended in THF (10 cm^3), and the suspension was added to **2a** (0.501 g, 1.45 mmol) (which had not previously been dried *in vacuo*) *via* Teflon cannula. After this, ^{t}BuOH (1 drop) was added and the reaction mixture was subsequently stirred at ambient temperature for 19 h. The supernatant of the resulting mixture was isolated *via* filter cannula and the remaining solid was

washed with THF (5 cm³) and the THF extracts were combined. The combined extract was concentrated *in vacuo*, followed by the addition of hexane (20 cm³) and on stirring a dark brown tar was deposited. The supernatant was decanted and the tar was washed with hexane (20 cm³), and identified as **2a** by ^{1}H NMR.

2.4.3.2 Attempted deprotonation of 2a with LDA in THF

^{n}BuLi (0.82 cm³, 1.6 M, 1.31 mmol) was added dropwise to a solution of diisopropylamine (0.2 cm³, 1.43 mmol), in THF (3 cm³) and stirred for 30 minutes. The reaction mixture was then added dropwise to a mixture of **2a** (0.501 g, 1.45 mmol) suspended in THF (5 cm³) in an ice bath. The ice bath was removed and the mixture was stirred at ambient temperature for 24 h, to give an orange supernatant with pale precipitate and undissolved dark solid. The supernatant was transferred *via* filter cannula and the remaining solid was washed with THF (5 cm³) and the washings were combined. An *in situ* ^{1}H NMR of the combined filtrates identified diisopropylamine with no trace of **2a** or **3** present.

2.4.3.3 Attempted deprotonation of 2a with 1 eq. LiHMDS in THF

LiHMDS (0.2425 g, 1.45 mmol) and **2a** (0.501 g, 1.45 mmol) were combined and THF (5 cm³) was added. The mixture was subsequently stirred at ambient temperature for 22 h. The solvent was removed under reduced pressure, which afforded a brown/cream solid. Attempted extraction into toluene (6 x 10 cm³) and the extracts were removed *via* a filter cannula and combined. However, the extraction was unsuccessful, as hardly any of the solid dissolved and an *in situ* ^{1}H NMR of the combined toluene filtrates suggested that no **3** or **2a** were present.

2.4.3.4 Attempted deprotonation of 2a with 1 eq. LiHMDS in THF, under reflux

LiHMDS (0.2424 g, 1.45 mmol), **2a** (0.501 g, 1.45 mmol) were combined and THF (5 cm³) was added. The mixture was subsequently refluxed for 25 h. The solvent was removed under reduced pressure and the residue was extracted into toluene (3 x 10 cm³), and the extracts were removed *via* a filter cannula and combined; however, the majority of the solid did not dissolve and therefore was presumed as **2a** and LiCl. The solvent was removed under reduced pressure from the combined extracts, affording a small quantity of a brown/orange tar. Subsequently, a solution of LiHMDS (0.2427 g, 1.45 mmol) in THF (5 cm³) was added to the leftover solid and

the reaction mixture was stirred at ambient temperature for 12 h. The resulting solution was dark brown with no solid present. The solvent was removed under reduced pressure and **3** was extracted into hot toluene (5 x 10 cm^3) and the extracts were removed *via* a filter cannula and combined, leaving behind a brown sludge. The combined extracts formed an orange/yellow supernatant with orange precipitate. The solvent was concentrated *in vacuo* to ~5 cm^3 and the supernatant was removed *via* filter cannula, and the remaining solid was washed with hexane (10 cm^3) and dried *in vacuo*. The resulting pale orange solid was identified as **2a** by ^{1}H NMR in *protio*-DCM and did not dissolve in benzene.

2.4.3.5 Attempted deprotonation of 2a (dried with Me₃SiCl) with 1 eq. LiHMDS in THF

2a (0.5038 g, 1.46 mmol) (dried with Me$_3$SiCl) and LiHMDS (0.2429 g, 1.45 mmol) were combined and THF (5 cm^3) was added. The reaction mixture was subsequently stirred at ambient temperature for 12 h. The solvent was removed under reduced pressure and the residue was extracted into toluene (4 x 10 cm^3), and the extracts were removed *via* a filter cannula and combined; the majority of the solid did not dissolve. The solvent was removed under reduced pressure from the combined filtrates, affording a small quantity of a yellow tar shown to be a mixture of **2a** and **3** by ^{1}H NMR in *protio*-DCM.

2.4.3.6 NMR-scale reactions

General procedure: In a J Young's NMR tube equipped with a DMSO-d_6 capillary, an imidazolium salt (**2a** or **2c**), base and solvent were combined and the tube was inverted for approximately 5 minutes. The reaction progress was monitored by *in situ* ^{1}H NMR.

2.4.3.6.1 Deprotonation of 2a (dried with Me₃SiCl) with 2 eq. LiHMDS in THF

2a (0.0348 g, 0.1 mmol) (dried with Me$_3$SiCl), LiHMDS (0.0333 g, 0.2 mmol), and THF (1 cm^3) were combined and allowed to stand for 20 h. The resulting mixture was a red/brown supernatant with a small amount of brown solid (presumed **2a**). The product was identified by *in situ* ^{1}H NMR as **3**.

2.4.3.6.2 Deprotonation of 2a (dried with Me₃SiCl) with 2 eq. ᵗBuOK in THF

2a (0.0344 g, 0.1 mmol) (dried with Me₃SiCl), ᵗBuOK (0.0229 g, 0.2 mmol), and THF (1 cm³) were combined and allowed to stand for 15 h, forming a bright-orange supernatant with a small amount of brown solid (presumed **2a**). The product was identified by *in situ* ¹H NMR as **3**.

2.4.3.6.3 Deprotonation of 2a (dried with Me₃SiCl) with 2 eq. ᵗBuOK in Et₂O

2a (0.0345 g, 0.1 mmol) (dried with Me₃SiCl), ᵗBuOK (0.0228 g, 0.2 mmol), and Et₂O (1 cm³) were combined and allowed to stand for 15 h, forming an orange/red supernatant with a small amount of brown solid (presumed **2a**). The product was identified by *in situ* ¹H NMR as **3**.

2.4.3.6.4 Deprotonation of 2a (dried with Me₃SiCl) with 2 eq. LiHMDS in THF

2a (0.0347 g, 0.1 mmol) (dried with Me₃SiCl) was suspended in THF (1 cm³) and *in situ* ¹H NMR data confirmed that only trace amounts of **2a** had dissolved. To this LiHMDS (0.0338 g, 0.2 mmol) was then added, forming a yellow supernatant with a small amount of brown solid (believed to be **2a** as it is poorly soluble in THF). The product was identified by *in situ* ¹H NMR as **3**.

2.4.3.6.5 Deprotonation of 2a (dried with Me₃SiCl) with 2 eq. ᵗBuOK in Et₂O

2a (0.0344 g, 0.1 mmol) (dried with Me₃SiCl) was suspended in Et₂O (1 cm³); *in situ* ¹H NMR data confirmed no traces of **2a** were present in solution. ᵗBuOK (0.0226 g, 0.2 mmol) was then added, forming a cream supernatant with brown and white solid present at the bottom, and signals ascribed to **3** were identified in the *in situ* ¹H NMR spectrum.

2.4.3.6.6 Deprotonation of 2c with 2 x 1 eq. LiHMDS in THF

2c (0.040 g, 0.1 mmol) (which had not previously been dried *in vacuo*) was suspended in THF (1 cm³); *in situ* ¹H NMR data confirmed only trace amounts of **2c** were present in solution. To this LiHMDS (0.0167 g, 0.1 mmol) was then added, forming a yellow/brown supernatant with a small amount of brown solid (**2a**), with signals ascribed to **3** seen by *in situ* ¹H NMR. Subsequently, another portion of LiHMDS (0.0172 g, 0.1 mmol) was added, resulting in a yellow/brown solution with no solid present. The *in situ* ¹H NMR spectrum showed no imidazolium C-H resonance, suggesting formation of **3**.

2.4.3.6.7 Deprotonation of 2c (dried *in vacuo*) with 1 eq. LiHMDS in THF

2c (0.0398 g, 0.1 mmol) (dried *in vacuo*) was suspended in THF (1 cm³); *in situ* ^{1}H NMR data confirmed only trace amounts of **2c** were present in solution. Subsequently, LiHMDS (0.0168 g, 0.1 mmol) was added, forming a brown solution with no solid present. The *in situ* ^{1}H NMR spectrum showed no imidazolium C-H resonance, suggesting formation of **3**.

2.4.3.6.8 Deprotonation of 2a (dried in a vacuum oven at 80 °C for 69 h) with 2 x 1 eq. LiHMDS in THF

2a (0.035 g, 0.1 mmol) (dried in a vacuum oven at 80 °C for 69 h) was suspended in THF (1 cm³); *in situ* ^{1}H NMR data confirmed only trace amounts of **2a** were present in solution. Subsequently, LiHMDS (0.0169 g, 0.1 mmol) was added, forming a bright red supernatant with a small amount of undissolved solid (**2a**); the *in situ* ^{1}H NMR data was consistent with formation of **3** in solution. Subsequently, another portion of LiHMDS (0.0166 g, 0.1 mmol) was added and the resulting solution was a bright red colour with no solid present; the *in situ* ^{1}H NMR spectrum was consistent with **3**.

2.4.3.7 Attempted deprotonation of 2b (dried *in vacuo*) with 1 eq. LiHMDS in toluene

2b (0.4363 g, 1 mmol) (dried *in vacuo*), LiHMDS (0.1677 g, 1 mmol), and toluene (5 cm³) were combined and subsequently stirred at ambient temperature for 12 h, affording a clear supernatant with a brown sticky residue and white solid. The mixture was filtered through Celite® and washed with toluene (3 x 5 cm³). The solvent was removed under reduced pressure from the filtrate to afford a yellow residue which was washed with hexane (2 x 5 cm³) and dried *in vacuo* to give a yellow solid (0.0412 g) whose ^{1}H NMR spectrum in *protio*-THF was ambiguous.

2.4.3.8 Deprotonation of 2c (dried *in vacuo*) with NaH/^{t}BuOH

NaH (0.0999 g, 60wt % in mineral oil, 4.16 mmol) was first washed with THF (2 x 5 cm³) and then suspended in THF (5 cm³), and the suspension was added to a mixture of **2c** (0.5035 g, 1.27 mmol) (dried *in vacuo*) and ^{t}BuOH (2 drops). The resulting mixture was stirred at ambient temperature for 19 h, forming a brown solution with some remaining solid. The supernatant was transferred *via* filter

cannula and the leftover solid was washed with THF (5 cm³) and the filtrates were combined and concentrated to ~5 cm³, followed by the addition of hexane (15 cm³) to induce precipitation. The supernatant was decanted and the precipitate was washed with hexane (2 x 5 cm³) and dried *in vacuo* to afford a brown solid (0.2532 g) which was identified as **3** along with a small amount of **2c** by ¹H NMR.

2.4.3.9 Deprotonation of 2a (dried *in vacuo*) with NaH/ᵗBuOH

NaH (0.1650 g, 60wt % in mineral oil, 6.88 mmol) was first washed with THF (2 x 5 cm³) and then suspended in THF (5 cm³), and the suspension was added to a mixture of **2a** (0.1728 g, 0.50 mmol) and ᵗBuOH (1 drop). The resulting mixture was stirred at ambient temperature for 22 h, forming a brown supernatant with some remaining solid. The supernatant was filtered *via* filter cannula and the residues extracted with THF (5 cm³). The combined filtrates were concentrated to 5 cm³ and hexane (25 cm³) was added, inducing precipitation. The supernatant was decanted and the precipitate was washed with hexane (2 x 5 cm³) and dried *in vacuo* to give a brown solid which was identified as **3** by ¹H NMR in *protio*-THF. Provisionally assigned **¹H NMR** (400 MHz, THF, 25.0 °C): δ 7.27 (m, 4H), 7.04 (d, J = 8.04 Hz, 2H), 6.93 (t, J = 7.06 Hz, 2H), and alkyl signals were masked by solvent signals. Attempts to record NMR in *protio*-DCM displayed very broad peaks in the ¹H NMR spectrum, suggesting **3** reacts with DCM.

2.4.4 Attempted syntheses of protected NHCs

2.4.4.1 Attempted synthesis of 1,3-bis(2-methoxyphenyl)-4,5-dimethylimidazolium-2-carboxylate (IAnis^Me.CO2), 4a

2.4.4.1.1 Attempted carboxylation of 2c using dry ice

2c (0.3129 g, 0.79 mmol), LiHMDS (0.2647 g, 1.58 mmol) and toluene (10 cm³) were combined and stirred at ambient temperature for 2 h. CO_2 was transferred *via* cannula from a Schlenk tube filled with dry ice (1/3 of the Schlenk) and bubbled though the solution for 10 minutes, inducing precipitation immediately. Subsequently, the solvent was removed under reduced pressure from the resulting mixture, affording a cream/white solid which was shown to be a mixture of **2c** and **4a** in a 2:3 ratio, respectively, by ¹H NMR by integration of signals for methyl groups on the backbone.

2.4.4.1.2 Attempted carboxylation of 2c using CO_2 gas

2c (0.4001 g, 1.01 mmol), LiHMDS (0.1859 g, 1.11 mmol), and THF (5 cm^3) were combined and stirred at ambient temperature for 30 minutes. CO_2 was bubbled though the solution for 5 minutes affording a biphasic solution. After 3 days, the bottom liquid phase had formed a solid. The supernatant was removed and the remaining solid was washed with Et$_2$O (2 x 10 cm^3) and dried *in vacuo* at 80 °C overnight to give an off-white solid which was shown to be a mixture of **2c** and **4a** in a 1:9 ratio, respectively, along with Et$_2$O and a small amount of LiHMDS by ^{1}H NMR by integration of signals for methyl groups on the backbone.

2.4.4.1.3 Attempted carboxylation of 2c using CO_2 gas passed though molecular sieves

2c (0.4004 g, 1.01 mmol), LiHMDS (0.2544 g, 1.52 mmol) and THF (5 cm^3) were combined and stirred at ambient temperature overnight. CO_2 was passed though molecular sieves before being bubbled through the solution for 5 minutes, during which a sludge precipitated. The resulting mixture was left to stir for 40 minutes and the solvent was removed under reduced pressure, affording a viscous oil. This was triturated with Et$_2$O (3 x 10 cm^3) and the supernatant was removed, affording a cream solid which was shown to be a mixture of **2c** and **4a** in a 1:9 ratio, respectively, along with Et$_2$O by ^{1}H NMR by integration of signals for methyl groups on the backbone.

2.4.4.2 Synthesis of 1,3-bis(2-methoxyphenyl)-4,5-dimethyl-2-(trimethylsilyl)imidazolium chloride (IAnis^{Me}.SiMe$_3$Cl), 4b

2.4.4.2.1 Attempted silylation by the generation of 3 *in situ*, followed by the addition of Me$_3$SiCl

2c (0.4009 g, 1.01 mmol), LiHMDS (0.1694 g, 1.01 mmol), and toluene (5 cm^3) were combined and stirred at ambient temperature for 2 days, forming a yellow supernatant with pale precipitate. The resulting mixture was filtered through Celite® and washed through with toluene (2 x 10 cm^3); *in situ* ^{1}H NMR data of the filtrate suggested the formation of the free carbene, **3**, and HMDS. Therefore Me$_3$SiCl (0.05 cm^3, 0.4 mmol) was added to the J Young's NMR tube and upon agitating the tube a pale precipitate formed. The supernatant was decanted and

the majority of the precipitate dissolved in DCM (1 cm^3); *in situ* ^{1}H NMR data indicated that the reaction was unsuccessful, producing a complex mixture of unknown species.

2.4.4.2.2 Attempted silylation of 3 *via* the addition of Me$_3$SiCl in THF

3 (0.0308 g, 0.1 mmol) and THF (1 cm^3) were combined in a J Young's NMR tube equipped with a DMSO-d_6 capillary, and confirmed to be free NHC, **3**, by ^{1}H NMR. Me$_3$SiCl (0.03 cm^3, 0.2 mmol) was added, causing immediate formation of copious precipitate, preventing further *in situ* ^{1}H NMR. As a chemical test for the protected NHC in solution, Ph$_2$PCl (0.02 cm^3, 0.11 mmol) was added but the resulting mixture was not amenable to NMR analysis. The supernatant was transferred into another J Young's NMR tube and ^{1}H NMR data confirmed none of the desired product was present. The leftover precipitate did not dissolve in DCM, indicating that the experiment was unsuccessful.

2.4.4.2.3 Attempted silylation of 3 *via* the addition of Me$_3$SiCl

3 (0.0196 g, 0.06 mmol), THF (1 cm^3), and Me$_3$SiCl (0.015 cm^3, 0.12 mmol) were combined in a J Young's NMR tube equipped with a DMSO-d_6 capillary, forming lots of pale precipitate with an orange supernatant. The solvent was removed under reduced pressure, followed by the addition of DCM (1 cm^3) and **2a** was confirmed as the majority product by ^{1}H NMR.

2.4.5 Synthesis of 1,3-bis(2-hydroxyphenyl)-4,5-dimethylimidazolium salts, 5

2.4.5.1 Synthesis of 1,3-bis(2-hydroxyphenyl)-4,5-dimethylimidazolium tetrafluoroborate (IPhenol^{Me}.HBF$_4$), 5a

2.4.5.1.1 Attempted demethylation of 2c with 2.1 eq. BBr$_3$, stirred for 1 h

2c (0.1987 g, 0.50 mmol) (dried *in vacuo*) and DCM (5 cm^3) were combined and stirred in an ice bath. BBr$_3$ (0.10 cm^3, 1.04 mmol) was added and the solution was left to stir at ambient temperature for 1 h. To this under air, a solution of NaBF$_4$ (0.056 g, 0.51 mmol) in ice cold water (30 cm^3) was added and the reaction was left to stir at ambient temperature for 2 h. The organic products were extracted into DCM (3 x 10 cm^3), combined, dried with MgSO$_4$, filtered, and the solvent was removed under reduced pressure to give a grey tar which was identified as a mixture of mono- and di-demethylated **5a** by ^{1}H NMR.

2.4.5.1.2 Attempted demethylation of 2c with 2.1 eq. BBr₃, longer reaction time

2c (0.1989 g, 0.50 mmol) (dried *in vacuo*) and DCM (5 cm³) were combined and stirred in an ice bath. BBr₃ (0.10 cm³, 1.04 mmol) was added and the solution was left to stir at ambient temperature for 17 h. To this under air, a solution of NaBF₄ (0.058 g, 0.53 mmol) in ice cold water (20 cm³) was added and the mixture was left to stir at ambient temperature for 3 h. The organic products were extracted into DCM (3 x 10 cm³), combined, dried with MgSO₄, filtered, and the solvent was removed under reduced pressure to give a grey tar which was identified as a mixture of mono- and di-demethylated **5a** by ¹H NMR.

2.4.5.1.3 Demethylation of 2c with 4.2 eq. BBr₃, overnight stirring

2c (0.1981 g, 0.50 mmol) (dried *in vacuo*) and DCM (5 cm³) were combined and stirred in an ice bath. BBr₃ (0.20 cm³, 2.08 mmol) was added and the solution was left to stir at ambient temperature for 15 h. To this under air, a solution of NaBF₄ (0.056 g, 0.51 mmol) in ice cold water (25 cm³) was added and the reaction was left to stir at ambient temperature for 1 h. The organic products were extracted into DCM (4 x 10 cm³). The organic extracts were combined, dried with MgSO₄ and filtered, and dried under reduced pressure. Afforded a grey/brown tar (0.146 g, 0.40 mmol, 80 %). **¹H NMR** (400 MHz, DCM, 25.00 °C): δ 8.11 (s, 1H), 7.42 (m, 2H), 7.32 (m, 4H), 6.98 (m, 2H), 2.13 (s, 6H). **¹¹B NMR** (128.27 MHz, DCM, 25.00 °C): δ -1.72 (s). **¹⁹F NMR** (376.17 MHz, DCM, 25.00 °C): δ -151.59 (s), -151.64 (s) [due to the primary isotope effect, ¹⁹F bound to ¹⁰B and ¹¹B].

2.4.5.2 Synthesis of 1,3-bis(2-methoxyphenyl)-4,5-dimethylimidazolium bromide (IPhenol^Me.HBr), 5b

2.4.5.2.1 Small-scale demethylation

2a (0.1723 g, 0.50 mmol) (dried *in vacuo*) and DCM (5 cm³) were combined and stirred in an ice bath. BBr₃ (0.20 cm³, 2.08 mmol) was added and the solution was left to stir at ambient temperature for 18 h. Under air, a solution of NaBr (0.053 g, 0.52 mmol) in ice cold water (20 cm³) was added and the reaction mixture was left to stir at ambient temperature for 1 h. The organic products were extracted into DCM (4 x 10 cm³), combined, dried with MgSO₄, filtered, and the solvent was removed under reduced pressure to give a brown tar (0.114 g, 0.32 mmol, 64 %),

which was identified as **5b** by ^{1}H NMR. X-ray quality crystals of **5b** were grown by the slow diffusion of hexane into a concentrated solution of DCM.

2.4.5.2.2 Large-scale demethylation

2a (1.0008 g, 2.90 mmol) (dried *in vacuo*) and DCM (20 cm^3) were combined and stirred in an ice bath. BBr$_3$ (1.17 cm^3, 12.14 mmol) was added and the solution was left to stir at ambient temperature for 16 h. Under air, a solution of NaBr (0.300 g, 2.92 mmol) in ice cold water (40 cm^3) was added and the reaction mixture was left to stir at ambient temperature for 1 h. The organic products were attempted to be extracted into DCM (4 x 20 cm^3), leaving an aqueous layer which was a yellow solution with dark solid present. The organic extracts were combined, dried with MgSO$_4$, filtered, and the solvent was removed under reduced pressure to give a small quantity of brown tar which was identified as **5b** by ^{1}H NMR. Therefore, repeated extraction of the aqueous layer into DCM (4 x 20 cm^3) and treatment as above afforded a small quantity of a light brown solid which was identified as **5b** by ^{1}H NMR; the aqueous layer still contained a dark solid.

The solid in the aqueous layer was identified as **5b** by ^{1}H NMR and so the aqueous layer was filtered and the solid was washed with water (10 cm^3), which afforded a brown solid which was identified as **5b** by ^{1}H NMR. All three isolated fractions were combined, dissolved in methanol (7 cm^3), and added dropwise to stirring hexane (30 cm^3). The clear top layer was decanted and the solvent was removed under reduced pressure, to give a brown tar which was washed with DCM (6 cm^3) and the resulting solid was dried in a Schlenk at 80 °C *in vacuo* overnight to afford **5b** as a light brown solid (0.2428 g, 0.67 mmol, 23 %). **^{1}H NMR** (400 MHz, DCM, 16.70 °C): δ 9.07 (s, 2H), 8.10 (s, 1H), 7.37 (m, 6H), 6.97 (m, 2H), 2.12 (s, 6H). **^{13}C{^{1}H} NMR** (100.52 MHz, DCM, 17.50 °C): δ 152.63 (NC(H)N), 134.60 (C phenyl or NC(CH$_3$)), 132.65 (CH phenyl), 129.37 (C phenyl or NC(CH$_3$)), 127.52 (CH phenyl), 120.69 (C phenyl or NC(CH$_3$)), 120.59 (CH phenyl), 119.80 (CH phenyl), 8.82 (CH$_3$). Extracting into DCM was not as successful as expected, which uncovered that **5b** is not very soluble in DCM.

2.4.5.2.3 Large-scale demethylation with altered work-up

2a (1.0004 g, 2.91 mmol) (dried *in vacuo*) and DCM (25 cm³) were combined and stirred in an ice bath. BBr$_3$ (1.2 cm³, 12.45 mmol) was added and the solution was left to stir at ambient temperature for 19 h. Under air, a solution of NaBr (0.299 g, 2.90 mmol) in ice cold water (40 cm³) was added and the mixture was left to stir at ambient temperature for 2 h. The resulting mixture was filtered to afford a brown solid which was identified as **5b** by ¹H NMR. The organic products in the filtrate were extracted into DCM (4 x 20 cm³) and the organic extracts were combined, dried with MgSO$_4$, filtered, and the solvent was removed under reduced pressure to afford a brown tar which was dissolved in methanol (2 cm³) and added dropwise to stirring hexane (10 cm³). The clear top layer was decanted and the solvent was removed under reduced pressure, to give a brown tar which was triturated with DCM (1 cm³). The solvent was removed under reduced pressure, to give a brown solid which was identified as **5b** by ¹H NMR. Both fractions were combined and dried in a Schlenk at 80 °C *in vacuo* overnight to give clean **5b** as a brown solid (0.7076 g, 1.96 mmol, 67 %).

2.4.6 Synthesis of potassium/sodium/lithium 2,2'-(4,5-dimethylimidazole-1,3-diyl)diphenolate (depending on the base employed) (IPhenolate^{Me}), 6

2.4.6.1 Attempted deprotonation of phenols and C$_{carbene}$ with NaH/^{t}BuOK

NaH (0.1650 g, 60wt % in mineral oil, 6.88 mmol) was first washed with THF (2 x 5 cm³) and then suspended in THF (5 cm³), and the suspension was added to a mixture of ^{t}BuOK (3.8 mg, 0.03 mmol) and **5b** (0.114 g, 0.32 mmol) (which was not completely dry). The resulting mixture was stirred at ambient temperature for 19 h, forming a brown supernatant with residual solid (presumed unconverted **5b**). The supernatant was removed *via* a filter cannula and the leftover solid was washed with THF (5 cm³). The combined filtrates were concentrated to ~5 cm³, followed by the addition of hexane (30 cm³) and the resulting solution was stirred to induce precipitation. The supernatant was decanted and the precipitate was washed with hexane (2 x 5cm³) and dried *in vacuo* to afford a cream solid (0.2532 g).

2.4.6.2 Deprotonation of phenols and C$_{carbene}$ with 2 x 3 eq. ^{t}BuOK (NMR-scale)

In a J Young's NMR tube equipped with a DMSO-d_6 capillary, **5b** (0.0362 g, 0.1 mmol) was suspended in THF (1 cm^3); *in situ* ^{1}H NMR data showed trace amounts of **5b** were present in solution. On addition of ^{t}BuOK (0.0338 g, 0.30 mmol), the resulting mixture formed a brown solution with solid remaining at the bottom, presumed to be **5b**; *in situ* ^{1}H NMR data suggested the presence in solution of mostly **6** with a small amount of **5b**. However, the peaks were very broad and therefore ^{1}H NMR data was not very informative. A further portion of ^{t}BuOK (0.0338 g, 0.30 mmol) was added, leading to sharper signals in the ^{1}H NMR spectrum and indicating formation of **6**.

2.4.6.3 Attempted deprotonation of phenols and C$_{carbene}$ with 6 eq. ^{t}BuOK (larger scale)

5b (0.0543 g, 0.15 mmol), ^{t}BuOK (0.1013 g, 0.90 mmol) and THF (5 cm^3) were combined and stirred at ambient temperature for 19 h. The solvent was removed under reduced pressure and the residue was washed with Et$_2$O (2 x 10 cm^3) and dried *in vacuo*, affording an off-white solid (5.2 mg) which was insoluble in THF and so not suitable for NMR analysis.

2.4.6.4 Deprotonation of phenols and C$_{carbene}$ with 2 x 3 eq. LiHMDS (NMR-scale)

In a J Young's NMR tube equipped with a DMSO-d_6 capillary, **5b** (0.0360 g, 0.1 mmol) (dried *in vacuo*) was suspended in THF (1 cm^3); *in situ* ^{1}H NMR data showed trace amounts of **5b** were present in solution. On addition of LiHMDS (0.0504 g, 0.30 mmol), the resulting mixture was a brown solution with dark solid present at the bottom, presumed to be **5b**; *in situ* ^{1}H NMR data identified **6** as the only arene containing species present. A further portion of LiHMDS (0.0503 g, 0.30 mmol) was added, resulting in consumption of further solid; *in situ* ^{1}H NMR data showed an increase in the intensity of the signals associated with **6**. Provisionally assigned **^{1}H NMR** (400 MHz, THF, 25.0 °C): δ 7.01 (bd, 2H), 6.78 (bt, 2H), 6.55 (bd, 2H), 6.30 (bt, 2H), 2.01 (s, 6H).

2.4.6.5 Assumed deprotonation of phenols and C$_{carbene}$ with 3.1 eq. LiHMDS (larger scale)

5b (0.1014 g, 0.28 mmol), LiHMDS (0.1454 g, 0.0.87 mmol) and THF (3 cm^3) were combined and stirred at ambient temperature for 19 h, forming a brown supernatant with small quantity of brown solid present, presumably residual **5b**. The supernatant was transferred *via* filter cannula into stirring hexane (15 cm^3), which induced precipitation. The supernatant was decanted, the precipitate was washed with hexane (2 x 5 cm^3) and dried *in vacuo* to afford a pale brown solid (0.0279 g, 0.10 mmol, 36 %) which was identified as **6** by ^{1}H NMR, although not unambiguously as the aryl peaks were broad and the alkyl resonances were obscured by the *protio*-THF.

2.5 References

1. M. Jahnke and F. Hahn, *N-Heterocyclic Carbenes: From Laboratory Curiosities to Efficient Synthetic Tools, 2nd Edition*, 2017, 1-45.

2. J. Dumas and E. Peligot, *Ann. Chim. Phys.*, 1835, **58**, 5-74.

3. a) L. Tschugajeff, M. Skanawy-Grigorjewa, A. Posnjak and M. Skanawy-Grigorjewa, *Z. Anorg. Allg. Chem.*, 1925, **148**, 37-42. b) L. *Tschugajeff*, M. *Skanawy-Grigorjewa, J. Russ*. Chem. *Ges*., *1915*, **47**, *776* (although could not be located).

4. W. Butler, J. Enemark, J. Parks and A. Balch, *Inorg. Chem.*, 1973, **12**, 451-457.

5. P. de Frémont, N. Marion and S. Nolan, *Coord. Chem. Rev.*, 2009, **253**, 862-892.

6. J. Moerdyk, D. Schilter and C. Bielawski, *Acc. Chem. Res.*, 2016, **49**, 1458-1468.

7. A. Arduengo, R. Harlow and M. Kline, *J. Am. Chem. Soc.*, 1991, **113**, 361-363.

8. K. Hirano, S. Urban, C. Wang and F. Glorius, *Org. Lett.*, 2009, **11**, 1019-1022.

9. H. Finkelstein, *Ber. Dtsch. Chem. Ges.*, 1910, **43**, 1528-1532.

10. C. Gibard, H. Ibrahim, A. Gautier and F. Cisnetti, *Organometallics*, 2013, **32**, 4279-4283.

11. F. Medici, G. Gontard, E. Derat, G. Lemière and L. Fensterbank, *Organometallics*, 2018, **37**, 517-520.

12. M. Fèvre, P. Coupillaud, K. Miqueu, J. Sotiropoulos, J. Vignolle and D. Taton, *J. Org. Chem.*, 2012, **77**, 10135-10144.

Chapter Three

Metal Complexes

"It always seems impossible until its done"

Nelson Mandela

3.1 Introduction to NHC metal complexes

NHCs' strong σ donor capability makes them excellent ligands for coordination to metal centres *via* formation of metal carbon bonds, and hence they are important ligands in modern organometallic chemistry. NHCs are capable of binding to virtually all transition metals[1,2] as well as metalloids such as selenium, with examples shown in *Figure 3.1*.[3,4]
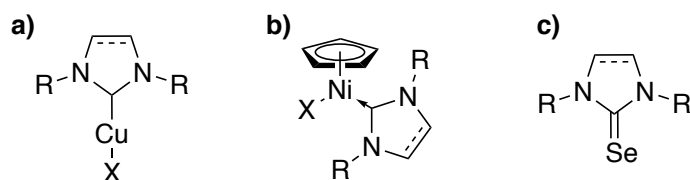
Figure 3.1. NHC-metal complexes: a) NHC-copper complex; b) Half-sandwich nickel(II) complex; c) NHC-selenium adduct.

Most metal carbene complexes can be split into two types according to the nature of their binding to the metal centre, binding either as 'singlet' Fischer or 'triplet' Schrock carbenes.[1] The coordination in Fisher-type complexes is regarded as donor-acceptor binding and results from the σ-donation from the lone pair on the singlet carbene to the metal (empty d-orbital) and π-back-donation from the metal (filled orbital with similar symmetry) to the carbene (vacant p_π orbital), illustrated in *Figure 3.2a*.[1] Fischer carbenes therefore, typically bind to low oxidation state metal fragments. In contrast, Schrock-type complexes coordinate in a more covalent manner which arises from the pairing of σ and π electrons between a triplet carbene and a triplet metal (*Figure 3.2b*).[1] Thus, Schrock carbenes generally bind with high oxidation state metal fragments.
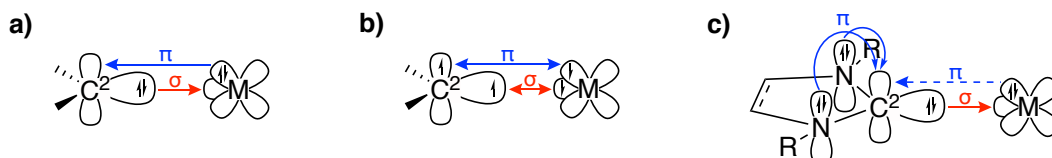
Figure 3.2. Bonding schematic of: a) Fischer-type complexes; b) Schrock-type complexes; c) NHC complexes.

However, NHC complexes where the carbene bears two π-donor substituents adjacent to the carbenic centre are not classified as either Fisher- or Schrock-type complexes since they coordinate to transition metals predominately by σ-donation;

the π-backbonding from the metal was historically considered to be negligible although in more recent years it has been shown that π-backbonding depends significantly on the NHC employed (*figure 3.2c*).[1] The presence of strongly π-donating substituents adjacent to the carbenic carbon increases the energy of carbenic carbon p_π orbital (compared to Fischer carbenes) enough to cause poor overlap between the metal and the NHC p_π orbital,[1] giving rise to negligible π-back-bonding. This is why NHCs can bind to metals which are incapable of π-back-bonding and thus why NHC complexes have been reported with nearly all transition metals.[1]

NHCs are very widely utilised in organometallic chemistry as they have properties which are highly tuneable and easily synthetically accessible.[4] They allow access to a wide range of complexes, of which half-sandwich nickel(II) complexes [Ni(η^5-C$_5$H$_5$)(X)(NHC)] [generally X = Cl, Br, I], NHC copper(I) complexes [(NHC)CuX], and bis-NHC copper(I) complexes [Cu(NHC)$_2$]X] [generally X = Cl, Br, I, BF$_4$] are relevant to this work. NHC-metal complexes have been shown to catalyse a range of reactions including styrene polymerisation, methyl methacrylate polymerisation, cross-coupling reactions, conjugate addition reactions, carbene transfer reactions, diboration reactions, hydrosilylation reactions and others.[4-8]

Coordination to selenium, forming NHC-selenium adducts, can be used to determine the σ-donor and π-acceptor properties of these NHC ligands.[9,10] The ^{77}Se coupling and NMR parameters of the NHC-selenium adducts offer a way of correlating the $^1J_{\text{C-Se}}$ coupling constant in the ^{13}C{^{1}H} NMR spectrum to the σ-donor ability of the respective carbene and alternatively the ^{77}Se chemical shift with the π-acceptor ability of the respective carbene.[9,10]

Having synthesised the imidazolium precursors (**2** and **5**) to two novel NHCs, see *chapter two*, a small selection of simple complexes were synthesised to determine the donor properties and behaviour of these new ligands. Copper, silver, nickel, and selenium complexes were targeted as cheap and accessible species whose

analogues with other NHCs have been used in a range of useful chemistry. Due to time constraints, only the coordination of **3** was explored.

3.2 Results and discussion

### 3.2.1 Synthesis of 1,3-bis(2-methoxyphenyl)-4,5-dimethylimidazole-2-selenone, 7

As mentioned above, the selenium adduct of NHC, **3**, which may also be regarded as a selenourea, was targeted to probe the potential donor and acceptor properties of this species.

3.2.1.1 Preparation

Selenourea adducts are typically prepared *via* oxidation of imidazolium salts with selenium in the presence of a base such as potassium carbonate or LiHMDS.[9-15] Initial attempts with **2a** or **2c** indicated the formation of the desired target, **7**, but produced either mixtures contaminated with side products or a mixture of **7** and imidazolium, **2**. Nevertheless, the crude, impure **7** was sufficient to allow the growth of a small number of single crystals which were separated manually from a contaminating poorly formed solid. Characterisation by SCXRD unambiguously confirmed the generation of **7**. Subsequently, a range of different purification methods were attempted to isolate clean product, in varying combinations of filtration through silica or Celite®, extraction, and precipitation, however all attempts were unsuccessful. Separation of the desired product from the imidazolium, **2**, was unfortunately not successful due to both compounds having similar solubilities. Therefore, complete (or very close to) conversion into **7** was required as purification of a mixture showed to be unviable.

Since *in situ* generation of the free NHC, **3**, with Se was ineffective, the formation of the selenourea adduct was attempted from the reaction of the isolated free NHC, **3**, with selenium in THF and Et$_2$O. However, neither effort proceeded cleanly and instead like before afforded impure **7**. After such results, further searching of the literature revealed a paper by Nelson[16] which reported the synthesis of selenourea adducts *via* a concentrated solution of imidazolium salt, selenium and potassium *tert*-butoxide in THF. In view of this, preparation was attempted by the reaction of the imidazolium chloride, **2a**, with excess potassium *tert*-butoxide and excess

selenium in minimal amounts of THF (*Scheme 3.1*), which after work-up yielded the desired product, **7**, which was characterised by multinuclear NMR spectroscopy.
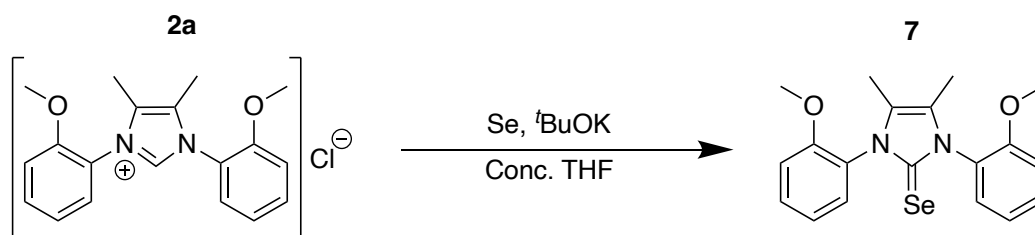
Scheme 3.1. Reaction of **2a** with selenium and potassium tert-butoxide in concentrated THF.

For characterisation, the selenourea adduct, **7**, was initially dissolved in *protio*-DCM. Surprisingly, however, it started to decompose after approximately one hour to give unidentified decomposition products (*Figure 3.3*). This raised the question of whether the selenourea adduct was light sensitive or unstable in DCM.
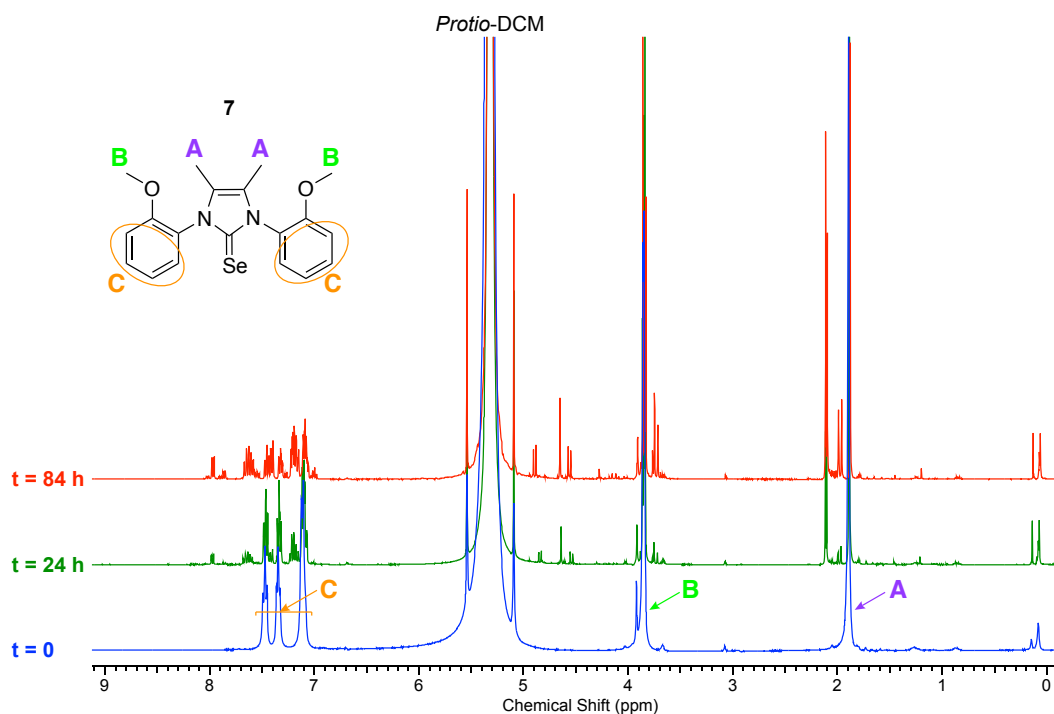
Figure 3.3. ^{1}H NMR spectra of **7** recorded in *protio*-DCM: a) t = 0; b) t = 24 hours; c) t = 84 hours.

As a preliminary test, two separate NMR samples of **7** in *protio*-DCM were made and one was exposed to light whilst the other was kept in the dark. Both ^{1}H NMR spectra revealed that the samples had decomposed, ruling out the light sensitive

theory and therefore indicating **7** is unstable in DCM. Therefore, characterisation of **7** was carried out in *protio*-MeCN.

The same method was attempted to generate **7** from the imidazolium tetrafluoroborate salt, **2c**. This was unsuccessful, and afforded a green solid which was identified as impure **7** by ^{1}H NMR.

3.2.1.2 Multinuclear NMR spectroscopy analysis

The ^{1}H NMR spectra of **7**, in both solvents (*protio*-DCM and -MeCN) displayed two separate, overlapping singlets in the 3.80 ppm region, corresponding to the protons on the methoxy group (A). It was therefore tentatively believed that the two overlapping singlets represented the presence of syn- and anti-conformers in slow exchange, illustrated in *Figure 3.4*. Nevertheless, all the other ^{1}H signals were coincident.
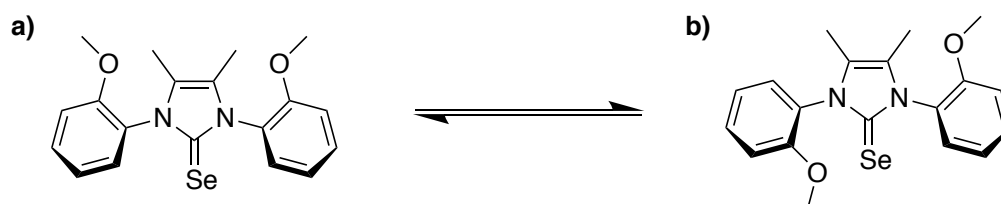
Figure 3.4. The two conformers that SeIAnis^Me, **7**, exists in: a) Syn-conformer; b) Anti-conformer.

This was further speculated by variable temperature ^{1}H NMR. Upon heating the solution from 298 K to 348 K, the two overlapping singlets due to the OMe groups (A) coalesce and upon cooling appear again, depicted in *Figure 3.5*. This tentatively demonstrates that at lower temperatures the rotation of the anisole rings is slow on the NMR timescale and hence two signals are displayed.
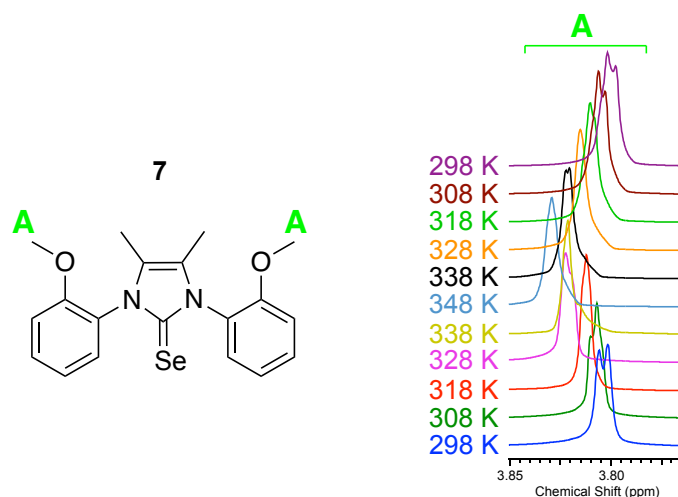
Figure 3.5. Variable temperature ^{1}H NMR spectra of SeIAnis^{Me}, **7**, displaying the OMe signals (B) coalescing.

The two conformers are also apparent in the ^{13}C{^{1}H} NMR spectrum of **7** where the majority of the carbon environments are represented by two signals. This is because ^{13}C chemical shifts are much more sensitive to changes in the chemical environment (a net effect of inherently narrower linewidths and wider shift-range). It was reported by Ganter[10] that there was no obvious correlation between the ^{77}Se and the C$_{carbene}$ ^{13}C chemical shifts of the selenourea compound studied in the paper and that such data are not informative, and do not indicate the electronic properties of the NHC. No $^1J_{C\text{-Se}}$ coupling was observed for the C$_{carbene}$ of **7** in the ^{13}C{^{1}H} NMR spectrum due to poor signal intensity and therefore the σ-donor capability of the NHC could not be inferred; and unfortunately, there was no time to return to this prior to the submission of this thesis.[9]

Ganter also reported that the ^{77}Se chemical shift of NHC-selenourea adducts can be used to determine the π-accepting abilities of NHCs.[9,10] Similarly, Bertrand reported that the ^{31}P chemical shifts of NHC-phosphinidene adducts can also be used to assess the π-accepting properties of NHCs.[17] Such measurements are independent of the adduct's NHC σ-donating ability, unlike Tolman electronic parameter (TEP) measurement which is commonly employed for the exploration of NHCs electronic properties.[18] Both the phosphinidene and selenourea adducts can be represented by two canonical structures, a polarised structure featuring a C-P/Se dative bond or

as a neutral hetero-alkene (*Figure 3.6*). The ^{31}P and [77]Se chemical shifts correlate to the relative contribution to bonding in the adduct of the two canonical structures.[9] Both Bertrand and Ganter demonstrated that the ^{31}P and ^{77}Se NMR chemical shifts of NHC-phosphinidene and NHC-selenourea adducts, which are shifted further downfield correspond to π-acidic NHCs with substantial π-backbonding and which are best described as neutral hetero-alkenes (a C=P/Se double bond), whereas signals shifted further upfield correspond to the dative polarised structures (C-P/Se single bond).[9]
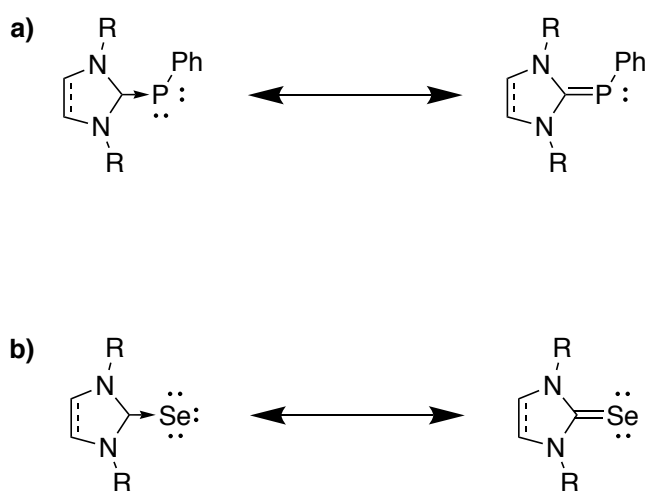
Figure 3.6. The two canonical structures of: a) NHC-phosphinidene adducts; b) NHC-selenourea adducts.

Two years later, Cavallo applied both methods to a broad range of NHCs and confirmed that either the ^{31}P or [77]Se chemical shifts of the corresponding adducts can be utilised to determine the π-accepting capabilities of NHC ligands.[18] They report the [77]Se chemical shifts (δ_{Se} in chloroform-*d*) for a range of selenourea compounds featuring different NHCs ligands with increasing π-accepting ability such as: ICy (δ_{Se} -22 ppm), I[i]Pr[Me] (δ_{Se} -18 ppm), IMes (δ_{Se} 27 ppm), IPr (δ_{Se} 90 ppm), SIMes (δ_{Se} 110 ppm), SIPr (δ_{Se} 190 ppm), IAd (δ_{Se} 197 ppm), and more in a scale which spans from -22 to 197 ppm.[18] The ^{77}Se NMR of **7** showed two signals, corresponding to the two conformers present at δ_{Se} 67.12 and 65.18 ppm in *protio*-MeCN. Since chemical shifts are very sensitive to temp, concentration, pH, and solvent, the comparison of such results can only tentatively indicate the π-accepting capability of the IAnis[Me], **3**, and should be used with caution.[18] Interpreted within the [77]Se chemical shift range described by Cavallo, the ^{77}Se NMR

chemical shifts of **7** lie in the middle which indicate that the complex is best described as neither dative nor neutral, but instead somewhat in the middle of both. Therefore, **3** cannot be described as either a strong or weak π-accepting ligand.

3.2.1.3 Single-crystal X-ray diffraction analysis

Crystals suitable for SCXRD analysis were obtained *via* the slow diffusion of hexane into a concentrated solution of **7** in DCM and X-ray crystal structure data unambiguously confirmed the formation of the selenourea (*Figure 3.7*). Compound **7** crystallises in the space group Pnma with half a molecule of **7** and half a molecule of DCM in the asymmetric unit with the anisole rings of the NHC adopting a syn-configuration. The DCM molecule shows short C-H...OMe contacts (d_{O-C} = 3.150 Å), longer than the sum of the van der Waals radii but suggesting some electrostatic interaction. The crystal structure has a C-Se bond distance of 1.849(4) Å and an N-C-N bond angle of 105.4(3)°, in accordance with other similar selenourea complexes.[9,11,19] Generally the C-Se bond lengths of NHC-selenourea adducts vary between 1.82 to 1.86 Å, however, complexes containing strongly π-acidic NHCs typically feature shorter bond lengths of around 1.78 Å.[9,11,19,20] Whereas, complexes with C-Se single bonds feature longer bond lengths of around 1.89 Å.[9,20] Therefore, the C-Se bond length of **7**, lies in the middle of the range.
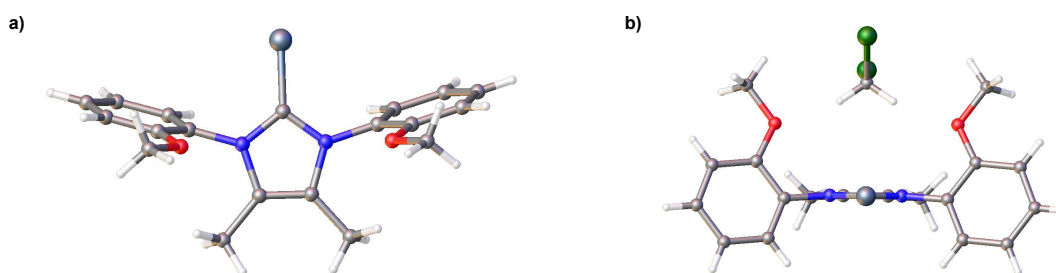

Figure 3.7. Crystal structure of SeIAnis[Me], **7**: a) Top-down view with solvent omitted for clarity; b) View down C=Se axis.

3.2.2 Synthesis of (η⁵-C₅H₅)NiCl(1,3-bis(2-methoxyphenyl)-4,5-dimethylimidaozl-2-ylidene, 8

3.2.2.1 Preparation

The preliminary attempt to prepare a half-sandwich nickel(II) complex by the reaction of nickelocene with **2a** by a modified preparation by Cowley *et al.*[21] was successful, affording red crystals of **8** (*Scheme 3.2*).

Scheme 3.2. Reaction of **2a** with nickelocene.
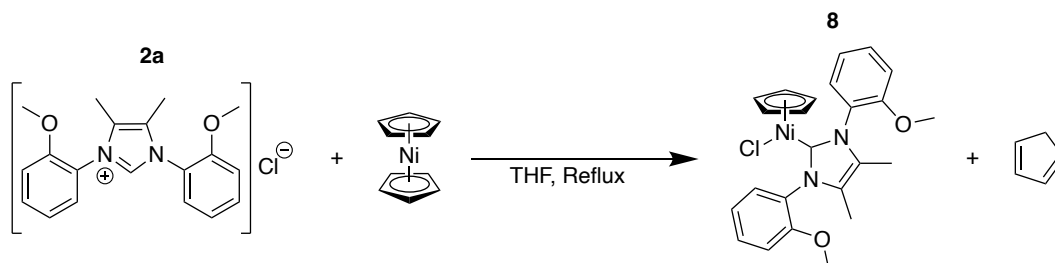
The structure was confirmed by SCXRD. However, the ^{1}H NMR spectrum of a concentrated sample prepared for ^{13}C{^{1}H} NMR displayed broader signals, as shown in *Figure 3.8*.
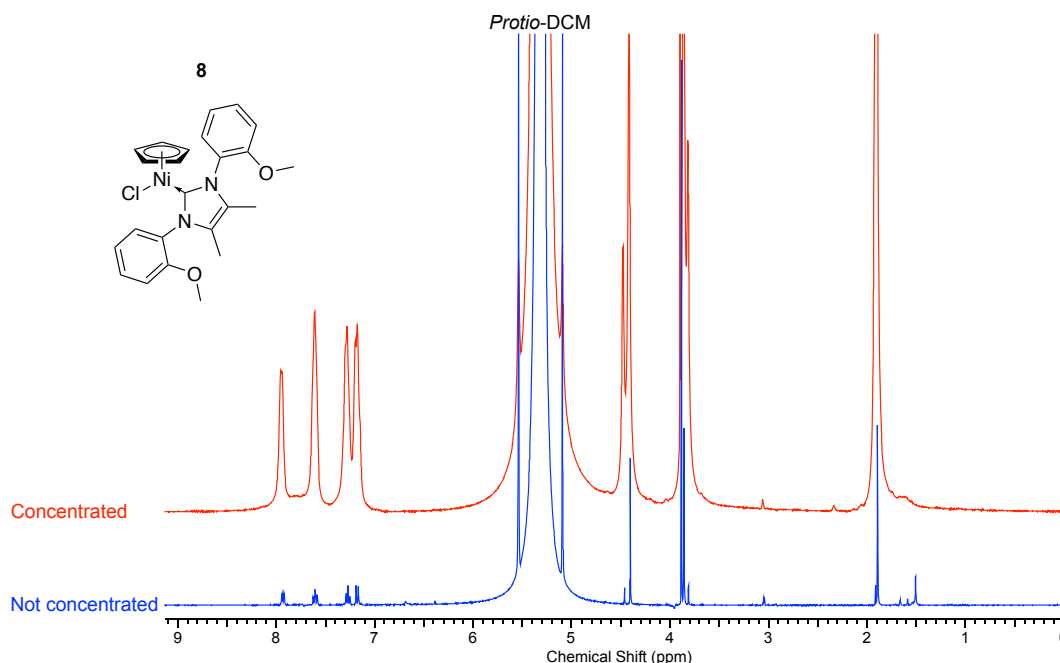
Figure 3.8. ^{1}H NMR spectra of [Ni(Cp)(Cl)(IAnis^{Me})], **8**: a) Not concentrated; b) Concentrated.

There are three typical causes for broad peaks in NMR: paramagnetic broadening, exchange broadening, or quadrupolar broadening. However, since **8** is not paramagnetic or doesn't contain any significant quadrupolar nuclei, this suggested

slow exchange as the cause but the nature of these processes could not be explained. However, further searching of the literature revealed that the work-up procedure used sometimes affords the desired product with paramagnetic impurities which cause the broadening of the peaks in the ^{1}H NMR spectra; an alternative work-up to circumvent this problem was reported.[22] The reaction of nickelocene with **2a** was thus repeated, followed by the alternative work-up reported; filtration though Celite® and removal of the solvent to afford a crude dark red solid which was washed with hexane and dried *in vacuo* was identified as impure **8** by ^{1}H NMR.[22] Subsequent crystallisation afforded red crystals that were confirmed by multinuclear NMR spectroscopy and elemental analysis to be pure **8**, with no broadening of signals in ^{1}H NMR spectra upon concentration of **8**.

3.2.2.2 Multinuclear NMR spectroscopy analysis

The ^{1}H NMR spectrum of **8** displays two separate singlets for three different groups: the η^5-Cp ring (two peaks at δ 4.48 and 4.42 ppm, with a total integration of 5H), the methoxy groups (two peaks at δ 3.86 and 3.82 ppm, with a total integration of 6H), and the methyls on the backbone (two peaks at δ 1.92 and 1.90 ppm, with a total integration of 6H); the ligand aryl peaks are not split. As before (*vide supra*), this is tentatively attributed to the presence of syn- and anti-conformers of the complex.

Variable temperature ^{1}H NMR studies revealed that upon heating the sample from 298 K to 348 K, the singlets corresponding to the η^5-Cp ring (A) and the OMe groups (B) did not coalesce, illustrated in *Figure 3.9*; the peaks corresponding to the methyls on the backbone were under the solvent peak (*protio*-MeCN) and therefore are not displayed. That the peaks did not coalesce indicates that the rotation of the anisole rings is either slow on the NMR timescale, or does not occur at all and a mixture of different static conformers are present in solution.
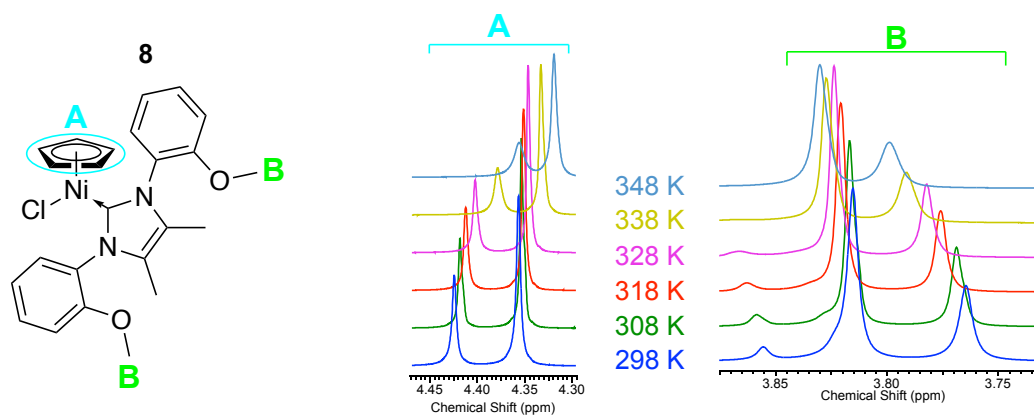
Figure 3.9. Variable temperature ^{1}H NMR spectra of [Ni(Cp)(Cl)(IAnis^{Me})], **8,** displaying that the peaks corresponding to the Cp ring (A) and the OMe groups (B) did not coalesce.

The ^{13}C{^{1}H} NMR spectrum of **8** likewise shows the presence of two conformers and the majority of the carbon environments are represented by two signals.

3.2.2.3 Single-crystal X-ray diffraction analysis

Crystals suitable for SCXRD analysis were obtained *via* gradual cooling of the saturated toluene solution, followed by additional cooling in the freezer to -20 °C, and X-ray crystal structure data was obtained for **8** (*Figure 3.10*) which unambiguously confirmed the formation of the desired half-sandwich nickel(II) complex. Compound **8** crystallises in the space group Pbca with one molecule of **8** in the asymmetric unit with the anisole rings of the NHC adopting a syn-configuration. The structure has C-Ni, Ni-Cl, and Ni-Cp (to centroid) bond lengths of 1.8651(19), 2.1994(6), and 1.7687(12) Å, respectively and C-Ni-Cl, C-Ni-Cp (to centroid), Cl-Ni-Cp (to centroid), and N-C-N bond angles of 95.22(6), 129.10(7), 135.65(4), and 104.51(16)°, respectively. These values are similar to those of other half-sandwich nickel(II) complexes reported in the literature.[4,21,23] The most relevant example is [Ni(η^5-C$_5$H$_5$)(Cl)(IMes)] and has C-Ni, Ni-Cl, and Ni-Cp (to centroid) bond lengths of 1.917(9), 2.185(2), and 1.760(7) Å, respectively, and C-Ni-Cl, C-Ni-Cp (to centroid) and Cl-Ni-Cp (to centroid) bond angles of 98.4(2), 132.4(2), 129.2(2)°, respectively.[21]
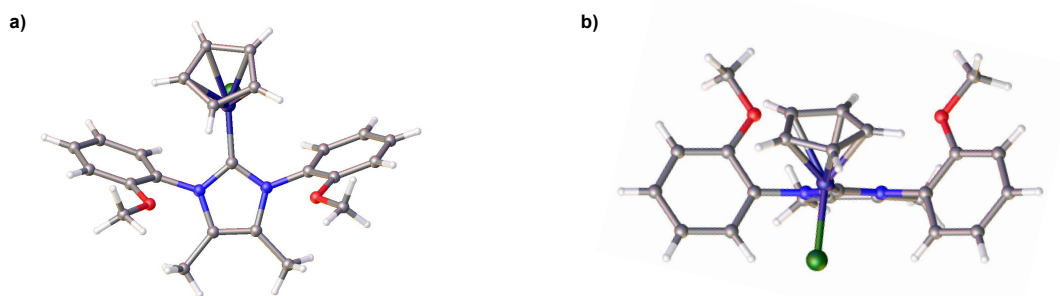
**Figure 3.10.** Crystal structure of [Ni(Cp)(Cl)(IAnis^{Me})], **8**: a) Top-down view; b) Profile view.

3.2.3 Synthesis of (1,3-bis(2-methoxyphenyl)-4,5-dimethylimidazol-2-yl)silver chloride, 9

3.2.3.1 Preparation

A preliminary preparation, using a modified method developed by Cazin[24], of the silver(I) complex, **9**, from **2a** and silver(I) oxide in H$_2$O in an argon purged glass vial proceeded successfully (*Scheme 3.3*). Formation of the product **9** was readily identified in the ^{1}H NMR spectrum with two peaks for the OMe groups being observed and the absence of the imidazolium C-H resonance. Compound **9** was also characterised by SCXRD.
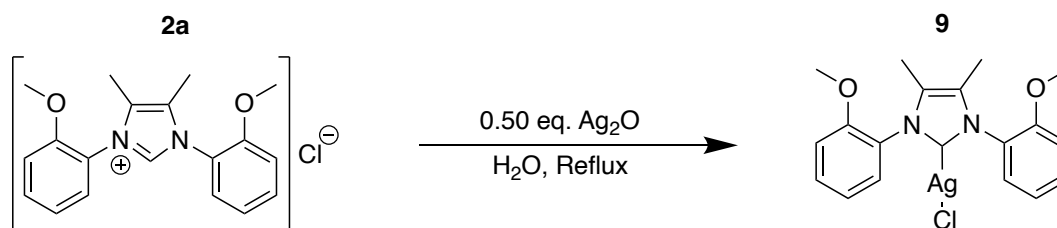
Scheme 3.3. Reaction of **2a** with silver(I) oxide.

However, upon scaling-up the reaction only a yield of 31 % was obtained. This was substantially lower than Cazin's reported yields ranging from 58 to 92 %.[24] Therefore, the reaction was repeated under inert atmosphere to see if higher yields could be obtained. This afforded **9** as a beige solid in a good yield (59 %), which was confirmed as pure by ^{1}H NMR and elemental analysis.

Although a 59 % yield was good, it was hoped that enhanced yields could be obtained by alternative routes. In view of this two-other preparations were

attempted. The first was a modified procedure reported by Leitner[25] with the reaction of **2a**, silver(I) oxide, and potassium hydroxide in degassed H_2O followed by a work-up in air. The reaction proceeded well, to give a good yield of 70 %; the product was, however, shown to contain water and therefore that is just a crude yield. Simultaneously, a modified procedure from Gimeno[26] was attempted. **2a** and silver nitrate were combined in DCM, followed by the addition of potassium carbonate and the reaction mixture was stirred at ambient temperature for two hours. After work-up, this afforded a cream solid which was identified as a mixture of **9** and **2a** by ^{1}H NMR in 7:3 ratio, respectively. As the reaction did not go to completion, it was repeated with a longer reaction time (20 hours). This afforded a 54 % yield contaminated with Et_2O. In view of all these results, the modified Leitner method could potentially be the best yielding procedure but further work would be required to acquire pure product.[25] As such, the Cazin method is currently the most efficient procedure at producing **9**.[24]

3.2.3.2 Multinuclear NMR spectroscopy analysis

Like **7** the ^{1}H NMR spectrum of **9**, contains two overlapping singlets at δ 3.85 and 3.83 ppm, corresponding to the OMe groups (A) which are tentatively assigned as syn- and anti-conformers (*vide supra*). This is the only environment which displays this effect; the signals for the other environments are coincident between conformers. Variable temperature ^{1}H NMR data showed that upon heating the solution from 298 K to 348 K the two overlapping singlets coalesced and upon cooling separated again, depicted in *Figure 3.11* (explanation *vide supra*).
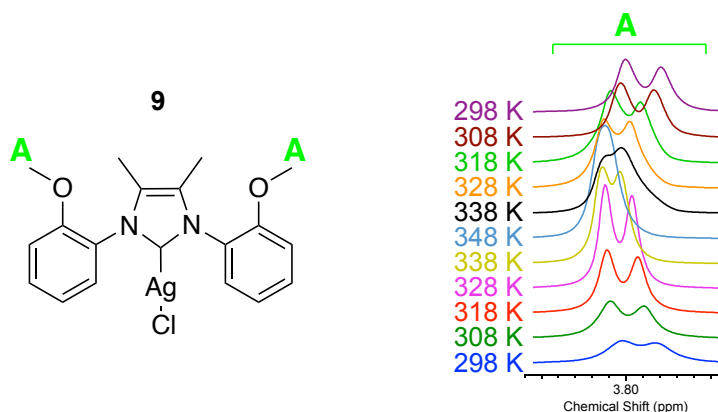

Figure 3.11. Variable temperature ^{1}H NMR spectra of [AgCl(IAnis^Me^)], **9**, displaying the OMe signals (A) coalescing.

The $^{13}C\{^1H\}$ NMR spectrum of **9**, as for **7**, displays two (generally overlapping) singlets for majority of the signals corresponding to different carbon environments. No $C_{carbene}$ signal was observed in the $^{13}C\{^1H\}$ NMR spectrum (i.e. up to 220 ppm); the absence of $C_{carbene}$ signal may be due to the quaternary $C_{carbene}$'s long relaxation time.

3.2.3.3 Single-crystal X-ray diffraction analysis

Crystals suitable for SCXRD analysis were obtained *via* the slow diffusion of hexane into a concentrated solution of DCM and X-ray crystal structure data was obtained for **9**, (*Figure 3.12*) which unambiguously confirmed the formation of the silver(I) complex with the anisole rings adopting an anti-configuration. Compound **9** crystallises in the space group P2$_1$/c with one molecule of **9** in the asymmetric unit. The complex has a two-coordinate silver(I) centre with a C-Ag-Cl bond angle of 175.94(10)°, in a near linear environment (close to 180°). The C-Ag and Ag-Cl bond distances are 2.073(4) and 2.3147(12) Å, respectively and the N-C-N bond angle is 104.3(3)°, which are in accord with other silver(I) complexes.[27-30]
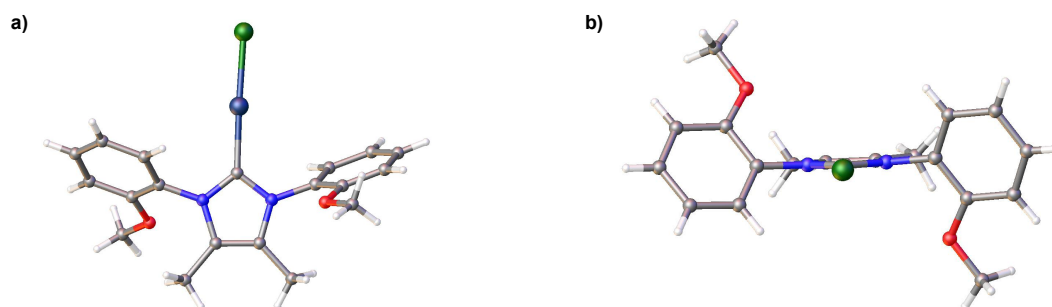
**Figure 3.12.** Crystal structure of [AgCl(IAnis^{Me})], **9**: a) Top-down view; b) View down C-Ag axis.

3.2.4 Synthesis of (1,3-bis(2-methoxyphenyl)-4,5-dimethylimidazol-2-yl)copper chloride, 10

3.2.4.1 Preparation

Synthesis of **10** was attempted *via* a modified method developed by Cazin[24] from **2a** and copper(I) oxide in H$_2$O in a glass vial purged with argon (*Scheme 3.4*), and isolated *via* an alternative work-up; the supernatant was removed by filtration, the filtered solid was extracted into DCM, and the product precipitated by addition of either EtOAc or hexane. This proceeded successfully and the structure was confirmed by SCXRD to be **10**. The disappearance of the C-H imidazolium

resonance in the ^{1}H NMR spectrum did not conclusively indicate the formation of the copper(I) complex and could have also been attributed to the formation of the corresponding urea, an imidazolidin-2-one with a carbon-oxygen double bond instead, as reported by Cazin.[24]
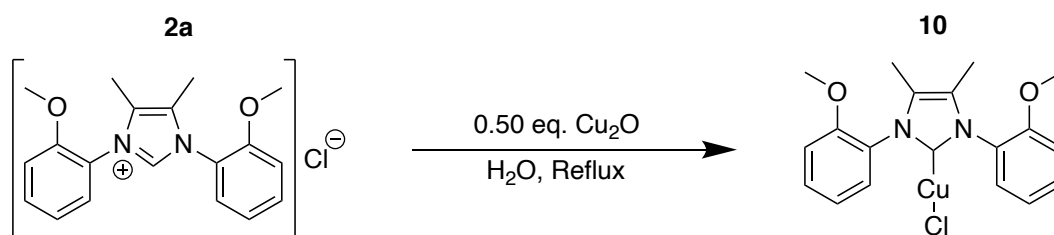

Scheme 3.4. Reaction of **2a** with copper(I) oxide.

However, upon scale up, the reaction produced a minuscule yield of 13 %. However, when making a concentrated solution for ^{13}C{^{1}H} NMR, not all the solid added dissolved, which indicated that **10** has low solubility in DCM and so may be being lost in work-up. As for **10**, the reaction was repeated under inert atmosphere to see if enhanced yields could be obtained. This increased the yield substantially but nevertheless still only afforded a 39 % yield. This yield, although improved, was still very low especially when compared to yields reported by Cazin *via* this route which produced yields ranging from 72 to 88 %.[24]

3.2.4.2 Multinuclear NMR spectroscopy analysis

As for **7** and **9**, the OMe resonances (A) of **10** are seen as two overlapping singlets at δ 3.87 and 3.85 ppm in the ^{1}H NMR spectrum, tentatively assigned as syn- and anti-conformers (vide supra). Variable temperature ^{1}H NMR data showed that the two singlets coalesced (at 318 K) upon heating the solution from 298 K to 348 K, illustrated in *Figure 3.13*, and upon cooling separated out again. This occurs at a temperature 30 K lower than **9** (at 348 K), indicating a lower barrier to exchange.
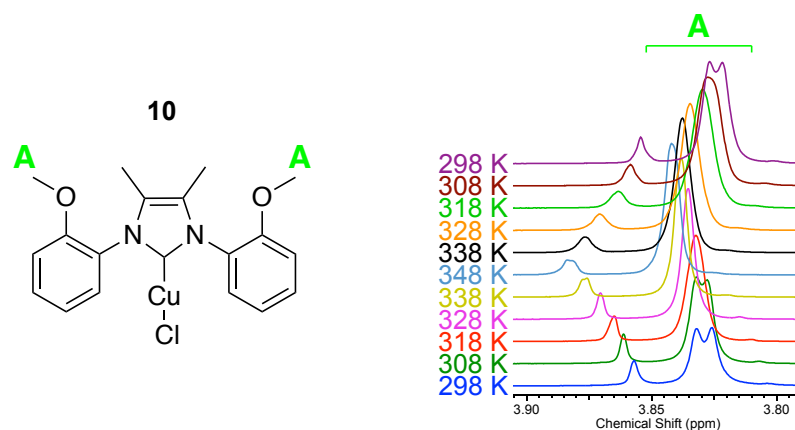
Figure 3.13. Variable temperature ^1H NMR spectra of [CuCl(IAnis^{Me})], **10**, showing the coalescence of the OMe signals (A).

The $^{13}C\{^1H\}$ NMR spectrum of **10**, as for [AgCl(IAnis^{Me})], **9**, exhibits two singlets (corresponding to the syn- and anti-conformers) for the majority of its carbon environments. In this case, the C$_{carbene}$ signal for **10** was observed as two overlapping singlets at δ 176.40 and 176.37 ppm, in line with other mono-NHC copper(I) complexes in the literature.[31-34]

3.2.4.3 Single-crystal X-ray diffraction analysis

Crystals of **10** suitable for SCXRD analysis were obtained *via* the slow diffusion of hexane into a concentrated solution of DCM and the X-ray crystal structure for **10** (*Figure 3.14*), unambiguously confirmed the formation of the monomeric copper(I) complex.
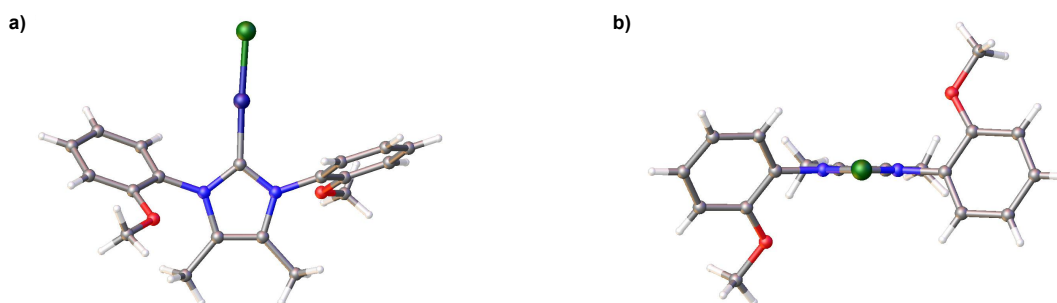
Figure 3.14. Crystal structure of [CuCl(IAnis^{Me})], **10**: a) Top-down view; b) View down C-Cu axis.

Compound **10** crystallised in the space group P2$_1$/c with one molecule of **10** in the asymmetric unit, with the anisole rings of the NHC adopting an anti-configuration. The monomeric complex has a two-coordinated copper(I) centre in a close to linear environment with a C-Cu-Cl bond angle of 177.39(13)˚. The C-M-Cl (M= Ag or Cu)

bond angle of **10** is closer to the ideal linear geometry 180˚ than **9** (175.94(10)°). The C-Cu and Cu-Cl bond distances are 1.896(5) and 2.0885(13) Å, respectively, and the N-C-N bond angle is 103.9(4)°; these are in accordance with other monomeric copper(I) complexes, as shown in *table 3.1*.[31-36]

Compounds	Bond lengths (Å)		Bond angles (°)		Reference
	C-Cu	**Cu-Cl**	**C-Cu-Cl**	**N-C-N**	
10	1.896(5)	2.0885(13)	177.39(13)	103.9(4)	---
[CuCl(IMes)]	1.956(10)	2.091(2)	180.000(1)	109.3(8)	34
[CuCl(IMes^{Me})]	1.92(1)	2.124(4)	179.5(5)	108(1)	35
[CuCl(IPr)]	1.881(7)	2.106(2)	176.7(2)°	*	36

Table 3.1. Bond lengths and angles of monomeric copper(I) complexes (*not reported).

3.2.5 Synthesis of bis(1,3-bis(2-methoxyphenyl)-4,5-dimethylimidazol-2-yl)copper tetrafluoroborate, 11

3.2.5.1 Preparation

The synthesis of **11** was initially attempted by the treatment of **2a** with 0.25 equivalents of Cu_2O and one equivalent of $NaBF_4$ (for *in situ* anion metathesis) in H_2O in a glass vial purged with argon. This was not successful, and instead the isolated solid was identified as an imidazolium salt (either **2a** or **2c**) by ^{1}H NMR. The procedure was repeated using the imidazolium tetrafluoroborate salt, **2c**, instead and therefore without the addition of $NaBF_4$, but like before the afforded solid was identified as **2c** by ^{1}H NMR.

Alternative methods were therefore sought out. The first to be pursued was a modified preparation by Nolan.[7] **2c**, 0.5 equivalents of $Cu(MeCN)_4BF_4$, and one equivalent of $^{t}BuOK$ were combined in THF for a one-pot metalation reaction. After work-up, this afforded a green tar which was shown to be impure **2c** by ^{1}H NMR with the possibility of a tiny amount of the desired product present. In view of this, a modified procedure from Cisnetti[37] was attempted. The treatment of **2a** with 0.24 equivalents copper(I) oxide in EtOH, followed by the addition of aq. NH_3 to form a soluble copper(I)-ammine complex $[Cu(NH_3)_2]^+$ with Cu_2O (*Scheme 3.5*).[37]
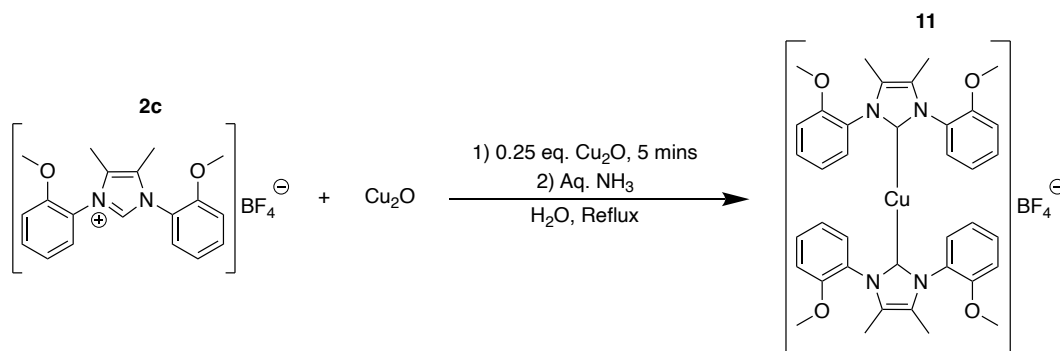
Scheme 3.5. Reaction of **2a** with 0.25 eq. copper(I) oxide and aq. NH_3.

After work-up, this yielded an off-white solid which was confirmed as **11** by ^1H NMR and SCXRD. The reaction was repeated on a larger-scale, but without the same success. The scaled-up reaction yielded a yellow tar after work-up which was identified as a mixture of **11** and **2c** by ^1H NMR. It was suggested that the reaction mixture did not contain enough water as Cisinetti's syntheses were carried out in aqueous conditions. Thus, the reaction was repeated with the addition of water and proceeded efficiently to give a wet, white solid in ~56 % yield (only an approximate yield, as the solid was wet with water) which was confirmed as **11** by multinuclear NMR. The elemental analysis was not as expected, however, and therefore, drying the material was attempted by precipitations, multiple drying *in vacuo*, and recrystallisation. Unfortunately, all attempts were found to be unsuccessful as the presence of EtOH and hexane now remained in the ^1H NMR spectra, instead of water and subsequent combustion analysis was also unsatisfactory.

3.2.5.2 Multinuclear NMR spectroscopy analysis

The ^1H NMR spectrum of **11**, displayed five singlets corresponding to the OMe protons (A) and three singlets corresponding to the backbone methyl protons. All the aryl peaks coincide, appearing as two multiplets integrating to 18 protons. The appearance of multiple singlets is explained by the non-equivalence of the NHC ligands and the different conformations possible for the NHC ligands (syn or anti).[38] Variable temperature ^1H NMR spectra confirmed presence of dynamic processes involving the NHC ligands. On heating from 298 K to 348 K, all the five singlets coalesced, illustrated in *Figure 3.15*, and upon cooling the peaks separated out

again. The backbone methyl protons were not observed in the variable temperature ^{1}H NMR spectra as they are under the solvent peak (*protio*-MeCN).
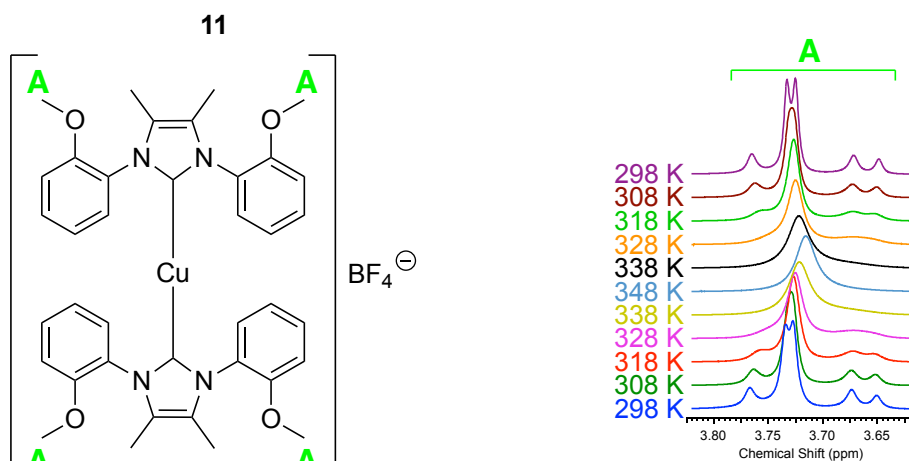

Figure 3.15. Variable temperature ^{1}H NMR spectra of [Cu(IAnis^{Me})$_2$]BF$_4$, **11**, showing the coalescence of the OMe signals (A).

This phenomenon was also observed in the ^{13}C{^{1}H} NMR spectrum of **11**. The majority of the signals corresponding to each carbon environment were split into multiple peaks, including the C$_{carbene}$ signal for **11** which were observed in the region of δ 175.78 to 175.13 ppm.

3.2.5.3 Single-crystal X-ray diffraction analysis

Only poor-quality crystals of **11** were obtained *via* the slow diffusion of hexane into a concentrated solution of DCM at 4 °C. The SCXRD data was sufficient to unambiguously confirm the connectivity and nature of **11** in its homoleptic form as shown in *Figure 3.16*, but not for detailed analysis of the bond metrics. The asymmetric unit of compound **11** consists of two crystallographically inequivalent quarters of **11** and half a molecule of BF$_4$. The anisole rings of each NHC adopt anti-configuration and are also anti with respect to the opposite rings on the other bound NHC.
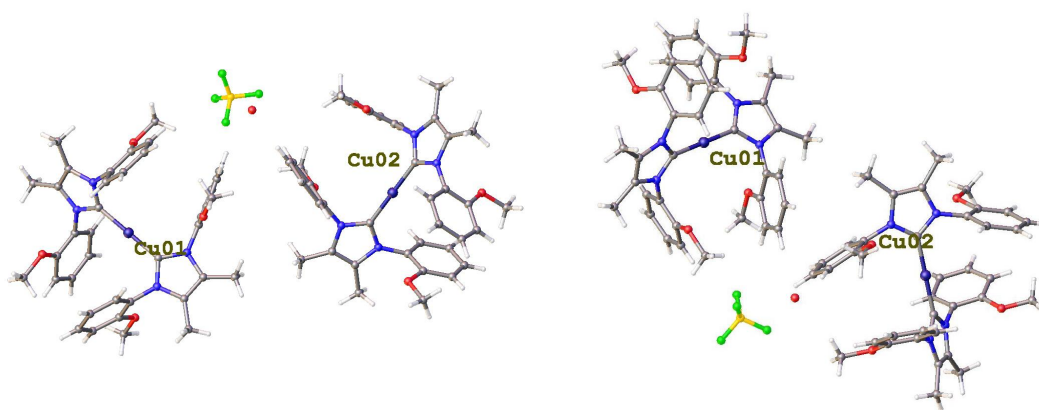
Figure 3.16. Crystal structure of ([Cu(IAnis^{Me})$_2$]BF$_4$), **11**, depicted in two different projections (left and right). The lone oxygen is unresolved water.

3.2.6 Percent buried volumes (%V$_{Bur}$)

To evaluate the steric bulk, the software SambVca 2.0[39] was used to generate %V$_{Bur}$ for the four metals complexes **7**, **8**, **9**, and **10** with good single crystal data, all bound to the same ligand IAnis^{Me}; the results are shown in *table 3.2*.

Metal complexes	%V$_{Bur}$
SeIAnis^{Me}, **7**	26.5
[Ni(Cp)(Cl)(IAnis^{Me})], **8**	28.1
[AgCl(IAnis^{Me})], **9**	28.5
[CuCl(IAnis^{Me})], **10**	28.2

Table 3.2. %V$_{Bur}$ of the synthesised metal complexes.

Upon comparing the %V$_{Bur}$ of **9** to [AgCl(IMes)] (%V$_{Bur}$ = 34.8)[40] and of **10** to [CuCl(IMes^{Me})] (%V$_{Bur}$ = 30.5)[35], the steric demand of the IAnis^{Me} ligand is significantly less than that of IMes and IMes^{Me}.[41]

3.3 Conclusion

The IAnis^{Me} (NHC) ligand, **3**, has been shown successfully to coordinate to selenium, nickel, silver, and copper. A number of mono-NHC complexes were synthesised, and in the case of copper, also a homoleptic, cationic copper complex. The metal complexes were all characterised by multinuclear NMR and single-crystal X-ray diffraction. The π-accepting ability (an electronic property) of the ligand was also investigated by the ^{77}Se chemical shift of the selenourea adduct. In some cases, poor yields were obtained and therefore, if intended to use in subsequent reactions, more viable methods would need to be sought out for atom efficiency.

3.4 Experimental

3.4.1 Synthesis of 1,3-bis(2-methoxyphenyl)-4,5-dimethylimidazole-2-selenone [Se(IAnis^{Me})], 7

3.4.1.1 Attempted synthesis of the selenourea adduct *via* generation of 3 *in situ* using bis(benzyltriethylammonium) carbonate

Selenium (0.107 g, 1.36 mmol), **2a** (0.316 g, 0.92 mmol), potassium carbonate (0.149 g, 1.08 mmol) and benzyltriethylammonium chloride (0.036 g, 0.16 mmol) were combined and THF (5 cm^3) was added. The resulting mixture was subsequently stirred at 85 °C for 24 h. The resulting mixture was filtered through silica in air and was washed with THF (5 cm^3). The solvent was removed under vacuum to give a brown tar (0.103 g, ~0.27 mmol, ~29 %) shown to be impure **7** by ^{1}H NMR. The silica was also washed through with DCM (10 cm^3) and the solvent was removed under vacuum which afforded a dark brown bubbly solid (0.22 g) which was identified as **2a** by ^{1}H NMR. X-ray quality crystals of **7** were grown by the slow diffusion of hexane into a concentrated DCM solution.

3.4.1.2 Attempted synthesis of the selenourea adduct *via* generation of 3 *in situ* using LiHMDS

2c (0.4004 g, 1.01 mmol), selenium (0.1235 g, 1.56 mmol), LiHMDS (0.1860 g, 1.11 mmol) were combined and THF (5 cm^3) was added. The resulting mixture was subsequently stirred at ambient temperature for 27 h. The solvent was removed under vacuum to afford a grey solid and the organic products were extracted into DCM (4 x 10 cm^3). The solvent was removed from the combined extracts to give a residue which was washed with hexane (2 x 5 cm^3) and dried *in vacuo* to afford a light brown solid which was identified as a mixture of **7**, **2c** and possibly **3** by ^{1}H NMR. In air, the light brown solid was dissolved in DCM (7 cm^3) and filtered through silica and the solvent was removed to afford a brown tar (0.063 g, ~0.16 mmol, ~16 %) which was identified as impure **7** by ^{1}H NMR. The silica was rewashed twice with DCM (30 cm^3) and the extracts were kept separate. The solvent was removed from both the extracts to afford yellow tars and both were identified as impure **7** by ^{1}H NMR.

3.4.1.3 Attempted synthesis of the selenourea adduct *via* generation of 3 *in situ* using LiHMDS, refluxed overnight

2c (0.4004 g, 1.01 mmol), selenium (0.1212 g, 1.53 mmol), LiHMDS (0.1857 g, 1.11 mmol) and THF (5 cm^3) were combined. The resulting mixture was subsequently stirred at 85 °C for 16 h. The solvent was removed under vacuum and the organic products were extracted into DCM (4 x 10 cm^3) and the extracts were filtered through Celite®. An *in situ* ^{1}H NMR of the filtrate suggested that both **7** and **2c** were present. The solvent was removed under vacuum and extracting the organic products into THF (3 x 10 cm^3) was attempted however the majority of the solid did not dissolve. The solvent was removed under vacuum from the THF extracts to give a minuscule quantity of a golden residue which was identified as a mixture of **7** and **2c** by ^{1}H NMR. The remaining solid was identified as a mixture of **7** and **2c** by ^{1}H NMR. Dissolving in hot THF (20 cm^3) was attempted, the supernatant was decanted, and was identified as a mixture of **7** and **2c** by ^{1}H NMR. The undissolved solid was washed with hexane (2 x 5cm^3) and dried *in vacuo* to give an off-white solid (0.126 g), which was also identified as a mixture of **7** and **2c** in a 9:1 ratio, respectively by ^{1}H NMR by integration of signals for methyl groups on the backbone.

3.4.1.4 Attempted synthesis of the selenourea adduct *via* isolated 3 in THF

3 (0.1359 g, 0.44 mmol), selenium (0.0350 g, 0.44 mmol) and THF (5 cm^3) were combined and the reaction mixture was subsequently stirred at ambient temperature for 17 h. The solvent was removed under vacuum to afford a solid. The crude solid was dissolved in DCM (15 cm^3), filtered through Celite® in air, and the filtrate was reduced in volume to ~10 cm^3. Hexane (40 cm^3) was added and the resulting solution was stirred, inducing precipitation. The resulting mixture was filtered and the residue washed with hexane (10 cm^3) to yield a light brown solid (0.072 g, ~0.19 mmol, 43 %) which was identified as impure **7** by ^{1}H NMR.

3.4.1.5 Attempted synthesis of the selenourea adduct *via* isolated 3 in Et$_2$O

3 (0.1555 g, 0.50 mmol), selenium (0.0413 g, 0.52 mmol), and Et$_2$O (5 cm^3) were combined and the resulting mixture was subsequently stirred at ambient temperature for 23 h. The solvent was removed under vacuum and the organic products were extracted into DCM (3 x 10 cm^3) and filtered through Celite®. The

filtrate was reduced in volume to ~5 cm^3 and hexane (30 cm^3) was added. The resulting mixture was stirred inducing precipitation. The supernatant was decanted *via* a filter cannula and the solid was washed with hexane (5 cm^3) to give a dark brown solid (0.0331 g, ~0.09 mmol, ~18 %) which was shown to be impure **7** along with trace amounts of imidazolium, **2**, by ^{1}H NMR.

3.4.1.6 Synthesis of the selenourea adduct *via* generation of 3 *in situ* from 2a using ^{t}BuOK in THF at high concentration.

2a (0.1378 g, 0.40 mmol), selenium (0.0912 g, 1.16 mmol), ^{t}BuOK (0.1795 g, 1.60 mmol), and THF (2 cm^3) were combined under the absence of light. The resulting mixture was subsequently stirred at ambient temperature for 66 h. The solvent was removed under vacuum to afford a solid which was dissolved in DCM (10 cm^3) and the solution was filtered through Celite®. The residue was washed with further DCM (10 cm^3), and the washings were combined. The solvent was removed under vacuum to afford a solid which was washed with hexane (3 x 5 cm^3) and dried *in vacuo* to yield **7**, as a brown solid (0.1256 g, 0.32 mmol, 80 %). **^{1}H NMR** (400 MHz, DCM, 16.20 °C): δ 7.47 (t, *J* = 15.22, 2H), 7.34 (t, *J* = 13.15 Hz), 7.11 (m, 4H), 3.86 and 3.85 (overlapping s, 6H), 1.90 (s, 6H). **^{1}H NMR** (400 MHz, MeCN, 16.20 °C): δ 7.47 (t, *J* = 15.83 Hz, 2H), 7.26 (m, 2H), 7.17 (d, *J* = 8.40 Hz), 7.08 (t, *J* = 15.10 Hz), 3.80 (overlapping s, 6H). **^{13}C{^{1}H} NMR** (100.52 MHz, MeCN, 17.20 °C): δ 158.49 and 158.41 ($C_{carbene}$), 155.69 and 155.63 (*C* phenyl or N*C*(CH$_3$)), 131.45 and 131.40 (*C*H phenyl), 131.26 and 131.22 (*C*H phenyl), 127.08 and 126.98 (*C* phenyl or N*C*(CH$_3$)), 125.00 (*C* phenyl or N*C*(CH$_3$)), 121.33 and 121.27 (*C*H phenyl), 113.26 and 113.21 (*C*H phenyl), 56.27 and 56.22 (O*C*H$_3$), 9.40 (*C*H$_3$). **^{77}Se NMR** (76.24 MHz, MeCN, 25.00 °C): δ 67.12, 65.18. Elemental analysis of the isolated brown solid was not as expected, therefore the brown solid was dissolved in MeCN (1 cm^3) followed by the addition of Et$_2$O (10 cm^3) and the resulting solution was stirred inducing precipitation. The supernatant was transferred *via* a filter cannula and the precipitate was washed with Et$_2$O (3 cm^3) and dried *in vacuo* to give a brown solid. However, despite this, no satisfactory combustion analysis was obtained for **7**.

3.4.1.7 Attempted synthesis of the selenourea adduct *via* generation of 3 *in situ* from 2c using ᵗBuOK in THF at high concentration

2c (0.1589 g, 0.40 mmol), selenium (0.0921 g, 1.17 mmol), ᵗBuOK (0.1804 g, 1.61 mmol), and THF (1 cm³) were combined and the resulting mixture was stirred at ambient temperature for 23 h. The solvent was removed under vacuum to afford a solid which was dissolved in DCM (20 cm³) and the solution was filtered through Celite®. The residue was washed with further DCM (10 cm³) and the washings were combined. The solvent was removed under vacuum and washed with hexane (3 x 5 cm³) to give a green solid (0.106 g, ~0.14 mmol, 35 %), which was identified as impure **7** by ¹H NMR.

3.4.2 Synthesis of (η⁵-C₅H₅)NiCl(1,3-bis(2-methoxyphenyl)-4,5-dimethylimidaozl-2-ylidene [Ni(Cp)(Cl)(IAnisᴹᵉ)], 8

3.4.2.1 Synthesis of the half-sandwich nickel(II) complex along with paramagnetic impurities

2a (0.100 g, 0.29 mmol), nickelocene (0.0611 g, 0.28 mmol), and THF (5 cm³) were combined and the resulting mixture was refluxed for 18 h. The solvent was removed under vacuum and, under air, the resulting red residue was extracted twice with hot toluene (5 cm³). The filtrate was then reduced in volume until solid was observed, heated to re-dissolve the solid, and then placed in a -20 °C freezer for two days. The resultant red crystals were isolated (small quantity kept for SCXRD analysis) and washed with hexane (5 cm³) to give **8** as red crystals (0.011 g, ~0.02 mmol, ~7 %). Upon making concentrated solutions, it became apparent that the crystals contained a paramagnetic impurity which caused broadening of the signals in the ¹H NMR spectrum.

3.4.2.2 Synthesis of the half-sandwich nickel(II) complex with altered work-up

2c (0.401 g, 1.16 mmol), nickelocene (0.2433 g, 1.11 mmol), and THF (10 cm³) were combined. The resulting mixture was refluxed for 67 h, during which time the colour of the solution changed from green to dark red. The resulting solution was filtered through Celite® and washed through with THF (2 x 5 cm³). The solvent was removed under vacuum to give a dark red solid which was washed with hexane (2 x 5 cm³) and dried *in vacuo* to afford a crude dark red solid which was identified as

impure **8** by ^{1}H NMR. The organic products from the crude dark red solid were extracted into toluene (4 x 10 cm^3), which was then reduced in volume to ~10 cm^3, heated to re-dissolve the solid, and then placed in a -20 °C freezer for four days. The resultant red crystals were isolated, washed with hexane (3 x 10 cm^3), and dried *in vacuo* to give **8** as a red crystalline solid (0.3081 g, 0.66 mmol, 57 %). **^{1}H NMR** (400 MHz, DCM, 25.10 °C): δ 7.95 (d, *J* = 7.43 Hz), 7.61 (m, 2H), 7.29 (m, 2H), 7.17 (m, 2H), 4.48 and 4.42 (two s, 5H), 3.86 and 3.82 (two s, 6H), 1.92 and 1.90 (overlapping s, 6H). **^{13}C{^{1}H} NMR** (100.52 MHz, DCM, 25.00 °C): δ 161.26 (*C*$_{carbene}$), 155.50 and 155.13 (*C* phenyl or N*C*(CH$_3$)), 132.27 (*C*H phenyl), 130.63 (*C*H phenyl), 128.66 and 128.38 (*C* phenyl or N*C*(CH$_3$)), 120.95 and 120.65 (*C*H phenyl), 112.01 and 111.47 (*C*H phenyl), 91.44 and 90.62 (Cp), 55.85 and 55.77 (O*C*H$_3$), 9.21 and 9.16 (*C*H$_3$). Elemental analysis: Calculated for C$_{24}$H$_{25}$ClN$_2$NiO2: C, 61.65; H, 5.39; N, 5.99. Found: C, 61.44; H, 5.23; N, 5.82.

3.4.3 Synthesis of (1,3-bis(2-methoxyphenyl)-4,5-dimethylimidazol-2-yl)silver chloride [AgCl(IAnis^{Me})], 9

3.4.3.1 Synthesis of the silver(I) complex with Ag$_2$O in H$_2$O (glass vial)

2a (0.101 g, 0.29 mmol), Ag$_2$O (0.045 g, 0.19 mmol), and H$_2$O (2 cm^3) were combined in a glass vial sealed with a septum, and sparged with argon. The reaction mixture was then refluxed for 24 h. The resulting mixture was filtered in air and the crude solid was extracted with DCM (20 cm^3). The resulting mixture was then filtered, the solvent removed under vacuum, and the resulting residue was dried on an oven to give a brown crystalline solid which was shown to be wet (with H$_2$O) **9** (0.019 g, ~0.04 mmol, ~14 %) by ^{1}H NMR. X-ray quality crystals of **9** were grown by the slow diffusion of hexane into a concentrated DCM solution.

3.4.3.2 Larger scale synthesis of the silver(I) complex with Ag$_2$O in H$_2$O (glass vial)

2a (0.302 g, 0.88 mmol), Ag$_2$O (0.132 g, 0.57 mmol), and H$_2$O (2 cm^3) were combined in a glass vial sealed with a septum, and sparged with argon. The reaction mixture was refluxed for 89 h. The resulting mixture was filtered in air and the residue washed with H$_2$O (15 cm^3). Majority of the crude solid was dissolved in DCM (10 cm^3), filtered and the solvent was removed under vacuum. To afford a solid which was dissolved in DCM (3 cm^3) and added dropwise to stirring hexane (9

cm^3) which induced precipitation. The resulting mixture was then filtered and washed with hexane (10 cm^3) to give a brown crystalline solid (0.123 g, 0.27 mmol, 31 %). **^{1}H NMR** (400 MHz, DCM, 25.10 °C): δ 7.50 (m, 2H), 7.33 (br, 2H), 7.10 (m, 4H), 3.85 and 3.83 (overlapping s, 6H), 1.96 (s, 6H). **^{13}C{^{1}H} NMR** (100.52 MHz, DCM, 25.00 °C): δ 154.90 and 154.78 (*C* phenyl or N*C*(CH$_3$)), 131.02 and 131.00 (*C*H phenyl), 129.47 and 129.44 (*C*H phenyl), 127.66 and 127.63 (*C* phenyl or N*C*(CH$_3$)), 126.97 and 126.82 (*C* phenyl or N*C*(CH$_3$)), 121.12 and 121.04 (*C*H phenyl), 112.45 and 112.34 (*C*H phenyl), 56.01 and 55.88 (O*C*H$_3$), 9.16 (*C*H$_3$).

3.4.3.3 Larger scale synthesis of the silver(I) complex with Ag$_2$O in H$_2$O (Schlenk)

2a (0.402 g, 1.17 mmol), Ag$_2$O (0.174 g, 0.75 mmol), and degassed H$_2$O (5 cm^3) were combined and the reaction mixture was refluxed for 41 h. The supernatant was decanted *via* filter cannula and the resulting solid was washed with degassed H$_2$O (2 x 10 cm^3) and was dried *in vacuo*. The crude solid was extracted with DCM (10 cm^3 then 3 cm^3), and the supernatant was transferred *via* filter cannula. The combined filtrates were reduced in volume to ~5 cm^3, followed by the slow addition of hexane (20 cm^3) which induced precipitation. The precipitate was then isolated and dried *in vacuo* to give a beige solid (0.3099 g, 0.69 mmol, 59 %). Elemental analysis: Calculated for C$_{19}$H$_{20}$AgClN$_2$O$_2$: C, 50.52; H, 4.46; N, 6.20. Found: C, 50.46; H, 4.50; N, 6.12.

3.4.3.4 Synthesis of the silver(I) complex with Ag$_2$O, KOH in DCM

A suspension of Ag$_2$O (0.075 g, 0.32 mmol), KOH (0.102 g, 1.82 mmol) and H$_2$O (3 cm^3) was added to **2a** (0.1725 g, 0.50 mmol) in DCM (10 cm^3) and the resulting mixture was subsequently stirred at ambient temperature for 24 h. The aqueous layer was decanted under air, and the organic products in the aqueous layer were extracted into DCM (5 cm^3) and the organic layers were combined. The combined organic phases were washed with H$_2$O (3 x 10 cm^3), dried with MgSO$_4$, filtered, and the solvent removed under vacuum, to afford a crude brown tar which was identified as impure **9**. The crude tar was triturated with hexane (20 cm^3), filtered, and the residue was washed with hexane (10 cm^3) to give a cream solid which was identified as wet (with water) **9** (0.156 g, ~0.35 mmol, ~70 %) by ^{1}H NMR.

3.4.3.5 Attempted synthesis of the silver(I) complex with AgNO$_3$ and K$_2$CO$_3$ in DCM

2a (0.1724 g, 0.50 mmol), AgNO$_3$ (0.085 g, 0.50 mmol), and DCM (15 cm^3) were combined and stirred for 5 minutes. Subsequently, K$_2$CO$_3$ (1.152 g, 8.34 mmol) was added and the reaction mixture was stirred at ambient temperature for 2 h. The resulting mixture was filtered through Celite® and the solvent was reduced in volume to ~2 cm^3. Et$_2$O (10 cm^3) was added which induced precipitation. The precipitate was isolated by filtration and dried *in vacuo* to give a cream solid (0.0892 g) which was identified as a mixture of **9** and **2a** in a 7:3 ratio, respectively by ^{1}H NMR by integration of signals for methyl groups on the backbone.

3.4.3.6 Synthesis of the silver(I) complex with AgNO$_3$ and K$_2$CO$_3$ in DCM, overnight stirring

2a (0.1726 g, 0.50 mmol), AgNO$_3$ (0.087 g, 0.51 mmol), and DCM (5 cm^3) were combined and stirred for 5 minutes. K$_2$CO$_3$ (1.151 g, 8.33 mmol) was then added and the reaction mixture was subsequently stirred at ambient temperature for 20 h. The resulting mixture was filtered through Celite® and washed through with DCM (10 cm^3). The solvent was reduced in volume to ~2 cm^3, followed by the addition of Et$_2$O (10 cm^3) which induced precipitation. The precipitate was isolated by filtration, washed with Et$_2$O (3 x 5 cm^3), and dried *in vacuo* to give a cream solid which was identified as wet (with Et$_2$O) **9** (0.1198 g, ~0.27 mmol, ~54 %) by ^{1}H NMR.

3.4.4 Synthesis of (1,3-bis(2-methoxyphenyl)-4,5-dimethylimidazol-2-yl)copper chloride [CuCl(IAnis^{Me})], 10

3.4.4.1 Synthesis of the copper(I) complex with Cu$_2$O in H$_2$O (glass vial)

2a (0.100 g, 0.29 mmol), Cu$_2$O (0.028 g, 0.20 mmol), and H$_2$O (2 cm^3) were combined in a glass vial sealed with a septum, and sparged with argon. The reaction mixture was then refluxed for 22 h. The resulting mixture was filtered in air and the residue washed with H$_2$O (10 cm^3). The solid residue was extracted into DCM (5 cm^3) which was filtered and the solvent was removed under vacuum to afford a crude solid. This was dissolved in DCM (3 cm^3) and the solution was added dropwise to stirring hexane (9 cm^3) which induced precipitation. The resulting mixture was filtered and ^{1}H NMR suggested a mixture of **10** and **2a**. The solvent was

removed under vacuum to afford a solid which was suspended in EtOAc (5 cm^3) and filtered through silica. The solvent was removed under vacuum to yield minimal amounts of a brown/orange solid which was shown to be **10** or the urea complex by ^{1}H NMR. X-ray quality crystals of **10** were grown by the slow diffusion of hexane into a concentrated DCM solution.

3.4.4.2 Larger synthesis of the copper(I) complex with Cu$_2$O in H$_2$O (glass vial)

2a (0.603 g, 1.75 mmol), Cu$_2$O (0.162 g, 1.13 mmol), and H$_2$O (3.5 cm^3) were combined in a glass vial sealed with a septum, and sparged with argon. The reaction mixture was refluxed for 112 h. The resulting mixture was filtered in air, and the residue washed with H$_2$O (20 cm^3). The solid residue was dissolved in DCM (10 cm^3) and filtered, and i*n situ* ^{1}H NMR suggested a mixture of **10** and **2a**. The solvent was removed under vacuum to afford a solid which was subsequently stirred in EtOAc (10 cm^3); only a small quantity of the solid dissolved. The resulting mixture was filtered through silica and the solvent was removed under vacuum to give a brown oil which was identified as a mixture of **10** and **2a** by ^{1}H NMR. The silica was washed through with DCM (15 cm^3) and the solvent was removed under vacuum to give a crude brown solid which was identified as impure **10** by ^{1}H NMR. Solubility tests of impure **10** confirmed that it was only barely soluble in THF, EtOH, EtOAc, and toluene. Therefore, the crude solid was dissolved in DCM (2 cm^3) and was added dropwise to stirring EtOAc (10 cm^3) which induced precipitation. The resulting mixture was filtered and washed with EtOAc (10 cm^3) and dried on top of the oven to give **10** as a light brown solid (0.09 g, 0.22 mmol, 13 %). **^{1}H NMR** (400 MHz, DCM, 25.00 °C): δ 7.50 (t, *J* = 15.83 Hz, 2H), 7.38 (br m, 2H), 7.11 (m, 4H), 3.87 and 3.85 (overlapping s, 6H), 1.97 (s, 6H). **^{13}C{^{1}H} NMR** (100.52 MHz, DCM, 25.00 °C): δ 176.40 and 176.37 ($C_{carbene}$), 154.85 and 154.74 (*C* phenyl or N*C*(CH$_3$)), 130.89 (*C*H phenyl), 129.65 and 129.60 (*C*H phenyl), 127.45 and 127.42 (*C* phenyl or N*C*(CH$_3$)), 126.48 and 126.36 (*C* phenyl or N*C*(CH$_3$)), 121.07 and 120.99 (*C*H phenyl), 112.46 and 112.32 (*C*H phenyl), 56.01 and 55.88 (O*C*H$_3$), 9.06 (*C*H$_3$).

3.4.4.3 Larger synthesis of the copper(I) complex with Cu$_2$O in H$_2$O (Schlenk)

2a (0.403 g, 1.17 mmol), Cu$_2$O (0.108 g, 0.75 mmol), and degassed H$_2$O (5 cm^3) were combined and the reaction mixture was refluxed for 41 h. The supernatant was

decanted *via* filter cannula and the residue washed with degassed H_2O (2 x 10 cm³)

and dried *in vacuo*. The solid residue was extracted into DCM (10 cm³ then 3 cm³)

and the supernatant was transferred *via* filter cannula. The combined filtrates were

reduced in volume to ~5 cm³, followed by the slow addition of hexane (20 cm³)

which induced precipitation. The precipitate was isolated by filtration and dried *in*

vacuo to give **10** as a light brown solid (0.1863 g, 0.46 mmol, 39 %). Elemental

analysis: Calculated for $C_{19}H_{20}ClCuN_2O_2$: C, 56.02; H, 4.95; N, 6.88. Found: C, 55.87;

H, 4.93; N, 6.78.

3.4.5 Synthesis of bis(1,3-bis(2-methoxyphenyl)-4,5-dimethylimidazol-2-yl)copper tetrafluoroborate ([Cu(IAnis^{Me})$_2$]BF$_4$), 11

3.4.5.1 Attempted synthesis of the bis-NHC copper(I) complex *via* 2a, 0.25 eq. Cu$_2$O, and NaBF$_4$ in H$_2$O

2a (0.102 g, 0.30 mmol), Cu_2O (10 mg, 0.07 mmol), $NaBF_4$ (0.036 g, 0.33 mmol), and

H_2O (2 cm³) were combined in a glass vial sealed with a septum, and sparged with

argon. The reaction mixture was refluxed for 64 h. The resulting mixture was

filtered in air, and the residue washed with H_2O (5 cm³) to give a solid. The solid

was extracted into DCM (5 cm³), filtered and *in situ* ^1H NMR of the filtrate indicated

the presence of an imidazolium salt (either **2a** or **2c**).

3.4.5.2 Attempted synthesis of the bis-NHC copper(I) complex *via* 2c, 0.25 eq. Cu$_2$O, and NaBF$_4$ in H$_2$O

2c (0.101 g, 0.25 mmol), Cu_2O (9 mg, 0.06 mmol), and H_2O (2 cm³) were combined

in a glass vial sealed with a septum, and sparged with argon. The reaction mixture

was refluxed for 64 h. The resulting mixture was filtered in air and the residue

washed with H_2O (5 cm³) to give a solid. The residue was extracted into DCM (5

cm³) and filtered; *in situ* ^1H NMR of the filtrate indicated only **2c** was present.

3.4.5.3 Attempted synthesis of the bis-NHC copper(I) complex *via* 2c, Cu(MeCN)$_4$BF$_4$, and ^{t}BuOK in THF

2c (0.100 g, 0.25 mmol), $Cu(MeCN)_4BF_4$ (0.0393 g, 0.12 mmol), ^{t}BuOK (0.0369 g,

0.33 mmol), and THF (5 cm³) were combined and stirred at ambient temperature

for 66 h. The resulting mixture was filtered through Celite® in air and the filtrate left

overnight. In the morning, all of the solvent had evaporated from the filtrate to give

a minuscule amount of green tar which was identified as impure **2c** with possibly a tiny amount of **11** present too by ^{1}H NMR.

3.4.5.4 Synthesis of the bis-NHC copper(I) complex *via* 2c, 0.25 eq. Cu₂O, and aq. NH₃ in EtOH

2c (0.1005 g, 0.25 mmol), Cu_2O (9 mg, 0.06 mmol), and EtOH (1.2 cm^3) were combined in a glass vial sealed with a septum, and sparged with argon. Aq. NH_3 (0.1 cm^3, 2.57 mmol) was then added and the reaction mixture stirred at 40 °C for 66 h. The resulting mixture was placed in an ice bath for 2 h, filtered in air, and washed with cold EtOH (2 cm^3), cold H_2O (2 cm^3), and cold EtOH (2 cm^3) to give a crude cream/grey solid with red specks (presumed to be Cu_2O) which was identified as impure **11** by ^{1}H NMR. The crude solid was washed with THF (2 cm^3), filtered and the residue was washed with THF (2 cm^3) to give **11** as an off-white solid (0.037 g, 0.05 mmol, 40 %). Poor quality X-ray crystals of **11** were grown by the slow diffusion of hexane into a concentrated DCM solution.

3.4.5.5 Attempted larger synthesis of the bis-NHC copper(I) complex *via* 2c, 0.25 eq. Cu₂O, and aq. NH₃ in EtOH

2c (0.3964 g, 1.00 mmol), Cu_2O (0.035 g, 0.24 mmol), and EtOH (5 cm^3) were combined in a glass vial sealed with a septum, and sparged with argon. This was followed by the addition of aq. NH_3 (0.39 cm^3, 10.01 mmol), after which the reaction mixture was stirred at 40 °C for 65 h. The resulting mixture was placed in an ice bath for 1 h, filtered in air, and the residue was washed with cold EtOH (3 cm^3), cold H_2O (3 cm^3), and cold EtOH (3 cm^3) to give a crude red/peach solid. The crude solid was washed with THF (5 cm^3) and filtered to afford a cream/red solid. The solid was extracted into DCM (10 cm^3) and the resulting mixture was filtered to remove residual Cu_2O. The solvent was removed under vacuum to give a yellow tar, which was shown to be a mixture of **11** and **2c** by ^{1}H NMR. The solvent was removed from the decanted THF solution under vacuum to give a yellow tar which was also identified as a mixture of **11** and **2c** in a 4:1 ratio, respectively by ^{1}H NMR by integration of signals for methyl groups on the backbone.

3.4.5.6 Larger synthesis of the bis-NHC copper(I) complex *via* 2c, 0.25 eq. Cu₂O, aq. NH₃, and H₂O in EtOH

2c (0.3965 g, 1.00 mmol), Cu_2O (0.036 g, 0.25 mmol), H_2O (0.5 cm^3), and EtOH (5 cm^3) were combined in a glass vial sealed with a septum, and sparged with argon, followed by the addition of aq. NH₃ (0.39 cm^3, 10.01 mmol). The reaction mixture was then stirred at 40 °C for 88 h. The resulting mixture was placed in an ice bath for 5 h, filtered in air, and was washed with cold EtOH (3 cm^3), cold H_2O (4 cm^3), cold EtOH (2 cm^3), and cold H_2O (2 cm^3) to give a white solid (0.218 g, ~0.28 mmol, ~56 %) which was identified as wet (with water and trace amounts of EtOH) **11** by ¹H, ¹¹B, and ¹⁹F NMR. **¹H NMR** (400 MHz, DCM, 25.0 °C): δ 7.49 (m, 2H), 6.95 (m, 6H), 3.81, 3.78, 3.76, 3.72, and 3.70 (overlapping s, 6H), 1.88, 1.87, and 1.85 (overlapping s, 6H). **¹³C{¹H} NMR** (100.52 MHz, DCM, 25.00 °C): δ 175.78 - 175.13 ($C_{carbene}$), 154.72 - 154.28 (*C* phenyl or N*C*(CH₃)), 130.97 - 130.73 (*C*H phenyl), 129.26 - 128.94 (*C*H phenyl), 127.14 - 126.60 (*C* phenyl or N*C*(CH₃)), 121.07 - 120.92 (*C*H phenyl), 112.50 - 112.18 (*C*H phenyl), 55.93 - 55.72 (O*C*H₃), 8.87 (*C*H₃) [apparent multiplets due to multiple different conformations, therefore signals given in ranges]. **¹¹B NMR** (128.27 MHz, DCM, 25.00 °C): δ -1.72 (s). **¹⁹F NMR** (376.17 MHz, DCM, 25.00 °C): δ -153.90 (s), -153.95 (s) [due to the primary isotope effect, ¹⁹F bound to ¹⁰B and ¹¹B]. Elemental analysis of the white solid was not as expected and therefore a variety of drying methods were tested using inert atmosphere techniques. The afforded solid was dissolved in DCM (5 cm^3) and hexane (25 cm^3) was added which induced precipitation. The precipitate was isolated and then dried *in vacuo* at 80 °C overnight to give a white solid, which was shown still to be wet (with both water and EtOH) **11** by ¹H NMR. The solid was further dried *in vacuo* at 80 °C for 114 h, but was still contaminated with water and EtOH by ¹H NMR. Crystallisation from a concentrated solution in DCM layered with hexane (6 cm^3) and allowed to diffuse over 3 days afforded colourless/white crystals which were isolated, washed with hexane (2 cm^3) and dried *in vacuo* for 1 h, but which were nevertheless shown to be contaminated with EtOH and hexane. The overall yield of **11** (0.0509 g, ~0.07 mmol), was thus approximately 7 %. Unfortunately, the combustion analysis for **11** was still not satisfactory.

3.5 References

1. D. Bourissou, O. Guerret, F. Gabbaï and G. Bertrand, *Chem. Rev.*, 2000, **100**, 39-92.

2. a) W. Herrmann and C. Köcher, *Angew. Chem. Int. Ed. Engl.*, 1997, **36**, 2162-2187. b) W. Herrmann, *Angew. Chem. Int. Ed.*, 2002, 41, 1290-1309.

3. J. Moerdyk, D. Schilter and C. Bielawski, *Acc. Chem. Res.*, 2016, **49**, 1458-1468.

4. Ł. Banach, P. Guńka, D. Górska, M. Podlewska, J. Zachara and W. Buchowicz, *Eur. J. Inorg. Chem.*, 2015, **2015**, 5677-5686.

5. P. de Frémont, N. Marion and S. Nolan, *Coord. Chem. Rev.*, 2009, **253**, 862-892.

6. C. Citadelle, E. Nouy, F. Bisaro, A. Slawin and C. Cazin, *Dalton Trans.*, 2010, **39**, 4489.

7. S. Díez-González, E. Stevens, N. Scott, J. Petersen and S. Nolan, *Chem. - Eur. J.*, 2007, **14**, 158-168.

8. O. Santoro, F. Lazreg, D. Cordes, A. Slawin and C. Cazin, *Dalton Trans.*, 2016, **45**, 4970-4973.

9. K. Verlinden, H. Buhl, W. Frank and C. Ganter, *Eur. J. Inorg. Chem.*, 2015, **2015**, 2416-2425.

10. A. Liske, K. Verlinden, H. Buhl, K. Schaper and C. Ganter, *Organometallics*, 2013, **32**, 5269-5272.

11. S. Vummaleti, D. Nelson, A. Poater, A. Gómez-Suárez, D. Cordes, A. Slawin, S. Nolan and L. Cavallo, *Chem. Sci.*, 2015, **6**, 1895-1904.

12. D. Nelson, F. Nahra, S. Patrick, D. Cordes, A. Slawin and S. Nolan, *Organometallics*, 2014, **33**, 3640-3645.

13. A. Collado, A. Gómez-Suárez, A. Martin, A. Slawin and S. Nolan, *Chem. Comm.*, 2013, **49**, 5541.

14. R. Savka and H. Plenio, *Dalton Trans.*, 2015, **44**, 891-893.

15. O. Santoro, A. Collado, A. Slawin, S. Nolan and C. Cazin, *Chem. Comm.*, 2013, **49**, 10483.

16. F. Nahra, K. Van Hecke, A. Kennedy and D. Nelson, *Dalton Trans.*, 2018, **47**, 10671-10684.

17. O. Back, M. Henry-Ellinger, C. Martin, D. Martin and G. Bertrand, *Angew. Chem. Int. Ed.*, 2013, **52**, 2939-2943.

18. S. Vummaleti, D. Nelson, A. Poater, A. Gómez-Suárez, D. Cordes, A. Slawin, S. Nolan and L. Cavallo, *Chem. Sci.*, 2015, **6**, 1895-1904.

19. H. Baier, A. Kelling, U. Schilde and H. Holdt, *Z. Anorg. Allg. Chem.*, 2016, **642**, 140-147.

20. V. Landry, M. Minoura, K. Pang, D. Buccella, B. Kelly, G. Parkin, *J. Am. Chem. Soc.*, 2006, **128**, 12490-12497.

21. C. Abernethy, Alan H, Cowley and R. Jones, *J. Organomet. Chem.*, 2000, **596**, 3-5.

22. J. Cooke and O. Lightbody, *J. Chem. Educ.*, 2011, **88**, 88-91.

23. A. Oertel, V. Ritleng and M. Chetcuti, *Organometallics*, 2012, **31**, 2829-2840.

24. C. Citadelle, E. Nouy, F. Bisaro, A. Slawin and C. Cazin, *Dalton Trans.*, 2010, **39**, 4489-4491.

25. U. Hintermair, U. Englert and W. Leitner, *Organometallics*, 2011, **30**, 3726-3731.

26. R. Visbal, A. Laguna and M. Gimeno, *Chem. Comm.*, 2013, **49**, 5642.

27. J. Garrison and W. Youngs, *Chem. Rev.*, 2005, **105**, 3978-4008.

28. P. de Frémont, N. Scott, E. Stevens, T. Ramnial, O. Lightbody, C. Macdonald, J. Clyburne, C. Abernethy and S. Nolan, *Organometallics*, 2005, **24**, 6301-6309.

29. M. Samantaray, D. Roy, A. Patra, R. Stephen, M. Saikh, R. Sunoj and P. Ghosh, *J. Organomet. Chem.*, 2006, **691**, 3797-3805.

30. T. Ramnial, C. Abernethy, M. Spicer, I. McKenzie, I. Gay and J. Clyburne, *Inorg. Chem.*, 2003, **42**, 1391-1393.

31. A. Danopoulos, T. Simler and P. Braunstein, *Chem. Rev.*, 2019, **119**, 3730-3961.

32. S. Zhu, R. Liang and H. Jiang, *Tetrahedron*, 2012, **68**, 7949-7955.

33. H. Kaur, F. Zinn, E. Stevens and S. Nolan, *Organometallics*, 2004, **23**, 1157-1160.

34. S. Díez-González, E. Escudero-Adán, J. Benet-Buchholz, E. Stevens, A. Slawin and S. Nolan, *Dalton Trans.*, 2010, **39**, 7595.

35. a) K. Semba, M. Shinomiya, T. Fujihara, J. Terao and Y. Tsuji, *Chem. - Eur. J.*, 2013, **19**, 7125-7132. b) Bond lengths and angles measured and %V_{Bur} calculated from the single crystal structure deposited in the Cambridge crystallographic data centre (CCDC); CCDC number: 926626.

36. N. Mankad, T. Gray, D. Laitar and J. Sadighi, *Organometallics*, 2004, **23**, 1191-1193.

37. C. Gibard, H. Ibrahim, A. Gautier and F. Cisnetti, *Organometallics*, 2013, **32**, 4279-4283.

38. O. Santoro, F. Lazreg, D. Cordes, A. Slawin and C. Cazin, *Dalton Trans.*, 2016, **45**, 4970-4973.

39. L. Falivene, R. Credendino, A. Poater, A. Petta, L. Serra, R. Oliva, V. Scarano and L. Cavallo, *Organometallics*, 2016, **35**, 2286-2293.

40. S. Gaillard, X. Bantreil, A. Slawin and S. Nolan, *Dalton Trans.*, 2009, 6967-6971.

41. A. Gómez-Suárez, D. Nelson and S. Nolan, *Chem. Comm.*, 2017, **53**, 2650-2660.

Chapter Four

Attempted Synthesis of NHC-bound Phosphenium Cations

"Whatever the mind can conceive and believe, the mind can achieve"

Napoleon Hill

4.1 Introduction to phosphenium cations

Phosphenium cations are a phosphorus-centred, generally dicoordinate species in the +3 oxidation state and possess a vacant p-orbital and a lone pair of electrons.[1,2] As a result, they are classified as amphoteric and hence can function as either Lewis acids or bases, and thus can bind to metal centres as ligands.[1,3] The versatility of these cations makes them very useful and interesting species for both synthetic and reactivity utility as well as structural curiosities.[1] The majority of their functionality in reactions is attributed to their cationic (electrophilic) character.[2] The most investigated phosphenium cations are those which are incorporated into heterocyclic rings and stabilised by a π-conjugated system, and which are therefore denoted as *N*-heterocyclic phosphenium cations (NHPs, *figure 4.1*).[4,5] Such species show complementary properties to their NHCs congeners, and are strong π-acceptors but poor σ-donors, and thus dominated by their Lewis acid character.[4]
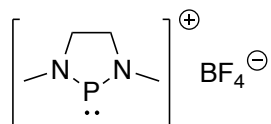
Figure 4.1. An example of an N-heterocyclic phosphenium cation.

Nevertheless, a substantial number of phosphenium cations are synthesised relying upon stabilisation *via* adduct formation with Lewis bases (electron pair donor ligands) such as NHCs (*figure 4.2a*), phosphines (*figure 4.2b*), nitrogen moieties (*figure 4.2c*) and so on.[6a-9] These stabilising interactions involve the donation of a lone pair bearing neutral ligand to the phosphorus centre.[10]
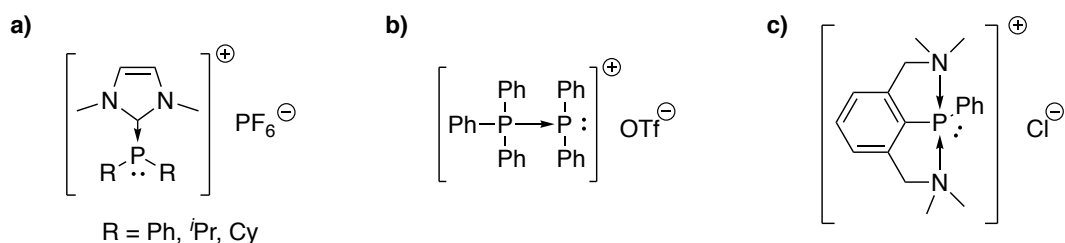
Figure 4.2. Stabilisation of phosphenium cations *via* coordination with: a) NHCs; b) Phosphines; c) Nitrogen moieties.

One approach to stabilising these species is by chelation with a dianionic, tridentate ligand; such complexes are known as geometrically constrained phosphenium cations and only a few examples have been described in the literature.[4,11-16] The

main one of interest to this project was reported by Dobrovetsky and depicted in *figure 4.3*. This compound is capable of activating E-H bonds such as H-OH, RO-H (R = H, Me, ^{i}Pr, ^{t}Bu) and H-NH$_2$; similar structures are also capable of such activation.[4]
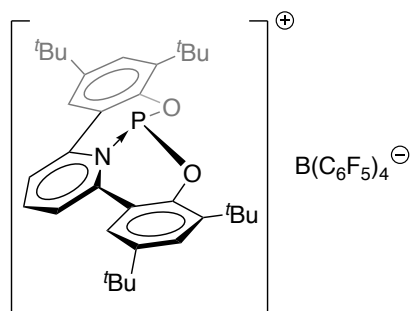
Figure 4.3. Dobrovetsky's geometrically constrained phosphenium cation.

All geometrically constrained phosphenium cations reported are stabilised *via* a nitrogen moiety for adduct formation. Therefore, this chapter sets out to synthesise a similar geometrically constrained phosphenium cation, illustrated in *figure 4.4*, which differs from those previously reported by using a carbene moiety for adduct formation. Furthermore, the absence of extra substituents on its phenyl rings would thus reduce the ligand's steric bulk and potentially increase its reactivity with a range of substrates. Therefore, this species was targeted with the intention to subsequently explore its Lewis acidity and potential as a main group Lewis acid catalyst.
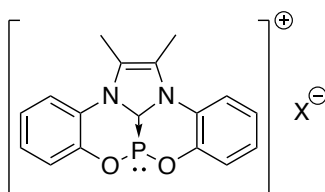
Figure 4.4. Targeted geometrically constrained phosphenium cation.

4.2 Results and discussion

Initially the intention was to synthesise the targets, **12** and **13** (*figure 4.5*) by the treatment of either the protected NHC (IAnis^{Me}.CO$_2$, **4a**) or the free NHC (IAnis^{Me}, **3**) with a phosphorus species such as chlorodiphenylphosphine or phosphorus trichloride in the hope that upon formation of the cationic species, either spontaneously or after halide abstraction, the OMe groups could be demethylated and therefore generate the geometrically constrained phosphenium cation, **14**, illustrated in *figure 4.4*.

R = Ph (**12**), Cl (**13**)
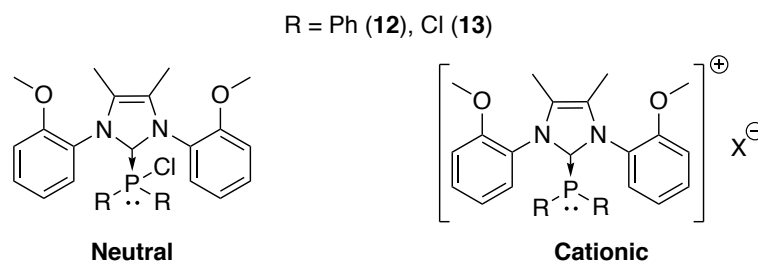
Neutral **Cationic**

Figure 4.5. Targeted IAnis^Me, **3**, carbene ligand coordinated to phosphorus species *via* C→P adduct formation, shown in its neutral or cationic state.

The first attempt at synthesis was by the reaction of **4a** with Ph_2PCl in DCM, illustrated in *scheme 4.1*; the *in situ* ^{1}H NMR spectrum was ambiguous and the ^{31}P NMR spectrum displayed residual Ph_2PCl, some minor peaks and two low resolution binomial quintets at δ -16.62 and -18.26 ppm (*figure 4.6a*), which collapse to singlets in the ^{31}P{^{1}H} NMR (*figure 4.6b*), which is as expected for **12** with [3]*J* coupling to 4 identical ortho protons.
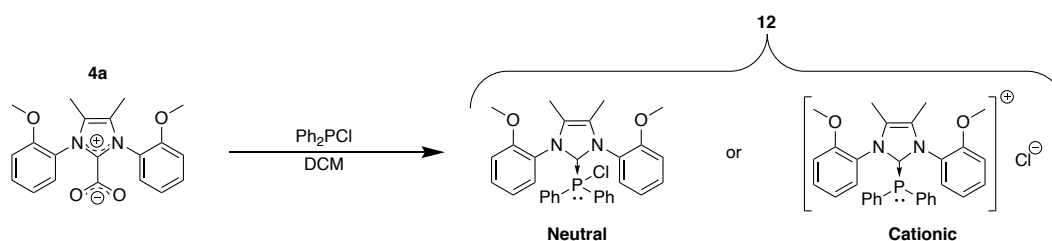
Scheme 4.1. Proposed reaction scheme for the synthesis of neutral or cationic **12** (*via* the autoionisation of neutral **12**).

Such quintets were thought to belong to the desired target, **12**, as similar carbene→PPh_2 cationic species have ^{31}P chemical shifts in the same region *e.g.* δ_P -26.95 and -12.9 ppm ((I^iPr^{Me}.PPh_2)Cl and (IDipp.PPh_2)Cl).[17,18] The two signals were tentatively assigned as the syn- and anti-conformations of the ligand, as found with the metal complexes.
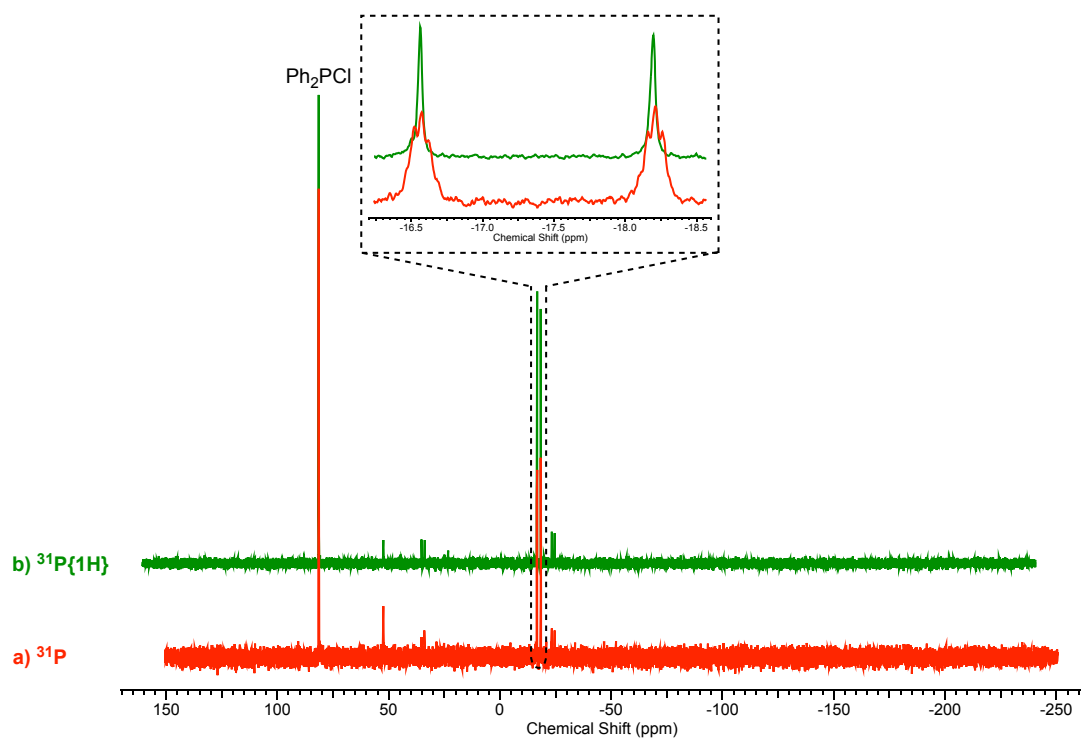
Figure 4.6. *In situ* NMR spectra of the reaction of **4a** with Ph$_2$PCl in DCM: a) ^{31}P NMR spectrum; and b) ^{31}P{^{1}H} NMR spectrum.

Unfortunately, crystallisation *via* slow diffusion was unsuccessful and therefore no single crystal structure was obtained to confirm unambiguously the formation of the desired target. Nevertheless, isolation of the residue from the crystallisation attempt did show removal of all the other unwanted phosphorus species and only two low resolution binomial quintets at δ -16.04 and -17.81 ppm remained in the ^{31}P NMR spectrum. In light of this, halide abstraction was attempted *via* the addition of aluminium trichloride to form the desired cationic target, **12** (*scheme 4.2*), leading to two binominal quintets at δ -16.04 and -17.81 ppm in the ^{31}P NMR spectrum and one singlet at δ 103.22 ppm in the ^{27}Al spectrum, corresponding to AlCl$_4$.
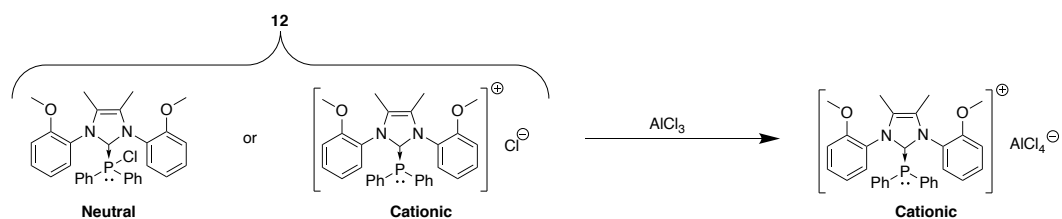
Scheme 4.2. Proposed synthesis of the phosphenium cation with the anion [AlCl$_4$]$^-$, from either the neutral or cationic **12**, *via* the addition of AlCl$_3$.

115

The lack of change of the ^{31}P chemical shifts tentatively suggested that if the displayed signals did correspond to the desired target, **12**, the desired complex was already cationic (*figure 4.7*).
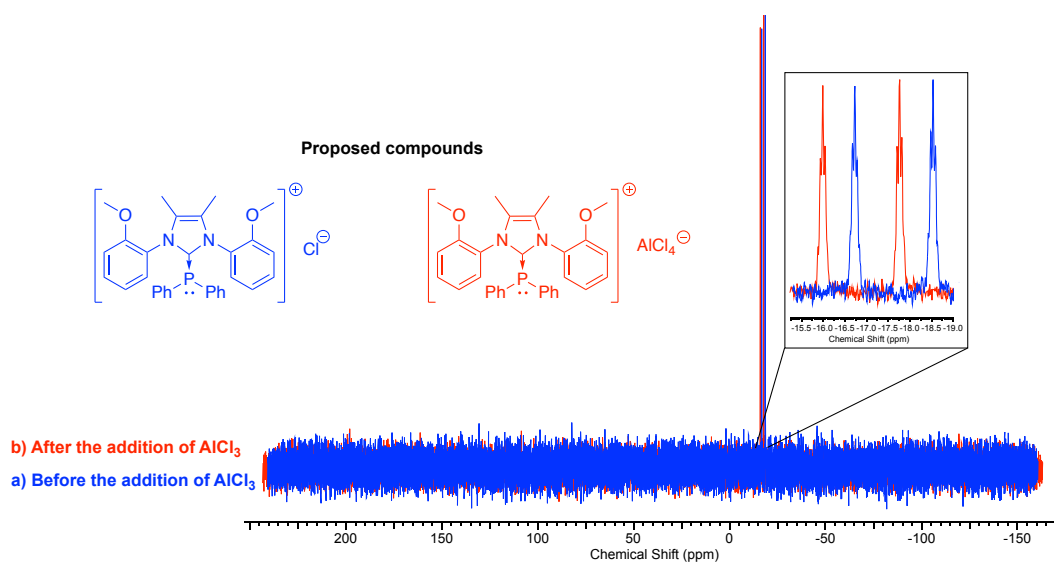
Figure 4.7. ^{31}P NMR spectra: a) Before the addition of AlCl₃; b) After the addition of AlCl₃.

However, the treatment of **4a** with PCl₃, gave very different results and instead multiple peaks presumed to be species afforded from hydrolysis and side reactions were seen in the ^{31}P NMR spectrum, depicted in *figure 4.8*.
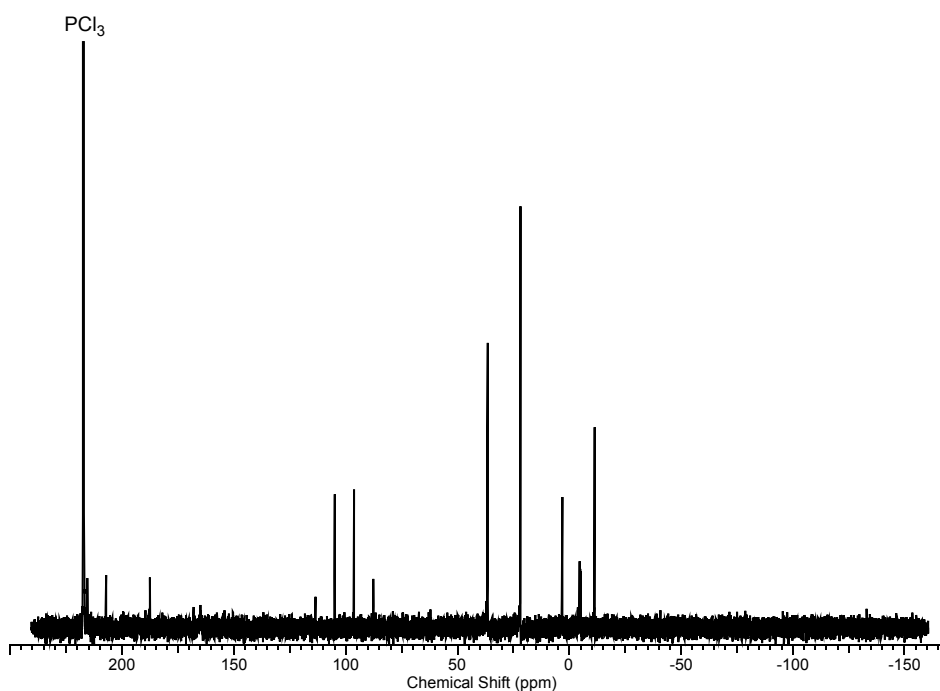
Figure 4.8. ^{31}P NMR spectrum of the reaction of **4a** with PCl₃.

For this sort of chemistry side reactions are known.[6,17,21] Potential side reactions that could have been occurring are as follows; exposure to small amounts of moisture could have led to the hydrolysis of chlorodiphenylphosphine and phosphorus trichloride resulting in the formation of the diphenylphosphine oxide or mixed chlorophosphonic acids, respectively, liberating HCl. The HCl could then have reacted rapidly to reform the corresponding imidazolium chloride. Alternatively, the reaction of PCl$_3$ with sterically unhindered NHCs is known to trigger a redox reaction and disproportionation,[6] yielding a P^I cation and 2-chloro-imidazolium chloride instead of the desired carbene→phosphorus adduct (*scheme 4.3*).
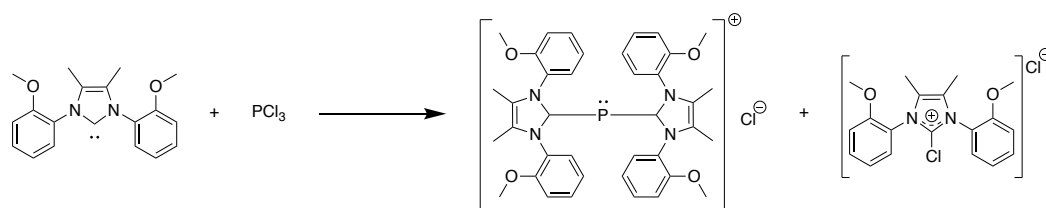
Scheme 4.3. Potential redox reaction.

Since neither the synthesised carboxylate adduct or the free NHC were pure, transmetalation from pure AgCl(IAnis^{Me}), **9**, was attempted since such silver(I) complexes are known for their use as carbene transfer reagents.[19,20] The treatment of **9** with neither phosphorus species (Ph$_2$PCl or PCl$_3$) in DCM proceeded cleanly, but were tentatively believed to have yielded the desired product, **12** or **13**, along with side products (*scheme 4.4*).
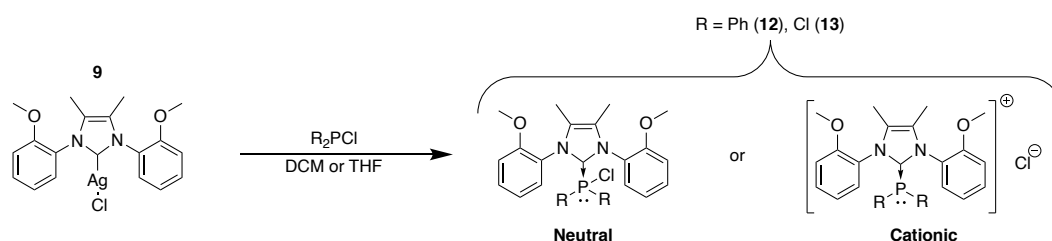
Scheme 4.4. Proposed transmetalation of **9** with Ph$_2$PCl or PCl$_3$.

The formation of the target compounds, **12** and **13**, were tentatively deduced as a few attempts displayed signals in the range of δ -11 to - 18 ppm and 70 to 82 ppm in their ^{31}P NMR spectra, respectively. These are as expected, for similar species are reported in the same region (carbene→PCl$_2$ cationic species ^{31}P chemical shift was reported at δ 107 ppm [(IMe.PCl$_2$)OTf]).[22] However, side reactions occurred too as the ^{1}H NMR spectra all confirmed the regeneration of imidazolium, **2**, and the ^{31}P
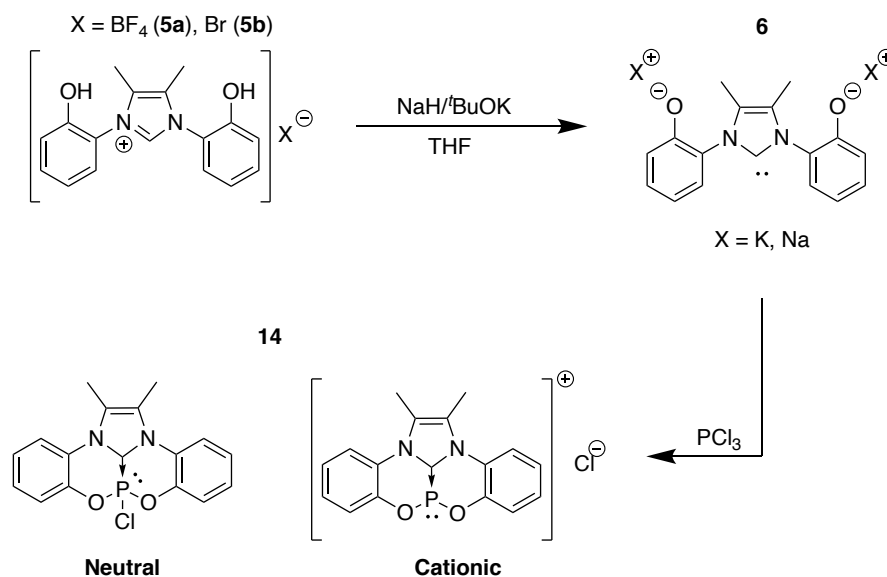
NMR spectra all displayed multiple other signals. These could possibly be due to hydrolysis and/or side reactions. Multiple crystallisations were attempted but all of them failed; since no crystal structure could be obtained to unambiguously confirm the structure, it is only tentatively believed that the desired product was synthesised.

Given the lack of success with the –OMe substituted NHC, the direct synthesis of the final target, the geometrically constrained phosphenium cation, **14** (*figure 4.9*), was attempted utilising the IPhenolate^{Me} NHC pincer ligand, **6**.

14
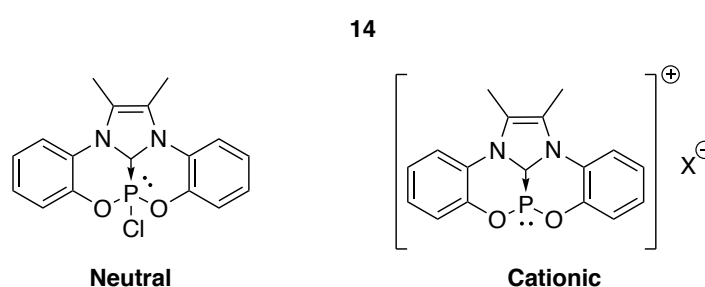
Figure 4.9. Targeted geometrically constrained phosphenium cation, **14**, shown in its neutral or cationic state.

The required IPhenolate^{Me} ligand, **6**, was initially generated *in situ* by the treatment of IPhenol^{Me}.HX (X = BF$_4$, Br; **5a**, **5b** respectively) with NaH/^{t}BuOK followed by the direct addition of PCl$_3$, in the hope of yielding the desired pincer ligand coordinated to phosphorus, **14** (*scheme 4.5*).

Scheme 4.5. Proposed reaction scheme for the direct synthesis of **14**.

For all the attempts, the ^{1}H NMR spectra were ambiguous and the ^{31}P NMR spectra all displayed multiple peaks, indicating that the reaction did not proceed cleanly and side reactions occurred. Nevertheless, a few attempts displayed one prominent signal at δ ~77 ppm (*figure 4.10*), which was thought could imply the formation of the desired product, **14**, in its neutral state as a similar species, albeit with a pyridine moiety instead of a carbene, has a ^{31}P chemical shift of δ ~92 ppm.[4]
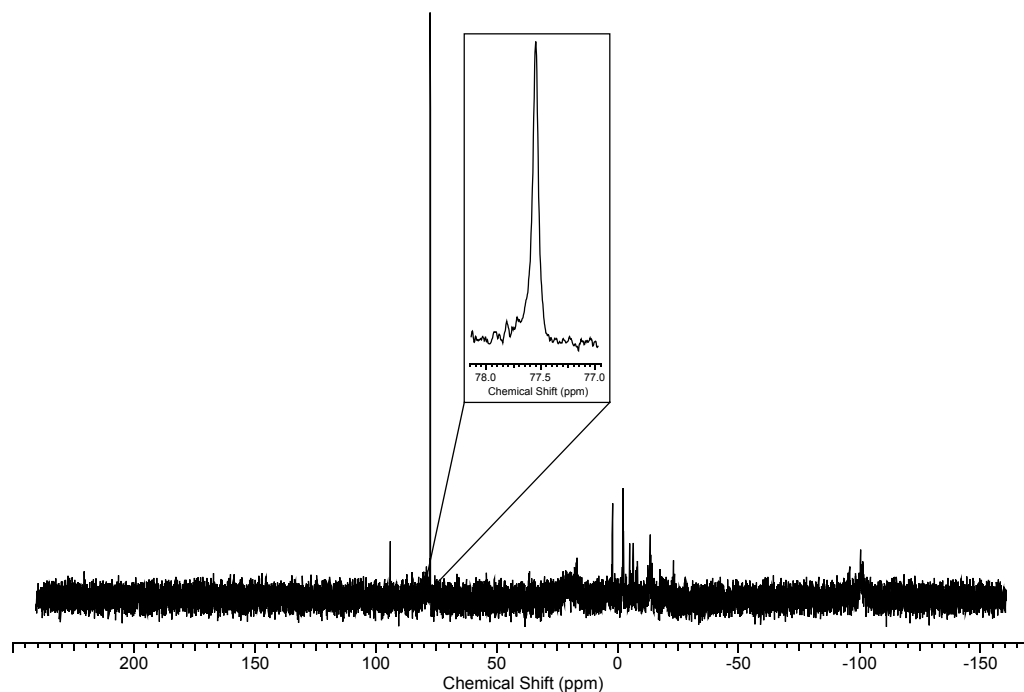
Figure 4.10. ^{31}P NMR spectrum of one of the attempts that displayed a signal at δ ~77 ppm, along with multiple other peaks.

Unfortunately, all attempts to grow single crystals suitable for X-ray diffraction studies failed and hence unambiguous confirmation of the structure of product, **14**, could not be obtained. However, halide abstraction was attempted on the putative impure **14**, and upon addition of NaBArᶠ significant amounts of precipitate formed. The ^{31}P NMR spectrum of the reaction mixture displayed three dominant signals at δ 177.46 (present before halide abstraction), 88.70, and 87.72 ppm. Upon removal of solvent and addition of THF, only small amounts of the precipitate dissolved and the ^{31}P NMR spectrum displayed only one signal at δ 177.64 ppm. Unfortunately, these peaks all remain unidentified.

4.3 Conclusion

Out of all the attempts it was only ever inferred that the three targeted compounds were synthesised by ^{31}P NMR, albeit never cleanly. No single-crystal X-ray measurements were ever acquired, and therefore no firm conclusions can be drawn. Due to time constraints, no further attempts were undertaken.

4.4 Experimental

4.4.1 Attempted synthesis of IAnis^{Me}.PPh$_2$(Cl) (halophosphine precursor), 12

4.4.1.1 Attempted synthesis *via* 4a and Ph$_2$PCl in DCM (NMR-scale)

In a J Young's NMR tube equipped with a DMSO-*d6* capillary, **4a** (0.0353 g, 0.10 mmol) was dissolved in DCM (1 cm^3); *in situ* ^{1}H NMR indicated that a mixture of the CO_2 adduct, **4a**, and imidazolium, **2c**, were present in a 7:3 ratio, respectively. Ph$_2$PCl (0.02 cm^3, 0.11 mmol) was added and after a few minutes a substantial amount of a fine cream precipitate appeared. The ^{31}P NMR showed the presence of residual Ph$_2$PCl and two binominal quintets at δ -16.62 and -18.26 ppm that were tentatively assigned to differing conformations of **12** amongst other minor impurities. Layering of the supernatant with hexane afforded an oil which was redissolved in DCM (1 cm^3). After tentatively confirming the presence of **12** by ^{31}P NMR, AlCl$_3$ (0.0137 g, 0.10 mmol) was added to the NMR tube. The *in situ* ^{31}P NMR showed two binominal quintets at δ -16.04 and -17.81 ppm whilst the ^{27}Al NMR spectrum showed one singlet at δ 103.22 ppm corresponding to the anion [AlCl$_4$]$^-$. The solution was layered with hexane, but this too gave an oil.

4.4.1.2 Attempted synthesis *via* 3 and Ph$_2$PCl in THF (NMR-scale)

In a J Young's NMR tube equipped with a DMSO-*d6* capillary, **3** (0.0312 g, 0.10 mmol) was dissolved in THF (1 cm^3); *in situ* ^{1}H NMR suggested **3** along with small quantities of **2c**. Ph$_2$PCl (0.018 cm^3, 0.10 mmol) was added and the solution changed from brown to orange with formation of a precipitate. The ^{31}P NMR spectrum displayed residual Ph$_2$PCl, one intense singlet at δ -18.09 ppm (tentatively assigned as **12** in one conformation) and multiple other, minor peaks. Further spectroscopic characterisation of this poorly soluble precipitate in DCM (1 cm^3) identified the presence of imidazolium in the ^{1}H NMR and only one binominal

quintet at δ -16.39 ppm. The above method was repeated with a different batch of **3,** but yielded the same result.

4.4.1.3 Attempted synthesis *via* 3 and Ph₂PCl in DCM (NMR-scale)

In a J Young's NMR tube equipped with a DMSO-*d6* capillary, Ph$_2$PCl (0.018 cm^3, 0.10 mmol) and DCM (1 cm^3) were combined. Subsequently, **3** (0.0309 g, 0.10 mmol) was added; the *in situ* ^{1}H NMR spectrum indicated the presence of imidazolium, **2**, but no other species could be identified. The corresponding ^{31}P NMR spectrum displayed residual Ph$_2$PCl, two small peaks at δ -16.44 and -18.24 ppm (tentatively attributed to the formation of the desired product, **12**), along with numerous small peaks.

4.4.1.4 Attempted synthesis *via* transmetalation of 9 with Ph₂PCl in DCM (NMR-scale)

In a J Young's NMR tube equipped with a DMSO-*d6* capillary, **9** (0.0450 g, 0.10 mmol) was dissolved in DCM (1 cm^3). Ph$_2$PCl (0.018 cm^3, 0.10 mmol) was added and a pale brown precipitate appeared; the ^{31}P NMR spectrum displayed three significant signals, a multiplet at δ 43.15 ppm and two binominal quintets at δ -11.86 and -16.94 ppm of which the two upfield signals are tentatively believed to indicate the desired product, **12**, and the one shifted furthest downfield is suggested to be diphenylphosphinic acid chloride. Other phosphorus species and Ph$_2$PCl were also present. The supernatant was transferred and layered with hexane but no crystals could be grown.

4.4.1.5 Attempted larger scale synthesis *via* transmetalation of 9 with Ph₂PCl in DCM

In the absence of light, **9** (0.1131 g, 0.25 mmol) was dissolved in DCM (5 cm^3) and Ph$_2$PCl (0.045 cm^3, 0.25 mmol) was added. The resulting solution was stirred at ambient temperature for 26 h, after which, the supernatant was transferred *via* filter cannula and the solvent was removed under reduced pressure, to give a residue which was triturated with hexane (10 cm^3). The supernatant was decanted *via* filter cannula and the cream solid was washed with hexane (2 x 5 cm^3) and dried *in vacuo* to afford a cream solid (0.126 g) which was identified as impure

imidazolium, **2**, by ^{1}H NMR. The ^{31}P NMR spectrum suggested the formation of diphenylphosphinic acid and other phosphorus species.

4.4.1.6 Attempted larger scale synthesis *via* transmetalation of 9 with Ph₂PCl in DCM (repeat)

In the absence of light, **9** (0.4009 g, 0.89 mmol) was dissolved in DCM (10 cm^3) and Ph$_2$PCl (0.16 cm^3, 0.89 mmol) was added and stirred at ambient temperature for 20 h. The supernatant was transferred *via* filter cannula and the solvent was removed under reduced pressure to give a sticky residue, which was triturated with hexane (10 cm^3). The supernatant was decanted *via* filter cannula and the cream solid was washed with hexane (2 x 5 cm^3) and dried *in vacuo*. The resulting cream solid (0.4794 g) was identified as impure imidazolium, **2**, by ^{1}H NMR. However, the ^{31}P NMR spectrum showed three significant signals, a multiplet at δ 27.53 ppm and two binominal quintets at δ -12.87 and -17.01 ppm of which the two upfield signals may tentatively indicate the desired product, **12**, and the third is suggested to be diphenylphosphinic acid.

4.4.1.7 Attempted larger scale synthesis *via* transmetalation of 9 with Ph₂PCl in DCM, over activated sieves

In the absence of light, **9** (0.1130 g, 0.25 mmol) was dissolved in DCM (10 cm^3) and stirred over activated molecular sieves for 70 h. Subsequently, Ph$_2$PCl (0.045 cm^3, 0.25 mmol) was added and the resulting solution was stirred at ambient temperature for 119 h to give a cloudy light brown mixture with copious precipitate. More DCM (10 cm^3) was added and the resulting mixture was stirred for 30 minutes, then the supernatant was transferred into a J Young's NMR tube which indicated imidazolium, **2**, as the major product by ^{1}H NMR. The ^{31}P NMR spectrum showed an absence of phosphorus signals.

4.4.2 Attempted synthesis of IAnis^{Me}.PCl₃ (halophosphine precursor), 13

4.4.2.1 Attempted synthesis *via* 4a and PCl₃ in THF (NMR-scale)

In a J Young's NMR tube equipped with a DMSO-*d6* capillary, **4a** (0.0354 g, 0.10 mmol) was suspended in THF (1 cm^3); *in situ* ^{1}H NMR showed a mixture of the CO$_2$ adduct, **4a**, and imidazolium, **2c**. Subsequently, PCl$_3$ (0.017 cm^3, 0.19 mmol) was added and even after inverting the tube to mix thoroughly, undissolved solid was

still present. The ^{31}P NMR spectrum showed residual PCl$_3$ and multiple other phosphorus species. Nevertheless, the supernatant was then transferred and layered with hexane, but no crystalline material was obtained, only an oil.

4.4.2.2 Attempted synthesis *via* transmetalation of 9 with PCl$_3$ in DCM (NMR-scale)

In a J Young's NMR tube equipped with a DMSO-*d6* capillary, **9** (0.0451 g, 0.10 mmol) was dissolved in DCM (1 cm^3) and PCl$_3$ (0.009 cm^3, 0.10 mmol) was added and a precipitate appeared; the *in situ* ^{1}H NMR spectrum suggested that a small amounts of imidazolium, **2**, was present, while the ^{31}P NMR spectrum showed residual PCl$_3$ and the presence of two singlets at δ 70.58 and 67.26 ppm, which were tentatively believed to be the desired product, **13**. The solvent in the NMR tube was removed under reduced pressure to remove the residual PCl$_3$ and the sample was re-dissolved in DCM (1 cm^3), although not all of the solid dissolved. Subsequently, AlCl$_3$ (0.0133 g, 0.10 mmol) was added for halide abstraction and more precipitate formed; the ^{1}H NMR spectrum was ambiguous but still showed imidazolium, **2**, to be present; the ^{31}P NMR spectrum displayed two singlets at δ 103.90 and 99.80 ppm (tentatively attributed to the desired product, **13**, with the anion [AlCl$_4$]$^-$) along with a few minor peaks and the ^{27}Al NMR spectrum showed one singlet at δ 103.17 corresponding to the anion [AlCl$_4$]$^-$.

4.4.2.3 Attempted larger scale synthesis *via* transmetalation of 9 with PCl$_3$ in DCM

In the absence of light, **9** (0.1127 g, 0.25 mmol) was dissolved in DCM (5 cm^3) and PCl$_3$ (0.022 cm^3, 0.25 mmol) was added and the resulting solution was stirred at ambient temperature for 16 h. The supernatant was transferred *via* filter cannula and the solvent was removed under reduced pressure, to give a residue which was washed with hexane (3 x 5 cm^3) and dried *in vacuo* to afford a cream solid (0.0596 g) which was identified as predominantly imidazolium, **2**, by ^{1}H NMR. The ^{31}P NMR spectrum of the cream solid displayed multiple minor peaks, however, no peaks appeared in the *δ* 70 to 80 ppm region.

4.4.2.4 Attempted larger scale synthesis *via* transmetalation of 9 with PCl₃ in DCM, over the weekend

In the absence of light, **9** (0.1127 g, 0.25 mmol) was dissolved in DCM (5 cm³) and PCl₃ (0.022 cm³, 0.25 mmol) was added and the resulting solution was stirred at ambient temperature for 73 h. The supernatant was transferred *via* filter cannula and the solvent was removed under reduced pressure, to give a residue which was triturated with hexane (10 cm³). The supernatant was transferred *via* filter cannula and the resulting solid was washed with hexane (2 x 5 cm³) and dried *in vacuo* to afford a brown solid (0.0969 g) which was identified as mainly imidazolium, **2**, by ^{1}H NMR. The ^{31}P NMR spectrum displayed two doublets which collapsed to singlets in the ^{31}P{^{1}H} NMR spectrum, indicating the presence of P-H species.

4.4.2.5 Attempted larger scale synthesis *via* transmetalation of 9 with PCl₃ (distilled) in DCM

In the absence of light, **9** (0.3999 g, 0.89 mmol) was dissolved in DCM (10 cm³). Subsequently, freshly distilled PCl₃ (0.078 cm³, 0.89 mmol) was added and the resulting solution was stirred at ambient temperature for 116 h. The supernatant was transferred *via* filter cannula and the solvent was removed under reduced pressure, to give a residue which was triturated with hexane (10 cm³). The supernatant was transferred *via* filter cannula and the resulting solid was washed with hexane (2 x 5 cm³) and dried *in vacuo* to afford a brown solid (0.3543 g) which was tentatively identified as the desired product, **13** (two major singlets in the ^{31}P NMR spectrum at δ 81.15 and 77.56 ppm) along with some imidazolium, **2**, and some other phosphorus species by ^{1}H NMR and ^{31}P NMR.

4.4.2.6 Attempted synthesis *via* transmetalation of 9 with PCl₃ (distilled) in THF (NMR-scale)

In a J Young's NMR tube equipped with a DMSO-*d6* capillary, **9** (0.0446 g, 0.10 mmol) was suspended in THF (1 cm³) and PCl₃ (0.009 cm³, 0.10 mmol) was added; ^{1}H NMR spectra were recorded at 1, 12 and 24 h which indicated the progressive generation of impure imidazolium, **2**, and the ^{31}P NMR spectra all indicated residual PCl₃ and other phosphorus species.

4.4.3 Attempted synthesis of Iphenolate^{Me}.PCl (halophosphine precursor), 14

4.4.3.1 Attempted synthesis *via in situ* generation of 6 using NaH/^{t}BuOH, followed by the addition of 2 eq. PCl$_3$

NaH (0.0678 g, 60wt % in mineral oil, 2.83 mmol) was first washed with THF (2 x 5 cm^3) and then suspended in THF (10 cm^3), followed by the addition of **5a** (stored in air) (0.087 g, 0.24 mmol) and ^{t}BuOH (5 drops, too much). The resulting mixture was subsequently stirred at ambient temperature for 19 h. PCl$_3$ (0.042 cm^3, 0.48 mmol) was added and the resulting mixture was stirred at ambient temperature for 23 h. The solvent was removed under reduced pressure and the organic products were extracted into DCM (2 x 10 cm^3) and extracts were combined. The solvent was removed under reduced pressure, to give a golden solid whose ^{1}H NMR spectrum showed imidazolium, **5**, was present. The ^{31}P NMR spectrum displayed one major singlet at δ 77.55 ppm, tentatively indicating the generation of **14**, along with multiple minor peaks. The growth of crystals for SCXRD was attempted by the slow diffusion of hexane into concentred DCM, but was unfortunately unsuccessful.

4.4.3.2 Attempted synthesis *via in situ* generation of 6 using NaH/^{t}BuOK, followed by filtration and then the addition of 2 eq. PCl$_3$

NaH (0.0419 g, 60wt % in mineral oil, 1.75 mmol) was first washed with THF (2 x 5 cm^3) and then suspended in THF (3 cm^3) and the suspension was added to a mixture of **5b** (0.0541 g, 0.15 mmol) and ^{t}BuOK (1.9 mg, 0.02 mmol) *via* a Teflon cannula. The resulting mixture was subsequently stirred at ambient temperature for 20 h, followed by filtration through Celite® and washing through with THF (3 x 5 cm^3). Subsequently, PCl$_3$ (0.026 cm^3, 0.30 mmol) was added to the filtrate and the resulting solution was stirred at ambient temperature for 19 h. The solvent was removed under reduced pressure, the organic products were extracted into DCM (2 x 10 cm^3) and the extracts were combined. The solvent was removed under reduced pressure, to give a dark golden sticky solid whose ^{31}P NMR spectrum displayed multiple signals, however, no signals in the region of δ 70 to 80 ppm. The ^{1}H NMR spectrum was ambiguous although did indicate imidazolium, **5**, was present.

4.4.3.3 Attempted synthesis *via in situ* generation of 6 using NaH/*t*BuOK, followed by the addition of 2 eq. PCl₃ and an altered work-up

NaH (0.0790 g, 60wt % in mineral oil, 3.29 mmol) was first washed with THF (2 x 5 cm^3) and then suspended in THF (10 cm^3) and the suspension was added to a mixture of **5b** (0.1009 g, 0.28 mmol) and ^{t}BuOK (3.2 mg, 0.03 mmol) *via* a Teflon cannula. The resulting mixture was subsequently stirred at ambient temperature for 20 h. PCl₃ (0.049 cm^3, 0.56 mmol) was added and the reaction mixture was stirred at ambient temperature for 29 h. The resulting supernatant was filtered through Celite® and washed through with THF (2 x 5 cm^3). The solvent was removed under reduced pressure, to give a yellow sticky residue whose ^{1}H NMR spectrum was ambiguous and whose ^{31}P NMR spectrum displayed one major signal at δ 77.09 ppm, tentatively attributed to the generation of **14**, along with multiple smaller peaks. The NMR solution was transferred and layered with hexane, but crystallisation was unsuccessful. The dark solid residue on the Celite® was extracted into DCM (3 x 5 cm^3) and the extracts were combined. The solvent was removed under reduced pressure, to yield a golden solid which was identified as impure imidazolium, **5**, by ^{1}H NMR.

4.4.3.4 Attempted synthesis *via in situ* generation of 6 using NaH/*t*BuOK, refluxed overnight, followed by the addition of 1 eq. PCl₃ and an altered work-up

NaH (0.0789 g, 60wt % in mineral oil, 3.29 mmol) was first washed with THF (2 x 5 cm^3) and then suspended in THF (10 cm^3) and the suspension was added to a mixture of **5b** (0.1016 g, 0.28 mmol) and ^{t}BuOK (1.9 mg, 0.02 mmol) *via* a Teflon cannula. The resulting mixture was subsequently refluxed for 17 h. PCl₃ (0.025 cm^3, 0.29 mmol) was added and the reaction mixture was stirred at ambient temperature for 3 h. The resulting mixture was filtered through Celite® and washed through with THF (5 x 5 cm^3). The solvent was removed under reduced pressure to afford a yellow residue, which was triturated with hexane (5 cm^3). The supernatant was decanted *via* filter cannula and the solid was further washed with hexane (3 cm^3) and dried *in vacuo* to give a yellow solid (4.1 mg). The ^{1}H NMR spectrum of the solid was ambiguous but confirmed that imidazolium, **5**, was present. The ^{31}P NMR spectrum showed only two singlets at δ 0.68 and -3.37 ppm corresponding to unidentified products.

4.4.3.5 Attempted synthesis *via in situ* generation of 6 using NaH/^{t}BuOK, refluxed overnight, followed by the addition of 2 eq. PCl$_3$ and further refluxed

NaH (0.0789 g, 60wt % in mineral oil, 3.29 mmol) was first washed with THF (2 x 5 cm^3) and then suspended in THF (10 cm^3) and the suspension was added to a mixture of **5b** (0.1015 g, 0.28 mmol) and ^{t}BuOK (3.4 mg, 0.03 mmol) *via* a Teflon cannula. The resulting mixture was subsequently refluxed for 18 h. PCl$_3$ (0.049 cm^3, 0.56 mmol) was added and the reaction mixture was refluxed again for 2 h. The solvent was removed under reduced pressure and the organic products were extracted into DCM (3 x 5 cm^3) and filtered through Celite®. The solvent was removed under reduced pressure, to afford a golden solid (0.0871 g) for which the ^{1}H NMR spectrum was ambiguous, and the ^{31}P NMR spectrum showed one major overlapping triplet at δ 177.51 ppm and one major singlet at δ 75.73 ppm (tentatively believed to be the desired product, **14**) along with a few minor peaks. The growth of crystals for SCXRD was attempted by the slow diffusion of hexane into concentred DCM, but was unfortunately unsuccessful.

Halide abstraction was attempted by addition of NaBAr^F (0.088 g, 0.10 mmol) to a J Young's NMR tube equipped with a DMSO-*d6* capillary and the afforded golden solid (0.0346 g, ~0.10 mmol) dissolved in DCM (1 cm^3), causing formation of copious precipitate; *in situ* ^{31}P NMR showed three major signals at δ 177.46 (multiplet), 88.70 (singlet) and 87.72 (singlet) ppm, but the ^{1}H NMR was ambiguous. BAr^F in solution was confirmed by the ^{11}B and ^{19}F NMR spectra. The solvent was removed from the NMR tube under reduced pressure and replaced by THF. However, there was still undissolved solid present and the multinuclear NMR spectra were almost identical, except for the ^{31}P NMR spectrum which only displayed one signal at δ 177.64 ppm.

4.5 References

1. H. Spinney, I. Korobkov, G. DiLabio, G. Yap and D. Richeson, *Organometallics*, 2007, **26**, 4972-4982.

2. A. Cowley and R. Kemp, *Chem. Rev.*, 1985, **85**, 367-382.

3. A. Cowley, M. Cushner and J. Szobota, *J. Am. Chem. Soc.*, 1978, **100**, 7784-7786.

4. S. Volodarsky and R. Dobrovetsky, *Chem. Comm.*, 2018, **54**, 6931-6934.

5. S. Fleming, M. Lupton and K. Jekot, *Inorg. Chem.*, 1972, **11**, 2534-2540.

6. a) J. Weigand, K. Feldmann and F. Henne, *J. Am. Chem. Soc.*, 2010, **132**, 16321-16323. B) B. Ellis, C. Dyker, A. Decken and C. Macdonald, *Chem. Comm.*, 2005, 1965-1967.

7. Y. Wang, Y. Xie, M. Abraham, R. Gilliard, P. Wei, H. Schaefer, P. Schleyer and G. Robinson, *Organometallics*, 2010, **29**, 4778-4780.

8. M. Azouri, J. Andrieu, M. Picquet, P. Richard, B. Hanquet and I. Tkatchenko, *Eur. J. Inorg. Chem.*, 2007, **2007**, 4877-4883.

9. N. Burford, T. Cameron, P. Ragogna, E. Ocando-Mavarez, M. Gee, R. McDonald and R. Wasylishen, *J. Am. Chem. Soc.*, 2001, **123**, 7947-7948.

10. N. Burford and P. Ragogna, *J. Chem. Soc., Dalton Trans.*, 2002, 4307-4315.

11. T. Robinson, S. Lo, D. De Rosa, S. Aldridge and J. Goicoechea, *Chem. - Eur. J.*, 2016, **22**, 15712-15724.

12. T. Robinson, D. De Rosa, S. Aldridge and J. Goicoechea, *Angew. Chem. Int. Ed.*, 2015, **54**, 13758-13763.

13. F. Carré, C. Chuit, R. Corriu, A. Mehdi and C. Reyé, *J. Organomet. Chem.*, 1997, **529**, 59-68.

14. W. Zhao, S. McCarthy, T. Lai, H. Yennawar and A. Radosevich, *J. Am. Chem. Soc.*, 2014, **136**, 17634-17644.

15. S. McCarthy, Y. Lin, D. Devarajan, J. Chang, H. Yennawar, R. Rioux, D. Ess and A. Radosevich, *J. Am. Chem. Soc.*, 2014, **136**, 4640-4650.

16. Y. Lin, J. Gilhula and A. Radosevich, *Chem. Sci.*, 2018, **9**, 4338-4347.

17. N. Kuhn, J. Fahl, D. Bläser and R. Boese, *Z. Anorg. Allg. Chem.*, 1999, **625**, 729-734.

18. D. Mendoza-Espinosa, B. Donnadieu and G. Bertrand, *J. Am. Chem. Soc.*, 2010, **132**, 7264-7265.

19. U. Hintermair, U. Englert and W. Leitner, *Organometallics*, 2011, **30**, 3726-3731.

20. M. Boronat, A. Corma, C. González-Arellano, M. Iglesias and F. Sánchez, *Organometallics*, 2010, **29**, 134-141.

21. S. Gaillard and J. Renaud, *Dalton Trans.*, 2013, **42**, 7255-7270.

22. F. Henne, A. Dickschat, F. Hennersdorf, K. Feldmann and J. Weigand, *Inorg. Chem.*, 2015, **54**, 6849-6861.

Chapter Five

Future Work

"The greatest pleasure in life is doing what people say you cannot do"

Walter Bagehot

5.1 Future work

The imidazolium salt (IAnis^{Me}.HCl), **2a**, was found to be wet even after special measures were used to try and dry the salt. Tests into whether the solid is hygroscopic would therefore be of great value, as understanding this would affect the way the solid is stored and handled, and could potentially make life easier for future experimentalists.

The inability to get satisfactory combustion analysis of the [Cu(IAnis^{Me})$_2$]BF$_4$ complex, **11**, suggests some form of decomposition process or contaminants. Since all other reported homoleptic cations are stable, this should be investigated. In conjugation to this, better signal to noise in a ^{13}C{^{1}H} NMR spectrum of the selenourea adduct would be useful in order to see if the $^1J_{C-Se}$ coupling constant can be observed for the C$_{carbene}$ to infer the σ-donor properties of the ligand.

Exploration of the metal complexes synthesised in catalysis would also be very interesting since similar complexes are all reported to catalyse numerous reactions. A more viable method for the synthesis of the mono-copper(I) complex, **10**, would be sought after if it were needed in large quantities. Additionally, synthesis of metal complexes coordinating to the IPhenol^{Me} ligand would also be highly desirable, as then these complexes can be contrasted and compared with other donor-substituted carbene complexes and indeed the parent IAnis^{Me} complexes, and observe if the methyl groups on the oxygens make a significant difference to the electronic properties of the NHC and subsequently catalysis.

The synthesis of the corresponding NHC precursors without the methyl groups on the backbone would be desirable to observe how the methyl groups on the backbone affect the NHCs, especially in light of the dynamic behaviour observed for the IAnis^{Me} complexes. Synthesis of the saturated analogues would also be of interest to see the difference in their electronic properties and if these species are indeed more reactive, as would be expected.

Initial reactions of free NHCs or the silver(I) complex with phosphorus species were performed at ambient temperature or above, to permit their rapid evaluation by ^{31}P NMR. However, it would be of great interest to try such reactivity at a lower temperature (preferably -78 °C), to see if this circumvents side reactions, which was not possible in the limited time available. Another possibility to try in conjugation to the one above is attempting the reactions of the free NHCs, **3** and **6**, generated *in situ,* over molecular sieves followed by subsequent addition of the phosphorus species to see if such preparation circumvents hydrolysis.

The reaction of Ph_2PCl with the carboxylate adduct (IAnis^{Me}.CO$_2$), **4a**, showed promise however the adduct was not clean. One potential method to try obtaining clean **4a** is the reaction of the imidazolium chloride (IAnis^{Me}.HCl), **2a**, with excess LiHMDS in Et$_2$O as **2a** is not even sparingly soluble in Et$_2$O. Subsequent reaction of the supernatant with dry CO_2 should provide the clean carboxylate adduct, **4a**.

When attempting halide abstraction on putative phosphenium cation samples, copious amounts of precipitate appeared. One possibility is that the desired products formed, but were not soluble in DCM. Thus, it may be helpful to try this reaction in solvents with higher dielectric constants like difluorobenzene (DFB), to see if the product remains in solution and so hopefully gain an indication of what the precipitate is, whether that be the desired phosphenium cation or decomposition products.

Appendix

"You can, you should, and if you're brave enough to start, you will"

Stephen King

A1 General experimental

A1.1 Starting material

All starting materials were used as received, unless otherwise stated, from Acros Organics, Alfa Aesar, Fisher, Fisons, Honeywell or Sigma Aldrich. Nickelocene was purified by vacuum sublimation from supplies synthesised by undergraduate students in teaching labs. Ph_2PCl and PCl_3 were distilled in vacuum prior to use (distilled PCl_3 used when specified).

A1.2 Drying of solvents

Prior to use all solvents were distilled over an appropriate desiccant and were stored in J Young's ampoules under an atmosphere of argon. DCM and MeCN were distilled over CaH_2 and stored over activated molecular sieves. THF was distilled over potassium and stored over activated molecular sieves. Hexane and Et_2O were distilled over sodium/benzophenone and stored over activated molecular sieves. Toluene was distilled over sodium and stored over activated molecular sieves. When reactions were carried out under air, then solvents were used as supplied.

A1.3 Air and moisture sensitive techniques

Unless otherwise specified, all reactions and product manipulations were carried out *via* standard Schlenk-line or glovebox techniques (MBraun MB10 compact glovebox maintained at < 0.5 ppm for H_2O and O_2) under an atmosphere of argon. Air and moisture sensitive reagents were stored in J Young's ampoules under an atmosphere of argon. All glassware used in manipulations were pre-dried at 80 °C and prior to use were flame-dried under vacuum, except when glassware was taken into the glovebox, when it was removed from the 80 °C oven and allowed to cool under vacuum in the ports.

A1.4 NMR spectroscopy

NMR spectra were recorded on either a Bruker AV II 400 MHz spectrometer, or a Bruker NEO 400 MHz NMR spectrometer. NMR spectra were reported in ppm, recorded in *protio*-solvent equipped with a DMSO-*d6* capillary and referenced to the appropriate residual solvent peak(s).

A1.5 Single-crystal X-ray diffraction

Diffraction data were recorded on a Rigaku Oxford Diffraction Supernova Dual Diffractometer with Cu-Kα (λ = 1.54184 Å) or Mo-Kα (λ = 0.71073 Å) radiation at 100 K. The single crystals were mounted on MiTeGen microloops. Unit cell determination, data reduction and absorption corrections were carried out using CrysAlisPro 1.171.39.46[1]. The structure was solved by direct methods and refined by full matrix least squares on the basis of F2 using SHELX 2013[2] within the Olex2 GUI[3]. Non-hydrogen atoms were refined anisotropically and hydrogen atoms were included using a riding model. Crystal structure images and data tables were generated using Olex2 GUI[3]. All data collections and refinements were carried out by Dr Ewan R Clark.

A1.6 Elemental analysis

Elemental analysis was performed at London Metropolitan University by Stephen Boyer.

A2 Multinuclear NMR data

A2.1 Multinuclear NMR data of 1a

A2.1.1 ^{1}H NMR spectrum
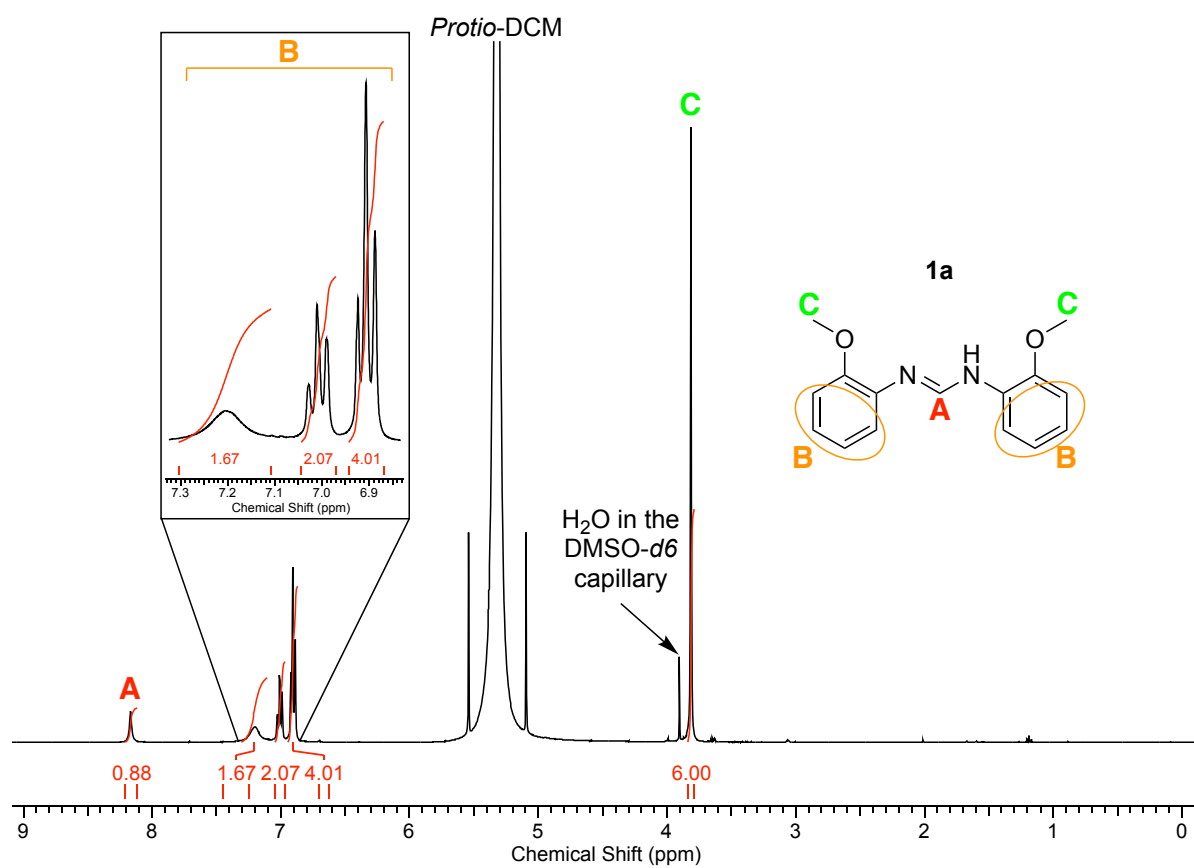
A2.1.2 $^{13}C\{^1H\}$ NMR spectrum
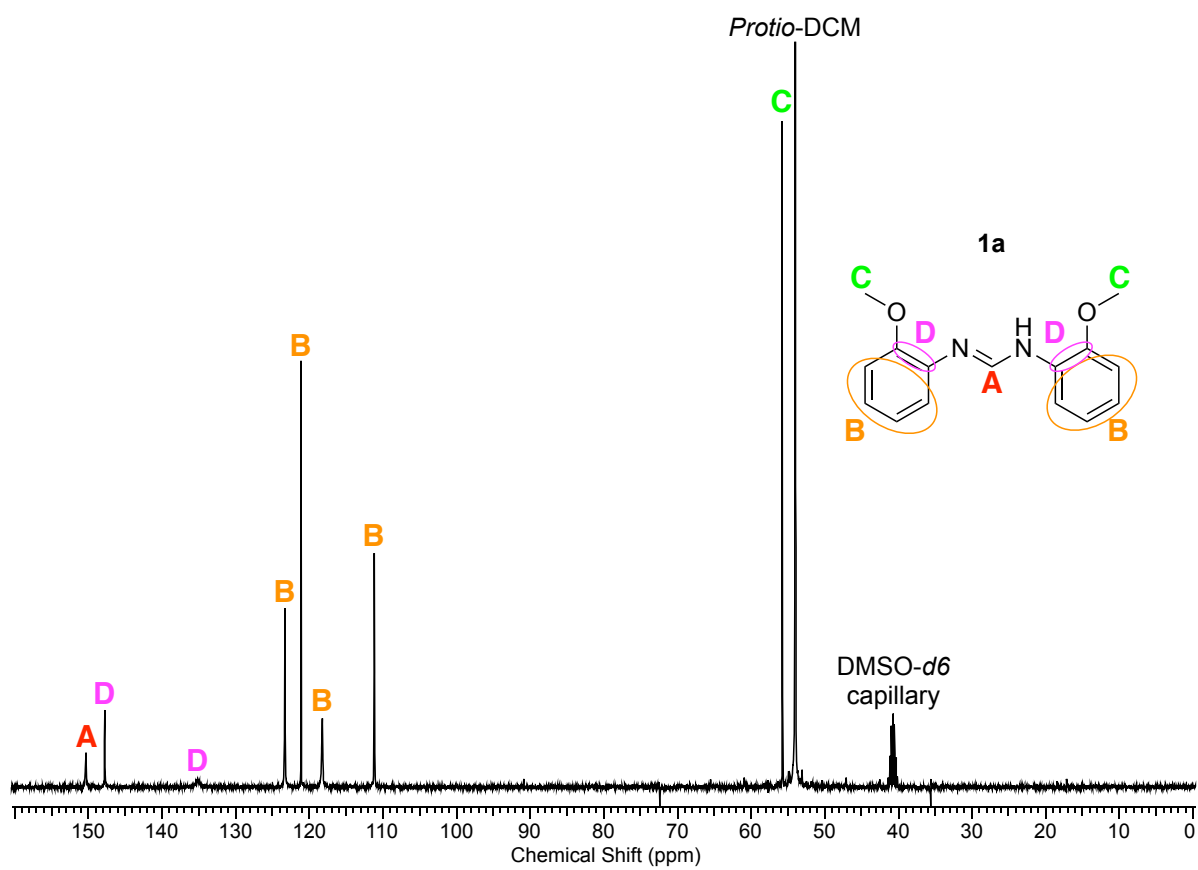
A2.2 Multinuclear NMR data of 2a

A2.2.1 ^{1}H NMR spectrum
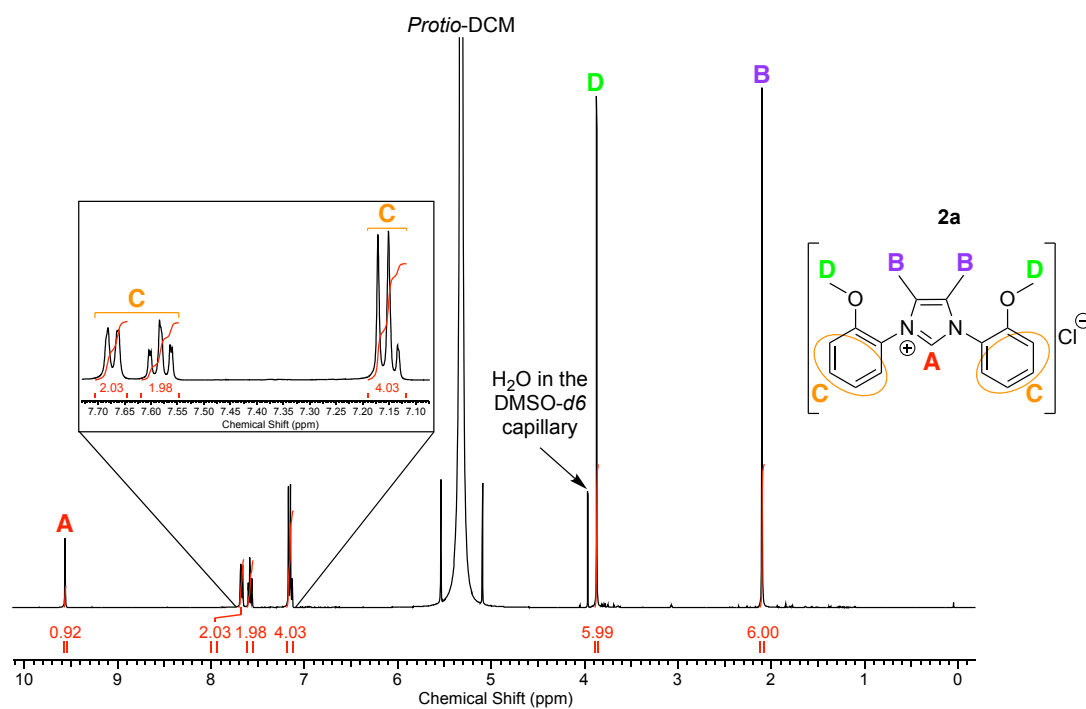
A2.2.2 ^{13}C{^{1}H} NMR spectrum
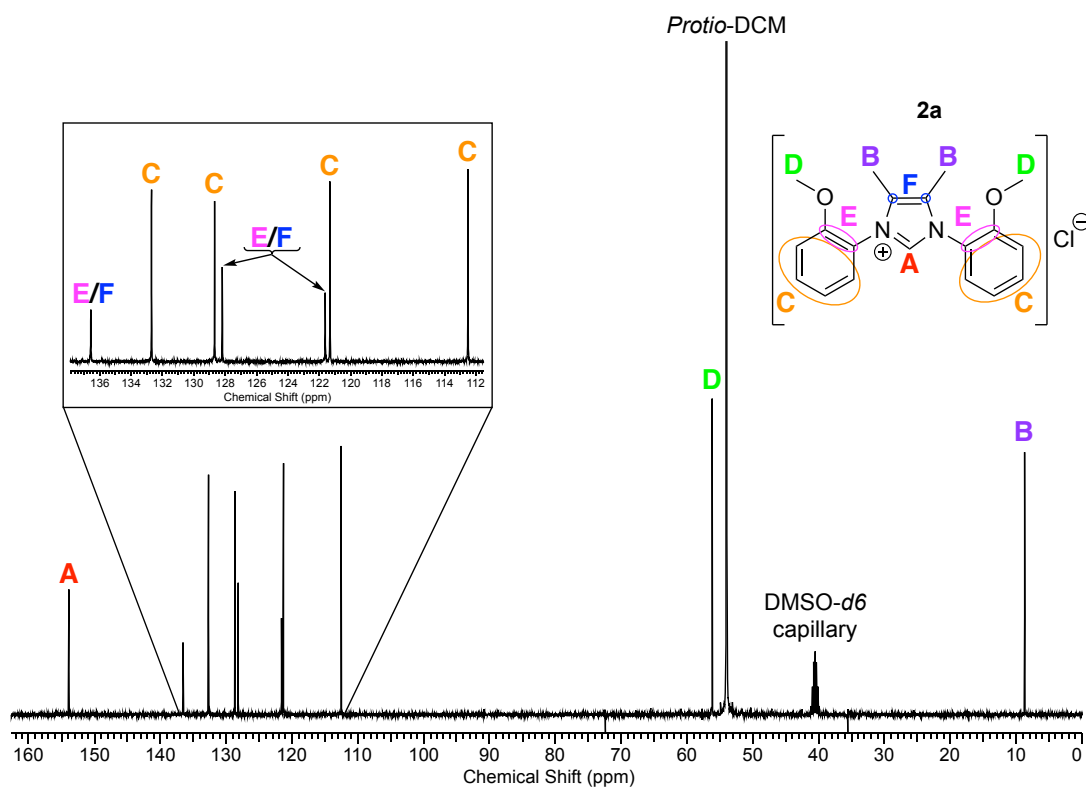
A2.3 Multinuclear NMR data of 2b

A2.3.1 ^{1}H NMR spectrum
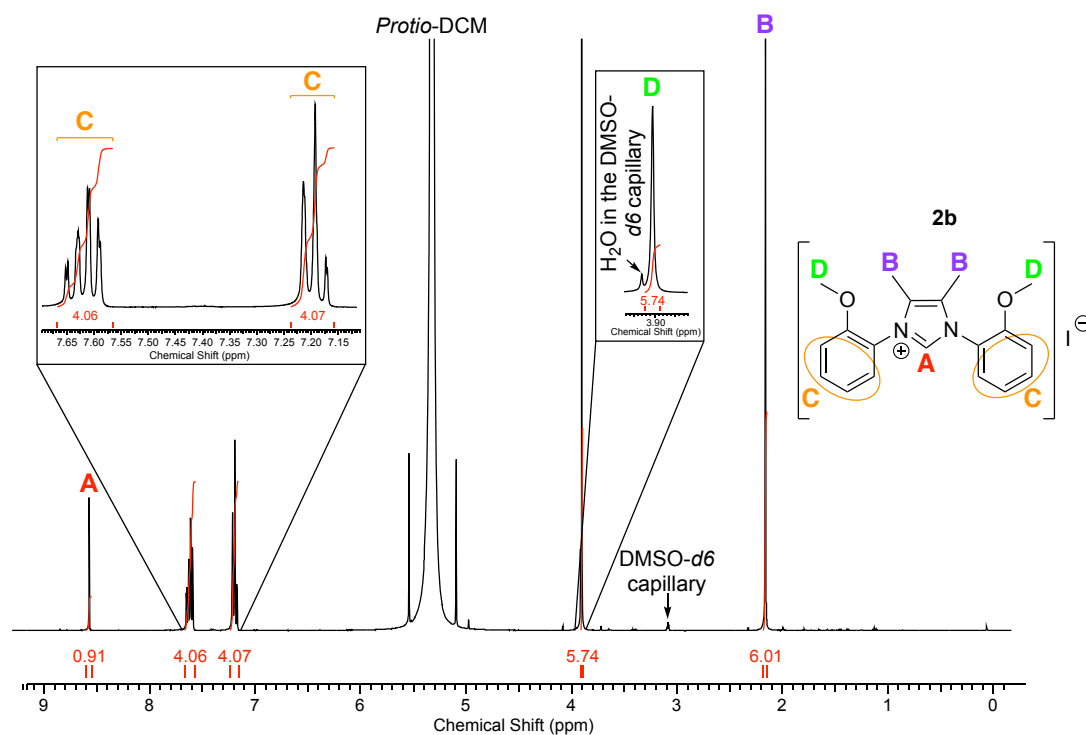
A2.3.2 ^{13}C{^{1}H} NMR spectrum
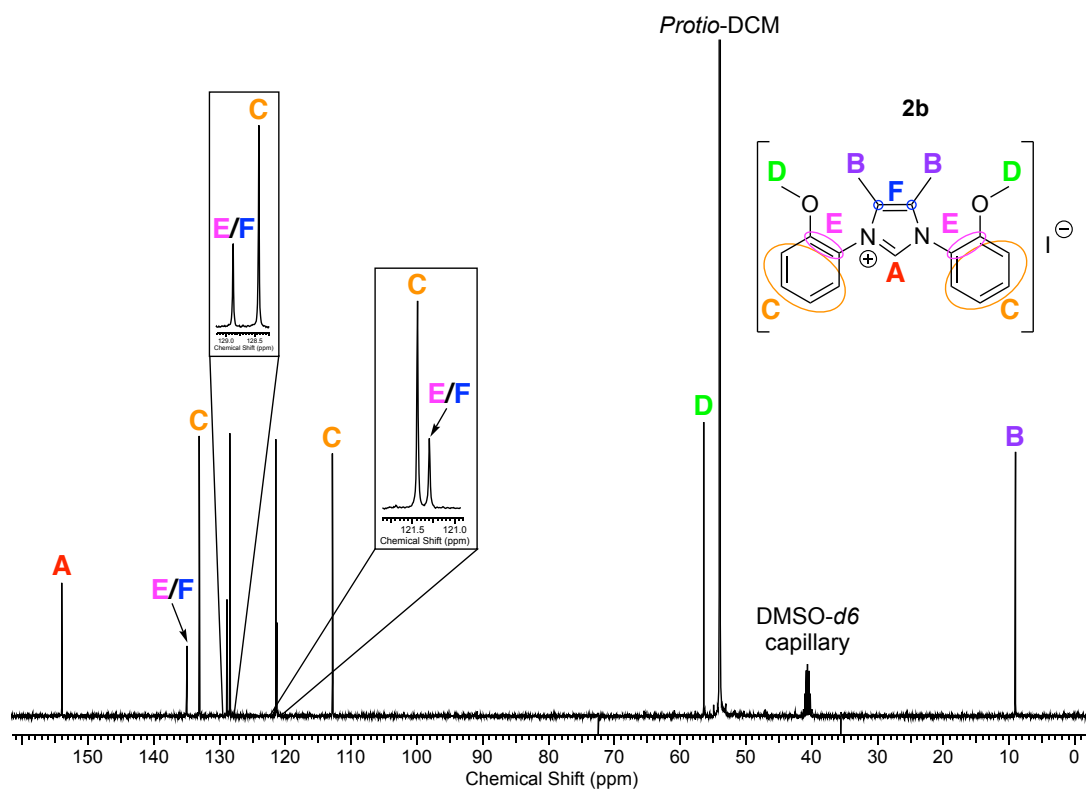
A2.4 Multinuclear NMR data of 2c

A2.4.1 ^{1}H NMR spectrum
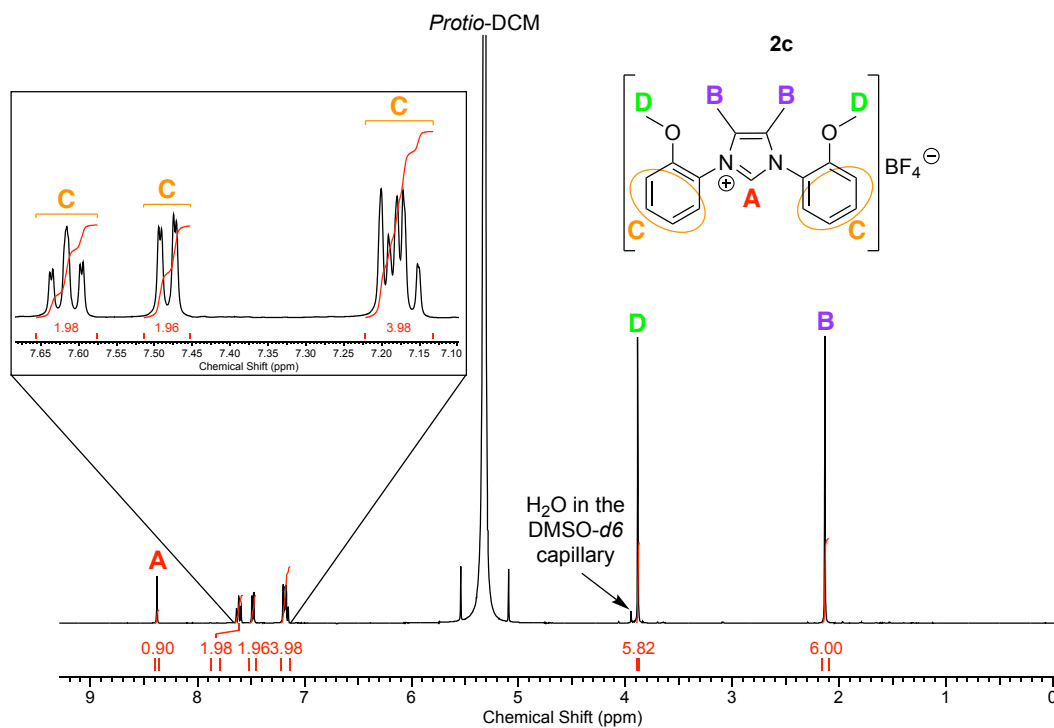
A2.4.2 ^{13}C{^{1}H} NMR spectrum
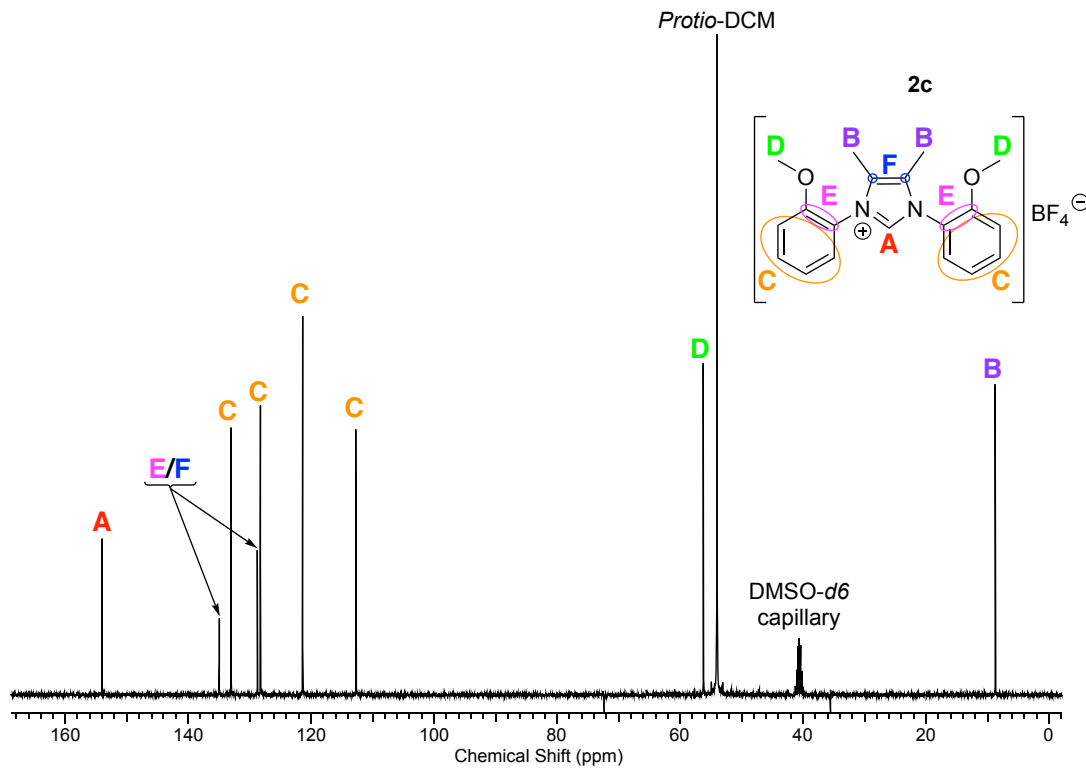
A2.4.3 ^{11}B NMR spectrum
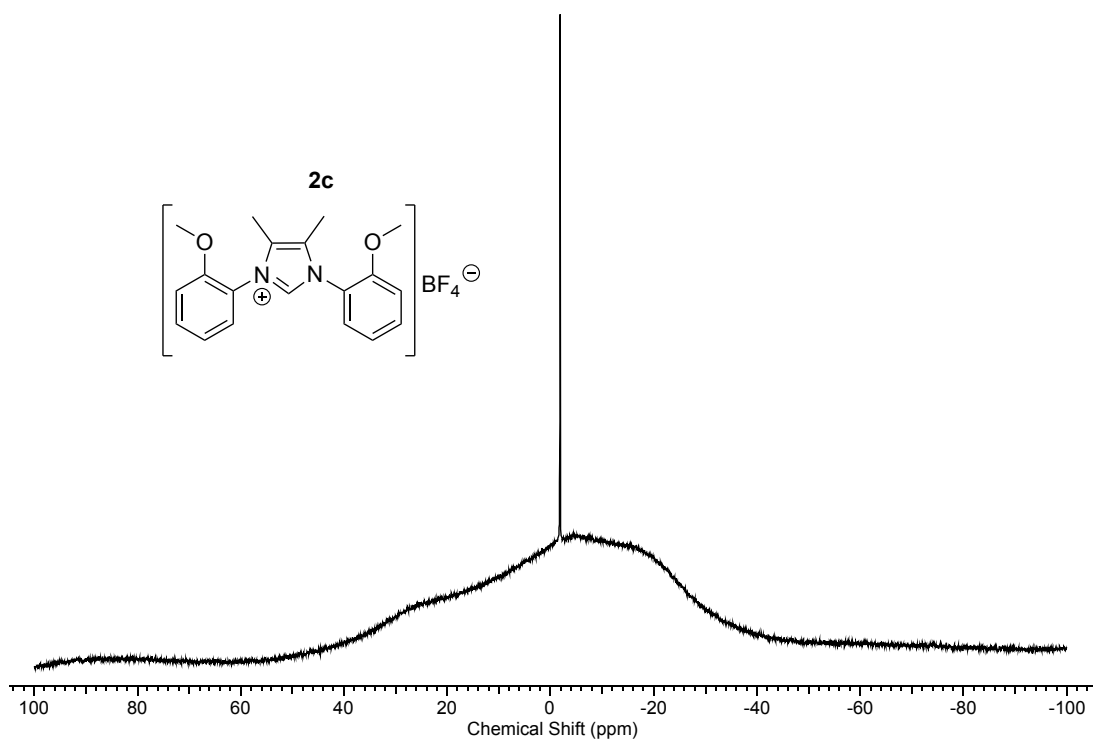
A2.4.4 ^{19}F NMR spectrum
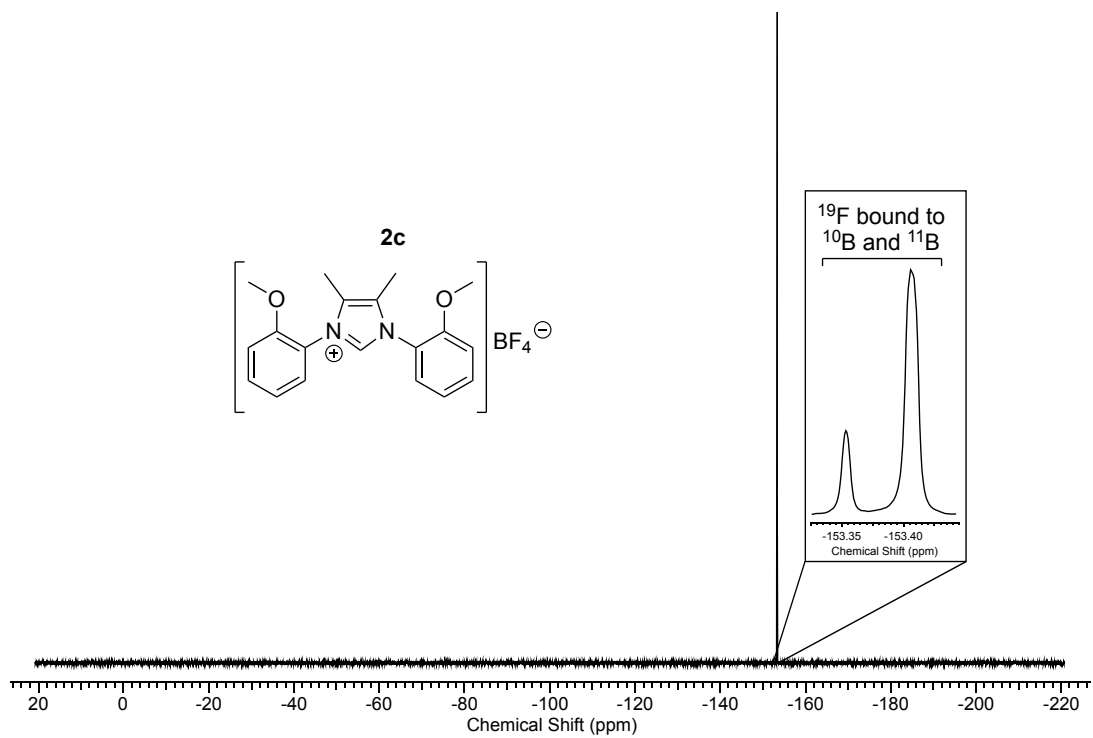
A2.5 Multinuclear NMR data of 3

A2.5.1 ^{1}H NMR spectrum (provisionally assigned)
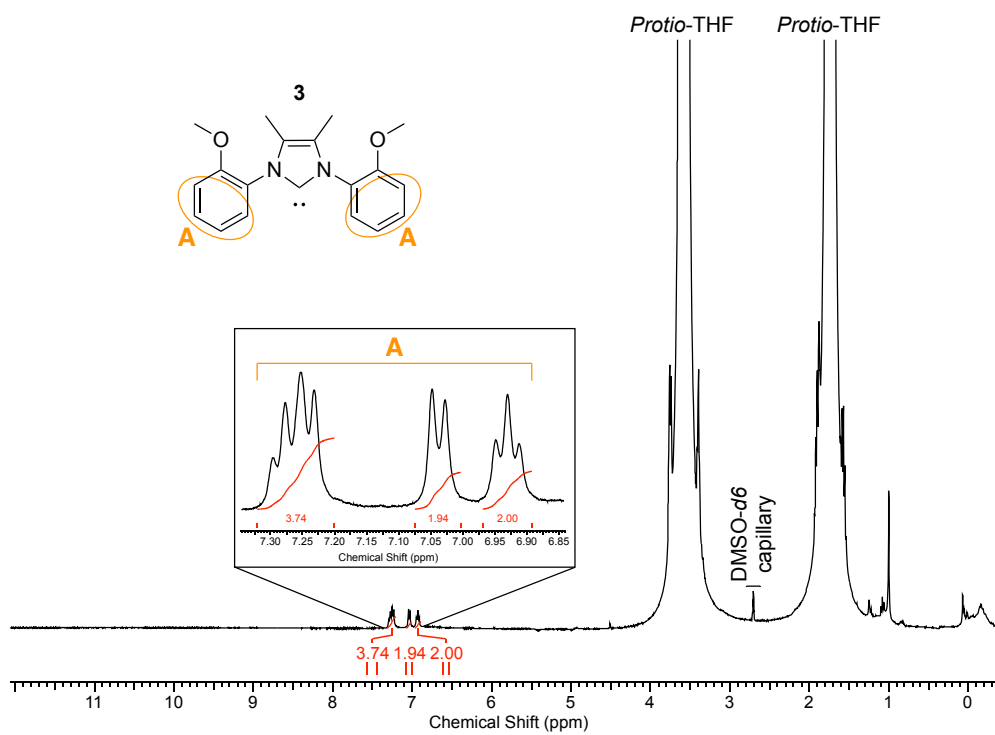
A2.6 Multinuclear NMR data of 5a

A2.6.1 ^{1}H NMR spectrum
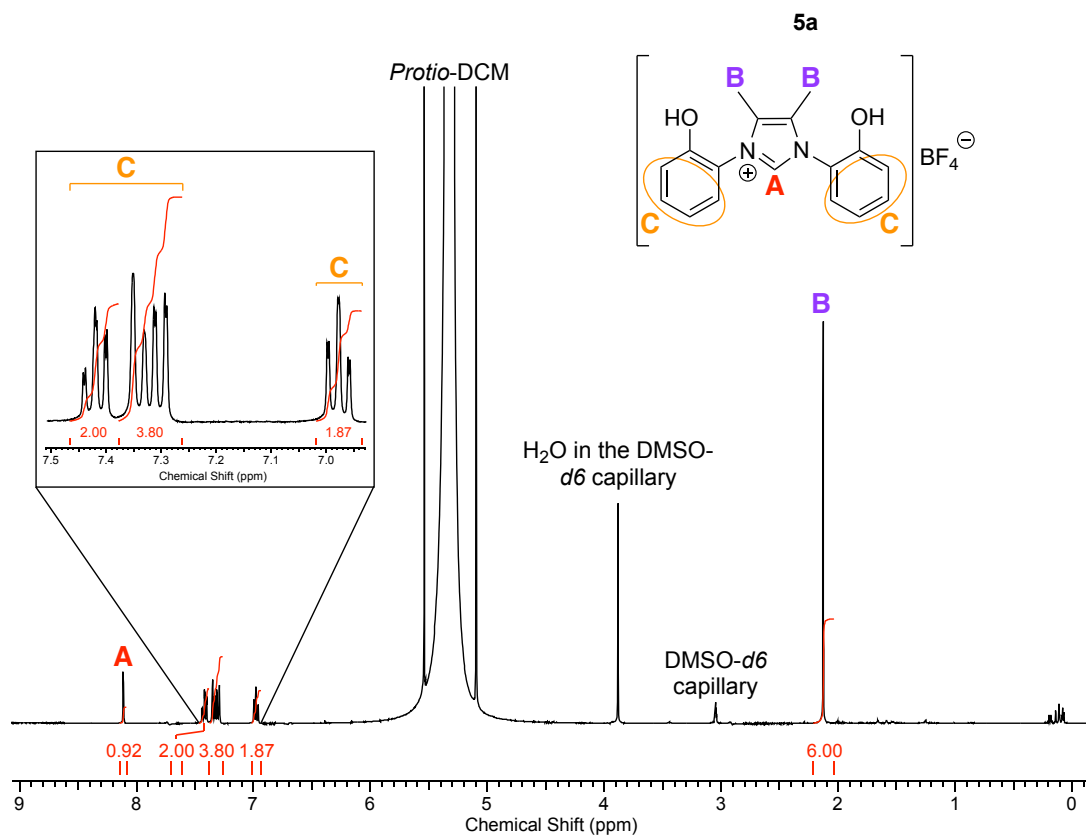
A2.6.2 ^{11}B NMR spectrum
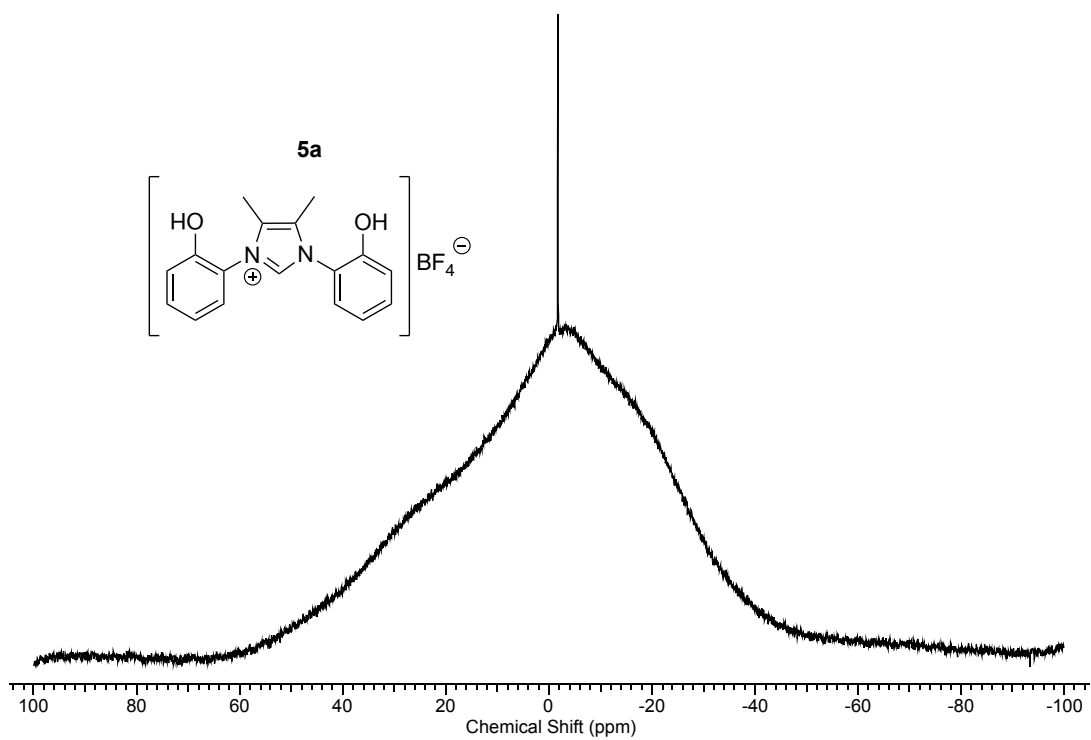
A2.6.3 19F NMR spectrum
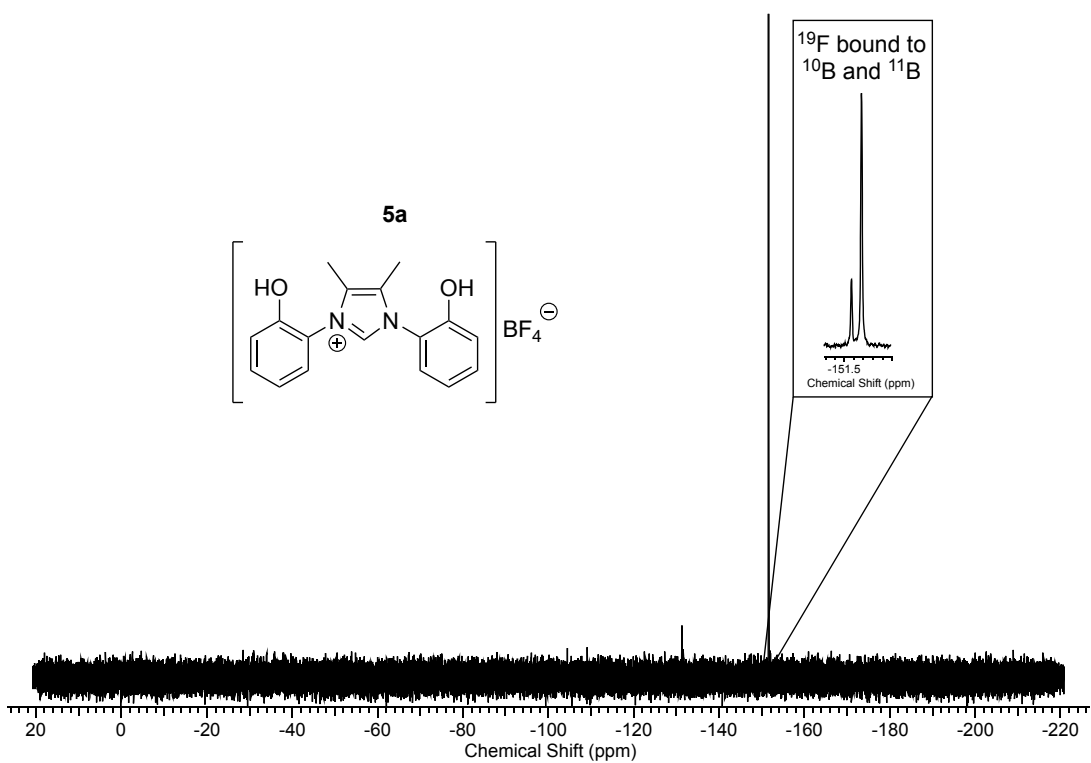
A2.7 Multinuclear NMR data of 5b

A2.7.1 ^{1}H NMR spectrum
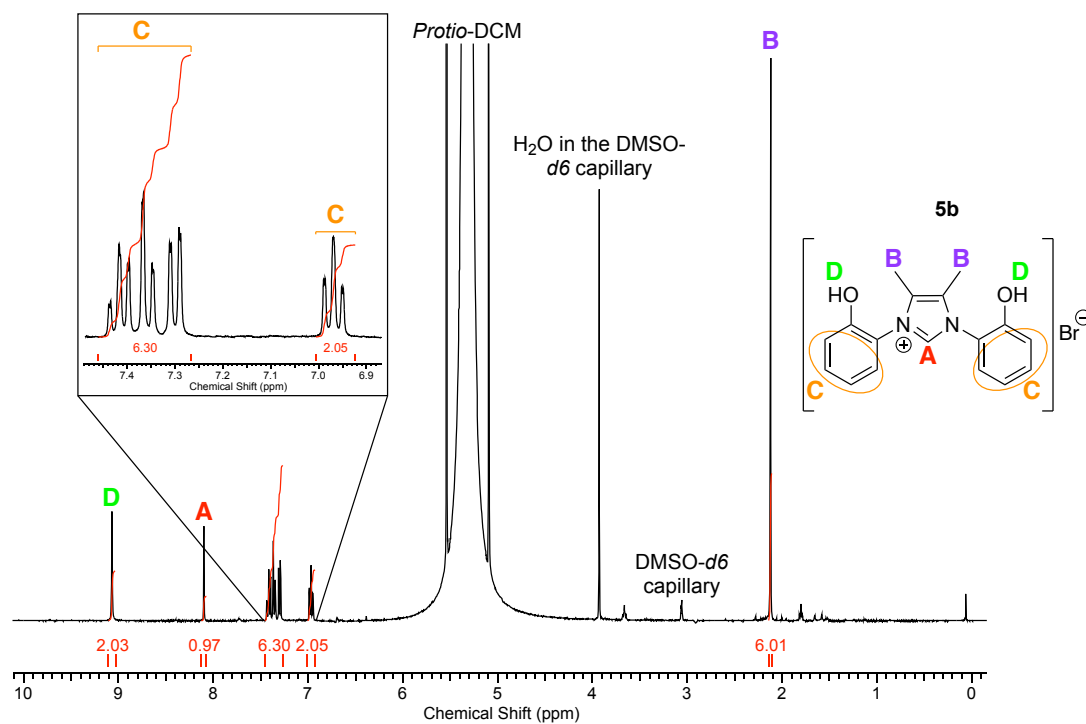
A2.7.2 ^{13}C{^{1}H} NMR spectrum
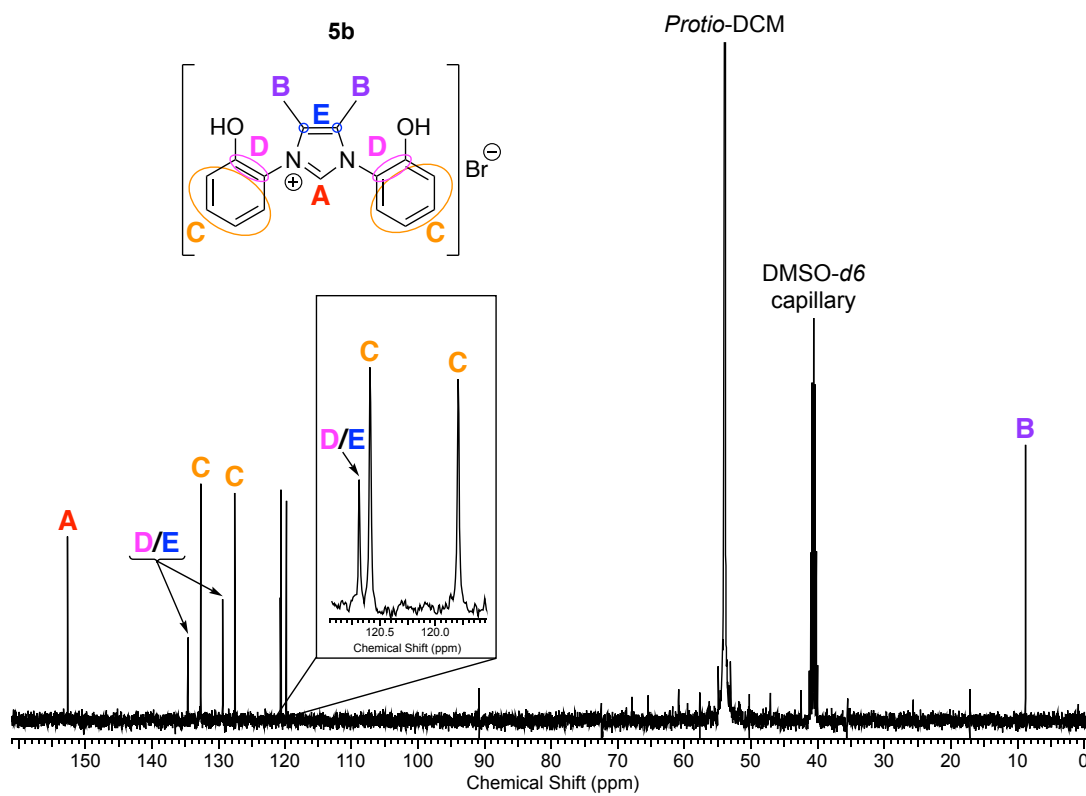
A2.8 Multinuclear NMR data of 6

A2.8.1 ^{1}H NMR spectrum (provisionally assigned)
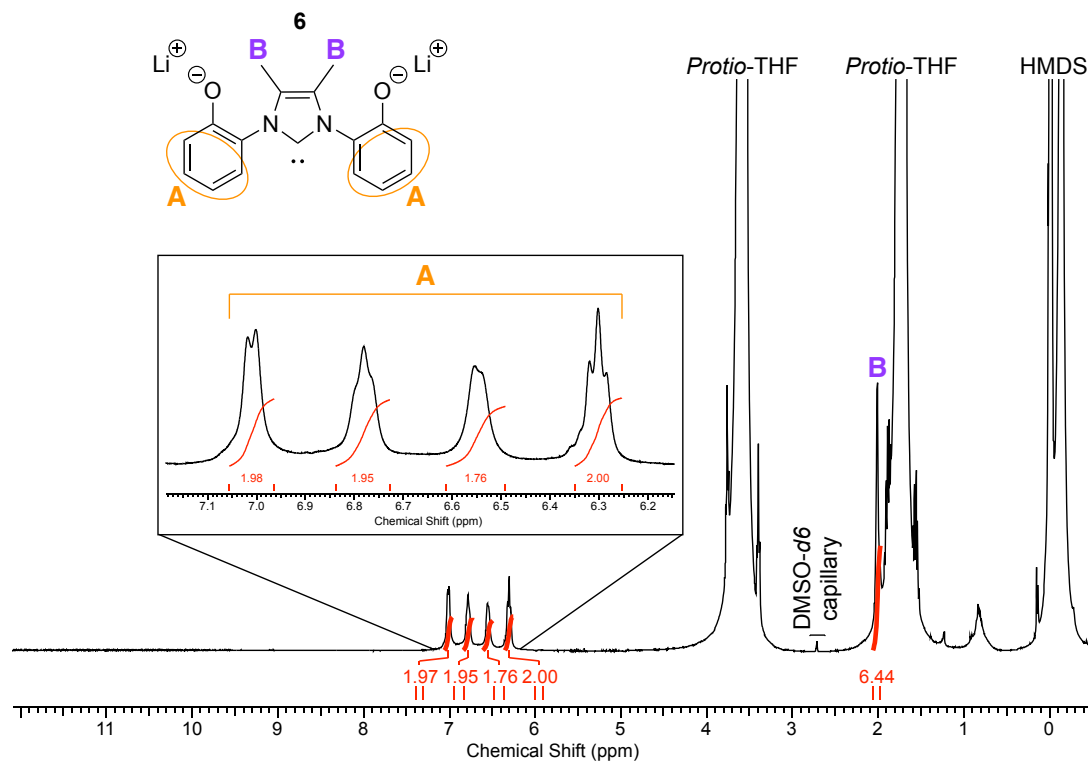
A2.9 Multinuclear NMR data of 7

A2.9.1 ^{1}H NMR spectrum recorded in *protio*-DCM
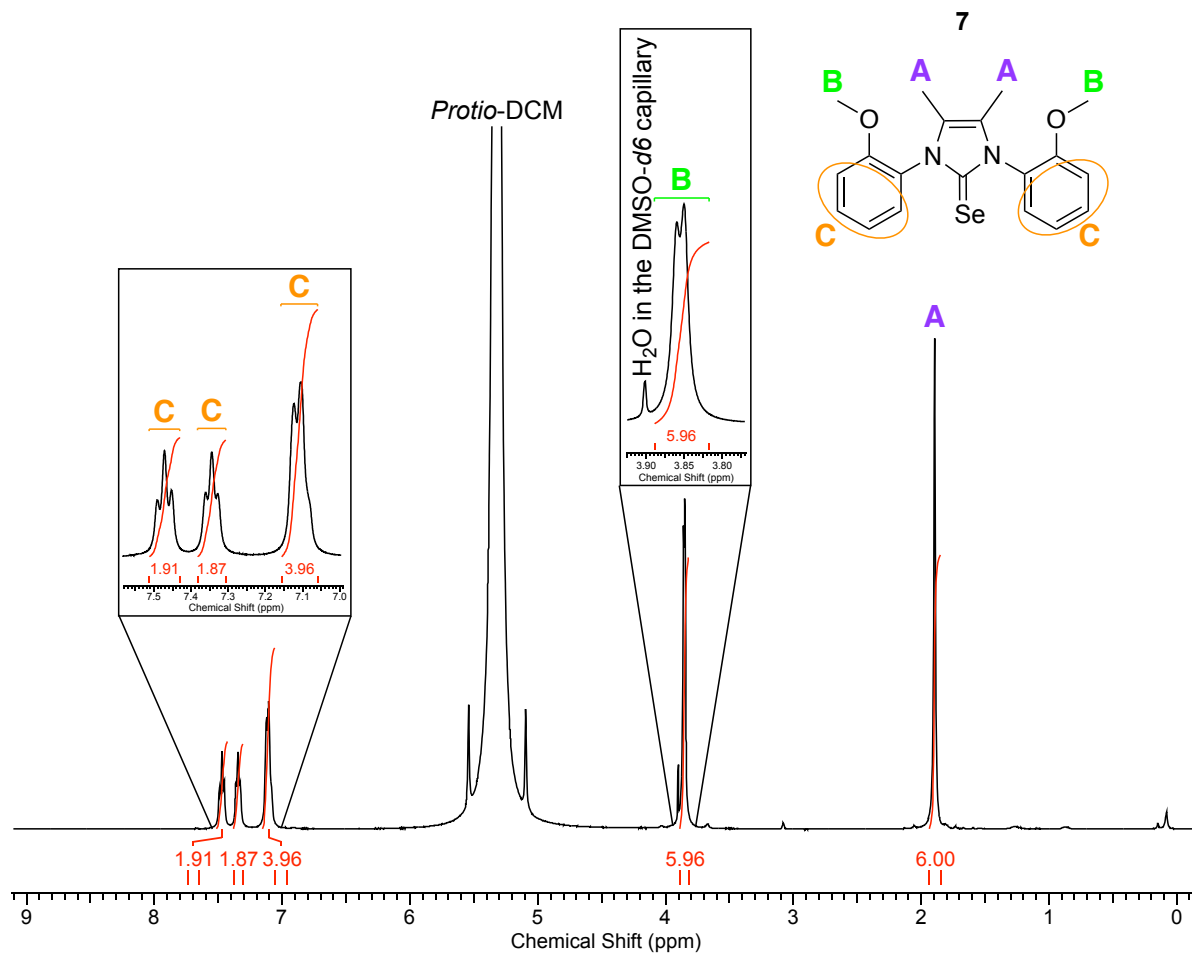
A2.9.2 ^{1}H NMR spectrum recorded in *protio*-MeCN
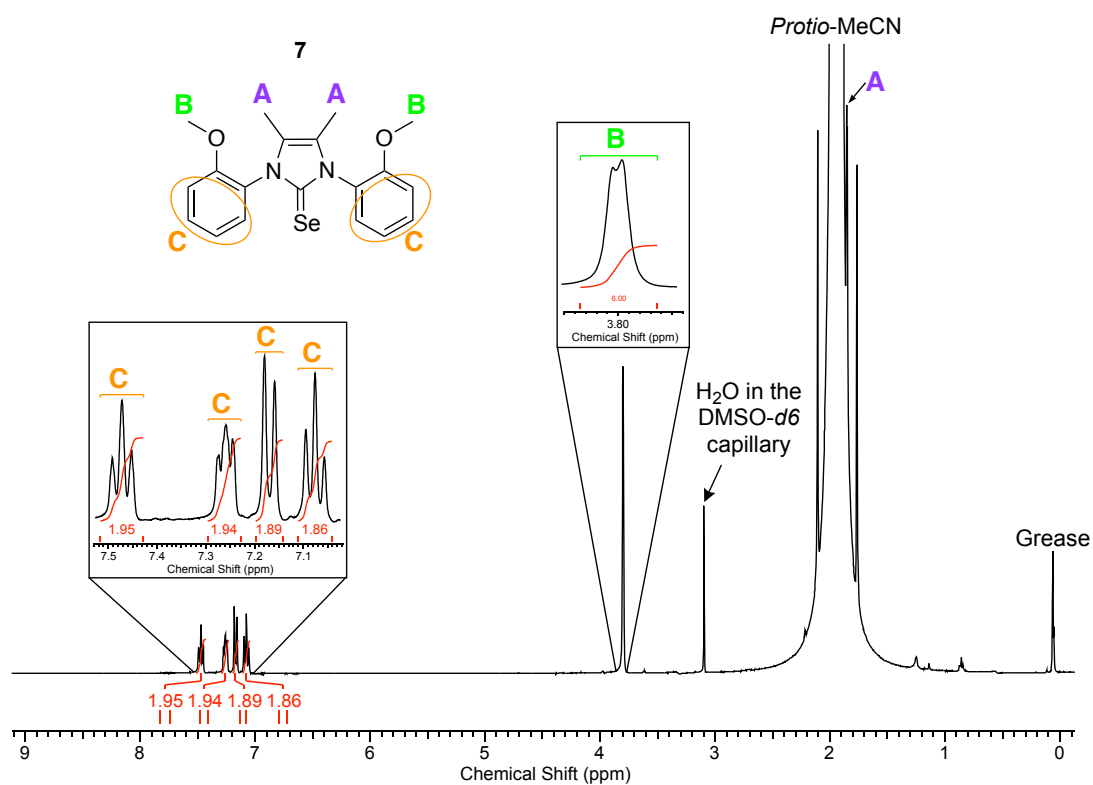
A2.9.3 ^{13}C{^{1}H} NMR spectrum
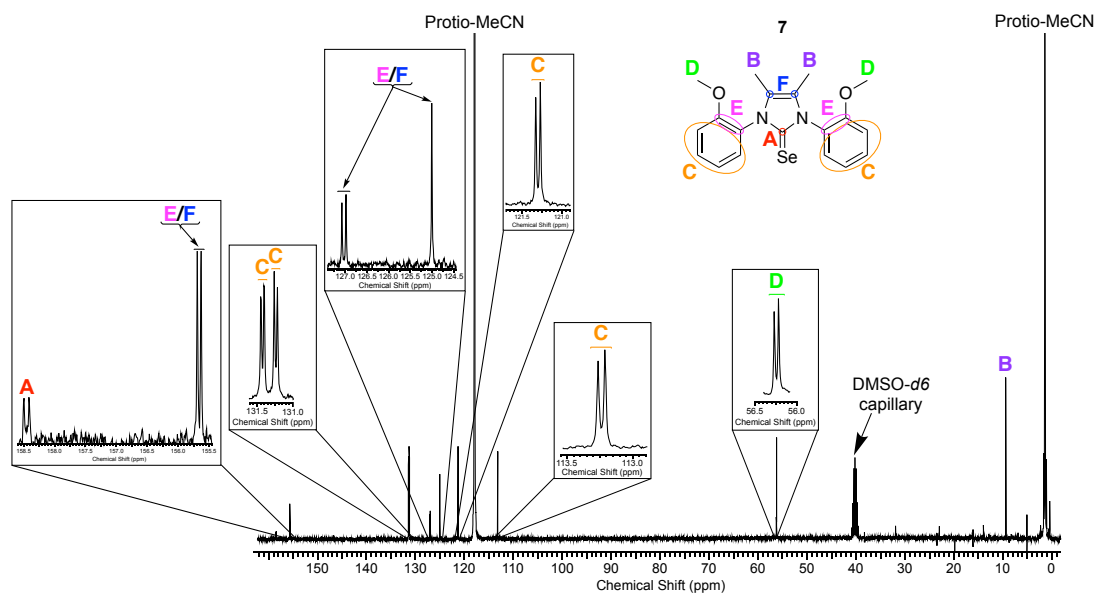
A2.9.4 ^{1}H VT NMR spectra
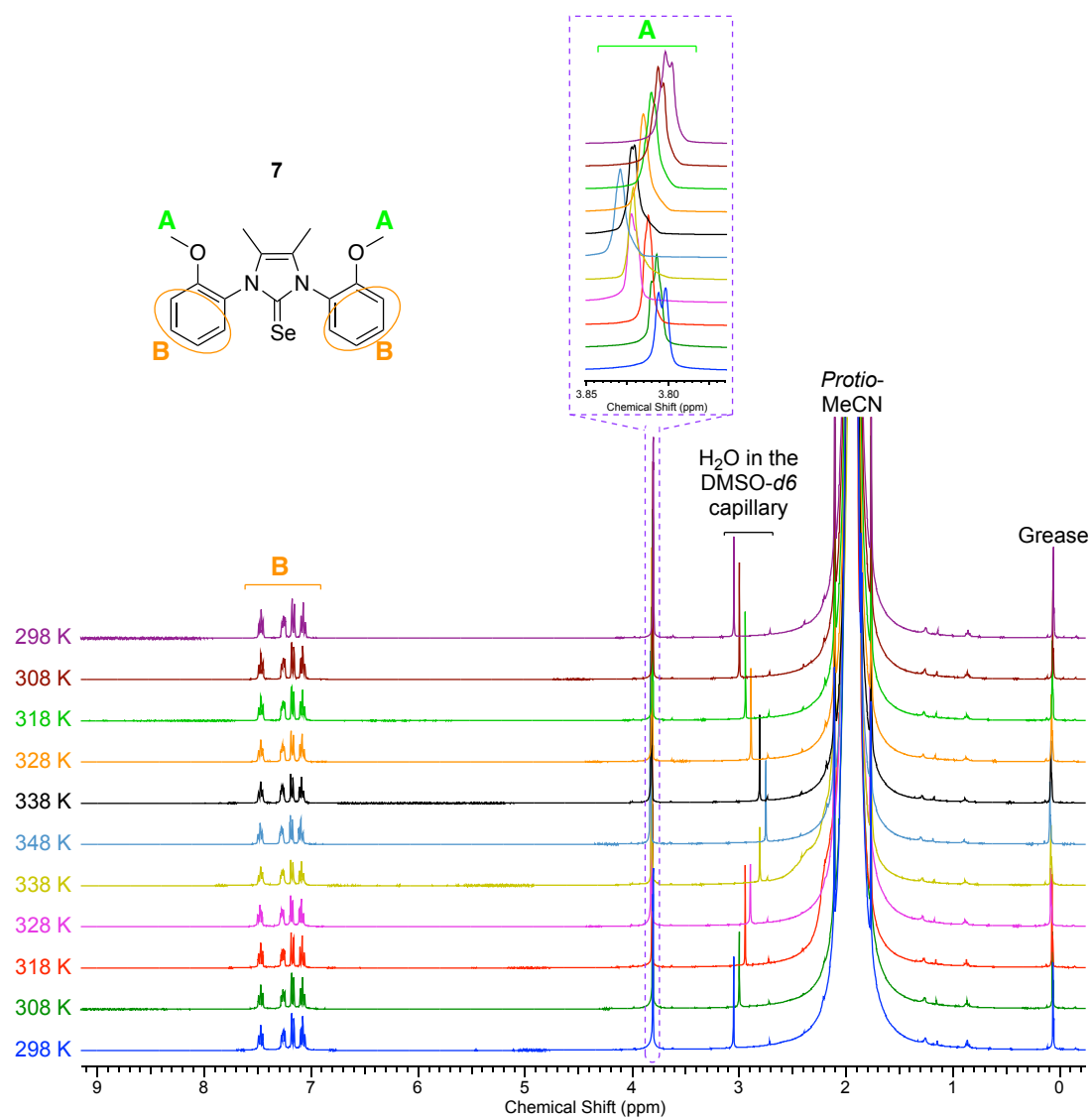
A2.9.5 ⁷⁷Se NMR spectrum
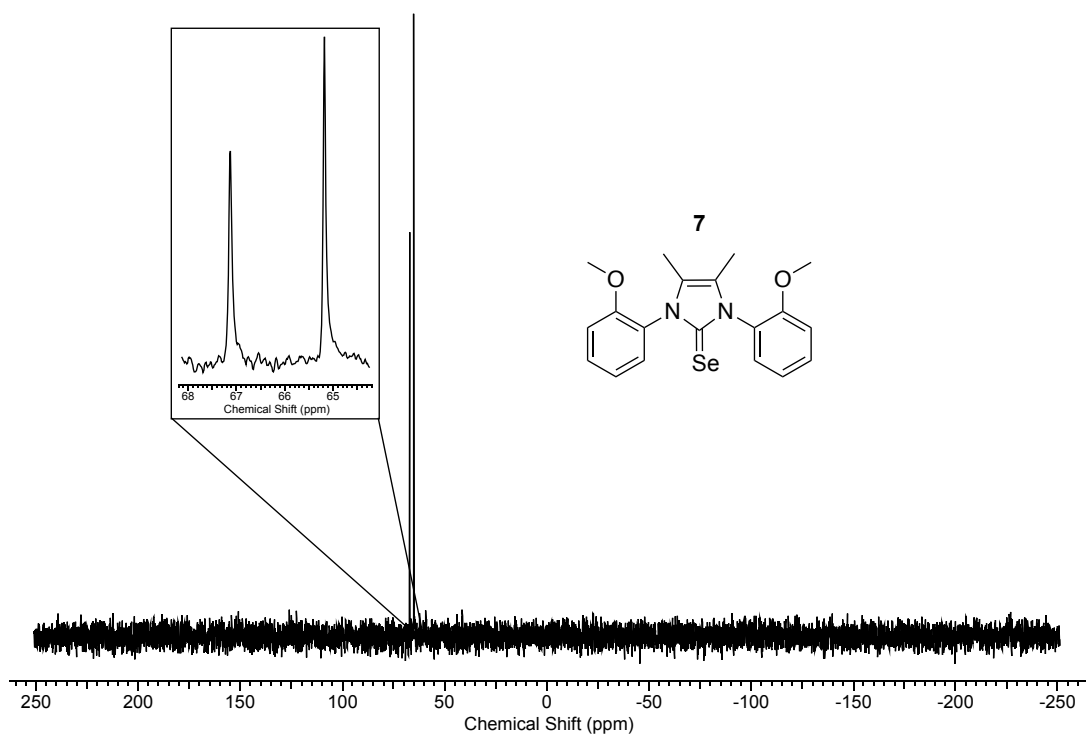
A2.10 Multinuclear NMR data of 8
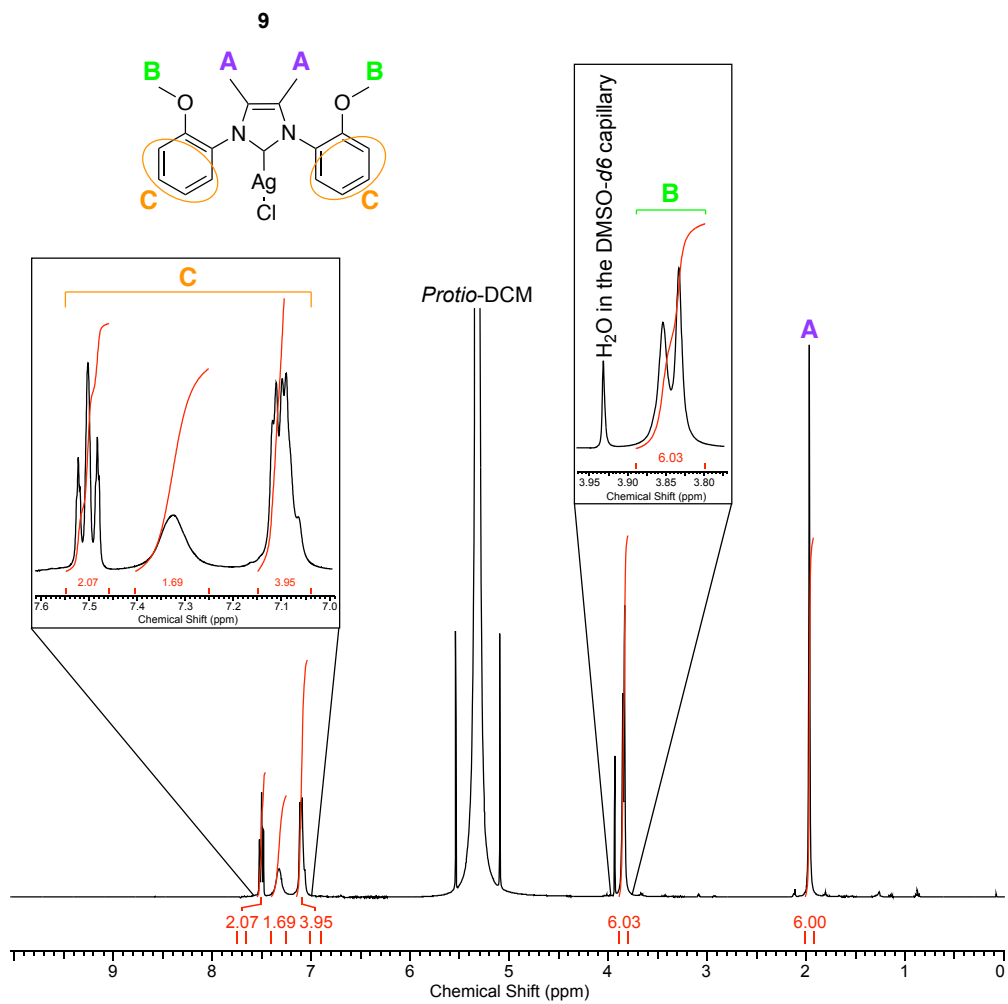
A2.10.1 ^{1}H NMR spectrum
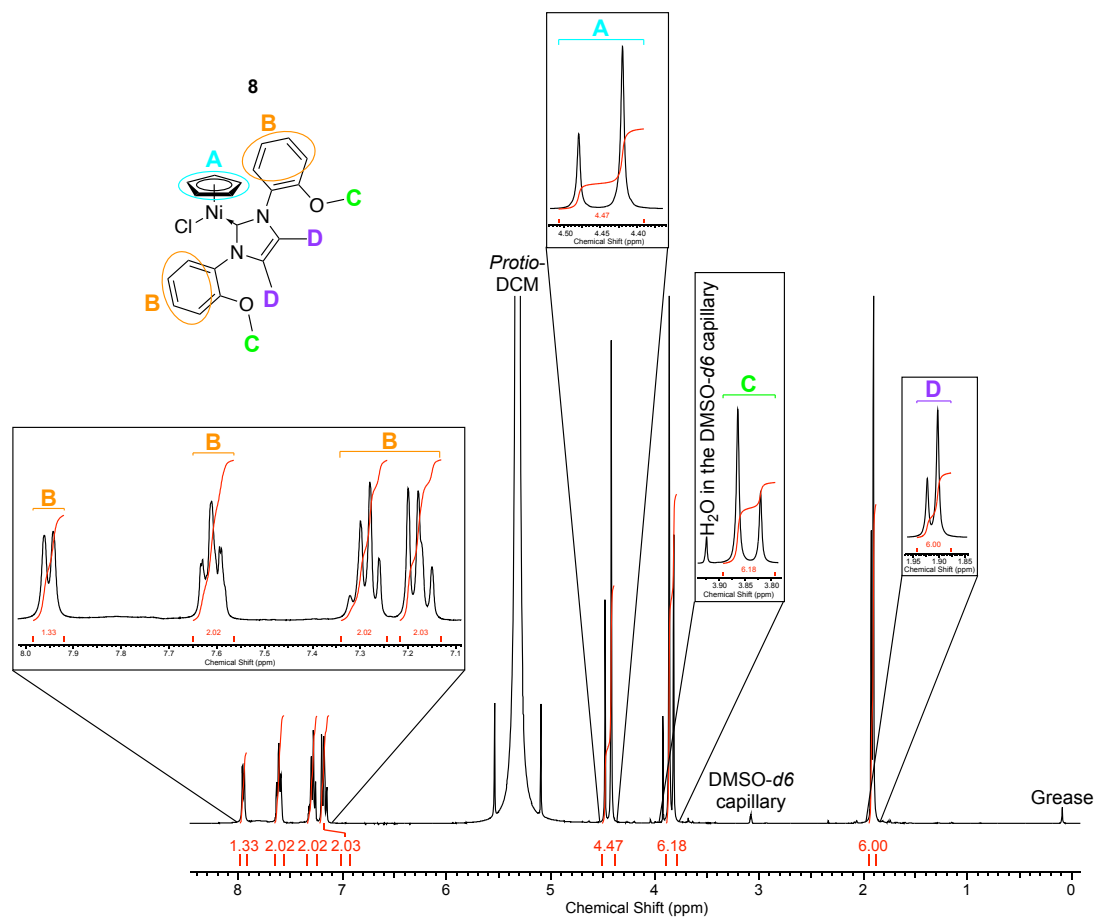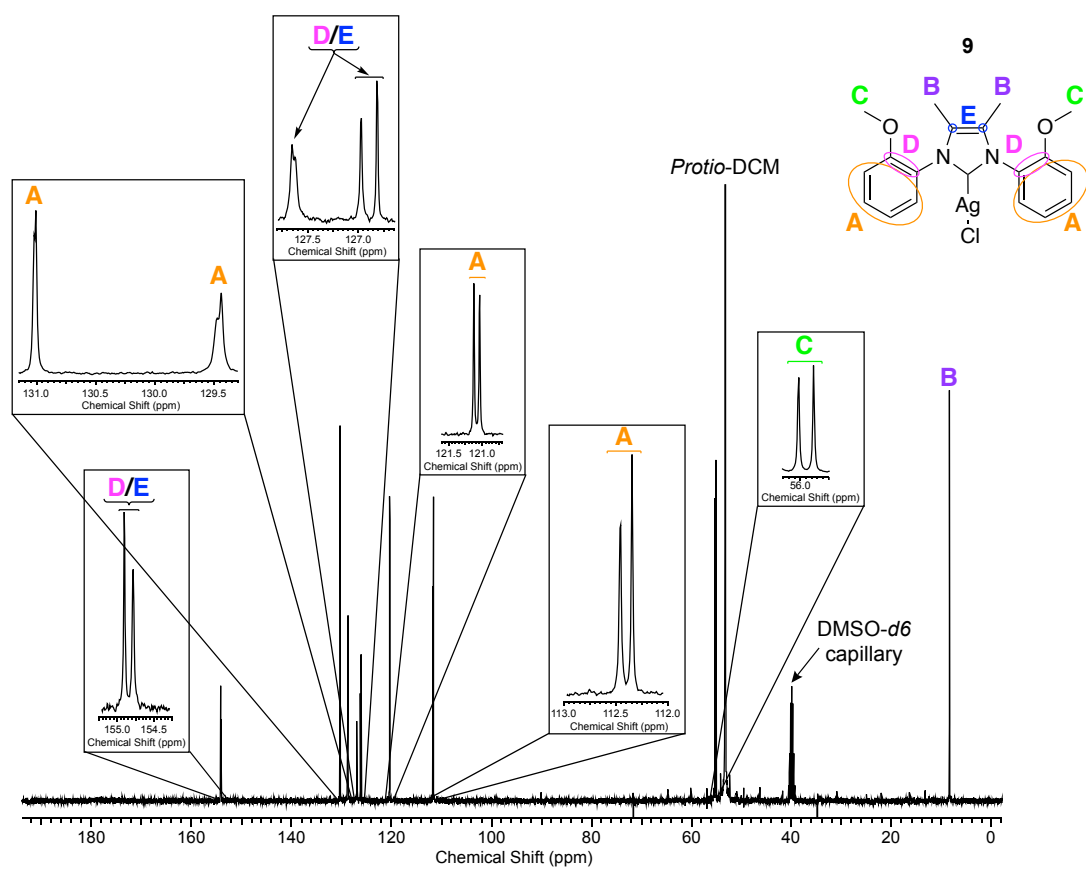
A2.10.2 ^{13}C{^{1}H} NMR spectrum
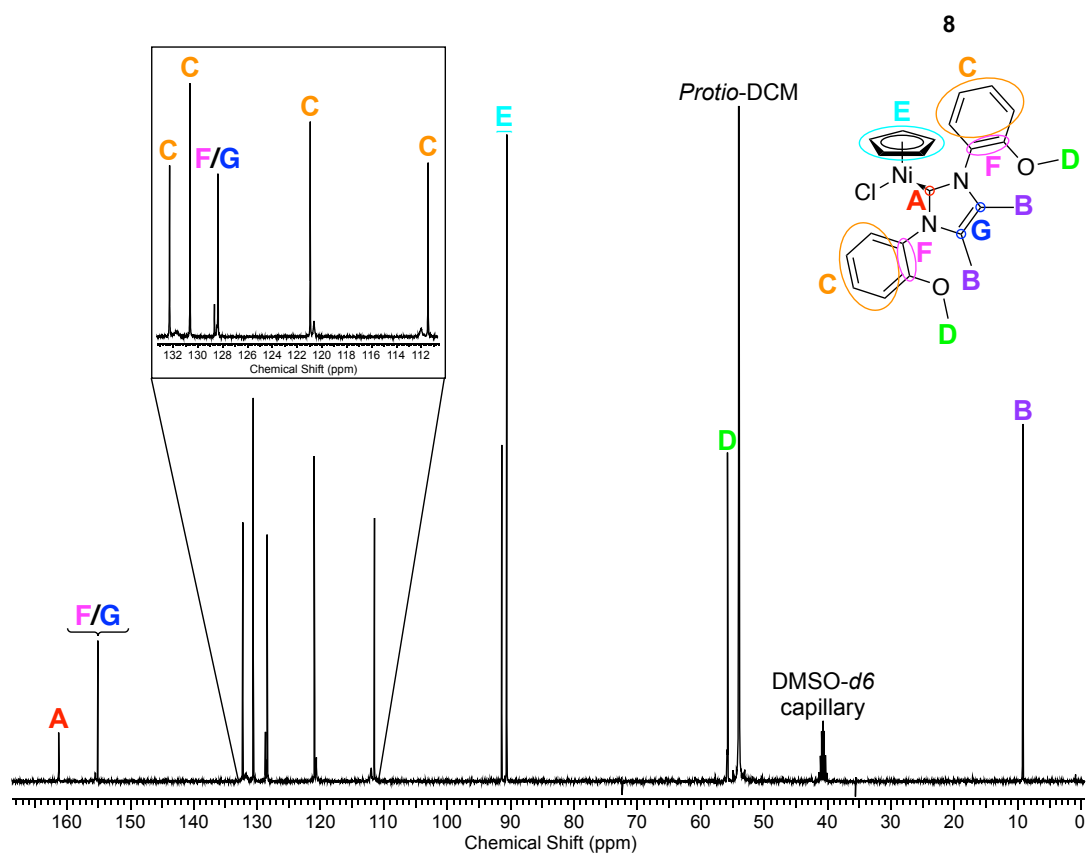
A2.10.3 ^{1}H VT NMR spectra
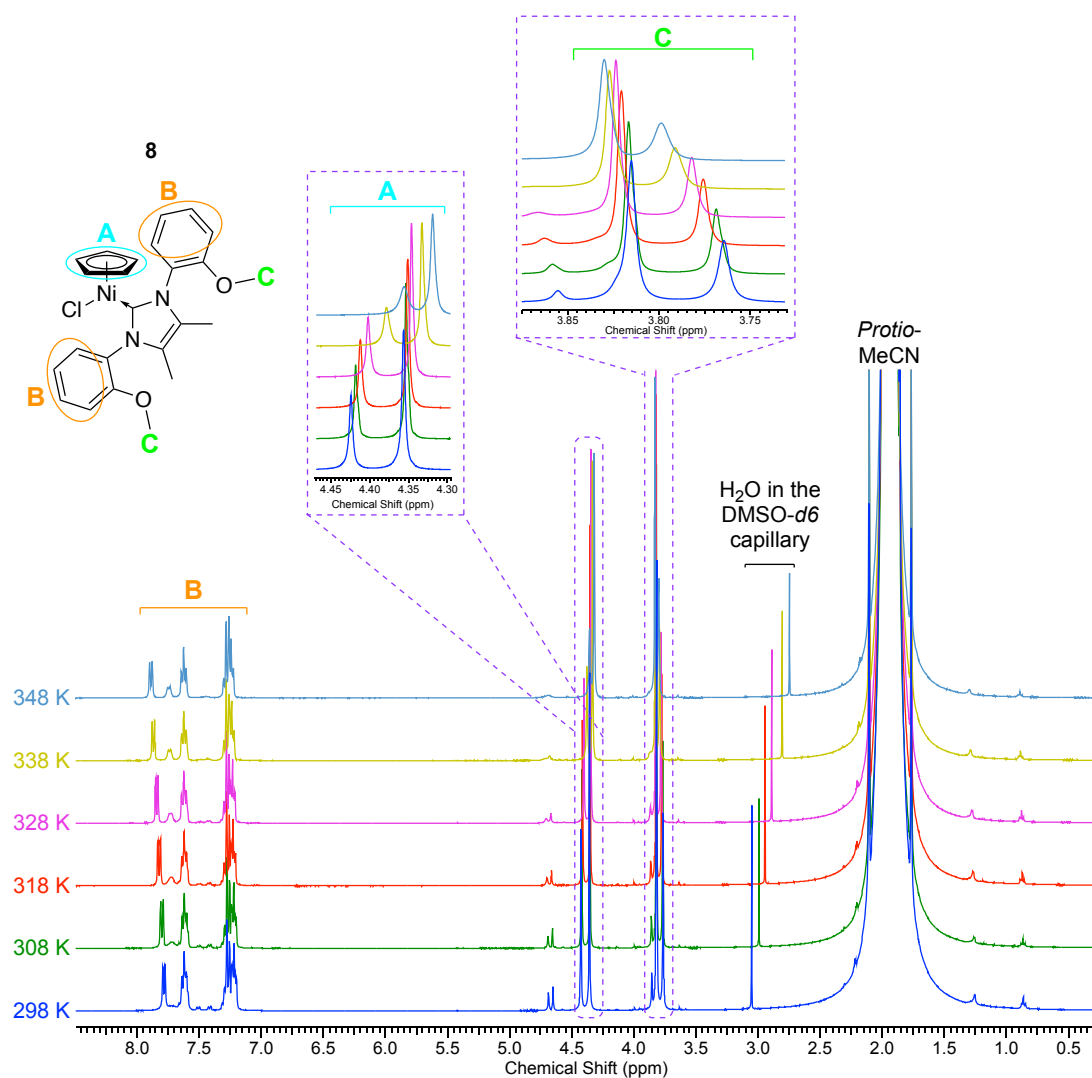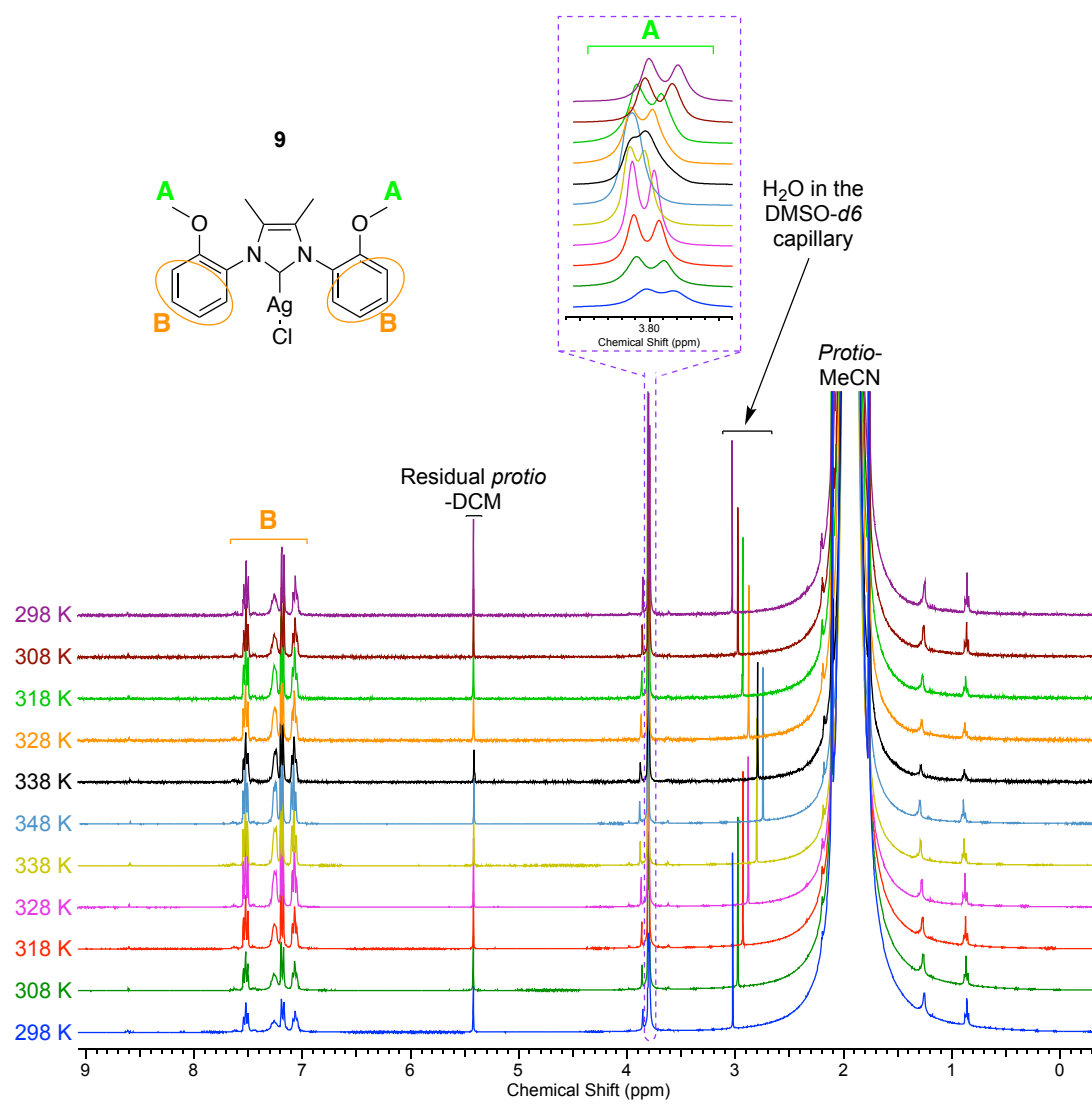
A2.11 Multinuclear NMR data of 9

A2.11.1 ^{1}H NMR spectrum

A2.11.2 $^{13}C\{^{1}H\}$ NMR spectrum

A2.11.3 ^{1}H VT NMR spectra
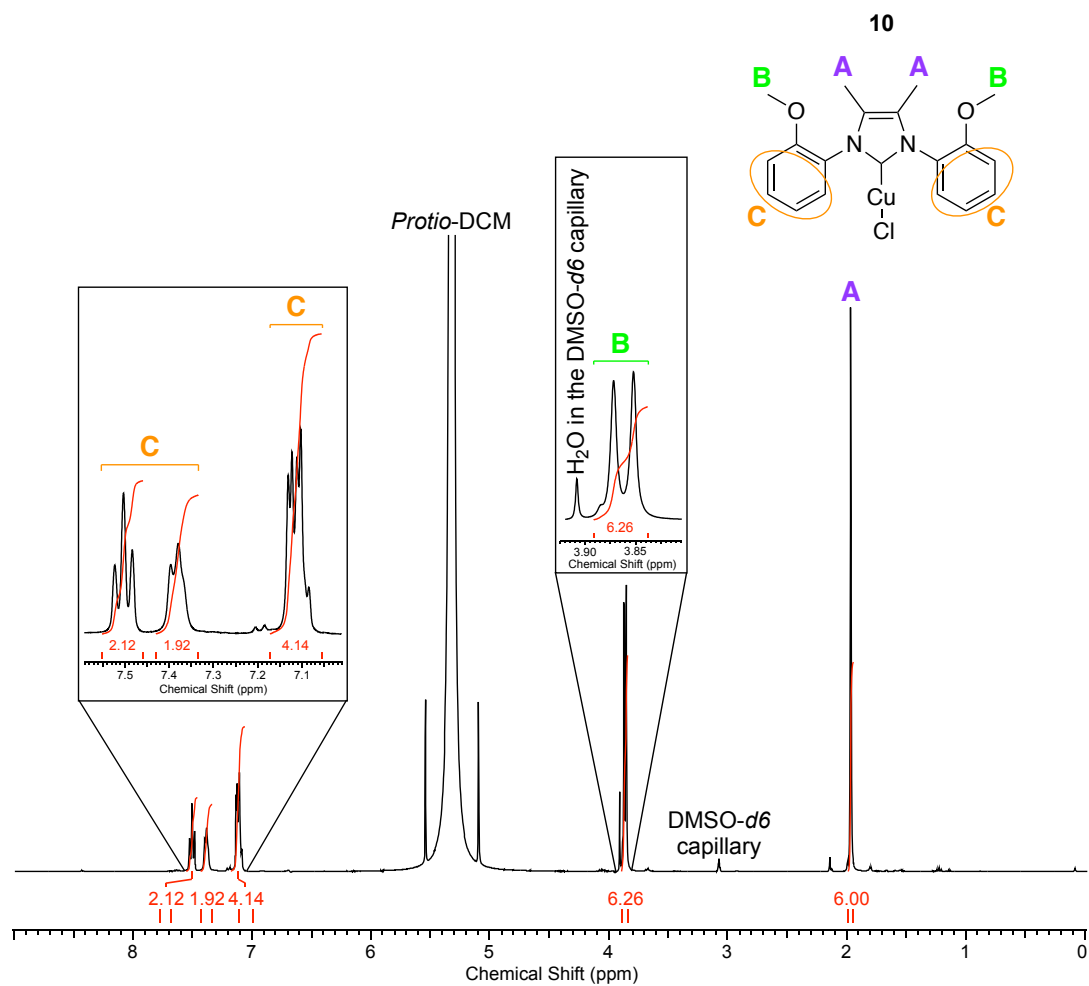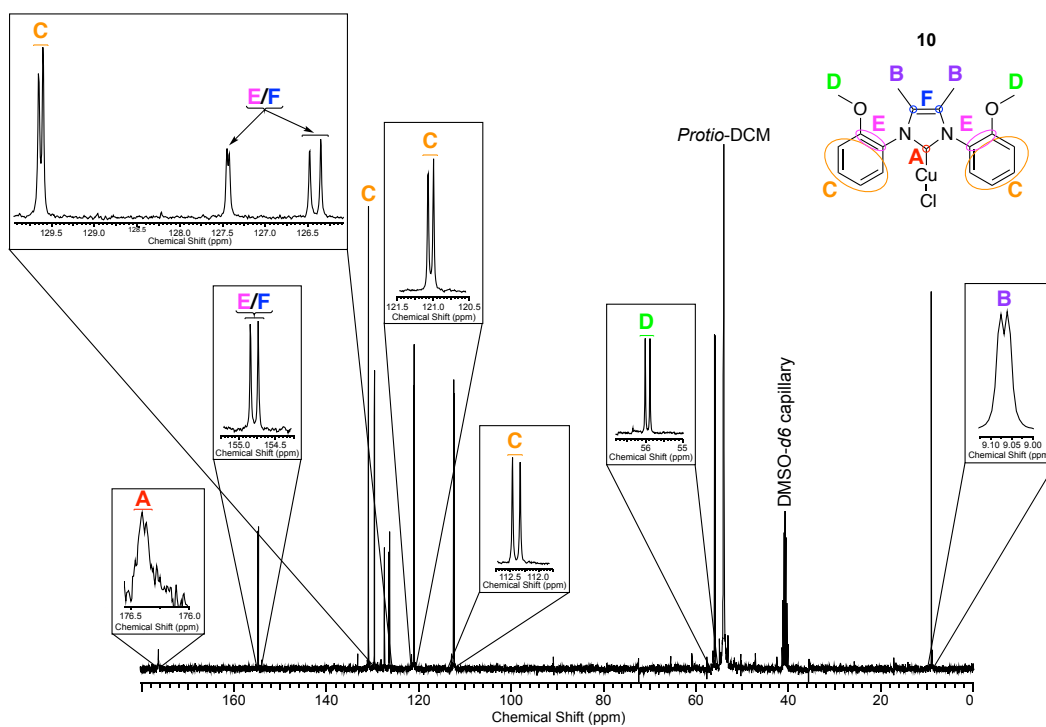
A2.12 Multinuclear NMR data of 10

A2.12.1 ^{1}H NMR spectrum

A2.12.2 $^{13}C\{^1H\}$ NMR spectrum
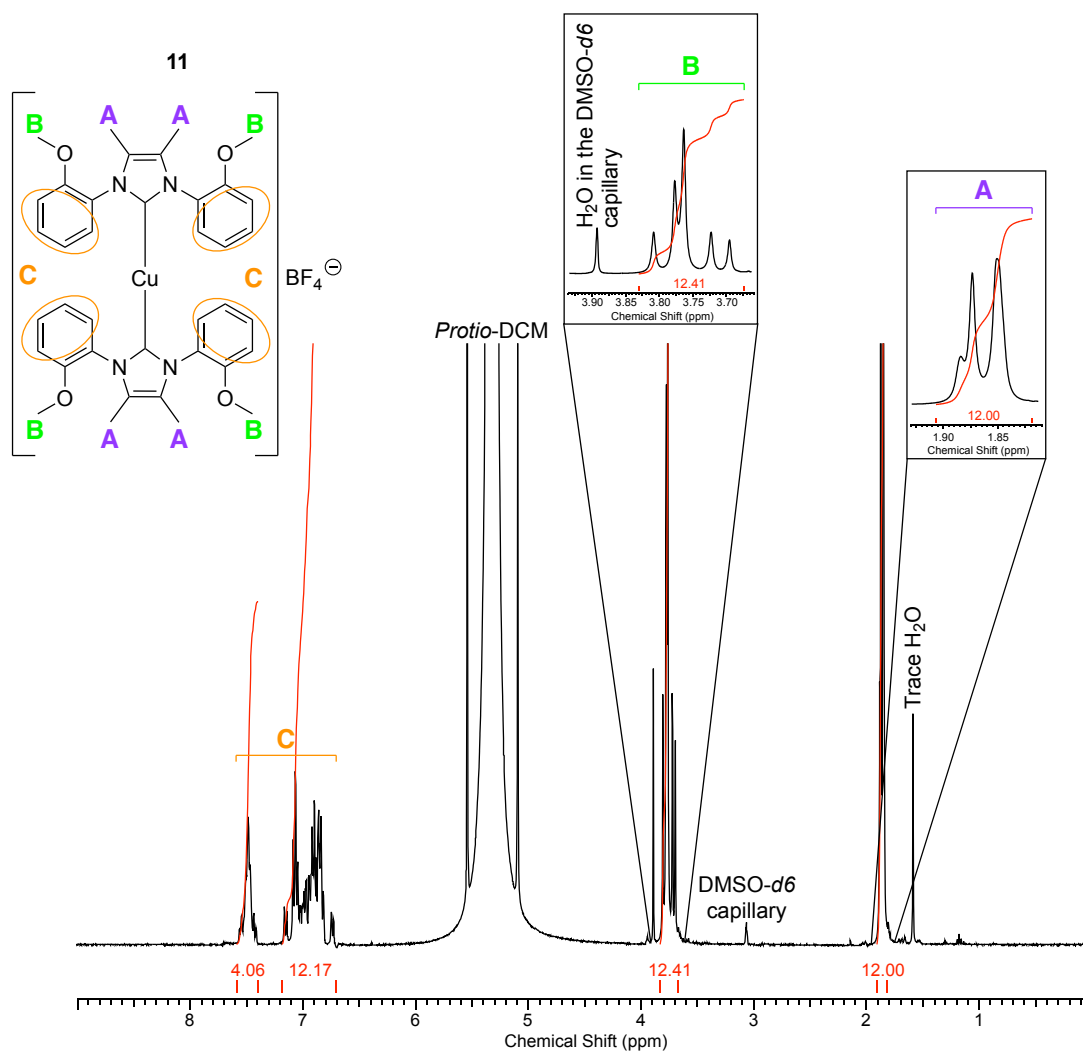
A2.12.3 ^{1}H VT NMR spectra
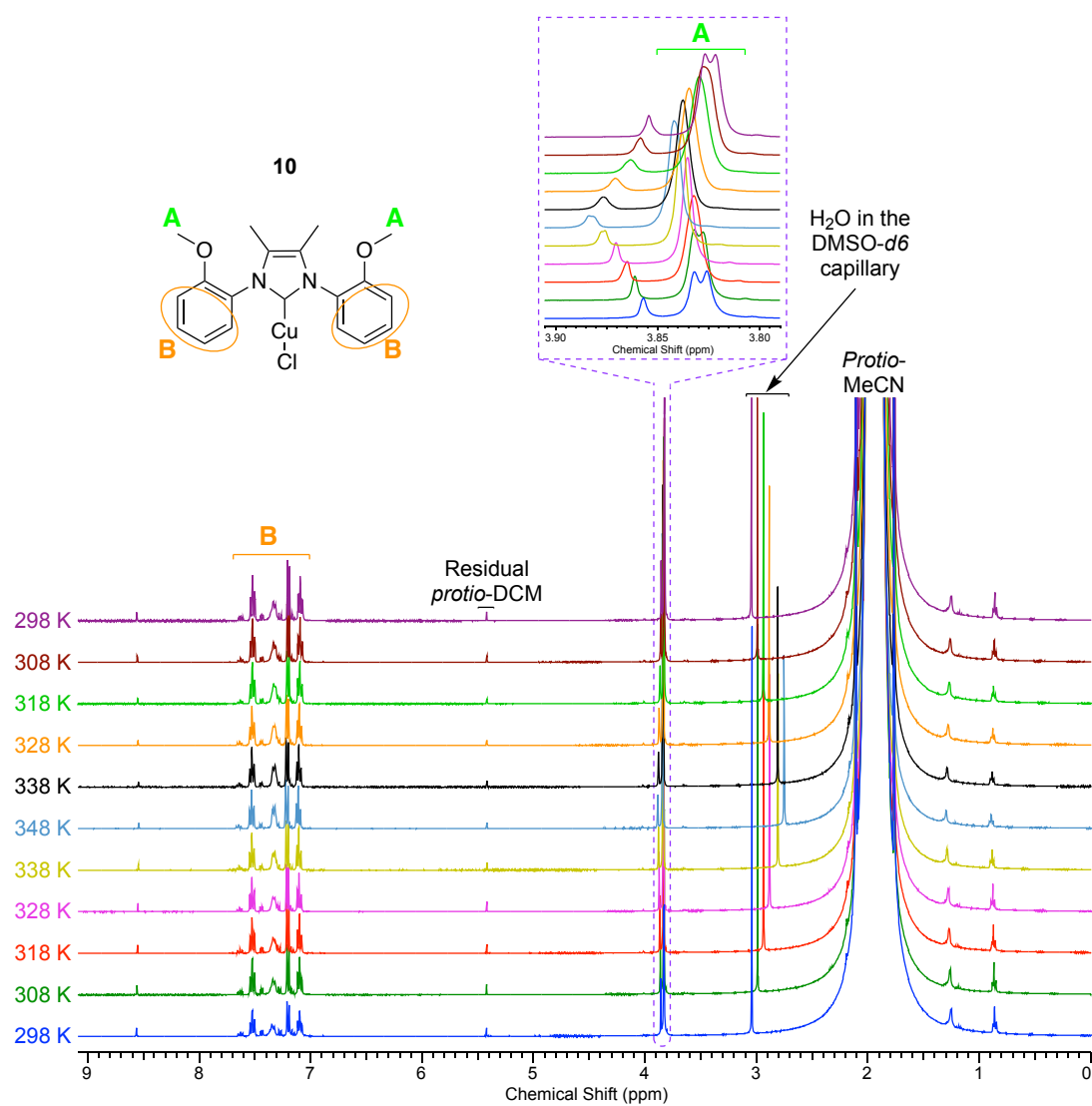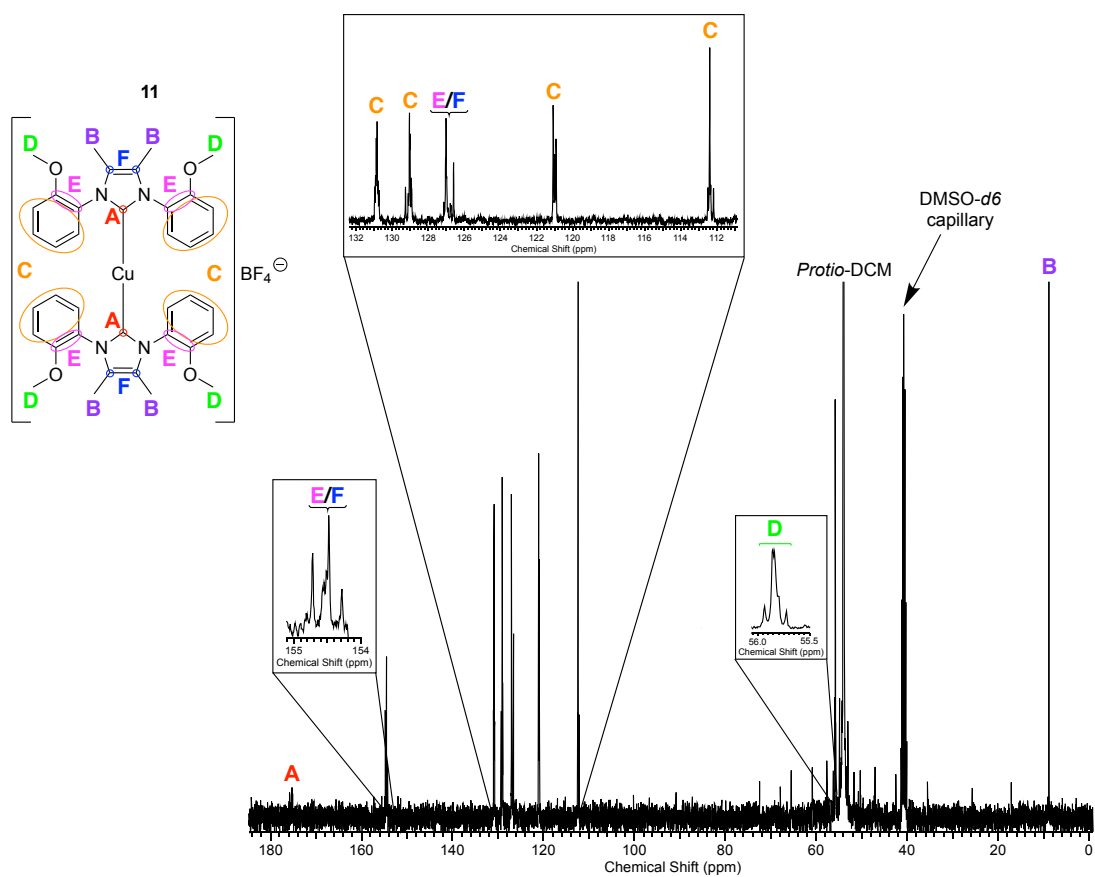
A2.13 Multinuclear NMR data of 11

A2.13.1 ^{1}H NMR spectrum
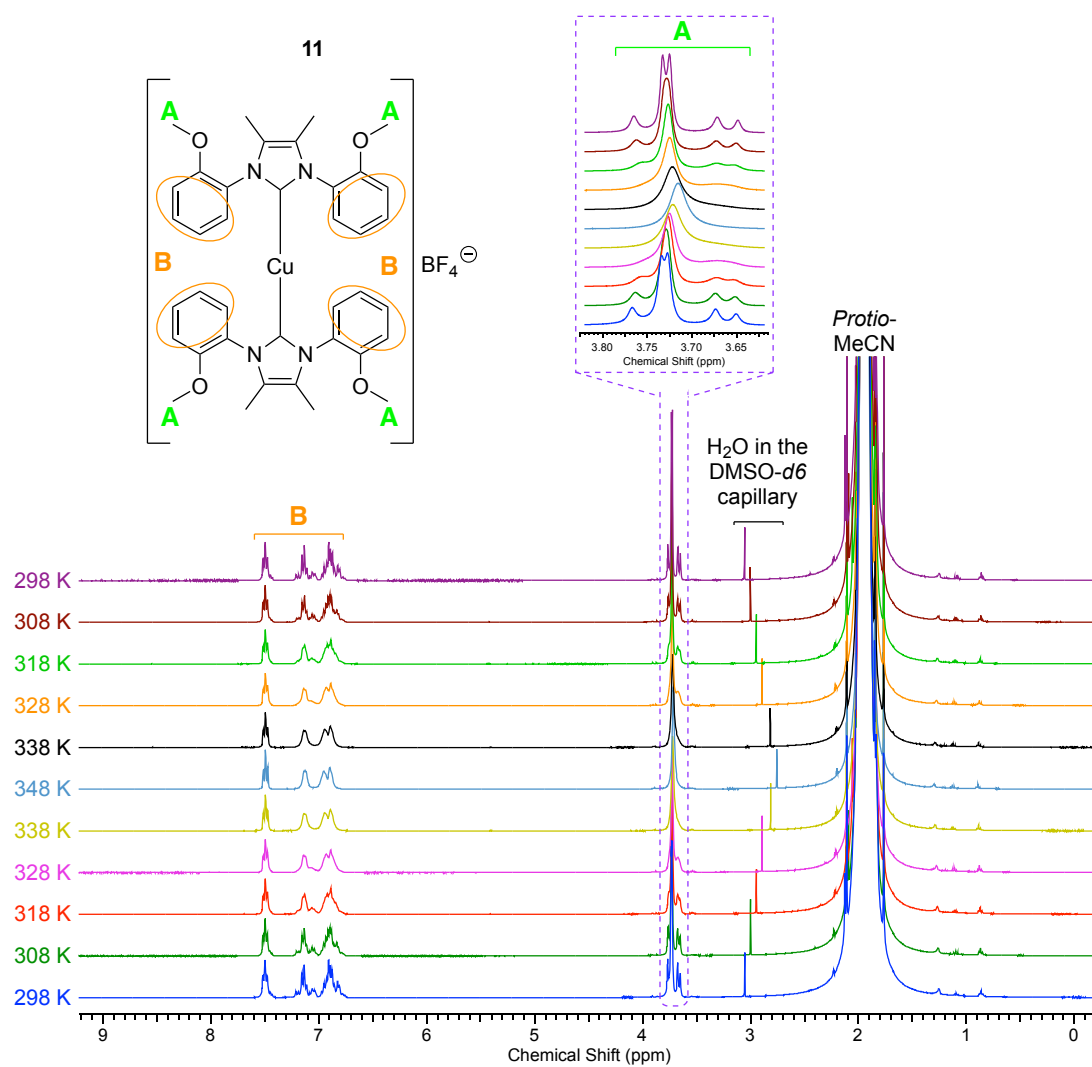
A2.13.2 ^{13}C{^{1}H} NMR spectrum
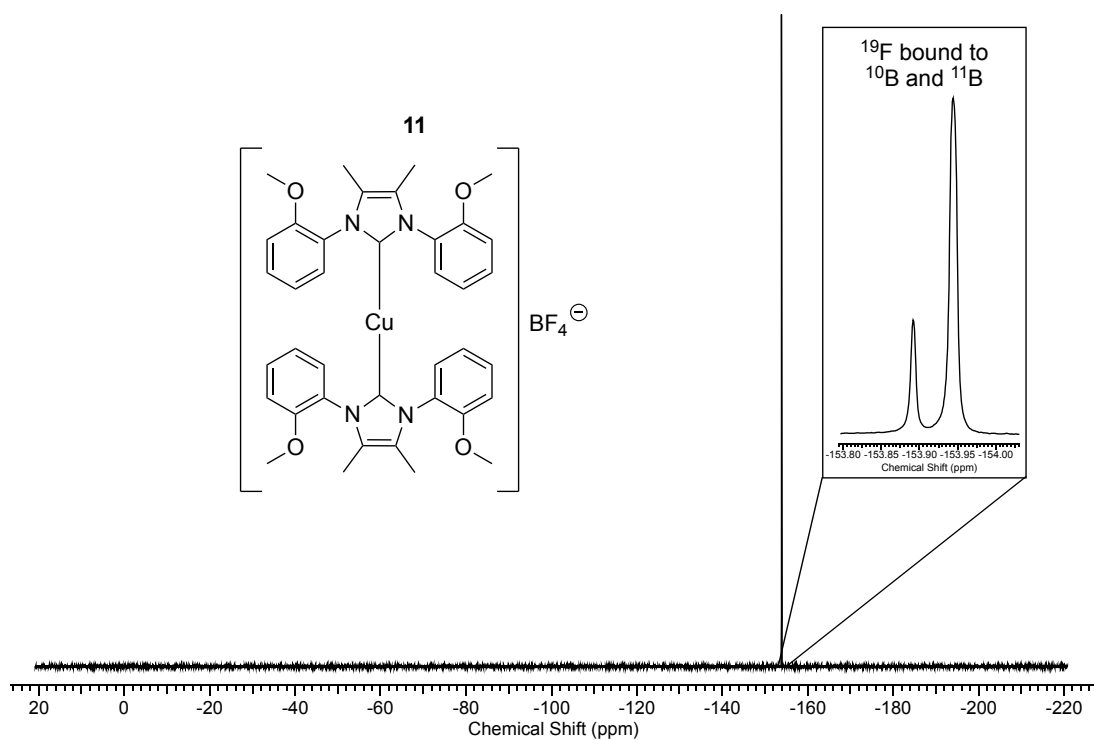
A2.13.3 ^{1}H VT NMR spectra

A2.13.4 ^{11}B NMR spectrum
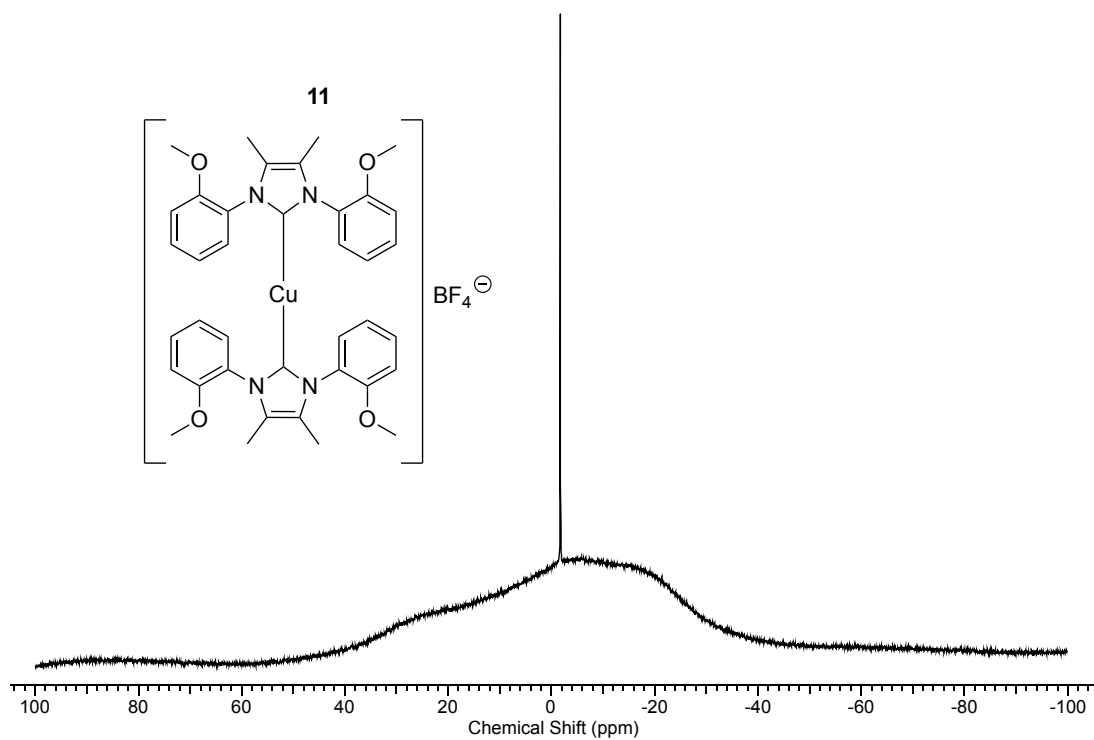
A2.13.5 ^{19}F NMR spectrum

A3 Crystallographic data tables

	2a	5b
Empirical formula	$C_{19}H_{11}ClN_2O_3$	$C_{17}H_{17}BrN_2O_2$
Formula weight	350.75	361.23
Temperature/K	99.9(6)	100.00(10)
Crystal system	triclinic	orthorhombic
Space group	P-1	Pbca
a/Å	9.3184(17)	8.75853(12)
b/Å	10.9017(18)	15.02900(18)
c/Å	11.264(2)	25.1401(4)
α/°	89.404(14)	90
β/°	66.039(17)	90
γ/°	66.474(17)	90
Volume/Å^3	942.9(3)	3309.24(8)
Z	2	8
ρ_{calc}g/cm^3	1.235	1.450
μ/mm^{-1}	1.954	3.455
F(000)	360.0	1472.0
Crystal size/mm^3	0.153 × 0.081 × 0.064	0.324 × 0.042 × 0.023
Radiation	CuKα (λ = 1.54184)	CuKα (λ = 1.54184)
2Θ range for data collection/°	8.736 to 131.648	7.032 to 144.234
Index ranges	-11 ≤ h ≤ 11, -12 ≤ k ≤ 11, -11 ≤ l ≤ 13	-10 ≤ h ≤ 10, -11 ≤ k ≤ 18, -31 ≤ l ≤ 31
Reflections collected	5677	26929
Independent reflections	3267 [R_{int} = 0.0612, R_{sigma} = 0.0471]	3265 [R_{int} = 0.0334, R_{sigma} = 0.0167]
Data/restraints/parameters	3267/0/245	3265/0/203
Goodness-of-fit on F^2	1.565	1.058
Final R indexes [I>=2σ (I)]	R_1 = 0.1141, wR_2 = 0.3324	R_1 = 0.0268, wR_2 = 0.0728
Final R indexes [all data]	R_1 = 0.1165, wR_2 = 0.3397	R_1 = 0.0284, wR_2 = 0.0742
Largest diff. peak/hole / e Å^{-3}	0.69/-1.08	0.32/-0.38

	7	8
Empirical formula	$C_{20}H_{22}Cl_2N_2O_2Se$	$C_{24}H_{25}ClN_2NiO_2$
Formula weight	472.25	467.62
Temperature/K	100	100
Crystal system	orthorhombic	orthorhombic
Space group	Pnma	Pbca
a/Å	17.7978(2)	16.5062(3)
b/Å	14.2752(2)	13.4284(2)
c/Å	8.22130(10)	20.4108(3)
α/°	90	90
β/°	90	90
γ/°	90	90
Volume/Å^3	2088.76(5)	4524.09(13)
Z	4	8
ρ_{calc}g/cm^3	1.502	1.373
μ/mm^{-1}	4.930	2.498
F(000)	960.0	1952.0
Crystal size/mm^3	0.224 × 0.110 × 0.083	0.127 × 0.048 × 0.037
Radiation	CuKα (λ = 1.54184)	CuKα (λ = 1.54184)
2Θ range for data collection/°	9.94 to 136.5	8.664 to 136.486
Index ranges	$-21 \le h \le 21$, $-17 \le k \le 16$, $-9 \le l \le 9$	$-19 \le h \le 14$, $-16 \le k \le 15$, $-24 \le l \le 13$
Reflections collected	18861	11774
Independent reflections	1995 [R_{int} = 0.0284, R_{sigma} = 0.0120]	4142 [R_{int} = 0.0339, R_{sigma} = 0.0351]
Data/restraints/parameters	1995/0/132	4142/0/371
Goodness-of-fit on F^2	1.043	1.016
Final R indexes [I>=2σ (I)]	R_1 = 0.0452, wR_2 = 0.1044	R_1 = 0.0315, wR_2 = 0.0741
Final R indexes [all data]	R_1 = 0.0454, wR_2 = 0.1045	R_1 = 0.0414, wR_2 = 0.0792
Largest diff. peak/hole / e Å^{-3}	1.84/-1.49	0.29/-0.27

|	**9**	**10**
Empirical formula	$C_{19}H_{20}AgClN_2O_2$	$C_{19}H_{20}ClCuN_2O_2$
Formula weight	451.69	407.36
Temperature/K	100.0(4)	100.0(9)
Crystal system	monoclinic	monoclinic
Space group	$P2_1/c$	$P2_1/c$
a/Å	10.27469(18)	10.1796(6)
b/Å	17.2548(2)	17.0154(11)
c/Å	11.39754(19)	11.4539(8)
α/°	90	90
β/°	111.2749(19)	110.989(7)
γ/°	90	90
Volume/Å^3	1882.94(5)	1852.3(2)
Z	4	4
ρ_{calc}g/cm^3	1.593	1.461
μ/mm^{-1}	10.009	1.337
F(000)	912.0	840.0
Crystal size/mm^3	0.133 × 0.056 × 0.054	0.274 × 0.214 × 0.146
Radiation	CuKα (λ = 1.54184)	MoKα (λ = 0.71073)
2Θ range for data collection/°	9.236 to 140.104	7.094 to 52.74
Index ranges	-12 ≤ h ≤ 12, -21 ≤ k ≤ 18, -10 ≤ l ≤ 13	-9 ≤ h ≤ 12, -21 ≤ k ≤ 16, -14 ≤ l ≤ 11
Reflections collected	13655	8902
Independent reflections	3572 [R_{int} = 0.0286, R_{sigma} = 0.0266]	3791 [R_{int} = 0.0684, R_{sigma} = 0.0844]
Data/restraints/parameters	3572/0/230	3791/0/230
Goodness-of-fit on F^2	1.216	1.057
Final R indexes [I>=2σ (I)]	R_1 = 0.0358, wR_2 = 0.0825	R_1 = 0.0635, wR_2 = 0.1662
Final R indexes [all data]	R_1 = 0.0366, wR_2 = 0.0828	R_1 = 0.0786, wR_2 = 0.1794
Largest diff. peak/hole / e Å^{-3}	1.63/-0.71	1.16/-0.72

A4 Buried volume tables and maps

SambVca 2.0[4] settings:

- Bondi radii scaled by 1.17

- Sphere radius = 3.5 Å

- Distance of the coordination point from the centre of the sphere = -2.28 Å

- Mesh spacing = 0.10 Å

7

V Free	V Buried	V Total	V Exact
131.9	47.6	179.5	179.6

%V_Free	%V_Bur	% Tot/Ex
73.5	**26.5**	100.0

Quadrant	V_f	V_b	V_t	%V_f	%V_b
SW	31.7	13.2	44.9	70.6	**29.4**
NW	31.4	13.4	44.9	70.1	**29.9**
NE	34.5	10.4	44.8	76.9	**23.1**
SE	34.2	10.6	44.9	76.3	**23.7**

Steric map
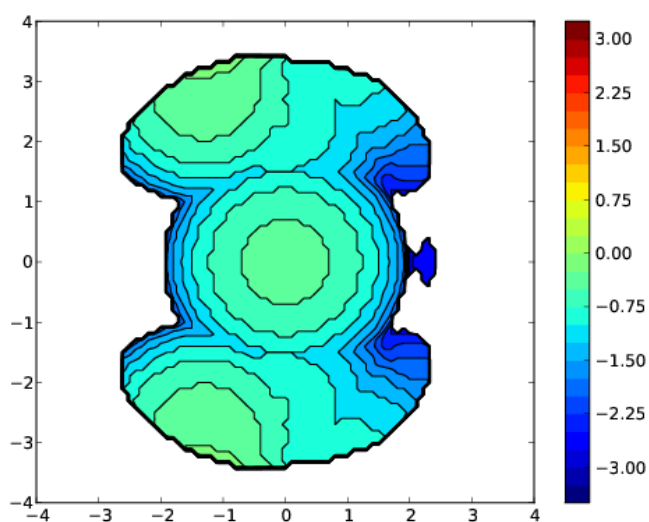
8

V Free	V Buried		V Total	V Exact
129.1	50.4		179.5	179.6

%V_Free	%V_Bur		% Tot/Ex
71.9	**28.1**		100.0

Quadrant	V_f	V_b	V_t	%V_f	%V_b
SW	35.2	9.7	44.9	78.4	**21.6**
NW	28.7	16.2	44.9	63.9	**36.1**
NE	37.2	7.7	44.8	82.8	**17.2**
SE	28.1	16.8	44.9	62.6	**37.4**

Steric map
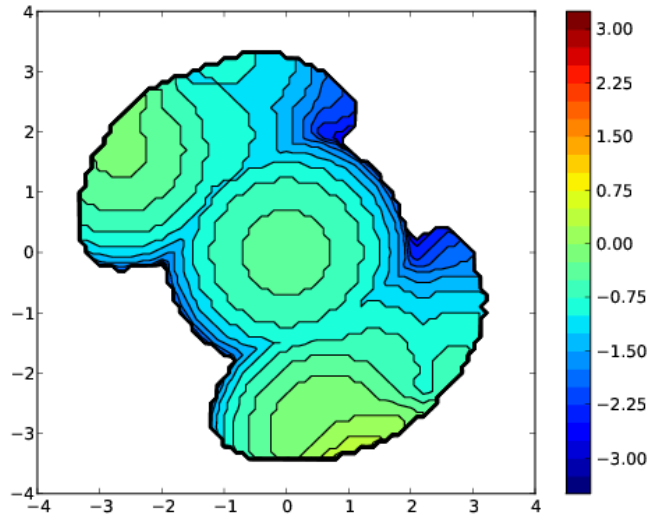
9

V Free	V Buried	V Total	V Exact
128.3	51.2	179.5	179.6

%V_Free	%V_Bur	% Tot/Ex
71.5	28.5	100.0

Quadrant	V_f	V_b	V_t	%V_f	%V_b
SW	29.3	15.6	44.9	65.2	34.8
NW	35.2	9.7	44.9	78.4	21.6
NE	29.5	15.4	44.8	65.7	34.3
SE	34.4	10.5	44.9	76.6	23.4

Steric map
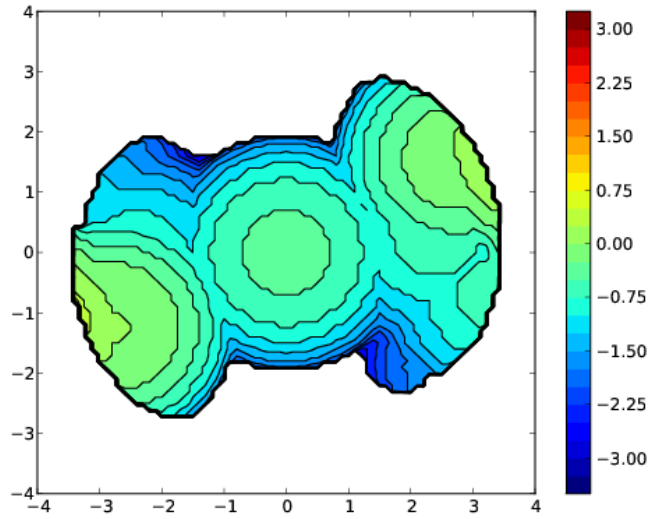
10

V Free	V Buried	V Total	V Exact
128.9	50.6	179.5	179.6

%V_Free	%V_Bur	% Tot/Ex
71.8	**28.2**	100.0

Quadrant	V_f	V_b	V_t	%V_f	%V_b
SW	37.0	7.9	44.9	82.5	**17.5**
NW	27.4	17.5	44.9	61.0	**39.0**
NE	36.3	8.6	44.8	80.9	**19.1**
SE	28.2	16.6	44.9	62.9	**37.1**

Steric map
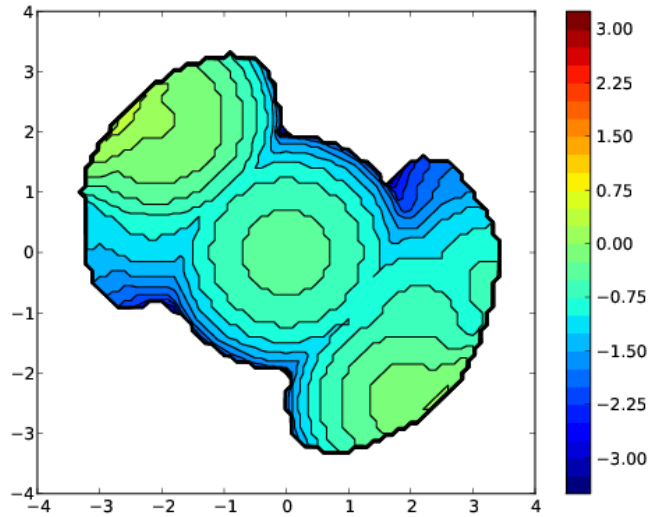
A5 References

1. Rigaku Oxford Diffraction, *CrysAlisPRO*, version 1.171.39.46 (2018), Agilent Technologies UK Ltd, Yarnton, England.

2.G. Sheldrick, *Acta Crystallogr., Sect. A: Found. Crystallogr.*, 2008, **64**, 112-122.

3. O. Dolomanov, L. Bourhis, R. Gildea, J. Howard and H. Puschmann, *J. Appl. Crystallogr.*, 2009, **42**, 339-341.

4. L. Falivene, R. Credendino, A. Poater, A. Petta, L. Serra, R. Oliva, V. Scarano and L. Cavallo, *Organometallics*, 2016, **35**, 2286-2293.